

**Cyclic AMP Modulation and its Effects on Chemo-resistant
Colon Cancer Cell Proliferation and Survival.**

by

David George McEwan

This thesis is submitted to the University of Glasgow as part fulfilment of the requirements for the degree of Doctor of Philosophy.

The Faculty of Medicine
University of Glasgow
Glasgow

The Beatson Institute for Cancer Research
Cancer Research UK Laboratories
Bearsden
Glasgow

Abstract

One of the major problems associated with colorectal cancer is resistance to cytotoxic chemotherapeutic agents. New strategies are therefore required to inhibit colon cancer proliferation and survival. Here I use modulators of cAMP pathways, including inhibitors of phosphodiesterase 4 (PDE4) enzymes, which are under clinical development for other disease states, to inhibit the breakdown of cAMP and to assess the effects of raising intracellular cAMP on colon cancer proliferation and survival. I found that some chemo-resistant cancer cells are addicted to keeping low cAMP in PDE4 regulated compartments, and modulation of this pool causes G1/S-phase arrest and apoptosis. I also show that PDE4 controlled cAMP negatively regulates the PI 3-Kinase/Akt pathway, which some cells are addicted to for survival. Furthermore, I investigated the expression and role of PDE4 enzymes in metastatic colon cancer cells and assessed the effects of modulating their expression on survival. Also, I used a clinically relevant analogue of forskolin, an agonist of adenylyl cyclase, to examine the general effect on growth of epithelial cancer cell lines. This work might provide new strategies for the treatment of advanced colon cancer.

Acknowledgements

First and foremost, I would like to thank my supervisors, Margaret Frame and Miles Houlsay for their continuous help and support during my PhD and without whom this thesis would not have completed. Also, I would like to thank George Baillie for his input, help and supply of reagents, again without which my project would have been that little bit more difficult.

Thanks to both the R1 and Gardiner lab members past and present.

Also I would like to thank Prof David Gillespie and Dr. Owen Sansom for their help throughout my PhD.

A big thank you to my partner Alison for her continued love and support.

Finally, I also wish to thank the Beatson Institute and Cancer Research U.K. for funding this project.

Table of Contents

Abstract	i
Acknowledgements	ii
Table of contents	iii
List of tables	vii
List of figures	viii
Abbreviations	ix
Declaration	xv
1. Introduction.....	1
1.1 Colorectal cancer.....	2
1.2 Oncogene addiction.....	4
1.3 Treatment of colorectal cancer.....	8
1.4 Chemoresistance.....	10
1.5 Cell-based models of colon cancer.....	11
1.6 Animal-based models of colon cancer.....	12
1.7 Fidler model of human colorectal metastasis.....	15
1.8 Previous work using the Fidler model of colorectal cancer cells.....	16
1.9 New strategies: Molecular targeted therapies.....	21
1.10 Cyclic nucleotide signalling.....	25
1.11 cAMP 2 nd messenger signalling.....	25
1.12 Compartmentalisation of cAMP signalling.....	26
1.13 GPCR signalling and cancer.....	28
1.14 cAMP effectors: PKA.....	30
1.15 cAMP effectors: Epac.....	33
1.16 Down stream effects of Epac activation.....	34
1.17 PKA and cancer.....	37
1.18 Epac/Rap1 and cancer.....	38
1.19 cAMP degradation.....	39
1.20 PDE3 enzymes.....	41
1.21 PDE3 enzymes and their role in cancer.....	42
1.22 PDE4 enzymes.....	45
1.23 PDE4 isoforms.....	45
1.24 PDE4s, cAMP and cross-talk with other signalling pathways.....	49
<i>ERK regulation of PDE4 activity</i>	49
<i>cAMP-mediated modulation of ERK activity</i>	50
<i>PI 3-kinase/Akt pathway</i>	51
<i>cAMP, PDE4s, and modulation of the PI 3-kinase/Akt pathway</i>	57
1.25 cAMP, PDE4s and the cell cycle.....	57
1.26 PDE4s and cancer.....	62
1.27 Summary.....	64
2. Materials and methods.....	65
Materials.....	66
2.1 Cell culture reagents.....	66
2.2 Cell culture plasticware.....	67
2.3 Treatments.....	67

2.4	MTT assay.....	67
2.5	PDE assay.....	68
2.6	Rap1 activity assay.....	68
2.7	Cell cycle analysis.....	68
2.8	Annexin-V staining.....	69
2.9	Immunofluorescence.....	69
2.10	Western blotting.....	70
2.11	Reverse-transcription (RT)-PCR.....	72
2.12	Stock solutions and buffers.....	72
2.13	Cells and plasmids.....	76
Methods.....		78
2.14	Routine cell culture.....	78
2.15	Treatment of cells.....	78
2.16	MTT proliferation assay.....	78
2.17	PDE assay.....	79
2.18	Preparation of protein extracts.....	79
2.19	Western blot analysis.....	80
2.20	Rap1 activation assay.....	81
2.21	Cell cycle analysis.....	81
2.22	Annexin-V detection of apoptosis.....	82
2.23	Transient transfection.....	83
2.24	Immunofluorescence.....	83
2.25	Sub-cellular fractionation.....	84
2.26	Immunoprecipitation (IP).....	84
2.27	RT-PCR.....	85
2.28	Preparation of DNA.....	86
2.29	Retroviral infection.....	87
2.30	Nucleofection.....	87
2.31	Stable knockdown of PDE4Din KM12L4A cells.....	87
2.32	Statistical analysis.....	88
2.33	Densitometry.....	88
3. cAMP effects of KM12C proliferation.....		89
3.1	Aims.....	90
3.2	cAMP inhibits the proliferation of KM12C cells.....	90
3.3	PDE enzymes can regulate anti-proliferative effects of cAMP.....	94
3.4	Epac did not regulate anti-proliferative effects of cAMP.....	98
3.5	Fsk/rolipram induces a partial G1/S-phase arrest.....	103
3.6	Fsk/rolipram induces specific G1/S-phase CKIs.....	106
3.7	Fsk/rolipram inhibits Rb/E2F regulated cell cycle proteins.....	106
3.8	Fsk/rolipram induces a cell death morphology.....	113
3.9	Fsk/rolipram induces DNA fragmentation.....	114
3.10	Fsk/rolipram induces apoptosis.....	114
Discussion.....		122
3.11	Inhibition of chemo-resistant colon cancer cells by cAMP.....	122
3.12	Is Epac or PKA regulating KM12C proliferation?.....	124
3.13	PDE3 vs PDE4 induced inhibition of proliferation.....	125
3.14	PDE4/cAMP controlled cell cycle arrest.....	127
3.15	Rolipram mediated apoptosis.....	128

3.16 Summary.....	129
4. cAMP interference with oncogene addiction.....	130
4.1 Aims.....	131
4.2 Loss of pAkt (Ser473) is an early event in PDE4/cAMP inhibition of proliferation.....	131
4.3 Fsk/rolipram perturbs PtdIns(3,4,5)P ₃ localisation.....	134
4.4 Fsk/rolipram displaces PI 3-kinase p85 α subunit from the cell periphery.....	135
4.5 PDE4/cAMP inhibits downstream effectors of the PI 3-kinase pathway.....	141
4.6 LY294002 induces similar effects to Fsk/rolipram.....	144
4.7 LY294002 induces apoptosis and inhibits proliferation.....	145
4.8 Exogenous expression of PTEN inhibits Akt phosphorylation and sensitises KM12C cells to Fsk.....	150
Discussion.....	155
4.9 PI 3-kinase localisation.....	155
4.10 PDE4/cAMP induced loss of Akt/PKB phosphorylation.....	156
4.11 PI 3-kinase regulation of proliferation.....	158
4.12 Effects of PTEN expression.....	160
4.13 Oncogene addiction and its inhibition.....	161
4.14 Summary.....	162
5. PDE4 expression and activity is altered in metastatic cells – consequences for Fsk sensitivity.....	163
5.1 Aims.....	164
5.2 Metastatic cells have increased resistance to Fsk mediated inhibition of proliferation.....	164
5.3 Metastatic cells have increased PDE4 activity and expression.....	168
5.4 PDE4D RNAi sensitises metastatic cells to Fsk.....	172
5.5 PDE4D3 does not regulate the apoptosis in KM12C cells.....	176
5.6 PDE4D5 may regulate apoptotic response to cAMP in KM12C cells.....	177
Discussion.....	182
5.7 Metastatic resistance to Fsk inhibition of proliferation.....	182
5.8 Increased PDE4 expression and activity in metastatic cell lines.....	183
5.9 PDE4D3 versus PDE4D5 regulation of proliferation and cell death.....	185
5.10 Summary.....	186
6. NKH477: A potentially clinically relevant Fsk analogue.....	188
6.1 Aims.....	189
6.2 Sensitivity to growth inhibition by cAMP modulation is not restricted to KM12C cells.....	189
6.3 NKH477 induces p27 ^{Kip1} and loss of pAkt in KM12C cells.....	194
6.4 NKH477 inhibits the proliferation of numerous cancer cell lines.....	195
Discussion.....	199
6.5 Cell lines sensitivity to Fsk/rolipram.....	199
6.6 NKH477 as an anti-cancer therapy.....	200
6.7 Summary.....	201

7. Concluding remarks and future perspectives.....	202
7.1 cAMP, PDE4s and their therapeutic potential in cancer.....	203
7.2 Does PDE4s elevation correlate with disease stage?.....	204
7.3 Can PDE4s be exploited as therapeutic targets for cancer?.....	206
7.4 Future work.....	210
8. References.....	214
Published material.....	252

List of tables

Table 1	The Dukes' classification of colorectal cancer and 5 year survival rates.....	3
Table 2	The TNM classification of colorectal cancer.....	3
Table 3	Correlation between TNM and Dukes staging of colorectal cancer.....	3

List of Figures

Figure number	Description	Page
Figure 1	Cancer development models	6
Figure 2	5-Fluorouracil mechanism of action	9
Figure 3	APC/ β -catenin pathway	14
Figure 4	Fidler mouse model of human colorectal metastasis	17
Figure 5	cAMP generation	27
Figure 6	cAMP effectors	32
Figure 7	Epac domain structure and regulation	35
Figure 8	Cyclic AMP hydrolysis	40
Figure 9	PDE3 domain structure and gene organisation	43
Figure 10	PDE4 domain structure	48
Figure 11	PI 3-Kinase/Akt pathway	55
Figure 12	PTEN domain structure	56
Figure 13	Cell cycle regulation by p21 ^{Cip1/Waf1} /p27 ^{Kip1}	61
Figure 14	cAMP inhibits the proliferation of KM12C cells	93
Figure 15	PDE enzymes regulate the anti-proliferative pool of cAMP	97
Figure 16	Epac/Rap1 did not mediate the anti-proliferative effects of cAMP	102
Figure 17	Fsk/rolipram induces partial G1/S arrest	105
Figure 18	Fsk/rolipram induces a specific G1/S-phase CKI	110
Figure 19	Fsk/rolipram treatment inhibits expression pRb/E2F regulated cell cycle proteins	112
Figure 20	Fsk/rolipram induces a cell-death like morphology	117
Figure 21	Fsk/rolipram induces DNA fragmentation	119
Figure 22	Fsk/rolipram induces apoptosis	121
Figure 23	Loss of pAkt (Ser473) is an early event in PDE4/cAMP inhibition of proliferation	133
Figure 24	Fsk/rolipram perturbs PtdIns(3,4,5)P ₃ localisation	138
Figure 25	Fsk/rolipram displaces PI3-Kinase p85 α from the cell periphery	140
Figure 26	PDE4/cAMP inhibits downstream effectors of the PI 3-kinase pathway	143
Figure 27	LY294002 induces similar effects to Fsk/rolipram	147
Figure 28	LY294002 induces apoptosis and inhibits proliferation	149
Figure 29.	Exogenous expression of PTEN inhibits Akt phosphorylation and sensitises KM12C cells to Fsk	154
Figure 30	Metastatic cells have increased resistance to Fsk	167
Figure 31	Metastatic cells have altered PDE4 expression and activity	171
Figure 32	PDE4D RNAi sensitises KM12L4A cells to Fsk	175
Figure 33	PDE4D3 does not regulate apoptosis in KM12C cells	179
Figure 34	PDE4D5 may regulate cAMP that controls KM12C apoptosis	181
Figure 35	Fsk/rolipram inhibits a number of cancer cell lines	193
Figure 36	NKH477 suppresses pAkt, pERK and proliferation of KM12C cells	197
Figure 37	NKH477 inhibits the proliferation of all cancer cell lines tested	198
Figure 38	NKH477 treatment of <i>APC</i> ^{fllox} / <i>PTEN</i> ^{fllox} mice	213

Abbreviations

5-FU	5-Fluorouracil
8-Br-cAMP	8-Bromo-cAMP
8-CPT	8-pCPT-2`OMe-cAMP
8-pMeOPT	8-pMeOPT-2'-O-Me-cAMP
AC	Adenylyl cyclase
AKAP	A-kinase anchoring protein
AMP	5'-adenosine monophosphate
APC	Adenomatous polyposis coli
Arg	Argenine (R)
ATP	adenosine 5'triphosphate
B-CLL	B-cell chronic lymphocytic leukaemia
BrdU	Bromodeoxyuridine
C-	Carboxy terminal
Ca ²⁺	Calcium
cAMP	3'5'-cyclic adenosine monophosphate
CDK	Cyclin dependent kinase
CFP	cyan fluorescent protein
cGMP	3'5'-cyclic guanosine monophosphate
CKI	Cyclin dependent kinase inhibitor
CLL	Chronic lymphocytic leukaemia
CML	Chronic myeloid leukaemia
CNB	Cyclic nucleotide binding domain
COPD	Chronic obtrusive pulmonary disease
CREB	Cyclic AMP responsive element binding protein

Cys	Cysteine (C)
DEP	Deshelved-Egl-10-pleckstrin
DLBCL	Diffuse large B-cell lymphoma
DMEM	Dulbeccos modified eagles medium
DNA	deoxyribonucleic acid
DPD	dihydropyrimidine dehydrogenase
E-cadherin	Epithelial cadherin
ECL	enhanced chemiluminescence
EGF	epidermal growth factor
EGFR	Epidermal growth factor receptor
Epac	Exchange protein directly activated by cAMP
ERCC1	Excision repair cross-complementing-1
ERK	extracellular regulated kinase
F	Phenylalanine
FACs	Fluorescent activated cell sorting
FAK	focal adhesion kinase
FAK	focal adhesion kinase
FAP	Familial adenomatous polyposis
FBS	foetal bovine serum
FITC	fluorescein isothiocyanate
FKHRL1	Forkhead homologue (rhabdomyosarcoma) like 1
FRET	Fluorescence resonance energy transfer
Fsk	Forskolin
GAPs	GTPase-activating proteins
GDP	Guanosine diphosphate
GEFs	guanine nucleotide exchange factors

GFP	green fluorescent protein
GI	Gastro intestinal
GIST	Gastrointestinal stromal tumour
GPCR	G-protein coupled receptor
GRP1	General receptor for phosphoinositides
GSK-3 β	Glycogen synthase 3-beta
GTP	guanosine 5'-triphosphate
HCC	Hepatocellular carcinoma
HNSCC	Head and neck squamous cell carcinoma
IBMX	3-Isobutyl-methylxanthine
kDa	Kilo-dalton
Krev	Kirsten-ras-revertant
LPA	lysophosphatidic acid
LV	Leucovorin
mAb	monoclonal antibody
MIN	Multiple intestinal neoplasias
MLC	Myosin light chain kinase
MLCK	Myosin light chain kinase
MMP	Matrix metallo-protease
mRNA	Messenger RNA
MSI	Micro-satellite instability
MTT	3-(4,5-dimethylthiazol-2-yl)-2,5-diphenyl tetrazolium bromide
N-	Amino terminal
NSAIDs	Non-steroidal anti-inflammatory drugs
NSCLC	Non-small cell lung carcinoma
p/m	Plasma membrane

PAR	Protease activated receptor
PBS	phosphate buffered saline
PCNA	Proliferating Cell Nuclear Antigen
PCR	Polymerase chain reaction
PDE	Phosphodiesterase
PDGF	platelet derived growth factor
PDK1	3-phosphoinositide dependent kinase-1
PGE2	Prostaglandin E2
PH	pleckstrin homology domain
PI	Propidium iodide
PI 3- Kinase	phosphatidylinositol 3 kinase
PKA	Protein kinase A
PKB	Protein kinase B
PP2A	Protein phosphatase 2A
PtdIns	Phosphatidylinositol
PtdIns(3,4)P ₂	phosphatidylinositol 3,4 bisphosphate
PtdIns(3,4,5)P ₃	phosphatidylinositol 3,4,5 triphosphate
PtdIns(4,5)P ₂	phosphatidylinositol 4,5 bisphosphate
PTEN	Phosphatase and tensin homolog deleted on chromosome 10
q-PCR	Quantitative-PCR
RA	Ras-association
rAb	Rabbit polyclonal antibody
RACK1	Receptor for activated C-kinase
Rb	Retinoblastoma
RBD	Rho binding domain
REM	Ras exchange motif

RGS	Regulators of G-protein signaling
RNA	Ribonucleic acid
RSVL	Resveratrol
RTK	Receptor tyrosine kinase
RT-PCR	Reverse transcription-PCR
RYR	Ryanodine receptor
SCC	Squamous cell carcinoma
SCF	Skp1, cullin, F-box protein
SDS	sodium dodecyl sulphate
Ser	Serine (S)
SH	Src Homology
SHIP	SH2-containing inositol phosphatase
Skp2	S-phase kinase-associated protein 2
Tcf	T-cell factor
TF	Transcription factor
TMA	Tissue micro array
TNM	Tumour, node metastasis
TRAIL	Tumour necrosis factor-related apoptosis-inducing ligand
TRITC	tetramethyl rhodamine isocyanate
TS	Thymidylate synthase
TSH	Thyroid stimulating hormone
TSHR	Thyroid stimulating hormone receptor
Tyr	Tyrosine (Y)
UCR	Upstream conserved region
VEGF	Vascular endothelial growth factor
VEGFR	Vascular endothelial growth factor receptor

VSV	Vesicular stomatitis virus
Wt	wild type
Y	tyrosine

Declaration

I declare that all of the work in this thesis was performed personally unless stated otherwise. No part of this work has been submitted for consideration as part of any other degree or award.

Chapter 1: Introduction

1. Introduction

1.1 Colorectal Cancer

Colorectal cancer is the third most commonly diagnosed cancer in the UK, after breast and lung, and makes up 13% of all cancers. Approximately 35,000 people in the UK are diagnosed with colorectal cancer every year and it accounts for 16,100 deaths per annum. This equates to approximately 10% of all cancer related deaths and is the second most common cause of cancer death in the UK (Cancer Research UK). The five-year survival rate after diagnosis is dependent upon the stage of the cancer at presentation. One method of colorectal cancer classification is Dukes' staging. The Dukes' stage describes extent of invasion/spread of the tumour and correlates with overall survival. For example, patients diagnosed with Dukes' stage A tumours have an 83% chance of survival over five years which is dramatically reduced to only 3% if diagnosed with Dukes' stage D (see Table 1) (Cancer Research UK and (1)). Another method of classification is the TNM (tumour, node and metastasis) system (2-4). TNM system allocates a number to each letter, where for T, the number correlates with the size of the tumour; for N the number indicates which lymph nodes have cancer cells in them and for M indicates whether the cancer has spread beyond the lymph nodes (Table 2)(2-4). For example, a colorectal cancer graded T1N0M0 indicates stage I colorectal cancer where the tumour has grown through the muscularis mucosa (the thin layer of smooth muscle) into the submucosa (layer of loose connective tissue that supports the mucosa) or that it may have grown into the muscular coat of the colon but has not spread to neighbouring lymph nodes or to distal sites. Table 3 shows how the TNM system is simplified (into stages 0-4) and how each stage correlates with Dukes stages (5).

The majority of colorectal cancers arise from pre-existing benign polyps in the mucosa of the bowel. The progression from early adenomatous polyp through to invasive carcinoma is a

Dukes Stage	Pathological Features	5 Year Survival
A	Tumour confined to intestinal wall	83%
B	Tumour has invaded through muscular mucosa of the bowel wall	70%
C	Tumour has spread to regional lymph nodes but no distal spreading	38%
D	Tumour present at distal sites (e.g. Liver and Lungs)	3%

Table 1. The Dukes' classification of colorectal cancer and 5 year survival rates

	TNM code	Description
T (Tumour)	T0	No evidence of tumour
	Tis	Cancer has not spread beyond first epithelial layer of cells
	T1	Cancer has reached inner layers of colon wall
	T2	The cancer has spread into the muscle layer of the colon
	T3	The cancer has spread beyond the muscle layer of the colon
	T4	The cancer extends from colon wall into adjacent tissues
N (regional lymph nodes)	N0	The cancer has not spread to the nearest lymph nodes
	N1	The cancer has spread to 1, 2 or 3 lymph nodes
	N2	The cancer has spread to 4 or more lymph nodes
M (distant metastases)	M0	The cancer has not metastasised
	M1	The cancer has spread to distal lymph nodes/ organs/tissues

Table 2. The TNM classification of colorectal cancer.

TNM code	Dukes Stage	TNM stage
Tis, N0, M0	-----	0
T1, N0, M0	A	1
T2, N0, M0	B	1
T3, N0, M0	B	2
Any T, N1, M0	C	3
Any T, Any N, M0	D	4

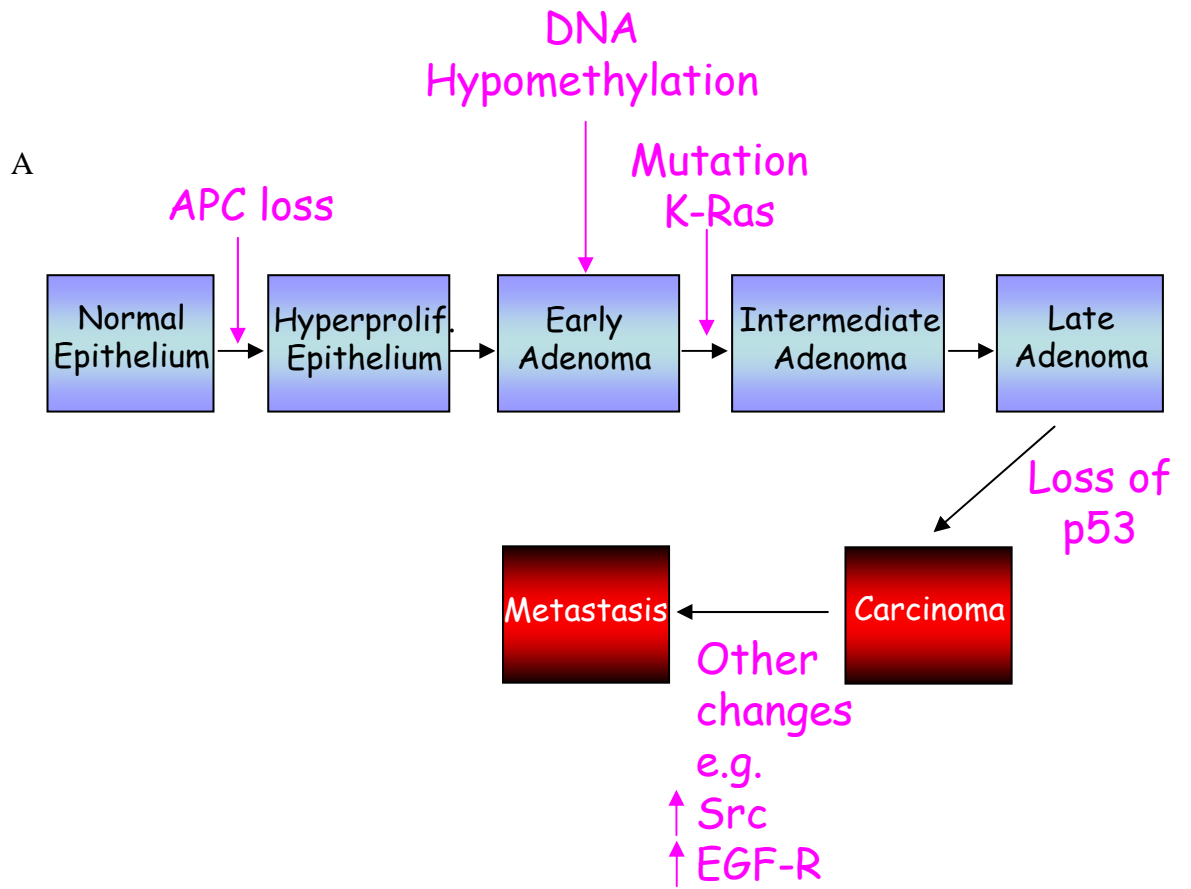
Table 3. Correlation between TNM and Dukes staging of colorectal cancer.

well documented process and a genetic pathway was initially proposed by Fearon and Vogelstein (6). This model proposes that there are a series of genetic alterations, each conferring a growth advantage, leading to the progressive conversion of normal cells into cancer cells (6). Examples of genetic changes that account for this transformation includes the inactivation of tumour suppressor genes (*p53*, *APC* and *PTEN*), through mutation or deletion, as well as activation of oncogenes including *KRas* and *PI3KCA* (reviewed in (7) (Figure 1 A). Alterations in key pathways that regulate cell proliferation, differentiation and survival do not always occur at once. Indeed, it has been proposed that a highly invasive, metastatic tumour has to acquire at least six essential alterations which are indicative of all cancer types. Alterations such as self-sufficiency in growth signals, evasion of programmed cell death (apoptosis), limitless replicative potential, sustained angiogenesis and tissue invasion and metastasis were proposed by Hanahan *et al* (8) (Figure 1 B). Often, these changes lead to the critical dependence of a cancer cell on one particular gene or signal transduction pathway for continued growth and survival, which has been termed ‘oncogene addiction’.

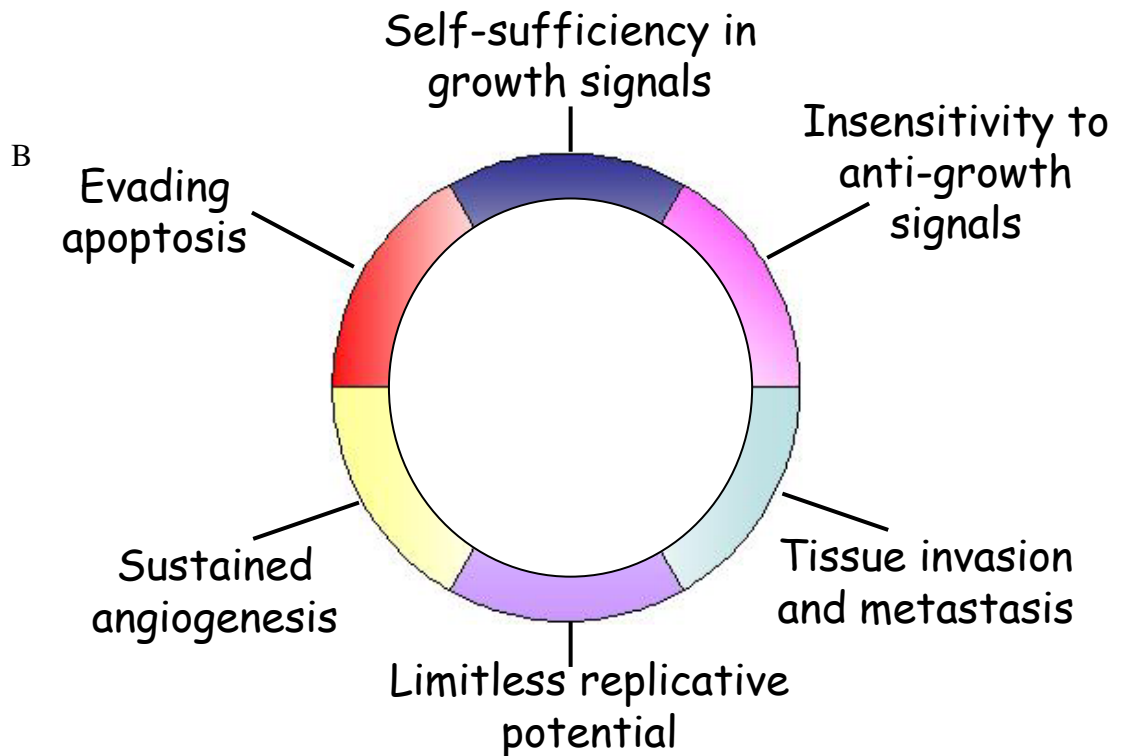
1.2 Oncogene addiction

Oncogene addiction is the phenomenon by which some cancers that contain multiple genetic and epigenetic alterations may become dependent upon (“addicted to”) one, or a small number of, genes for both maintenance of the malignant phenotype and cell survival (8, 9). There is now a large body of evidence to support the concept of tumour “oncogene addiction”. Diverse systems have contributed to our understanding of oncogene addiction, namely mouse models that have been genetically engineered to mimic human cancer, mechanistic studies in human cancer cell lines and clinical trials with molecularly targeted agents. For example, studies in mice have shown that sustained expression of *c-Myc* protooncogene resulted in both lymphoma and acute myeloid leukaemia formation (10). In

Figure 1. Cancer progression models. (A) Fearon and Vogelsteins genetic model of colorectal cancer progression. A normal epithelium goes through a series of genetic alterations that include activation of oncogenes (*K-Ras*) and inactivation of tumour suppressor genes (e.g. p53) all of which result in tumours of increasing size and dysplasia. (B) Hanahan and Weinburgs model of cancer. Most if not all, cancers acquire the same set of functional capabilities during their development. These are gaining self-sufficiency in growth signals, becoming insensitive to anti-growth signals, evading apoptosis, gaining limitless replicative potential, it must sustain angiogenesis and also to invade tissue and spread to distant organs.



Fearon & Vogelstein, (1990) *Cell* (61) 759-67



Hanahan & Weinburg, (2000) *Cell* (100) 57-70

this case, the conditional expression of a *c-Myc* transgene in haematopoietic cells resulted in tumours that were dependent on *c-Myc* expression for proliferation, and inactivation of *c-Myc* caused regression of established tumours. This underpinned the dependence on a single gene for generating and sustaining tumour formation. In breast cancer, c-Myc protein is often overexpressed and correlates with poor prognosis and clinical outcome (11). Induced human *c-Myc* oncogene expression in the mammary epithelium of mice resulted in the generation of invasive mammary carcinomas, many of which regress after *c-Myc* inactivation (12). However, it was noted that in tumours that did not regress, an activating mutation in *Kras* oncogene was present which limited the tumours dependence on c-Myc (12). Similar studies in mice have shown a critical dependence on c-Myc expression with numerous other cancer types, such as pancreatic β -cell tumours (13) and osteogenic sarcomas (14).

In human cancer cell lines, there is a plethora of data implicating a number of proteins in the maintenance of tumour viability, where loss of expression of a single protein is sufficient to inhibit proliferation and survival, despite these cells carrying numerous genetic and epigenetic abnormalities. Such proteins include genes encoding HER2, cyclin D1, K-ras, β -catenin, cyclin E and mutant B-Raf (15-20). Another pathway that is frequently deregulated, and to which tumours can be 'addicted' to, is the PI 3-kinase/Akt pathway, which I will discuss at a later point in this thesis.

Perhaps the most convincing evidence for targeting oncogene addiction is highlighted in clinical studies using molecular targeted therapies, such as Gleevec® (BCR-Abl target; chronic myeloid leukaemia) and Herceptin™ (HER2; breast cancer) (21-25). Some of the targeted therapies for the treatment of colorectal cancer will be discussed later in some detail (Chapter 1.5). I will now discuss current strategies for the treatment of colorectal cancer.

1.3 Treatment of colorectal cancer

Currently, treatment for colorectal cancer is dependent on stage of disease at presentation but consists primarily of surgical resection and chemotherapy. Surgery is the preferred option for primary tumours and regional lymph nodes, and is often curative. Unfortunately though, about 50% of patients, who undergo curative surgery for colorectal cancer, relapse with metastatic disease, usually within five years (26). The incidence of relapse is stage dependent with 20% of Dukes A, 30% of Dukes B and 50% of Dukes C patients will relapse. However, the incidence of metastatic disease can be reduced by giving those patients at high risk of recurrence adjuvant chemotherapy, to try to eliminate any micrometastatic deposits (27).

The vast majority of metastatic tumours are not resectable, and chemotherapy is therefore used to treat suitable patients. For more than 40 years the anti-metabolite 5-fluorouracil (5-FU) has been the frontline chemotherapeutic agent used in the treatment of advanced colorectal cancers. The mechanism of action of 5-FU has been well characterised in attempts to increase the efficacy of the drug. 5-FU acts by inhibiting thymidylate synthase (TS) and incorporating into DNA and RNA resulting in cell cycle arrest and apoptosis (28) (Figure 2). Understanding the mechanism of action has led to combinational therapies, for example with folinic acid (also known as leucovorin; LV), to improve the activity of 5-FU. The development of an orally available fluoropyrimidine, capecitabine has improved treatment administration greatly (28, 29). Capecitabine is a rapidly absorbed, prodrug that is metabolised by the liver to produce 5-FU by a three step process, the final of which is by thymidine synthase which is thought to be more active in tumour cells (Figure 2) (30, 31). Also, Capecitabine and its metabolites tend to be better tolerated and therefore offer significant advantages over standard 5-FU treatment (31). Increasingly, the third generation platinum

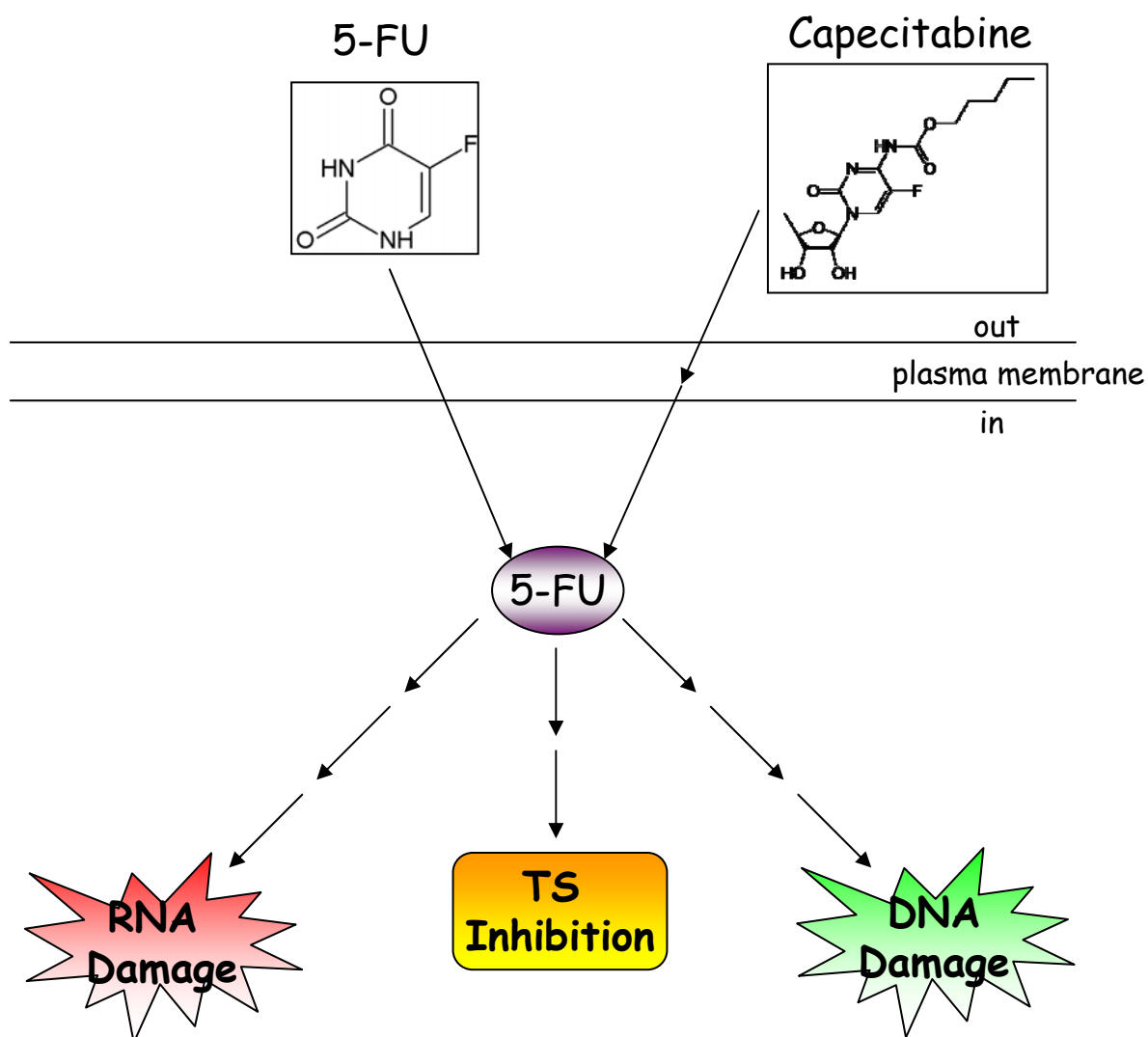


Figure 2. 5-Fluorouracil (5-FU) mechanism of action. 5-FU is an anti-metabolite that is readily absorbed by cells. The main mechanisms of action are the incorporation of its metabolites into either DNA or RNA thereby inducing damage responses as well as inhibition of thymidylate synthase (TS), which also results in DNA damage. Capecitabine is an orally available, pro-drug that is converted to 5-FU by a multistage process in both the liver and the target cells..

Figure adapted from Longley DB, Harkin DP, Johnston PG. (2003) *Nat. Rev Cancer* 3(5) ; 330-8

based compound oxaliplatin, is used in combination with 5-FU (or Capecitabine) and LV for the treatment of metastatic colorectal cancer (31). However, one of the major problems associated with colorectal cancer, is resistance, either natural or acquired, to chemotherapeutic agents, such as 5-FU and oxaliplatin (32).

1.4 Chemoresistance

Resistance to chemotherapeutic agents, such as 5-FU, limits the effectiveness of the current cancer treatments. The development of drug resistance causes approximately 90% of treatment failures in patients with metastatic cancer (28, 32). Also, drug-resistant micrometastatic tumour cells may contribute to decreased response to adjuvant chemotherapy. Resistance to chemotherapeutics, such as 5-FU, can be either natural (the cells have an inbuilt natural resistance to chemotherapy) or acquired, where the cells 'adapt' mechanisms to evade the effects of the chemotherapy agents (32). For example, 5-FU, resistance can occur by several mechanisms. Inhibition of TS by 5-FU acutely induces the expression of TS in both tumours and cell lines (33, 34). This induction may be due to inhibition of a negative feedback mechanism of TS binding to, and regulating, translation of its own mRNA (35). This is the case *in vivo* where increases in TS expression correlate with increased resistance to 5-FU (36, 37). Another mechanism of resistance is the overexpression of DPD (dihydropyrimidine dehydrogenase), which catabolises 5-FU to an inactive form, in 5-FU resistant cancer cell lines (38). Also, an alteration in DNA repair, namely a down-regulation of ERCC1 (excision repair cross-complementing 1) enzyme which prevents damage to DNA by nucleotide excision and repair, inversely correlates with survival and response in gastric cancer patients treated with 5-FU and oxaliplatin (39).

Therefore, there is now an impetus towards the generation of new, molecularly targeted therapies against proteins that are critical for the survival of the tumour cells, to help combat this disease, and which will be discussed in a later chapter (Chapter 1.9).

In order to test any potentially new therapeutic strategies to combat colorectal cancer, good cancer cell models are required. These include both cell-based, for example Fidler model of colorectal metastasis (40, 41), and animal-based models, such as the APC^{min} and APC^{flox} models (reviewed in (42)).

1.5 Cell-based models of colon cancer

Cell lines isolated from primary and metastatic tumours provide the main tool for research into the mechanisms involved in aspects of cancer, such as proliferation, evasion of apoptosis, and increased invasion and migration. Several cell lines that are routinely used to evaluate colorectal cancer are HT29, SW480 and SW620s. HT29s are an epithelial colorectal carcinoma cell line that can readily form tumour xenografts when injected subcutaneously into the hind region of nude mice (43-45). HT29 cells are frequently used to study the role of Src non-receptor tyrosine kinase, which shows increased expression and activity in colon cancer (46-48). Indeed, treatment of HT29 xenografts with either antisense oligonucleotides against Src (49) or treatment with a Src family inhibitor (43) inhibited the growth of these tumours. HT29 are also closely related to another cell line, WiDr (a human colorectal adenocarcinoma cell line) (50) and together these cell lines are useful tools for investigating cancer.

Other colon cancer cell lines frequently used are the SW480 and SW620s. SW480s are a colorectal adenocarcinoma cell line derived from a Dukes' stage B tumour (51). One year later, the SW620 cell line was isolated as a metastatic derivative of the SW480s, isolated from a lymph node metastasis in the same patient (51). Both SW480 and SW620 cells are

able to form tumour xenografts (52, 53) and in addition SW620 cells when injected into the caecum of nude mice, metastasise to the liver (54). As such, SW480 and SW620 cell lines are useful for studying genetic changes in late colon cancer progression. However, despite HT-29, WiDr, SW480 and SW620 cells being able to grow xenografts in nude mice, this method of *in vivo* analysis of tumour formation, and use as a model to test potential drug treatments, is not ideal. Genetically engineered animal-based models are far more useful tools for the study of colorectal cancer.

1.6 Animal-based models of colon cancer

The adenomatous polyposis coli (*APC*) gene is one of the best studied and perhaps one of the most important genes with respect to colorectal carcinogenesis. Germ line mutations in the *APC* gene results in the development of familial adenomatous polyposis (FAP) (55), which is one of the principal hereditary predispositions to colorectal cancer. Somatic mutations in the *APC* gene are also found in approximately 60% of sporadic colorectal adenomas and carcinomas (56).

One of the main functions of the APC protein is the inhibition of β -catenin, which is an essential component of mammalian cadherin adhesion complexes. β -catenin is also a downstream component of the Wnt signalling pathway and a key regulator of cell proliferation (42). Under unstimulated conditions, β -catenin is in a complex (termed ‘destruction complex’) which consists of scaffolding proteins axin and conductin, as well as glycogen synthase 3 β (GSK-3 β) and APC (Figure 3) (reviewed in (42, 57)). Whilst in a complex, GSK-3 β phosphorylates four critical Ser/Thr residues on the amino-terminus of β -catenin, thus targeting it for degradation by the proteasome (Figure 3)(58). In colorectal cancer, loss or mutation of APC results in constitutive activation of the Wnt/ β -catenin pathway, in the absence of external stimulation of Frizzled receptor. Loss or mutation of

APC suppresses GSK-3 β activity, resulting in decreased phospho- β -catenin, decreased degradative targeting and stabilisation of the protein (42, 59). β -catenin is then free to translocate to the nucleus, bind to DNA-binding proteins of the T-cell-factor (Tcf) family and initiate transcription of its target genes, such as *c-Myc* (60) and *cyclin D1* (61) (Figure 3; reviewed in (42, 59)).

APC also plays an important role in several other cellular processes such as cell adhesion (62, 63), migration (62, 64, 65) and chromosome segregation (66). However, its main function as a tumour suppressor is regulation of β -catenin levels (67). This function has been utilised in several mouse models of colorectal cancer where, truncated forms of APC are conditionally generated or the entire *APC* gene is selectively ‘deleted’. The best known of these models is the *APC*^{MIN} (multiple intestinal neoplasias) mouse. This transgenic mouse line was generated by random ethylnitrosourea mutagenesis and carries a nonsense mutation at codon 850 of the *APC* gene, generating a truncated (95kDa) APC polypeptide (68, 69). *APC*⁺/*APC*^{MIN} mice develop approximately 100 intestinal tumours per animal and mainly located in the upper gastro-intestinal (GI) tract over a period of approximately 100 days (68, 69).

Development of colorectal cancer is a multi-step process that can occur over long periods of time and the *APC*^{MIN} model is ideally suited to assess mutational events, caused in part by chromosome instability, that lead to the inactivation of the second, wild type allele in an *APC*⁺/*APC*^{MIN} mouse (reviewed in (42)). Another model, *APC*^{flox/flox}, is utilised to determine the immediate consequences of *APC* loss in normal, colonic epithelium (70). In this model, mice with lox-flanked *APC* alleles were crossed into a novel inducible *CRE* transgenic background, which uses a Cyp1A promoter to deliver inducible *CRE* expression in the intestine. Treatment of *CRE*⁺ *APC*^{flox/flox} mice with β -naphthoflavone for four consecutive days

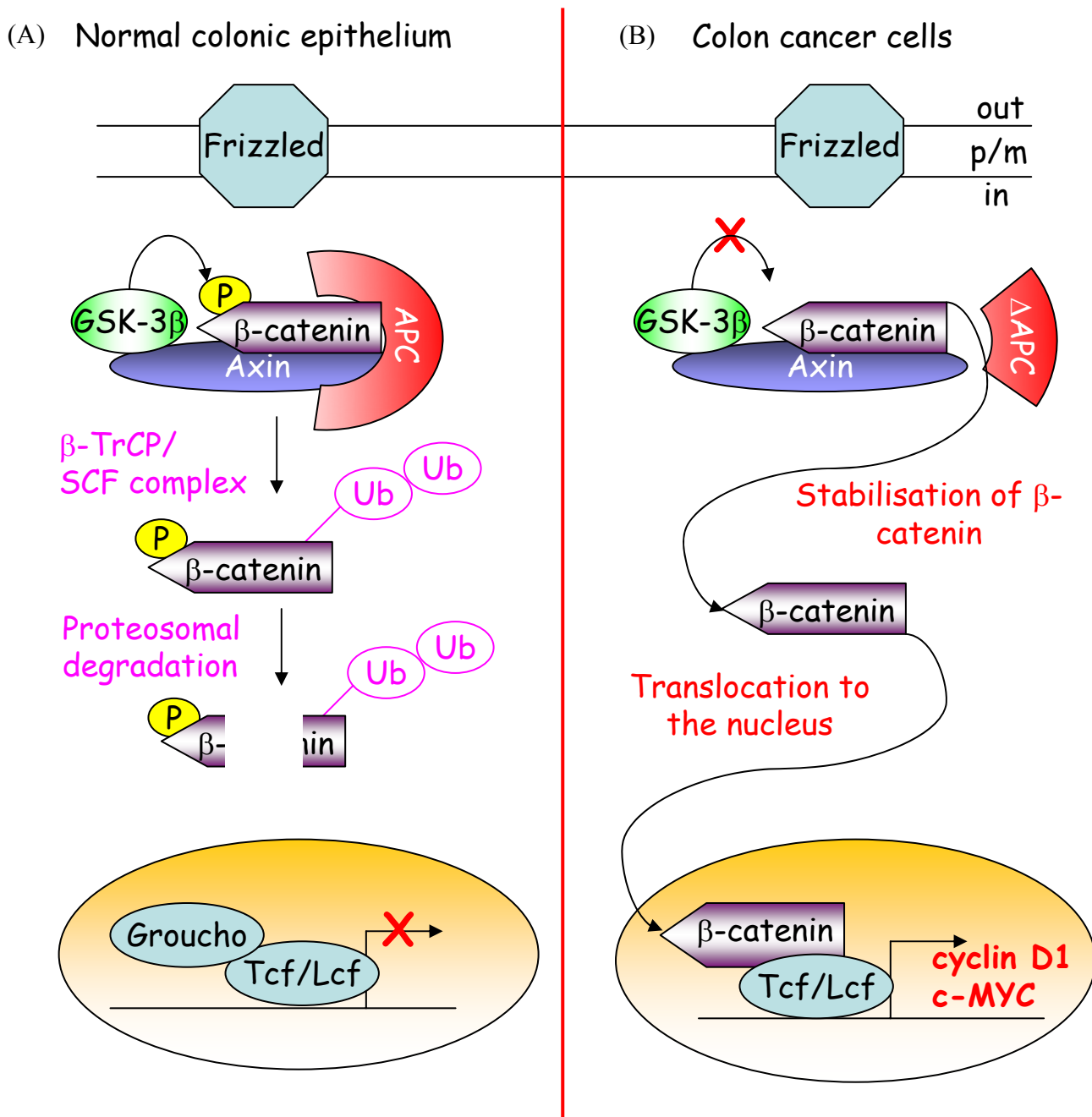


Figure 3. APC/ β -catenin pathway. (A) In normal unstimulated, colon epithelium β -catenin can be in a stable complex with Axin and adenomatous polyposis coli (APC) proteins. When present in this complex, GSK-3 β can phosphorylate β -catenin. This serves as a signal for the β -TRCP/SCF ubiquitin ligase complex. β -catenin is then poly-ubiquitinated and degraded by the 26S-proteasome, thereby preventing its accumulation in the nucleus. Its transcriptional cofactor Tcf/Lcf therefore remains bound to Groucho and no transcription is activated. (B) In colon cancer where APC is either mutated or lost (Δ APC above) β -catenin is no longer phosphorylated by GSK-3 β , is stabilised and is able to translocate to the nucleus. β -catenin can then accumulate and initiate transcription of target genes such as *c-MYC* and *cyclin D1*.

results in CRE recombinase expression and cleavage of the lox sites flanking the *APC* alleles and complete intestinal recombination and loss of *APC* (70). This leads to nuclear accumulation of β -catenin, increased *c-Myc* expression and perturbation of differentiation, migration, proliferation and apoptosis (Figure 3) (70). Therefore, the *APC*^{fllox/fllox} and *APC*^{MIN} mouse models of colorectal cancer are useful animal models for the study of both immediate/early and long-term effects of *APC* loss, which is a common occurrence in colorectal cancer.

However, in order to understand the molecular and biochemical events that regulate colon cancer proliferation and survival, as well as metastasis, a cell based system that also has applications in an *in vivo* setting would be advantageous. The Fidler mouse model of human colorectal metastasis provides just such a platform with which to do so.

1.7 Fidler model of human colorectal metastasis

The Fidler model cell lines were initially derived from a primary human colorectal carcinoma (HCC) designated as Dukes Stage B. These were established as a tissue culture cell line (KM12C). KM12C cells, when directly injected into the spleen of nude mice resulted in the generation of infrequent liver metastases (Figure 4 A). Isolation, re-culturing, expansion and injection of cells into the spleen from the few liver metastases that arose resulted in increased metastatic potential. This process was repeated a further two times (total of four successive rounds of culturing and injections), resulting in the highly metastatic KM12L4A cell line (Figure 4 B) (41). Also, the KM12C cells were used to generate another metastatic cell line, KM12SM, where the cells were injected into the cecum of nude mice to produce spontaneous hepatic metastases. The metastatic foci generated by this route were harvested as cell cultures and yielded the spontaneous metastasis (KM12SM) derivative of the KM12C cell line.

Thus, the Fidler model of colorectal metastasis provides an excellent platform for which the roles of specific pathways may be investigated in both the cells with relatively low-metastatic potential and the more metastatic derivatives.

1.8 Previous work using Fidler model of colorectal cancer cells

The expression and activity of the non-receptor tyrosine kinase Src is up-regulated in a number of tumour cell types including breast (71-73), ovary (74), lung (74, 75), head and neck (76) and colon (46-48) and is linked to the malignant potential of these tumours. Using the Fidler cells, Jones *et al* (77) showed that the expression and activity of Src were increased in the metastatic KM12L4A and KM12SM cells compared to the poorly-metastatic KM12C cells. Src kinase has been linked to the regulation of processes such as proliferation, migration, invasion and adhesion (reviewed in (78)). In HT-29 colon cancer cells, Src displays increased activity and expression. Using an anti-sense approach to knockdown Src expression suppresses HT-29 growth both *in vitro* and *in vivo* (49). However, in KM12C cells expression of a constitutively active form of Src, SrcY527F (KM12C/2C4 cells), where Tyrosine-527 (Tyr⁵²⁷) is mutated to a phenylalanine keeping Src in its 'open' and active conformation (reviewed in (78)), results in increased cell-matrix adhesion without any effect on proliferation (77).

Elevated Src kinase activity in KM12C cells also affects the regulation of the cell-cell junction protein, E-cadherin. Expression of SrcY527F in KM12C cells results in the internalisation of E-cadherin under high calcium conditions (79). Moreover, regulation of E-cadherin localisation by Src is dependent on its catalytic activity, as expression of Src lacking the kinase domain, but retaining its SH2 and SH3 domains, restores E-cadherin localisation to cell-cell junctions (79). In addition, Src induced de-regulation of cell-cell junctions requires adhesion to α_v and β_1 integrins, therefore blocking this interaction, using specific

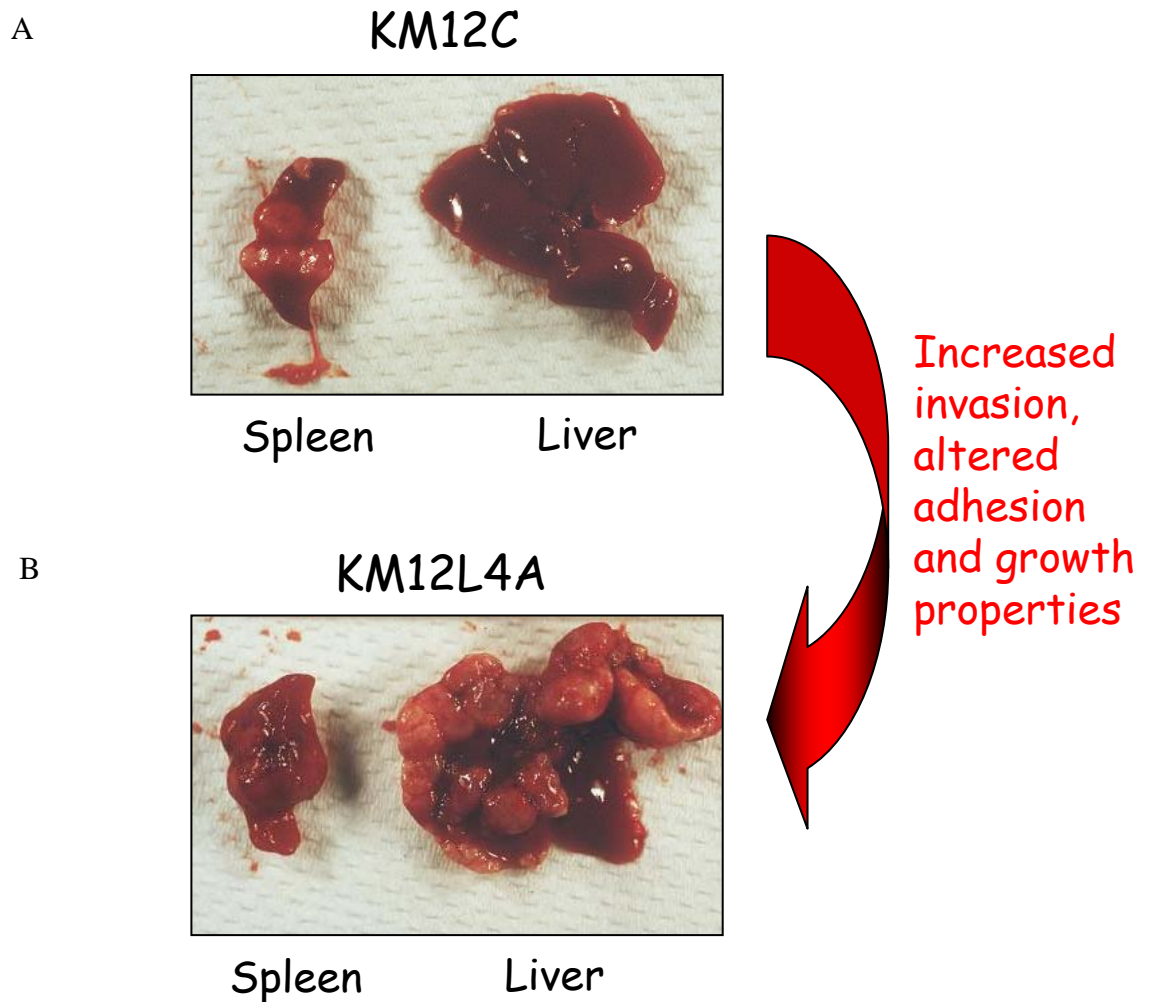


Figure 4. Fidler mouse model of human colorectal metastasis. (A) KM12C cells when injected into the spleen of nude mice produce few hepatic (liver) metastases. (B) KM12L4A cells were previously generated by four rounds of injection and sub-culturing KM12C cells that did produce liver metastases. The result of which is the highly metastatic KM12L4A cells that produce a high degree of liver metastases when injected into the spleens of nude mice. Photographs courtesy of R.J.Jones.

antibodies, prevents focal adhesion formation and causes de-localisation of E-cadherin (79). An important regulator of β_1 integrin downstream signalling is focal adhesion kinase (FAK). FAK is heavily phosphorylated by Src at multiple sites and the introduction of FAK mutated on all five tyrosine residues (FAK-Y407-925F) in KM12C/2C4 cells, restored the localisation of E-cadherin to cell-cell junctions, indicating that FAK is the major downstream substrate of Src and that it is required for cadherin-mediated junctions (79).

The altered cell morphology induced by active Src is consistent with an epithelial to mesenchymal (i.e. more migratory) phenotype and is accompanied by the expression of vimentin, a protein marker for mesenchymal cells (77, 80).

The epithelial to mesenchymal “switch” in KM12C/2C4 cells is dependent upon the activities of both ERK and its direct substrate MLCK (myosin light chain kinase). In KM12C cells, inhibition of either ERK or MLCK pathways results in reversion to an epithelial phenotype, with a loss of Src and integrin induced peripheral adhesion assembly and restoration of E-cadherin distribution to cell-cell junctions (80). The accumulation of the downstream target of MLCK, phospho-MLC (myosin light chain), at the cell periphery is dependent upon the SH2 (Src homology 2) and SH3 (Src homology 3) domains of Src as well as its kinase activity (80). In addition, mutation of either the SH2 or the SH3 domains results in the proper localisation of E-cadherin to cell-cell contacts (80). Thus, in KM12C cells, Src activity and its protein-protein interaction domains are important for the formation of integrin-adhesion structures and the redistribution of E-cadherin from cell-cell junctions.

The role of Src mediated phosphorylation of FAK and the effects on cell matrix adhesions has also been investigated in KM12C cells (81). Expression of kinase deficient Src mutants, namely SrcMF (full length Src with K295M (ATP binding site) and Y527F mutations) and Src251 (truncated Src minus the kinase domain), in KM12C cells did not alter proliferation

(81). However, phosphorylation of FAK (Tyr⁴⁰⁷, Tyr⁵⁷⁶, Tyr⁵⁷⁷ and Tyr⁸⁶¹) does increase and which are reported to be Src phosphorylation sites (81). Mutation of Src SH2 domain and use of a specific Src kinase inhibitor in cells expressing SrcMF showed that the increase in pTyr phosphorylation was dependent on an intact SH2 domain but independent of Src family (Src/Yes/Fin) kinase activity (81). Also, in cells expressing kinase defective Src, FAK phosphorylation on Tyr⁹²⁵ was reduced, indicating that this site was completely dependent upon the Src kinase activity (81). Moreover, reduced FAK (pTyr⁹²⁵) was associated with impaired extension and retraction of adhesions (81). Thus, based on evidence to date, Src's role in Fidler cells is to alter cell-matrix and cell-cell adhesions but does not alter their proliferation.

Other work carried out using Fidler cells include the analysis of expression patterns of approximately 1200 human genes in KM12C, KM12L4A and KM20 (a metastatic cell line derived from a Dukes stage D colon cancer tumour cells (41)) in order to identify alterations in genes that can contribute to the metastatic process. Of the 1,200 genes analysed by Hernandez *et al* (82), a greater than 3 fold alteration (either increase or decrease) in expression of genes associated with proliferation and survival was observed, including Zyxin (a gene implicated in regulating differentiation, proliferation and cell morphology), FRP1 (a member of the Phosphatidylinositol-related kinase family which controls cell cycle progression in the presence of DNA damage) and TRAIL (a member of the tumour necrosis family of protein that induces death of T-cells via apoptosis) (82). Proteins involved in the negative regulation of proliferation associated genes, such as the 26S proteasome, were found to be down regulated in the highly metastatic KM20 cells, compared to the KM12C and KM12L4A cells (82). Gene expression profiles, comparing the poorly-metastatic and metastatic Fidler cell lines have shown numerous alterations between the cell types (83, 84).

Perhaps one of the underlying causes of the changes associated with these cell lines is their genetic instability.

Two forms of genetic instability have been described in colorectal cancers: microsatellite instability (MSI) and chromosomal instability (CIN) (85). Microsatellites are short stretches of DNA repeats that vary from person to person and defects in DNA mismatch repair can give rise to microsatellite instability (85). In colon cancer, approximately 15% of tumours display microsatellite instability which contributes to colorectal carcinogenesis (86, 87). Camps *et al* have shown that KM12C cells have a near-diploid karyotype with high levels of chromosome instability and microsatellite instability, whereas the KM12L4A and KM12SM cells have polyploid karyotypes as well as chromosome and microsatellite instability (88).

Microsatellite instability also affects responses to 5-FU treatment, where patients who have high microsatellite instability tumours have a better response than those with microsatellite stable tumours (89-91). However, there are conflicting reports suggesting that MSI status does not correlate with prolonged survival after 5-FU treatment (92-94). Treatment of KM12C cells, which have high MSI, resulted in decreased proliferation (95). However, injection of KM12C cells into the spleens of nude mice and subsequent treatment with 5-FU had no effect on primary tumour formation, invasion or metastasis (95).

Overall, the genetic instability and alterations in the numerous pathways between the low-metastatic KM12C cells and the more highly metastatic KM12SM and KM12L4A cells, strongly reflects the alterations that are common in other human cancers. Historically, work in our lab has focused on the role of both Src and FAK tyrosine kinases in these cell lines. The work in my thesis will use the Fidler model cells to investigate novel approaches to inhibit the proliferation of chemoresistant colorectal cancer cells and, in particular, will focus on modulation of cyclic nucleotide signalling pathways. However, before discussing how

cyclic nucleotide signalling is perturbed in cancer and how these pathways might be exploited, I will discuss current the molecular targeted therapies that are now either approved, or in clinical trials, for the treatment of colorectal cancer.

1.9 New strategies: Molecular targeted therapies

Targeted therapies are classed into two distinct categories – monoclonal antibodies and small molecule inhibitors. Currently, there are two new promising strategies for the treatment of advanced colorectal carcinomas – epidermal growth factor receptor (EGFR) and vascular epidermal growth factor (VEGF) inhibitors, both of which have FDA approval for use in the treatment of colon cancer.

Aberrant signalling in cancer cells occurs during the development and progression of the disease. Considerable efforts in developing ‘targeted’ therapies, directed against specific components of these pathways that are hopefully more potent and less toxic than conventional chemotherapy are currently underway. The receptor tyrosine kinase (RTK) EGFR is frequently up-regulated in colorectal cancer (in 70-80% of cases (96, 97)) and can increase cell proliferation, invasion and metastasis of cancer cells (98). For those reasons it has become a target for new agents. Two monoclonal antibody therapies, namely Cetuximab (Erbix[®]; ImClone Systems/Bristol-Myers Squibb) and Panitumumab (Vectibix[™]; Amgen), have been developed as specific EGFR inhibitors (98-100). Both antibodies can bind and block the extracellular ligand binding domain of EGFR and prevent activation and downstream signalling (98-100). Clinical trials using both antibodies have shown good response rates, both alone and in combination with other frontline treatments for colorectal cancer. Patients treated with cetuximab and irinotecan (topoisomerase I inhibitor) had an objective response rate (proportion of patients who have either a partial response or a complete response) of approximately 23% and those receiving cetuximab alone had an objective response rate of approximately 11% (101). Out of a panel of 463 patients with

metastatic colorectal carcinoma, all expressing EGFR, treatment with panitumumab resulted in a statistically significant increase in progression free survival compared to those receiving best supportive treatment (not specified) alone (102). The overall response rate of patients to panitumumab was 8% but there was not an increase in overall survival of the patients (102). As well as monoclonal antibodies directed against the extracellular domain of EGFR, small molecule inhibitors of the kinase domain have been approved for the treatment cancer, and in particular, NSCLC (Non-Small Cell Lung Cancer) which approximately 50% of NSCLC is positive for EGFR (reviewed in(103)). Gefitinib (Iressa; AstraZeneca) and erlotinib (Tarceva®; OSI Pharmaceuticals) are two small molecule EGFR inhibitors approved for treatment of NSCLC in patients who have failed to respond to conventional chemotherapy (104). Both act as reversible, competitive inhibitors of ATP-binding at the active site of the EGFR kinase domain (105). However, sensitivity to these molecules correlates to a subset of patients with somatic gain-of-function mutations in EGFR (located in the kinase domain of the protein) and EGFR overexpression, with 77% of clinical responders harbouring alterations in EGFR, compared to approximately 7% of patients with NSCLC that are refractory to gefitinib or erlotinib (106-109).

The development of new blood vessels – angiogenesis – from pre-existing vasculature is a key process in normal tissue development but is also one of the hallmarks of cancer (8, 110). In order for a tumour to grow beyond a certain size, it requires a network of blood vessels to supply both oxygen and nutrients and to remove waste products, all of which are crucial for cell function and survival. One potent stimulator of angiogenesis is vascular endothelial growth factor (VEGF) and its cognate receptors, VEGF-receptor 1 (VEGFR1) and VEGFR2, all of which are frequently altered in colorectal cancer (110) and the angiogenic pathway has therefore become a key target in drug development. One of the first reports supporting anti-angiogenic treatments for cancer came from Kim *et al*, where they showed that an antibody

directed against VEGF inhibits angiogenesis and also suppress tumour growth *in vivo* (111). Bevacizumab (Avastin®; Genentech), a monoclonal antibody which binds VEGF and prevents its interaction with VEGFR1 and VEGFR2, has now been approved for first-line treatment of metastatic colon cancer in the US (110). In a clinical study with 813 patients, of which approximately 50% received Bevacizumab in combination with fluorouracil-based chemotherapeutic agents, like 5-FU, resulted in a statistically significant, and clinically meaningful, improvement in survival amongst patients with metastatic colorectal cancer (112). In addition, on-going studies into using Bevacizumab in an adjuvant therapy setting, in combination with other chemotherapeutics, may provide better survival and decreased metastatic disease in patients (113, 114).

Above, I have described two target therapies for the treatment of colorectal cancer. However, there are a number of other promising therapies that target other important pathways for tumour development. For example, matrix metalloproteases (MMPs) have been extensively studied in colorectal cancers and are believed to be key regulators of the invasive aspects of the metastatic process (reviewed in (115)). As such, orally available MMP inhibitors have shown considerable success in phase I/II trials (reviewed in (115)). However, a phase III trial of the BAY-129566 (broad spectrum MMP inhibitor) was terminated due to a lower survival rate of patients treated with the compound (116).

Chronic inflammation of the intestine is closely linked to colorectal cancer and patients with ulcerative colitis and familial adenomatous polyposis (FAP) which are both high risk conditions for the future development colorectal cancer (117, 118). Two potent stimulators of chronic inflammation are the cyclooxygenases Cox1 and Cox2 and are critical regulators of prostaglandin production which has been linked to the progression of colorectal cancer (118). Early studies identified elevated Cox2 expression was present in approximately 85% of human colorectal carcinomas and approximately 50% of colorectal adenomas (119-121).

Non-steroidal anti-inflammatory drugs (NSAIDs) are inhibitors of Cox1 and Cox2 and include both aspirin and ibuprofen and have been proposed as chemo-preventative agents (118). However, it is Cox2 appears to regulate inflammation and mitogenesis whereas Cox1 is associated with the production of cytoprotective prostaglandins in the gastrointestinal tract (122). Thus, NSAIDs targeted to Cox2 have been attributed to the anti-inflammatory effects of the drugs (122). Selective Cox2 inhibitors that have been developed include celecoxib (Searle/Pharmacia/Pfizer), rofecoxib (Merck), and valdecoxib (Pharmacia/Pfizer), all of which have been approved for use in the management of pain and inflammation (118).

Evidence for the involvement of Cox2 and therefore the use of specific inhibitors and NSAIDs in the treatment of colorectal cancer comes from a variety of animal model studies. Studies using a genetically engineered mouse expressing a targeted, truncated form of the APC tumour suppressor gene, APC^{Δ716}, showed that in the background of *Cox2*^{-/-} mice, both the number and size of intestinal polyps was reduced compared to the *Cox2*^{+/+} wild type mice (123). Also, treatment of APC^{Δ716}/*Cox2*^{+/+} mice with a Cox2 specific inhibitor resulted in a reduction in the number of polyps, compared to a NSAID which inhibited both Cox1 and Cox2 (123). However, therapeutic potential for the treatment of colorectal cancer is currently limited due to long term treatment of patients with selective Cox inhibitors resulting in adverse cardiovascular and thrombotic effects (118, 124-126).

It is also important to consider other signalling pathways that may be utilised in order to develop new therapeutic strategies to combat colorectal cancer. I will now discuss cyclic nucleotide signalling, its role in cancers of varying origin and its potential as a therapeutic strategy for the treatment of cancer.

1.10 Cyclic nucleotide signalling

Second messenger signalling, namely the generation of adenosine 3',5'-cyclic monophosphate (cyclic AMP; cAMP) or guanosine 3',5'-cyclic monophosphate (cyclic GMP; cGMP) has been investigated for over 50 years. This has provided key insights into signal transduction networks, including receptor-effector coupling, protein kinase cascades and down-regulation of drug responsiveness.

Cyclic nucleotide signalling is an important regulator of many cellular processes such as proliferation, migration, metabolism, growth and apoptosis, all of which can be altered in cancer.

1.11 cAMP 2nd messenger signalling

Research into hormone-receptor interactions and subsequent generation of intracellular second messengers, transducing extracellular signal into an intracellular response, has been central to our understanding of hormone action for several decades now. The generation and degradation of cAMP were previously thought to be confined to membrane fractions (127, 128). Generation of cAMP is achieved by the stimulation of G-protein coupled receptors (GPCRs) by hormones, such as adrenaline and prostaglandins, as well as many others. This in turn activates the stimulatory $G\alpha_s$ protein (by GDP-GTP exchange) and activated $G\alpha_s$ ($G\alpha_s$ -GTP) dissociates from the $G\beta\gamma$ subunits, then interacts and activates adenylyl cyclase (AC), leading to the generation of cAMP from ATP (Figure 5 and reviewed in (129)).

cAMP can elicit a diverse range of cellular processes with both short and long term consequences for cells. These include proliferation, migration, differentiation, neurotransmission, metabolism, growth and transcription (Figure 5) (130, 131). Transduction of intracellular cAMP into a cellular response can be achieved by effectors

such as the cAMP dependent protein kinase, PKA (Protein Kinase A;) (131), cAMP dependent guanine nucleotide exchange factor (cAMP-GEFs; or Epac (Exchange protein directly activated by cAMP)), which regulates the small GTPase Rap 1 (132, 133), or cAMP gated ion channels (Figure 5; (130)).

The action of cAMP specific phosphodiesterases (PDEs), which hydrolyses 3',5'-cyclic adenosine monophosphate to the inactive 5'-adenosine monophosphate (AMP), provides the sole route of degradation and can act as the 'off switch' for this signalling pathway (131, 134-136). Generation of specificity within cAMP signalling is achieved by partnering multiple components of the pathway that regulates the binding of hormones (GPCRs), intracellular transducers (G-proteins), cAMP generation enzymes (adenylyl cyclase) and cAMP degradation enzymes (PDEs). For example, there are approximately 335 7-trans-membrane GPCR receptors, 20 G-protein α subunits, 10 adenylyl cyclases and 11 PDE families. Eight of the PDE families can generate over 30 different isoforms with the ability to hydrolyse cAMP (131, 134-136). The sheer complexity of this system gives rise to almost unlimited combinatorial potential, which in turn, allows the cells to tailor their cAMP generation in a spatial and temporally regulated manner with a specific outcome. This is achieved by compartmentalisation of cAMP signalling.

1.12 Compartmentalisation of cAMP signalling

cAMP signalling controls a diverse range of signalling processes, and in order to do so it must activate or inhibit specific intracellular pathways. This is achieved by compartmentalisation of cAMP signalling, where stimulation of cAMP generation (by a specific receptor and/or adenylyl cyclase enzyme) is coupled to selective activation of cAMP effectors (such as PKA and Epac) (137). The concept of compartmentalised cAMP effects was first proposed nearly 30 years ago when it was shown that different Gs coupled GPCRs

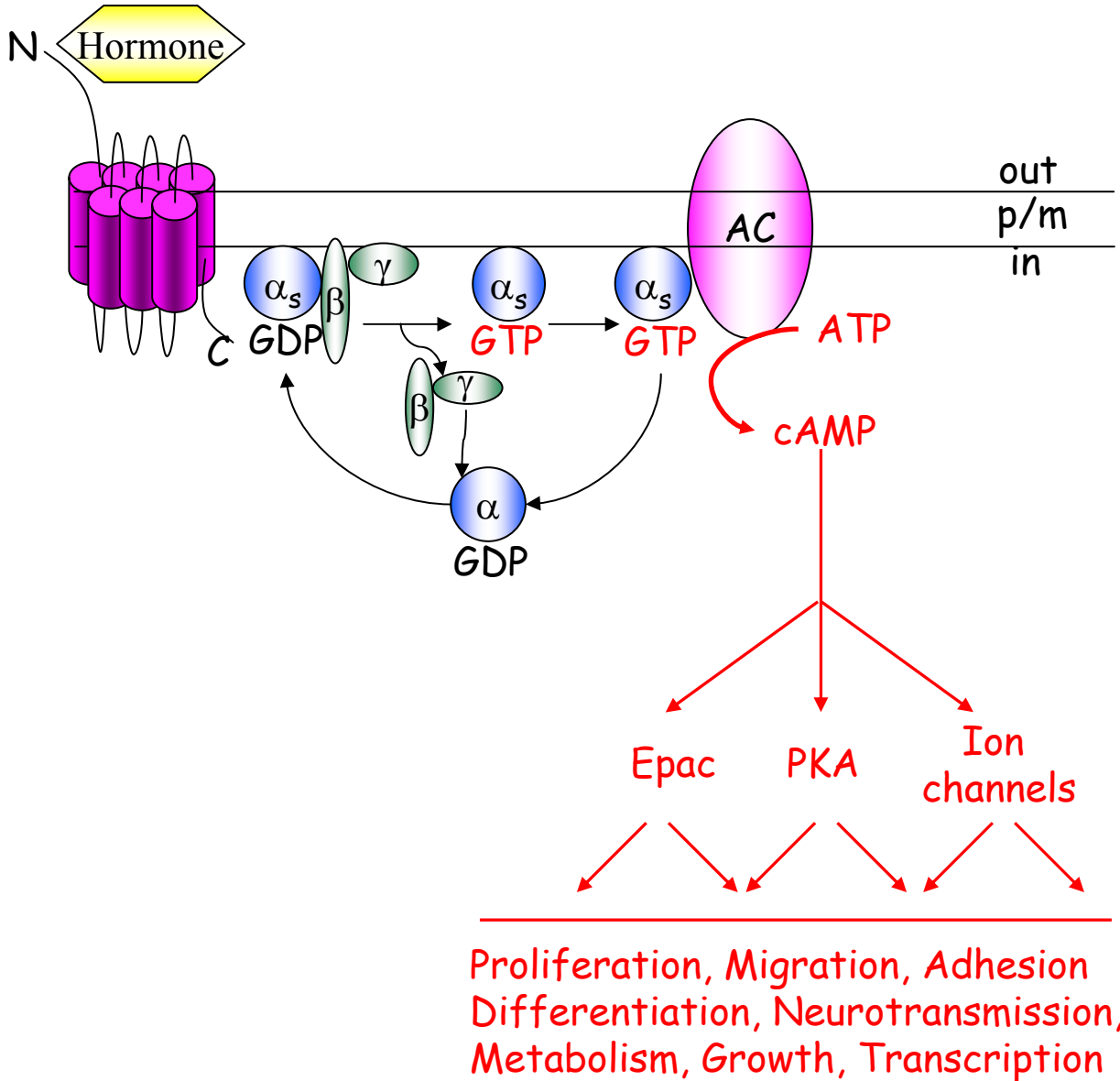


Figure 5. cAMP generation. Stimulation of a G-protein coupled receptor (GPCR) by a hormone results in a conformational change and the activation of G-proteins. G-proteins are heterotrimeric and upon stimulation, the G α_s subunit becomes activated by GDP/GTP exchange. G α_s subsequently dissociates from the regulatory G $\beta\gamma$ subunits (which can themselves activate other signalling pathways) and activates adenylyl cyclase (AC) to generate cyclic AMP (cAMP) from ATP. cAMP can then activate downstream effectors of the pathway, such as protein kinase A (PKA), Epac or cAMP gated ion channels which can elicit a diverse range of cellular processes. Switching off adenylyl cyclase is achieved by stimulation of G α_s intrinsic GTP hydrolysis, where the G α_s can then re-associate with the G $\beta\gamma$ subunits.

could selectively activate different isoforms of PKA in cardiac myocytes (138, 139). This then lead to the concept of PKA ‘sampling’ localised pools of cAMP (140-142). This can be achieved by tethering cAMP effectors to distinct sub-cellular locations, thereby positioning specific enzymes, for example PKA, to respond to local increases in cAMP concentrations. Proteins such as AKAPs (A-kinase anchoring proteins) are known to serve such a function (143). There are numerous other scaffolding proteins, some of which will be mentioned throughout this thesis, that serve to localise cAMP effectors, including RACK1 (144, 145), β -arrestin (137) and IQGAP1 (146).

The cAMP pathways, particularly at the level of PDEs, have become a key therapeutic target for many disease areas and, as such, inhibitors of PDE families are currently at various stages of clinical trials. In regards to developing a novel cancer treatment, components of the cAMP regulatory pathway may be perturbed in the malignant phenotype. Here I will discuss cAMP generators, effectors and degradation machinery, aspects of their regulation and how they are perturbed in cancer.

1.13 GPCR signalling and cancer

G-protein coupled receptors play vital roles in the regulation of a variety of biological and physiological functions. Numerous studies have shown that mutations or polymorphisms in GPCRs can result in a variety of human diseases or disorders (147-149). One of the first GPCRs with oncogenic properties was defined as the MAS oncoprotein, which is a GPCR which can transform NIH3T3 mouse fibroblast cells (150). The ability of *MAS* to transform these cells was attributed to over-expression of the oncoprotein, due to rearrangements in its 5' non-coding sequences.

Overexpression of GPCRs in cancer is commonly observed with many GPCRs over expressed in a variety of cancer types, which contribute to tumour cell growth after ligand

activation. Amongst these are the receptors for bioactive lipids, such as LPA (lysophosphatidic acid), and also the protease activated receptors (PARs). However, PAR receptors couple to the α_q , $\alpha_{12/13}$, α_i families of G-proteins, and not to the α_s family, stimulating a diverse signalling network, but not cAMP production (151). The PAR1 receptor is overexpressed or deregulated in a variety of human malignancies, including invasive breast carcinomas (152). In HNSCC (Head and Neck Squamous Cell Carcinoma) thrombin cleavage of PAR1 stimulates the growth and invasion of these cells (153) and PAR1 expression is also increased in advanced prostate cancer (154).

In colorectal cancer, several GPCRs and their ligands are linked to growth, survival, metastatic and angiogenic pathways. For example, prostaglandins, which are a product of the cyclooxygenases Cox1 and Cox2, provide a strong link between inflammation and cancer (118). The overexpression of Cox2, in conjunction with chronic inflammation, is now thought to play an important role in tumour development. The Cox2 regulated prostaglandin E2 (PGE2), as well as its cognate GPCRs, EP1-EP4, have all been linked to colorectal cancer progression (155-157). Of the PGE2 receptors, EP2 and EP4 have the most prominent roles in colon cancer and both are coupled to $G\alpha_s$, thereby stimulating cAMP production and accumulation (155). However, the main mechanism by which PGE2 exerts its oncogenic effects is through the stimulation of the APC/ β -catenin pathway (7, 57). In colon cancer cells, PGE2/EP2 stimulation of the β -catenin pathway, involves the G-protein subunits $G\alpha_s$ and $G\beta\gamma$. PGE2 causes $G\alpha_s$ association with the RGS (regulator of G protein signaling) domain of axin, thereby releasing GSK-3 β from the complex (158). PGE2 also causes release of the $G\beta\gamma$ subunits which activates the PI 3-kinase/Akt pathway and inhibits GSK-3 β released by axin by Akt mediated phosphorylation (158). Therefore, GSK-3 β can no

longer phosphorylate and inhibit β -catenin, allowing translocation to the nucleus and activation of target genes resulting in increased proliferation of the tumour cells (158).

As one of the major effectors of GPCR signalling, G-proteins have been linked with oncogenic transformation. In thyroid tissues, cAMP generation can stimulate cell proliferation. Mutationally-activated forms of $G\alpha_s$ (encoded by the *GSP* oncogene) are found in neoplastic growths in the thyroid tissue (159). The *GSP* oncogene encodes a protein that is mutated in the GTP hydrolysing domain, resulting in reduced GTP hydrolysis (approximately 30 times less than wild type $G\alpha_s$), thus effectively rendering the protein constitutively active (159, 160). $G\alpha_s$ activating mutations are found in approximately 40% of sporadic and growth-hormone secreting, pituitary tumours (159, 160).

All of the above alterations in GPCR/G-protein signalling can confer a 'high' activity status on the adenylyl cyclase molecule, where the basal production of cAMP is elevated.

1.14 cAMP effectors: Protein kinase A

The cAMP dependent protein kinase A (PKA) is the cAMP effector by which the vast majority of cAMP downstream signalling effects are thought to occur. In its inactive form, PKA is a heterotetramer of two regulatory (R) and two catalytic (C) subunits. Each subunit has multiple isoforms with 4 regulatory (RI_α , RI_β , RII_α and RII_β) and 3 catalytic (C_α , C_β , C_γ) subunits. This produces different isoforms of PKA holoenzymes with distinct physical and biological properties in the cell (161, 162). cAMP binds co-operatively to two sites termed A and B on each regulatory subunit (Figure 6). In the inactive holoenzymes, only the B-site is exposed and available for cAMP binding. When occupied, this enhances the binding of cAMP to the A site by an intramolecular steric change. The binding of a total of four molecules of cAMP results in a conformational change and dissociation of the catalytic subunits from the regulatory subunits (Figure 6) (reviewed in (161, 163, 164)). This release

of a molecular constraint on the catalytic subunits results in activation and subsequent phosphorylation of downstream targets on serine/threonine residues in a consensus motif (reviewed in (161, 163, 164)). The PKA consensus phosphorylation sites consists of R-R-X-S/T (Arginine-Arginine-X(any)-Serine/Threonine) and has been found in a plethora of targets that include regulators of cAMP signalling like the β_2 -Adrenergic receptor(165, 166), PDE4D3(167, 168)), Raf-1(169, 170), CREB (cAMP responsive element binding protein) transcription factor (171), regulators of apoptosis (BAD(172-174)) and the PI3-kinase p85 α regulatory subunit (175, 176).

The protein kinase A holoenzyme can be classified as either Type I or Type II depending on the association of either homo- or heterodimers of the R subunits, yielding holoenzyme complexes of PKA with distinct regulatory properties (Figure 6). Type I PKA contains either the regulatory subunits RI α or RI β ; Type II contains either RII α or RII β (162, 177, 178). Due to the significantly large number of PKA phosphorylation targets, several mechanisms are used to generate specificity and spatial/temporal activation of PKA. For example, the R subunits exhibit different binding affinities for cAMP, giving rise to PKA holoenzymes that require different thresholds of cAMP for activation (for type I 50-100nM cAMP; type II 200-400nM cAMP) (179). In addition, the R subunits are differentially expressed in cells and tissues and are able to form both homo- and heterodimers, thus generating a huge number of combinations, which further contributes to the compartmentalisation and specificity of cAMP signalling that can help generate a plethora of cellular outcomes.

Another mechanism, by which PKA activation is controlled, is by its spatial localisation. Sub-cellular localisation of PKA is controlled, at least in part, by anchoring of the R subunits by AKAPs (Figure 6). PKA type I is soluble and located in the cytoplasm, but conversely PKA type II is typically particulate and associated with sub-cellular structures and

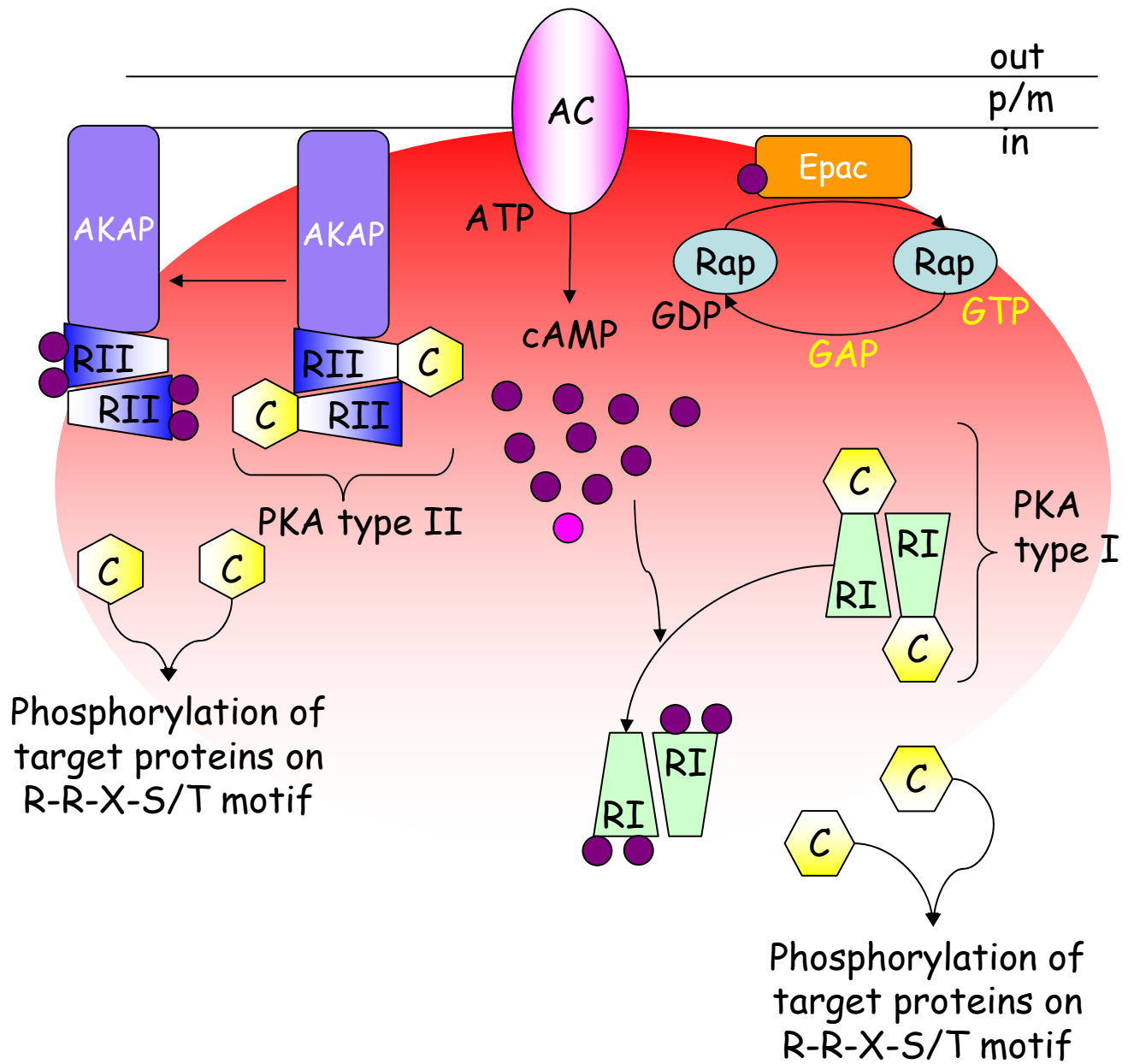


Figure 6. cAMP effectors. cAMP (purple circles) generation by adenylyl cyclase can diffuse (red area) until it encounters effectors, such as PKA-type I and –type II and Epac. Both PKA types exist as heterotetramers and each regulatory (R) subunits can bind two molecules of cAMP. Upon cAMP binding, the catalytic (C) subunits are released and can phosphorylate target substrates on RRXS/T motifs. PKA-type I is localised to the cytoplasm and type II is anchored to sub-cellular structures via interaction with AKAP scaffold proteins. Epac can bind one molecule of cAMP and catalyse the GDP-GTP exchange on Rap1, which is then free to activate downstream pathways.

compartments, being anchored by cell- and tissue-specific AKAPs (Figure 6; reviewed in (161)). AKAPs were originally identified due to the fact that they were contaminating purified PKA preparations (180-182).

Therefore, it is by a combination of differential expression, sub-cellular localisation and proximity to its substrates that cAMP activated PKA can act as an efficient and specific effector of cAMP signalling.

1.15 cAMP effectors: Epac

Early studies looking at the downstream effects of cAMP, attributed most of these effects to that of PKA. However, within the past 10 years another cAMP effector molecule has been identified. Epac (exchange protein activated by cAMP) proteins were first identified in 1998 during a database search of cAMP effectors and a screen of brain tissue for proteins containing second messenger binding motifs (132, 133, 183). Epac proteins, Epac1 and Epac2, are cAMP dependent Guanine Nucleotide Exchange Factors (GEFs) that activate the small GTPase proteins Rap1 and Rap2 (members of the Ras family) (Figure 6).

Epac1 and 2 are multi-domain proteins which consist of an amino-terminal regulatory region and a carboxy-terminal catalytic region; Epac2 has an additional cyclic nucleotide-binding domain (CNB) (Figure 7). X-ray crystallographic structure of Epac, in the absence of cAMP, has revealed that Epac2 exists in a compact structure in which the Rap binding site is completely hidden (Figure 7)(184). The 'open' conformation of Epac, in which cAMP is bound, has not yet been solved. However, binding of cAMP molecules to specific cAMP-binding pockets may induce a conformational change that disrupts an 'ionic latch' and re-orientates the second CNB domain towards the switchboard region (a β -sheet located in between the regulatory and catalytic regions), enabling the binding of Rap (Figure 7)(184).

Despite there not being any structural data available, the development of a fluorescence resonance energy transfer (FRET) probe of Epac, containing an amino-terminal cyan fluorescent protein (CFP) and a carboxy-terminal yellow fluorescent protein (YFP; CFP-Epac-YFP), supports the concept of cAMP 'opening-up' Epac (185).

1.16 Downstream effects of Epac activation

Activation of Epac by cAMP results in the stimulation of Rap1 or Rap2 the small GTPase proteins. Rap was originally identified as a small GTPase that could induce morphological reversion of Ras transformed cells (originally named Kirsten-ras-reverent-1; Krev-1 (186)). However, more recently Rap1s role in regulating integrin-mediated cell adhesion and E-cadherin mediated cell junction formation has received a lot of attention (187). This is due to the development of specific Epac activators that displays greater selectivity towards Epac, compared to PKA (188). The Epac specific agonist, 8-CPT (8-pCPT-2'OMe-cAMP), was developed by comparing the cAMP binding domains of several proteins including Epac1, Epac2 and PKA regulatory subunits. Epac proteins lack a critical and highly conserved glutamate residue present in all PKA isoforms and cAMP gated ion channels, and which forms high-affinity hydrogen bonds between the 2'-hydroxyl of the cAMP ribose group and PKA (189). Thus, a number of candidate compounds were synthesised and tested, and 8-CPT was selected due to its 10-fold better at activating Epac than cAMP alone (188). Also, another Epac agonist, 8-pMeOPT (8-pMeOPT-2'-O-Me-cAMP) is reported to have increased membrane permeability, increased PDE stability and increased Epac activating abilities (190, 191).

In Ovar3 cells, stimulation of Epac with 8-CPT results in increased β 1-integrin mediated adhesion to fibronectin coated dishes (192). Also, activation of Epac/Rap1 in epithelial cells results in adhesion to Laminin-5 by $\alpha_3\beta_1$ integrins, and which this interaction has been

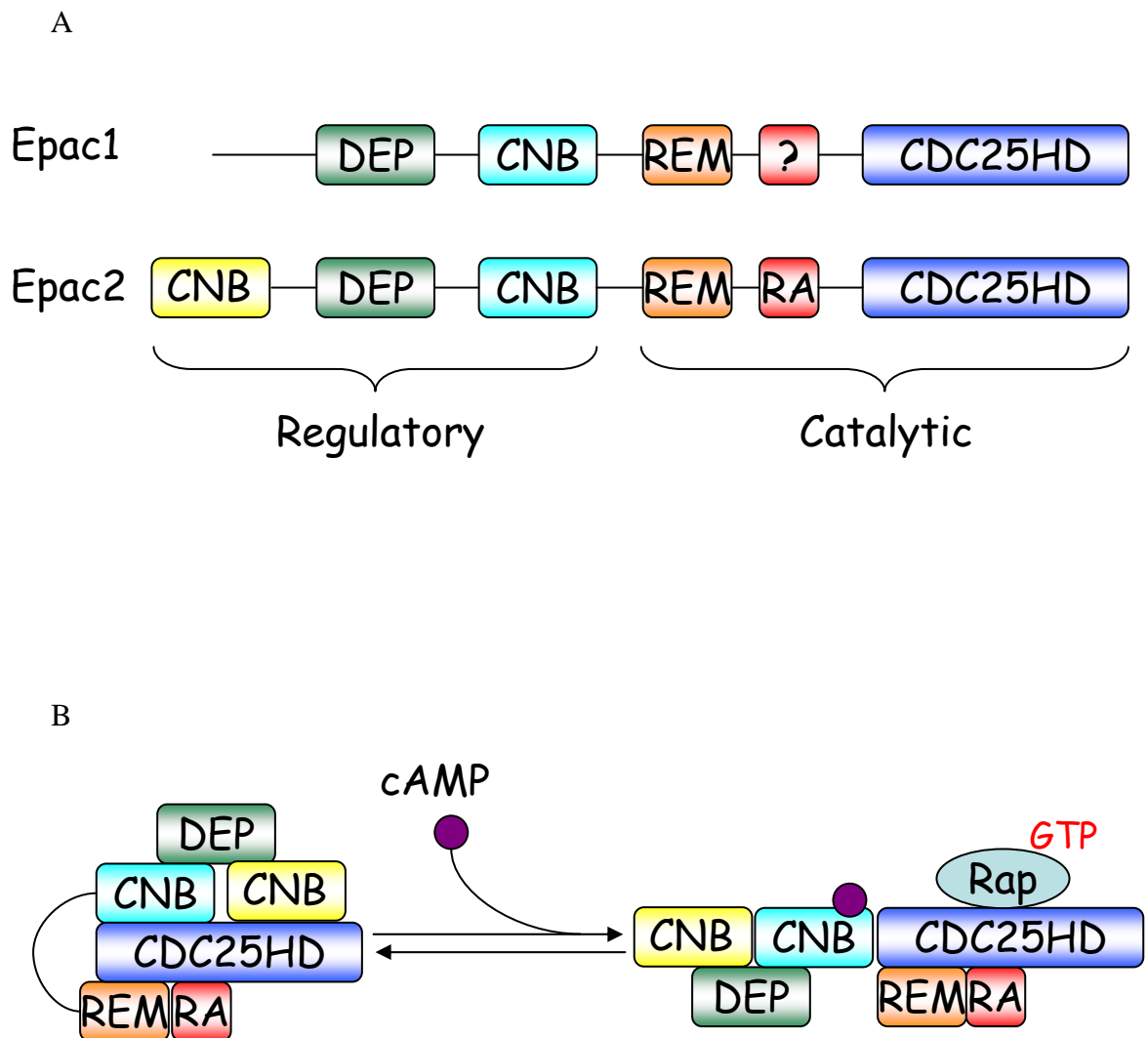


Figure 7. Epac domain structure and regulation. (A) The domain structure of Epac1 and Epac2 indicating the cyclic nucleotide binding domains (CNB), catalytic region with the CDC25 homology domain (CDC25HD) which is responsible for guanine-nucleotide-exchange activity. The DEP (Desheveled-Egl-10-pleckstrin (DEP) domain that is involved in membrane localisation; the Ras exchange motif (REM) which stabilises the catalytic helix of CDC25HD and the Ras-association domain (RA). (?) domain in a domain that is homologous to Epac2 RA domain but serves an unknown function. (B) Activation of Epac (shown for Epac2) by cAMP results in the opening of the protein, interaction with, and activation of, Rap.

implicated in epithelial wound repair and carcinoma invasion (193). Epac/Rap1 activation also promotes decreased cell permeability and increased VE-cadherin-dependent cell adhesion independently of PKA activity (194).

Rap1 is both a positive and negative regulator of the mitogenic Ras/Raf (B-Raf) /MEK/ERK pathway, in a cell type specific manner and binds the serine/threonine kinase Raf-1 *in vitro* and can inhibit downstream signalling(195-197). Using an activated form of Rap, RapV12, that is insensitive to GAP (GTPase activating protein) activity, ERK activation by either LPA or EGF (epidermal growth factor) was diminished but Ras activation was unaffected by RapV12 in Rat-1 fibroblasts (198). However, in another study using a number of different fibroblast cell lines and a number of different stimuli (platelet derived growth factor (PDGF), EGF, LPA, thrombin and endothelin and insulin) activation of Rap1 did not alter ERK activation, indicating that Rap1 activation is a common event but Rap1 function is not the modulation of Ras effector signalling and are possibly cell type specific (199).

In vitro, Rap1 is implicated in the activation of the ERK pathway via binding to, and activation of, B-Raf (200). In PC12 rat neuroendocrine tumour cells, activation of Rap1 results in Rap1 binding to, and activating, B-Raf and ERK signalling, causing differentiation of these cells (201, 202). Also, use of Rap1 inhibitors (Rap1GAP and RapN17 (dominant negative form of Rap)) completely abolishes B-Raf activation of ERK (201, 202). However, activation of Rap1 by Epac does not activate the ERK pathway in PC12 cells, due to differential localisation, with Epac normally present in the perinuclear region (203). Addition of a CAAX motif to Epac, which causes a translocation to the plasma membrane, results in cAMP/Rap1/B-Raf dependent activation of ERK, whereas wild type Epac cannot activate ERK in this fashion (203). Also, antisense depletion of C3G (Crk SH3 domain guanine nucleotide exchange factor), showed that C3G was responsible for cAMP activation

of Rap1, association with B-Raf and ERK activation in Epac wild type cells (203). Despite evidence of Rap1 regulation of the Ras/Raf/MEK/ERK pathway, treatment of a number of cell lines (including PC12) with the Epac specific agonist, 8-CPT, failed to activate or inhibit ERK (188). Where ERK was activated by cAMP, this was shown to be dependent upon Ras and PKA (188). Thus, B-Raf is a physiological target of Rap1 but its activation is dependent upon the guanine nucleotide exchange factor used by cells to activate it.

1.17 PKA and cancer

In the context of cancer, PKA activity and expression has been extensively studied. Alterations in the expression of RI and RII subunits have been well characterised during cell proliferation, differentiation and transformation. It has been suggested that RI α is preferentially expressed in proliferating and transformed cells and RII is associated with normal, non-proliferating and terminally differentiated cells (204). Indeed, PKA RI α is over-expressed in a variety of cancers and is associated with poor prognosis in breast cancer patients (205). Therefore, malignant transformation has mainly been associated with altered RI α expression or indeed, changes in the ration of PKA-I and PKA-II.

In colon carcinoma cell lines treated with either anti-sense oligodeoxynucleotides against RI or RII subunits, proliferation is inhibited in a cell line dependent fashion. This gave one of the first indications that PKA may be a potential anti-cancer target (206). Antisense knockdown of RI α is growth inhibitory in a number of cancer cell lines including breast, lung, prostate, leukaemia and jurkat T lymphoma cell lines, demonstrating that inhibition of RI α may also be a relevant target for future cancer therapies (207-209).

There may also be a similar role for PKA RII β in regulating the proliferation of colon cancer cells. Overexpression of RII β subunit in LS-174T human colon carcinoma cells results in down-regulation of PKA-I and an induction of growth inhibition in both 2- and 3-

dimensional substrates (210). This suggested that along with PKA-I, PKA-II may play an important role in the regulation of neoplastic growth and transformation in a cell-type dependent manner. Also, antisense suppression of PKA-RI α (which increases PKA-RII β expression) or overexpression of PKA-RII β increase differentiation associated genes and suppress proliferation and transformation associated genes in prostate cancer cells (211). Thus, switching the isoform expression profile of PKA regulatory subunits can cause a phenotypic reversion of malignant tumours.

Also, a number of mouse studies have been used to validate PKA regulatory subunits as an anti-cancer targets. For example, an antisense oligonucleotide against the RI α results in inhibition of tumour growth but for complete cessation, frequent dosing was required (210). PKA RI α antisense oligonucleotides used in combination with CpG DNA (CpG DNA mimics bacterial DNA due to absence of methylation and can elicit an immune response (212)) results in an enhanced anti-tumour effect on HCT-15 cancer cell growth in nude mice (213). Therefore, PKA regulatory subunits have distinct roles in cell proliferation and differentiation making them attractive targets for anti-cancer therapies.

1.18 Epac/Rap1 and cancer

Rap1/2 has previously been shown to have either increased or decreased activity in cancer cells. For example, in breast epithelial cells Rap1 activity is increased in malignant T4-2 cells and inhibition of this activity leads to the formation of acinars (apico-basal polarised, three-dimensional pseudo-tissue structures) with the correct polarity, and restored architecture (214). Whereas increasing Rap1 activity further led to increased invasiveness and tumorigenicity of these cells (214). Also, in studies using cells derived from metastatic melanoma tumours, elevated Rap1 activity correlates with increased activation of the MAPK pathway and increased integrin activation, which promotes cell migration (215). In ovarian

cancer cells, despite an interesting role for Epac in the regulation of cell-cell and cell-matrix adhesion (192), no definitive evidence as yet has directly implicated Epac in driving the progression of cancer. For example, in thyroid tumours, where cAMP plays a pivotal role in mitogenesis, there are no activating mutations in the Epac – Rap1 signalling pathway and neither plays a role in the abnormal proliferation of these cells (216). Thus, a role for Epac in the progression of a variety of cancers requires further study.

1.19 Cyclic AMP degradation

Cyclic nucleotide phosphodiesterases (PDEs) provide the sole route for the degradation of key second messengers, such as cAMP and cGMP, thus providing a crucial method by which cells can regulate cyclic nucleotide levels. The importance of these enzymes is reflected in the sheer diversity and number of PDE families encoded by the human genome. It has been reported that there are approximately 11 different PDE families (PDEs 1-11), comprising of approximately 21 gene products many of which can produce multiple, alternatively spliced mRNA and with different transcription start sites. Currently, there are reported estimates for >100 different PDE mRNA products (217). PDE enzymes are responsible for the hydrolytic cleavage of the 3' cyclic phosphate bond of adenosine and/or guanosine 3' 5' cyclic monophosphate (Figure 8). This reaction is shown for cAMP in Figure 8. Of the 11 PDE families, 8 of these are able to hydrolyse cAMP, 3 of which does so exclusively, where as others can hydrolyse both cAMP and cGMP as well as only cGMP (130, 217). All of these enzymes, with the exception of PDE9, can be inhibited by the inhibitor 3-Isobutyl-methylxanthine (IBMX) (134).

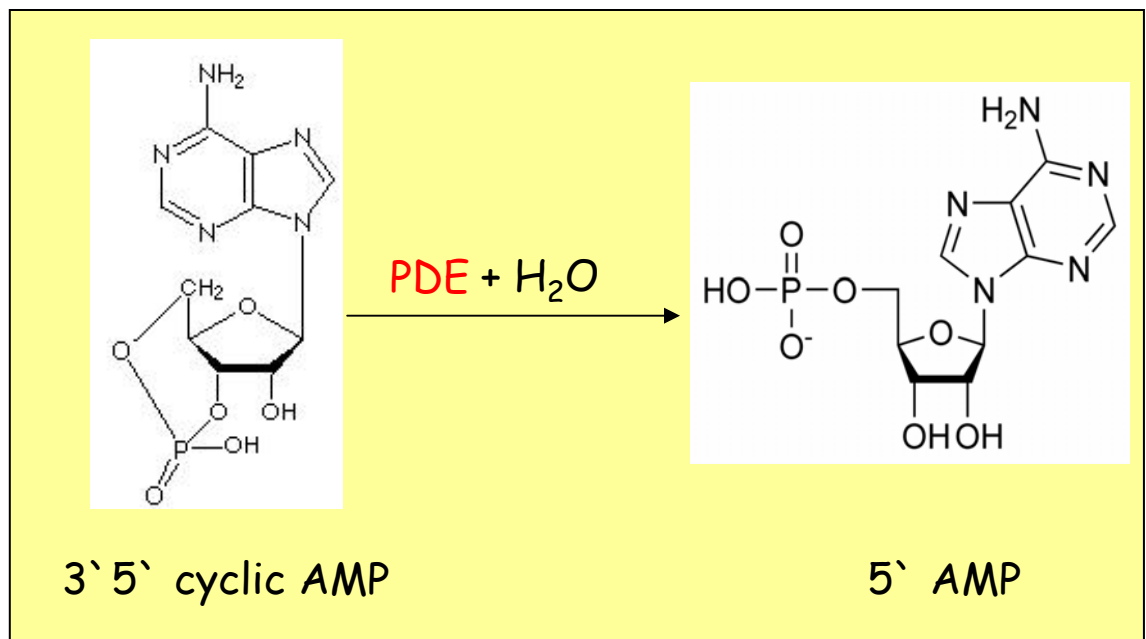


Figure 8. Cyclic AMP hydrolysis. Phosphodiesterase (PDE) enzymes catalyse the hydrolysis of 3`5` cyclic adenosine monophosphate (cAMP) to 5` AMP via the cleavage of the 3` phosphodiester bond. Therefore, the PDE enzymes regulate the localisation, duration and amplitude of cAMP signalling within sub-cellular domains.

The sheer complexity of the cyclic nucleotide PDE system has led to a wealth of research focused on understanding the roles of PDEs in the regulation of cAMP and cGMP in cells. It is now widely accepted that any cell type can express a number of different PDEs and that local concentrations of cAMP are highly regulated in cells. This compartmentalisation of cAMP signalling allows different cell types to specifically tailor their responses to cAMP generation through controlling the duration of the cAMP “clouds”, as well as localised activation of downstream effectors (131, 134, 136). Also, it has been proposed that PDEs may not only function as hydrolytic enzymes, but as scaffold proteins themselves, ensuring the correct receptors are in the vicinity of the cAMP generation and that the activity of these enzymes would serve to terminate the activation signal (131, 134, 136). This is highlighted extremely well in the case of PDE compartmentalisation in cardiac myocytes, where both PDE3 (cGMP inhibited, dual specificity enzyme) and PDE4 (cAMP specific) enzymes are expressed. Both enzymes are localised at distinct sub-cellular localisations within the myocytes and can generate distinct effects within these cells. But, it is PDE4s that are solely responsible for modulating the amplitude and duration of the cAMP response to β -adrenergic receptor stimulation in these cells (218).

1.20 PDE3 enzymes

One of the more extensively studied families of phosphodiesterases is the PDE3 enzymes as they have several roles in physiological and pathological processes making them a target for drug intervention (134). PDE3s have the ability to hydrolyse both cAMP and cGMP, with the *in vivo* cAMP hydrolysis activity seemingly being able to be inhibited by cGMP. PDE3 enzymes can hydrolyse both cAMP and cGMP with relatively high affinities where the K_{mcAMP} is $<0.4 \mu\text{M}$ and the K_{mcGMP} $<0.3 \mu\text{M}$. However, the maximum rate at which PDE3 enzymes hydrolyse cAMP (V_{max}) is approximately 10 fold higher than the V_{max} for cGMP. This has regulatory implications as it is possible that cGMP can then act as

an inhibitor of cAMP hydrolysis, first demonstrated in intact cells using blood platelets as the model system (219).

The PDE3 family of enzymes consist of two genes, PDE3A and PDE3B, but with only 3 splice variants giving rise to multiple isoforms present in the PDE3A gene (PDE3A1/2/3) (Figure 9 A)(217, 220).

Localisation of PDE3 enzymes is thought to be regulated primarily by two hydrophobic motifs, one large and one small, located in the N-terminus of the protein. The larger of the two, which is approximately 195 amino acids in length, is predicted to form approximately 6 transmembrane helices; however the exact number of these that actually transect the membrane still remains undermined (Figure 9 B) (221). Activation of both PDE3A and PDE3B enzymes can be achieved through direct phosphorylation by PKA and/or PI 3-kinase/Akt pathways, thus giving these enzymes the ability to act as a point of convergence between two distinct second messenger pathways (Figure 9 B). Phosphorylation of these enzymes occurs in response to hormonal stimulation in a variety of cell types. For example, prostaglandins and epinephrine (adrenaline) can activate PDE3A through phosphorylation by PKA and PDE3B can also act as a substrate for this enzyme (221). Other hormonal signals can activate PDE3 enzymes also. For example, insulin, IGF1 and leptin can activate the PI 3-kinase/Akt pathway which can subsequently go on and induce the phosphorylation of PDE3B, and possibly PDE3A, thereby stimulating its activity (221).

1.21 PDE3 enzymes and their role in cancer

Although the potential role of PDE3 enzymes in tumour development has not been extensively studied, there are reports highlighting differential expression and/or activity of PDE3s in tumour cell lines of various origins. For example, one of the earliest studies using

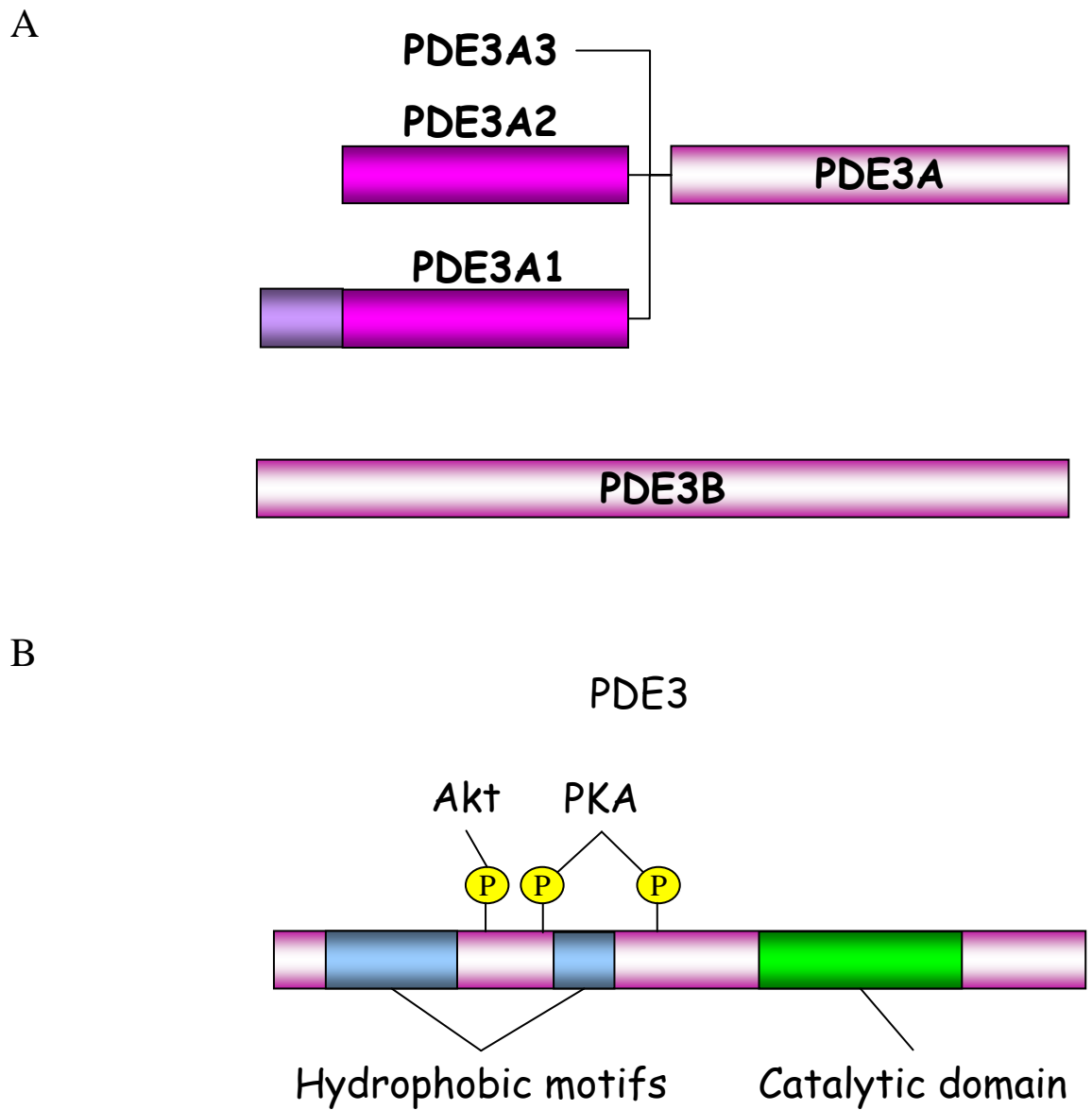


Figure 9. PDE3 domain structure and gene organisation. (A) Gene arrangement of PDE3s. Three variants of the PDE3A isoform (PDE3A1/2/3) have been identified and are thought to exist as truncated forms of PDE3A1. Only one variant of PDE3B has been identified. (B) PDE3 domain organisation, with two hydrophobic motifs and a catalytic region. PDE3 activity can be regulated by both PKA and PKB phosphorylation. The hydrophobic domains are thought to be involved in protein localization.

hepatocellular carcinoma cell lines indicated that PDE3 mRNA was indeed present in the majority of the cell lines tested (222). As well as studies examining PDE3 expression, PDE3 specific inhibitors, such as cilostamide (223), have been used extensively and has provided invaluable clues to the role of PDE3s in both normal and malignant cells. Shimizu *et al* showed that PDE3 genes (both PDE3A and PDE3B) were expressed in squamous cell carcinoma cells and that inhibition of PDE3 enzymes inhibits proliferation (224). This indicated that PDE3 enzymes may be a therapeutic target for skin cancer (224). In a malignant melanoma cell line (HMG), both PDE3A and PDE3B were expressed, but inhibition of the enzymes had no functional consequences on the proliferation of these cells and their role remains unknown (225). Also, studies carried out using cells derived from malignant tumours of the salivary submandibular gland showed that treatment with cilostamide resulted in inhibition of proliferation, suggesting that PDE3 inhibitors may be important in the treatment of some cancers (226).

In the context of colon cancer, the PDE3 specific inhibitor cilostazol, which has previously been used to treat patients with thrombosis, was used to assess the effects of PDE3 inhibition on aspects of cell motility. This study revealed that treatment with this drug inhibited the invasion and migration of colon cancer cells, indicating that it may be used in some instances as an anti-metastatic agent in the clinical setting (227). Thus, although the studies of PDE3 involvement in cancer are limited at present, they do hint that PDE3s may be a potential drug target in an anti-proliferative or anti-metastatic setting. However, due to PDE3s prominent role in cardiovascular function (228, 229) this could have adverse side effects, limiting their potential as therapeutic targets in cancer.

1.22 PDE4 Enzymes

The cAMP specific PDE4 family of enzymes is one of the best characterised. Enzymes of this class are widely expressed and they play key regulatory roles in a variety of cellular processes and disease areas. The role for these enzymes has been elucidated using highly specific inhibitors (including rolipram) (230), targeted gene knock outs (231-236), dominant-negative disruption of endogenous enzyme intracellular targeting (237) and RNA silencing techniques (238). Expression of PDE4s has been extensively studied and found in leukocytes (232, 239-242), vascular smooth muscle (234, 243, 244), vascular endothelium (241, 245) and brain tissues (235, 236, 246, 247). Through their ability to modulate intracellular cAMP, PDE4 enzymes regulate processes including pro-inflammatory responses (231, 241, 248, 249), smooth muscle contraction (234), and neurotransmitter signalling mediated by GPCR activation of adenylyl cyclase (250-253).

PDE4s have been linked to a wide range of diseases including chronic obstructive pulmonary disease (COPD), asthma, rheumatoid arthritis, Parkinson's disease, schizophrenia, HIV/AIDS depression and cancer (239-241, 248, 254-257). Indeed, the PDE4 specific inhibitor rolipram was initially developed as a novel anti-depressant, (258). However, rolipram suffered from dose limiting side effects, including nausea and emesis, which severely restricted its therapeutic use (259), but is utilised routinely *in vitro* to explore the functions of PDE4 enzymes in cells (131, 239, 260-262).

1.23 PDE4 Isoforms

Currently, there are approximately 20 known PDE4 isoforms which all exhibit distinct targeting and regulatory properties that offers diversity and tailoring of cAMP signalling on a cell specific basis (262, 263). This complex array of highly conserved enzymes indicates that the PDE4 family of enzymes is critically important to cellular function under normal physiological conditions.

PDE4 enzymes are generated by four different genes PDE4A, B, C and D and each gene has the ability to generate multiple PDE4 isoforms by utilising specific promoters (244, 264, 265) as well as alternative splicing of mRNA (247).

Knockout studies of PDE4 genes have given valuable insight into the specific roles of PDE4 sub-families *in vivo*. Mice deficient in PDE4A, PDE4B and PDE4D have been generated successfully and several studies have been published on the 4B and 4D mice but only preliminary data is available on PDE4A^{-/-} (266). Mehats *et al* showed that the airways of mice deficient in PDE4D were refractory to bronchoconstriction by cholinergic stimulation of the parasympathetic nervous system (234). Furthermore, PDE4D plays a role in controlling β_2 - (which activates both G α_s and G α_i to regulate myocytes contraction), and not β_1 -adrenergic responses in cardiac myocytes (267). Moreover, PDE4D^{-/-} mice have progressive and accelerated heart failure after myocardial infarction which is due to a deficiency in the PDE4D3 isoform (268). A lack, or deletion, of PDE4D3 results in the hyperphosphorylation of the ryanodine receptor (RyR2)/calcium-release-channel complex and hence altered Ca²⁺ flux control leading to cardiac dysfunction (268).

Utilising mice deficient in PDE4B, it was demonstrated that these enzymes play an important regulatory role in the immune system. PDE4B was found to be essential for the successful mounting of an inflammatory response lipopolysaccharide in monocytes (232) and macrophages (269). More recently, PDE4B was implicated in mediating the antipsychotic effects of rolipram in conditioned avoidance responding of mice and that the PDE4B-regulated cAMP signaling pathway may play a role in the pathophysiology and pharmacotherapy of psychosis (270).

Insight into emesis induced by PDE4 inhibitors has also been gained by knockout mice studies. Using this method, it has been shown that it is PDE4D, and not PDE4B, which is

primarily responsible for the emesis reaction to PDE4 inhibition (235). Taken together, these studies have implications for future development of PDE4 sub-family specific inhibitors for neurological and inflammatory disorders.

PDE4 isoforms themselves can be classed into three distinct groups: Long, short and super-short isoforms (Figure 10) (262). All isoforms have a unique amino-terminal region, long isoforms have paired regulatory domains, namely UCR1 (Upstream Conserved Region 1) and UCR2, which is followed by the conserved catalytic domain and then a sub-family specific domain (Figure 10) (262). Short PDE4 isoforms have no UCR1 domain but do have an intact UCR2 domain and super-short isoforms have no UCR1 and a truncated form of UCR2 (Figure 10) (262). The catalytic domain of all PDE4 isoforms contains a key aspartate residue (D556 in PDE4D5 (271, 272)), that when mutated to an alanine can render the enzyme catalytically inactive (271, 272). This can be used to express ‘dominant negative’ (DN) isoforms, where their expression displaces the endogenous enzymes and prevents any break down of cAMP generated. This method has been used extensively to analyse the role of specific PDE4 isoforms in a variety of cell types (237, 238, 273).

A key functional role of the UCR modules is the regulation of PDE4 activity. This can occur by PKA mediated phosphorylation of specific residues in the protein. The PKA site, located in the UCR1 domain, allows PKA to activate long forms of the enzymes (Figure 10) (134, 262), thereby increasing PDE4 activity in the regions of high intracellular cAMP and allowing the desensitisation of signalling by increased cAMP degradation (168, 274). The UCR1 and UCR2 domains also confer specific interactions with a variety of scaffolding proteins such as the immunophilin XAP2 (246), allowing further compartmentalisation and targeting of these enzymes to specific sub-cellular localisations. The unique amino-terminal

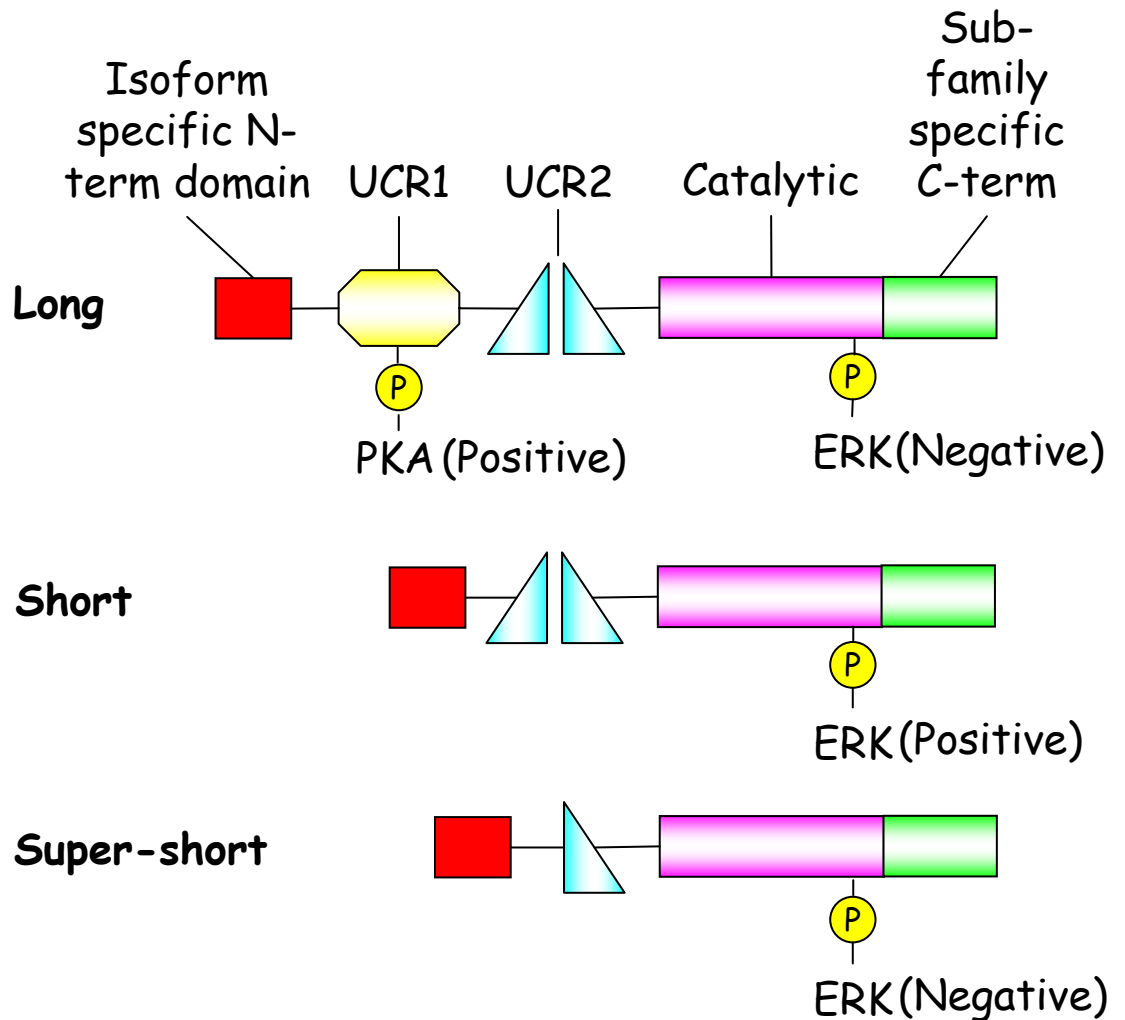


Figure 10. PDE4 domain structure. There are approximately 21 PDE4 isoforms generated by alternative splicing and transcription start sites. Each protein generated is classed as either a long, short or a super-short isoform. Long isoforms contain paired regulatory domains, upstream conserved regions 1 and 2 (UCR1 and UCR2). Short isoforms lack UCR1 but have an intact UCR2 module and super-short isoforms have no UCR1 and a truncated form of UCR2. PDE4 activity can also be regulated by either PKA or ERK and the nature of their regulation is indicated above. In the case of ERK phosphorylation, only PDE4A enzymes lack this site. In addition to the UCR1, UCR2 and catalytic domains, each isoform has a unique N-terminal region as well as a sub-family specific C-terminal domain.

region of each isoform also confers targeting to distinct intracellular sites and signalling complexes, by interaction with scaffolding proteins. These include β -arrestin (144, 271, 275, 276), RACK1 (144, 145) and AKAPs (237, 238, 277, 278). Therefore, the molecular structure of PDE4 isoforms and their interaction with binding partners, underpins the compartmentalisation of cAMP signalling within cells and tissues (262, 263, 279).

1.24 PDE4s, cAMP and cross-talk with other signalling pathways

PDE4 isoforms play a crucial role in regulating distinct sub-cellular pools of cAMP and are uniquely positioned at pivotal points, by interactions with scaffolding proteins, allowing the integration of numerous signalling pathways that involve cAMP. Two pathways that can either regulate PDE4 activity or, in turn, be themselves regulated (either in a positive or negative manner) are the Raf/MEK/ERK and PI 3-kinase/Akt pathways. Both are important regulators of cell proliferation and survival and are heavily implicated in tumourigenesis.

ERK regulation of PDE4 activity

Regulation of PDE4s by ERK occurs by phosphorylation of a conserved serine residue in the catalytic domain of the PDE4 enzymes, with the exception of PDE4A (Figure 10) (280-282). Phosphorylation of Ser⁵⁷⁹ (PDE4D3) results in inhibition of PDE4 activity in long isoforms, activation in short isoforms and inhibition is observed in super-short PDE4 isoforms (Figure 10) (280-282). For PDE4D3 and PDE4D5, two of the most commonly expressed PDE4 isozymes, phosphorylation by ERK2 causes a marked inhibition of the enzymes, leading to a localised increase of cAMP concentrations (247, 281, 282). The consequences of this type of regulation is generation of a feedback-loop, whereby the increase in cAMP leads to activation of PKA and phosphorylation of PDE4D3/4D5 in the UCR1 (Ser⁵⁴ in PDE4D3)

domain and ultimately an increase in cAMP hydrolysing activity (281, 282). This type of regulation has also been shown for both PDE4B and PDE4C isoforms (280).

cAMP mediated modulation of ERK activity

The mechanisms by which cAMP exerts its effects on ERK are still under investigation. One hypothesis is that phosphorylation of Raf-1 by PKA can negatively regulate its kinase activity. *In vitro*, PKA has been shown to phosphorylate Raf-1 at several sites – namely serines 43, 233, 259 and 621 (283, 284). Phosphorylation at these sites inhibits Raf-1 kinase activity by numerous mechanisms, including suppressing the interaction between Raf-1 and Ras (170), binding and sequestration of Raf-1 by 14-3-3 proteins (285) and inhibition of Raf-1 auto-phosphorylation (283). The net result of these phosphorylation events is the inhibition of Raf-1 activity and decreased downstream signalling to MEK and ERK.

Unlike PKA phosphorylation of Raf-1, phosphorylation of B-Raf does not inhibit its activity. Truncation of B-Raf at the amino-terminal allows PKA to phosphorylate and inhibit B-Raf *in vitro* (286). However, PKA cannot inhibit full length B-Raf immunoprecipitated from cells, indicating that the amino-terminal region of B-Raf interferes with PKA regulation of B-Raf (286).

In addition to Raf-1 phosphorylation, PKA can also phosphorylate and, in this case, activate B-Raf. In human uveal melanoma cells, both the inhibition of PKA, and RNAi depletion of PKA, reduced B-Raf activity as well as ERK1/2 activation and cell proliferation in wild type B-Raf cells, whereas it did not affect B-Raf (V600E) (constitutively active B-Raf) containing cells (287). This mode of B-Raf and ERK activation was independent of Rap1 and Ras, although no phosphorylation site on B-Raf was identified (287). PKA activity has been shown to be required for B-Raf mediated activation of ERK in a number of other systems, for

example, in human kidney cyst cells (288) as well as in response to elastin peptides (κ -elastin) in dermal fibroblasts (289).

cAMP mediated inhibition of ERK can occur by activation of Rap1 but a role for either PKA or Epac activation of Rap1 was not shown (290). Thus, the ability of cAMP to inhibit the proliferation of cells is both cell type and context specific. Although not directly implicated in the above mechanisms of ERK inhibition, PDE4s have previously been shown to regulate Epac/Rap1 activity (291) and PKA activity (237) and therefore may be a mechanism by which ERK is inhibited.

PI 3-kinase/Akt Pathway

PI 3-kinases are a large family of proteins, initially characterised by an ability to phosphorylate the 3' position of the inositol ring structure on a number of lipid substrates (292). PI 3-kinase is composed of three classes: I, II and III. Class I catalyse the conversion of $\text{PtdIns}(4,5)\text{P}_2$ to $\text{PtdIns}(3,4,5)\text{P}_3$ and are extremely important in mediating the proliferative effects of growth factors. Class I PI 3-kinase enzymes are heterodimeric and the most widely expressed subunits are p85 α regulatory and p110 α and p110 β catalytic subunits which are all ubiquitously expressed (293-296). Class II enzymes are poorly understood but it is thought that they act further downstream of surface receptors and also associate with clathrin(297) and their physiological substrates are still under investigation. Class III enzymes can phosphorylate PtdIns to form PtdIns-3-P and are involved in vesicular transport to endosomal compartments (298, 299). This thesis will focus solely on the class I PI 3-kinase due to their critical involvement in proliferative processes.

Under normal, unstimulated conditions, p85 and p110 are present in the cell as preformed, inactive dimers. PI 3-kinase is recruited to sites of receptor activation by interaction of p85 SH2 domain with specific pTyr residues within activation motifs on the intracellular

carboxy-terminal tails of the receptors (receptor tyrosine kinases (RTKs) or integrins) (293). This interaction brings the catalytic subunit into close proximity to its substrate, PtdIns(4,5)P₂, and the interaction of p85 with the RTK causes the p85/p110 complex to adopt an active conformation, resulting in PtdIns(3,4,5)P₃ production (Figure 11) ((294) and reviewed in(300, 301)). It is this localisation of PI 3-kinase to regions of high substrate concentration that is thought to regulate its activity.

Negative regulation of PI 3-kinase signalling is achieved by the activity of the tumour suppressor *PTEN* (phosphatase with tensin homology). PTEN protein is a dual lipid/protein phosphatase whose main function is catalysing the dephosphorylation of PtdIns(3,4,5)P₃ to PtdIns(4,5)P₂, thereby terminating PI 3-kinase signalling in cells (Figure 11) (302). PTEN is a 403 amino acid protein and analysis of its crystal structure revealed an amino-terminal phosphatase domain, followed by a tightly associated carboxy-terminal C2 domain (Figure 12)(303). Both of these domains form the minimal catalytic unit of the protein, with only a short amino-terminal region and a 50 amino acid sequence at the carboxy-terminal (Figure 12) (303).

Despite, PTEN lacking regulatory domains, such as a SH2 domain, its activity can be controlled by several mechanisms, such as phosphorylation, membrane recruitment and oxidation. For example, phosphorylation of PTEN on serine and threonine residues occurs in a highly acidic region of its extreme carboxy-terminus (Figure 11) and cellular PTEN appears to be constitutively phosphorylated on these residues. However, the role of PTEN phosphorylation in its carboxy-terminal tail region is shown to influence several aspects of PTEN function including recruitment to cell-cell junctions (304), PTEN protein stability (305-307) and suppression of its activity (308, 309). Phosphorylation of tyrosine residues has also been reported, but the functional consequences are, as yet, undefined (310, 311).

PTEN contains two highly reactive cysteine (Cys) residues within its phosphatase domain, making PTENs catalytic activity highly sensitive to oxidation. (Figure 12; (312)) and which may also be a physiologically relevant mechanism for inactivating PTEN. Oxidation of PTEN results in a disulphide bond forming between a highly conserved Cys71 (that is not required for catalytic activity) and Cys124 (which if mutated, inactivates PTEN lipid phosphatase activity), which in the crystal structure both lie very close to each other (303, 313). Regulation of PTEN activity by oxidation occurs during both experimental oxidative stress and endogenous reactive oxygen species and oxidative regulation of PTEN does play a role in redox regulation of PI 3-kinase-dependent signalling (314).

PtdIns(3,4,5)P₃ can also be dephosphorylated, on the 5' phosphate of the inositol ring by SHIP (SH2-containing inositol phosphatase) generating PtdIns(3,4)P₂. However, in the absence of stimulation SHIP does not appear to regulate the basal levels of PtdIns(3,4,5)P₃, as cells lacking SHIP do not have elevated basal levels of PtdIns(3,4,5)P₃ and Akt activity that is characteristic of PTEN-null cells (302, 315-319). Indeed, the loss of SHIP regulates the duration and magnitude of stimulated increases in PtdIns(3,4,5)P₃ or Akt activity (315-319). Thus, it is possibly the long-term sustained elevation of phosphoinositol increases, caused by loss of PTEN, that is important for tumour development and progression.

Production of PtdIns(3,4,5)P₃ by PI 3-kinase allows the recruitment of PH (Pleckstrin Homology) domain containing proteins, which act as effectors of the PI 3-kinase pathway. One of the major downstream effectors of PI 3-kinase is the serine/threonine kinase Akt (Figure 11) (also known as protein kinase B; PKB). This cytoplasmic kinase is recruited to sites of PtdIns(3,4,5)P₃ generation by its PH domain, wherein it becomes activated through phosphorylation of two residues – threonine 308 (Thr³⁰⁸) and serine 473 (Ser⁴⁷³) (Figure 11). Akt phosphorylation at Thr³⁰⁸, in its kinase activation loop, is sufficient for activity, but requires Ser⁴⁷³ phosphorylation for maximal activity (320). Phosphorylation at Thr³⁰⁸ is

carried out by the PH domain containing protein, 3-phosphoinositide dependent kinase-1 (PDK1) and this site is specific for PDK1 (Figure 11). Ser⁴⁷³ is phosphorylated by a number of kinases including mTOR and DNA-PK (Figure 11) (321, 322). When activated, Akt can phosphorylate its target substrates and promote cell survival and contribute to growth and proliferation (Figure 11).

PI 3-kinase is often deregulated in a large number of sporadic human tumours, due to its role in cell survival and proliferation, and current estimates indicate that one or more components of the pathway is mutated in approximately 30% of all human tumours (323). For example, mutations in the p110 catalytic subunit have been reported, with the most frequent 'hot spot' mutations enhancing PI 3-kinase activity and drive cell transformation (324). These activating point mutations have been reported in 20-30% of colon, brain and gastric tumours (325), and amplification of p110 catalytic subunit has been reported in ovarian, breast and pancreatic cancers (323). The gene encoding the p85 regulatory subunit is also frequently mutated and can give rise to new fusion proteins (326, 327), with mutant p85 proteins lacking the carboxy-terminal SH2 domain (328, 329) as well as the inter-SH2 domain (330) also occurring in some cancers, resulting in the constitutive activation of PI 3-kinase.

Mutations or deletions of the *PTEN* gene, which produce an inactive lipid phosphatase protein or loss of *PTEN* expression, results in sustained or uncontrolled PI 3-kinase signalling. These alterations are common in sporadic tumours and can also predispose to Cowdens syndrome, an inherited disorder characterized by benign growths (hamartomas) and increased risk of cancer (331). In fact, *PTEN* is perhaps one of the most frequently mutated or deactivated genes in the PI 3-kinase pathway in human cancers, with sporadic mutations found in a high percentage of tumour types including colon, breast, ovarian and glioblastoma (332).

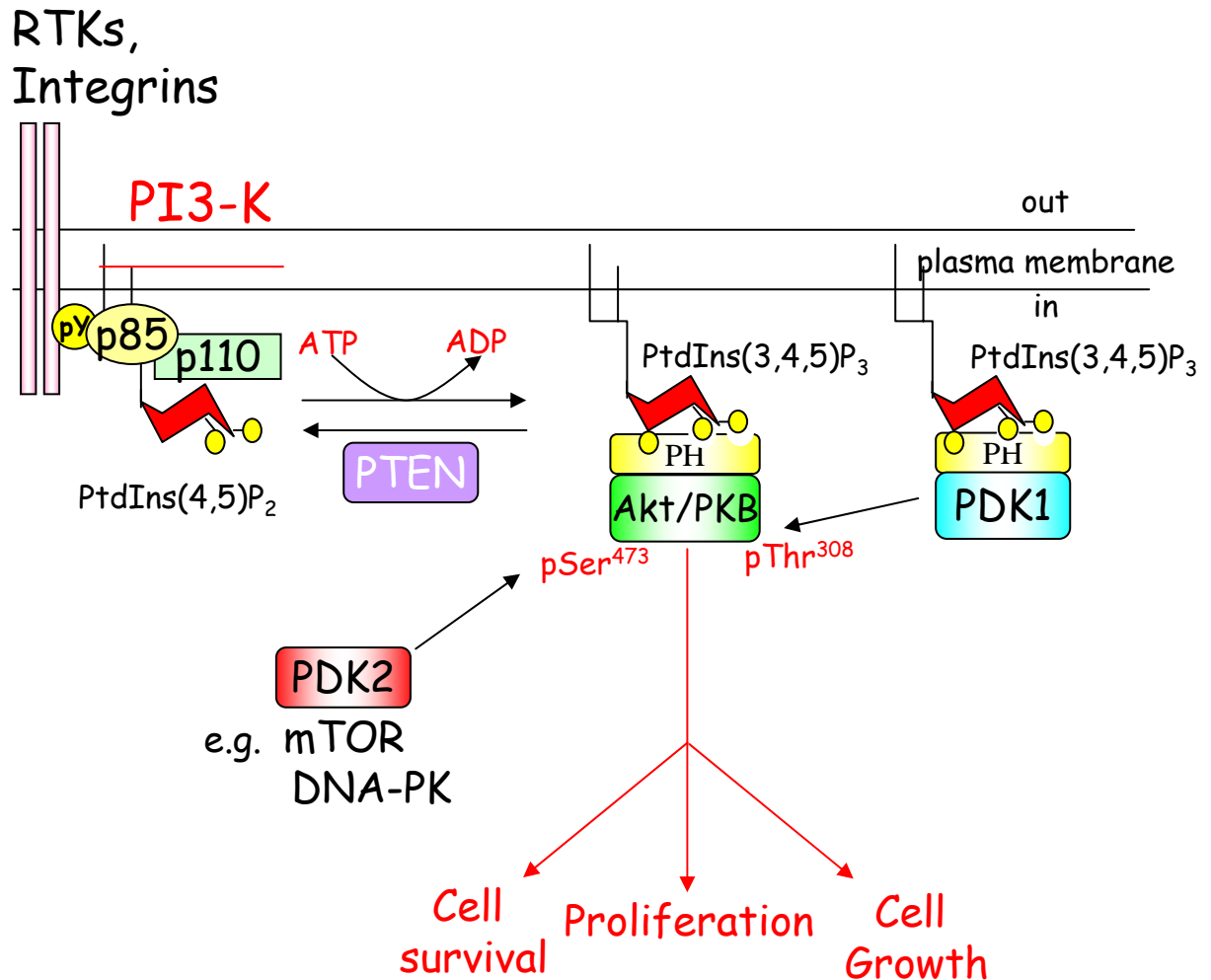


Figure 11. The PI 3-kinase/Akt pathway. Activation of the pathway is achieved by the autophosphorylation of RTKs or integrins on tyrosine residues in conserved motifs. The PI 3-kinase heterodimer is recruited to the activated receptors via its SH2 domain and phosphorylates PtdIns(4,5)P₂ to generate PtdIns(3,4,5)P₃. Effector proteins, such as PDK1 and Akt, are recruited via their PH domains to sites of PtdIns(3,4,5)P₃ generation. PDK1 can phosphorylate and activate Akt on Thr³⁰⁸. Akt can also be phosphorylated on Ser⁴⁷³ by so called PDK2s such as mTOR or DNA-PK. Once phosphorylated on both sites, and therefore fully active, Akt can then regulate cell fates such as apoptosis, proliferation and growth via phosphorylation of downstream proteins. Negative regulation of the pathway is achieved by the dual protein/lipid phosphatase PTEN which removes the 3' phosphate on the inositol ring and converts PtdIns(3,4,5)P₃ to PtdIns(4,5)P₂.

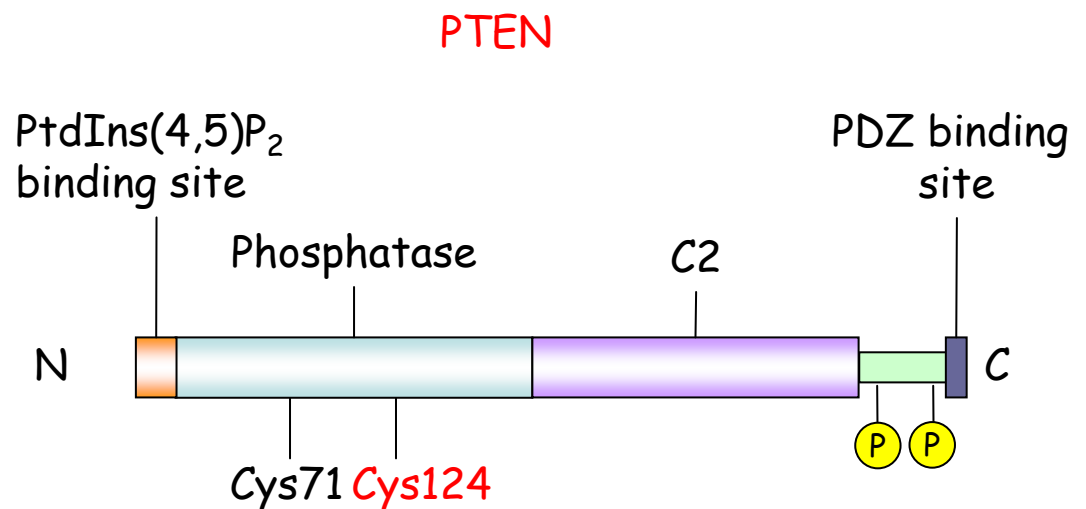


Figure 12. PTEN domain structure. Full-length PTEN protein domain structure is represented above. The N-terminal phosphatase domain and the C2 domain are required for PTEN catalytic activity. The catalytic cysteine residue (Cys124) along with cysteine 71 (Cys71) form a reversible disulphide bond when the enzyme becomes oxidised. The PtdIns(4,5)P₂ binding domain and the extreme carboxy-terminal PDZ-binding domain are also shown. The phosphorylation sites within the carboxy-terminal tail is represented by a yellow circled letter P.

cAMP, PDE4s, and modulation of the PI 3-kinase/Akt pathway

The ability of cAMP to negatively regulate the PI 3-kinase/Akt pathway occurs by a variety of mechanisms. For example, cAMP can inhibit Akt by blocking PDK1 membrane localisation (333) and can also inhibit Akt phosphorylation by other means that are poorly understood (334-336). cAMP can also activate the downstream effector Akt, by both PI 3-kinase dependent and independent mechanisms. For example, Fillippa *et al* (337) showed that forskolin (a direct activator of adenylyl cyclase) treatment of Cos cells (monkey kidney cells) resulted in the PKA-dependent, PI 3-kinase independent, activation of Akt. Also, mutation of Akt Ser⁴⁷³ did not abolish PKA activation of Akt, indicating that this was not the direct phosphorylation site and mechanism of action (337). cAMP can also activate Akt in a manner independent of both PI 3-kinase and PKA-phosphorylation of Akt (338).

PDE4 regulated cAMP has previously been shown to be able to inhibit PI 3-kinase/Akt in a number of cell types. For example, the PDE4B family can negatively regulate the proliferation of diffuse large B-cell lymphomas by inhibiting the PI 3-kinase/Akt pathways (339). Also, in adipocytes, PDE4 inhibition can partially inhibit the insulin-stimulated phosphorylation of Akt (340). Thus, PDE4s can act as pivotal regulators of both ERK and PI 3-kinase/Akt pathways that are often hyper-activated in human malignancies and may provide potential therapeutic strategies to inhibit cancer cells critically dependent on them for survival.

1.25 cAMP, PDE4s and the cell cycle

The cell cycle consists of several stages, namely G1, S, G2 and M, and all of which contribute to the process of cell division. During S-phase DNA is replicated and is preceded by a gap (G1) phase during which the cell is preparing for DNA synthesis (for example checking growth factor availability and that no DNA damage checkpoints are activated). A

second gap (G2) phase occurs after S-phase and is when DNA is checked to ensure it has been replicated faithfully prior to proceeding to mitosis (M), at which point the cell divides and the chromosomes are segregated into two daughter cells (Figure 13; reviewed in (341, 342)). Cells can also be in a non-replicating phase of the cell cycle, namely G₀, which accounts for the majority of the non-growing, non-proliferating cells of the body (341, 342).

Regulation of the cell cycle is achieved by the activity of key regulatory proteins such as cyclin dependent kinases (CDKs). CDKs are serine/threonine kinases that are activated and phosphorylate a number of downstream target proteins at specific points during the cell cycle to allow the progression from one phase to another. During G1 CDK4, CDK6 and CDK2 are all active, during S CDK2 and during G2 and M phases CDK1 (also known as Cdc2) is active (Figure 13 A). CDKs are activated by specific cyclins that are specifically expressed during the phases of the cell cycle. For example, during G1 cyclins D1, D2 and D3 are expressed and bind to, and activate, CDK4 and CDK6 which is essential for G1 entry (Figure 13) (343). Other cyclins expressed include cyclin E (which associates with CDK2 and which is essential for G1/S-phase progression), cyclin A (which binds CDK2 and is required during S-phase and also binds CDK1 for entry into M) and cyclin B, which binds CDK1 and regulates mitosis (Figure 13 A) (344-347). One method of inactivating CDK/cyclin activity is by proteolysis of the cyclin component and this occurs by ubiquitin mediated proteolysis at the end of a cell cycle phase (348).

Another method of counteracting CDK activity is by the action of cell cycle inhibitory proteins, namely CDK inhibitors (CKIs), which bind to CDKs either alone or in CDK/cyclin complexes. Two distinct families of CKIs are the INK4 family and Cip/Kip family (349). The INK4 family consist of several members including p15 (INK4b), p16 (INK4a), p18 (INK4c) and p19 (INK4d), all of which can bind CDKs in their inactive form and therefore prevent cyclin D binding and entry into G1 phase. Cip/Kip CKIs include p21^{Cip1/Waf1} (p21^{Cip1}

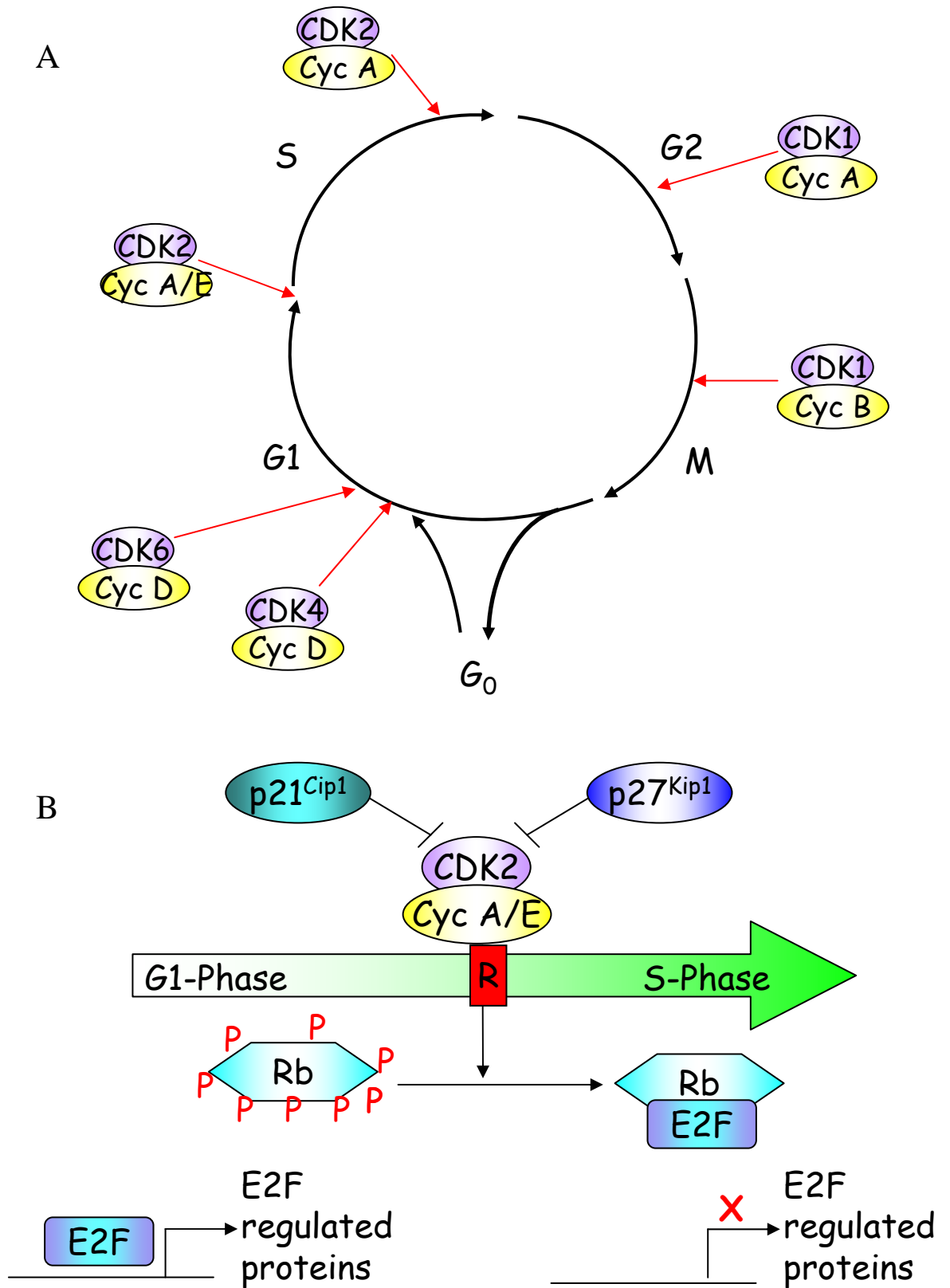
henceforth), p27^{Kip1/Cip2} (p27^{Kip1} henceforth) and p57^{Kip2}. These CKIs bind to, and inhibit, CDK/cyclin complexes and, in particular, G1-phase CDK/cyclins such as CDK2/cyclin E (Figures 13 A and B)(350-353). Induction of CKIs is achieved by several mechanisms such as DNA damage and growth factor withdrawal, all of which can regulate CKI on numerous levels. Regulation of CKI expression and activity is achieved by phosphorylation, localisation, transcription and degradation. For example, p21^{Cip1} is a direct transcriptional target of p53 tumour suppressor, where it is expressed in response to DNA damage, thereby preventing replication of damaged DNA (354). Also, p27^{Kip1} can be phosphorylated by both CDK/cyclin complexes and Akt, which regulates its localisation, nuclear import and interaction with 14-3-3 proteins (355-359). p27^{Kip1} is also regulated by transcription (by FOXO transcription factors) and by degradation (by SCF/Skp2 ubiquitin ligase complex) (360-363).

Downstream of CDK/cyclins is one of the major target substrates, retinoblastoma (Rb) protein (Figure 13 B). During early G1, Rb is hyperphosphorylated (ppRb), leading to disruption of a complex containing Rb and the E2F transcription factor (amongst others). Hyperphosphorylated Rb dissociates from E2F leading to E2F transcription of target genes including proteins that are essential for S-phase progression including cyclin A, B1 and E as well as CDK1 (364-367). Rb remains phosphorylated for the majority of the cell cycle and CDK2/cyclin E contributes to the maintenance of the hyperphosphorylated state and loss of hyperphosphorylated Rb results in re-association of the Rb/E2F complex and suppression of E2F activity (Figure 13 B) (347).

In cancer, numerous components of the cell cycle, as well as cell cycle regulators, are commonly mutated or overexpressed in cancer, leading to hyper-activation and contributing to the increased proliferative potential of tumour cells. For example, the most commonly mutated protein is the tumour suppressor p53 (reviewed in (368)) and subsequent

Figure 13. Cell cycle regulation by p21^{Cip1/Waf1}/p27^{Kip1}. (A) Cell cycle progression is regulated at key points by the activity of several CDK/cyclin complexes. These are in turn, regulated in a manner dependent on the transcription of the cyclins during the various stages of the cell cycle. Proteins such as p21^{Cip1/Waf1} and p27^{Kip1} act as inhibitors of specific CDK/cyclin complexes (such as CDK/cyclin A/E), resulting in a loss of their activity and cell cycle arrest. (B) p27^{Kip1} binding to these complexes results in suppression of CDK/cyclin activity. This results in the loss of phosphorylation on a key downstream substrate, retinoblastoma (Rb) protein. Under normal conditions Rb is hyperphosphorylated and is prevented from binding E2F transcription factors. Loss of hyperphosphorylated Rb results in binding of E2F and inhibition of its transcription factor activity. Rb/E2F target genes include cyclins A, B and E as well as CDK1, all of which are required for the progression of the cell cycle into S-phase and through G2/M phases.

Figure 13. Cell cycle regulation by p21^{Cip1}/Waf1/p27^{Kip1}



loss of p53 activity prevents the activation of p21^{Cip1} and inhibition of the cell cycle. Cyclin D1 is commonly overexpressed in breast, lung, oesophageal and bladder cancer and is linked to cancer progression (reviewed in (369)). Also, Rb was the first tumour suppressor identified and is commonly lost in several types of cancer (reviewed in (370)). Also, a key regulator of p27^{Kip1} stability, Skp2, is commonly overexpressed in ovarian, breast, colorectal and NSCLC cancers (371-374).

PDE4 enzymes can also regulate aspects of the cell cycle progression which can be utilised to address the possible therapeutic benefits of PDE4 inhibition, especially in the context of cancer. The role PDE4s play in regulating the cell cycle will be examined in the discussion section of Chapter 3.

1.26 PDE4s and cancer

Previously, the involvement of PDE4s in human disease has been focused on COPD and asthma. However, there is a growing body of evidence that PDE4s may be a potential drug target for several human malignancies.

For nearly 10 years, PDE4 inhibition in chronic lymphocytic leukaemia (CLL) is known to induce apoptosis and has been proposed as a potential therapeutic target (375, 376). PDE4 inhibition in CLL activates a mitochondrial apoptotic pathway involving caspases 3 and 9 along with cytochrome c release (377). This process is dependent upon the activity of protein phosphatase 2A (PP2A), as inhibition using okadaic acid, prevented loss of phosphorylated Bad protein and dissociation from 14-3-3 protein (377). This process was also shown to be independent of Epac mediated Rap1 activation, despite a forskolin/rolipram combination activating Rap1 (291). Cell cycle arrest and apoptosis can be induced in acute lymphoblastic leukaemia (ALL), by both forskolin and rolipram (378). In addition, PDE4B is often overexpressed in diffuse large B-cell lymphoma (DLBCL) which correlates

with poor clinical outcome (379). Moreover, DLBCL cells overexpressing PDE4B were resistant to cAMP induced apoptosis but modulation of PDE4B activity, by either inhibition or the expression of dominant negative enzymes, resulted sensitisation and subsequent apoptosis in a PI 3-kinase/Akt dependent fashion (339).

In addition to haematological malignancies, PDE4 inhibition causes a G1 cell cycle arrest and apoptosis in malignant glioma cells (380). Also, osteoblastic osteosarcoma cells, which express PDE4A and PDE4C enzymes, show proliferative inhibition when treated with rolipram (381).

As well as a direct role in inhibiting cancer cell proliferation, PDE4s inhibitors block angiogenic responses of endothelial cells (ECs). In human umbilical vein endothelial cells (HUVECs), VEGF mediated proliferation is blocked by PDE4 inhibition, involving suppression of ERK signalling, loss of cyclin A expression and cell cycle arrest (245). Also, PDE4 inhibition blocks VEGF-mediated EC migration (382). Thus, the use of PDE4 selective inhibitors may be a useful anti-angiogenic treatment, where pathological angiogenesis is driven by VEGF.

PDE4 inhibition has also been shown to ablate Rho-driven migration of fibroblasts on Laminin substrates, which highlights their potential as anti-invasive or anti-metastatic agents in certain circumstances (383).

Taken together, these studies that PDE4s may be useful drug targets several different types of malignancies. However, what is not clear is how, if at all, PDE4 activity and/or expression influences any aspects of solid epithelial cancer behaviour, and how their modulation may be exploited as a potential therapeutic strategy.

1.27 Summary

Although not thought of as a ‘classical’ cancer pathway, cAMP and in particular, PDE4 regulated cAMP pathways, have been shown to be altered in some malignancies. Also, cAMP can cross-talk with other pathways, such as ERK and PI 3-kinase/Akt pathways which are frequently deregulated in cancer, and is therefore an attractive target for therapeutic intervention. Thus, modulation of specific pools of cAMP, using pharmacological tools that are under development for other disease conditions, could provide a much needed way to treat cancers which may be resistant to conventional therapies.

Thus, there is some tantalising evidence that cAMP pathways may play critical roles in regulating the proliferation of cancer cells. It is the role of cAMP and how it may be modulated, to therapeutic benefit, in colorectal cancer that I wish to investigate in this thesis.

Chapter 2:
Materials and Methods

2. Materials and Methods

Materials

2.1 Cell culture reagents

Supplier: Autogen bioclear, Wiltshire, UK

Foetal bovine serum (FBS)

Supplier: Beatson Institute Central Services

Sterile PBS

Sterile PBS/1 mM EDTA

Supplier: Invitrogen, Paisley, UK

Eagles Minimal Essential Medium with Earles salts (MEM)

Dulbecco's modified Eagle's medium (DMEM)

RPMI

200 mM L-glutamine

MEM vitamins (100x)

MEM Non-essential amino acids (NEAA) (100x)

2.5% trypsin solution

Supplier: Qiagen, Crawley, UK

Polyfect transfection reagent

Supplier: Roche Diagnostics Ltd, Sussex, UK

Hygromycin

Supplier: Sigma Chemical Co, Poole, UK

100 mM Sodium pyruvate

2.2 Cell culture plasticware

Supplier: BD Biosciences, Oxford, UK

Falcon tissue culture dishes (60 mm, 90 mm and 120 mm)

12 and 96 well plates

Supplier: Fisher Scientific, Loughborough, UK

Nunc tissue culture flasks

Nunc cryotubes

2.3 Treatments

Supplier: Sigma Chemical Co, Poole, UK

IBMX

Forskolin

Rolipram

H-89

Supplier: MERK Chemicals Ltd, Nottingham, UK

Cilostamide

8-Br-cAMP

LY294002

Supplier: Axxora, Nottingham, UK

8-pMeOPT-2'-O-Me-cAMP

Supplier: TOCRIS, Bristol, UK

NKH 477 (Colforsin daropate hydrochloride)

2.4 MTT assay

Supplier: Sigma Chemical Co, Poole, UK

Thiazolyl blue tetrazolium bromide

Supplier: Fisher Scientific, Loughborough,, UK

Dimethylsulphoxide (DMSO)

2.5 PDE assay

Supplier: Sigma Chemical Co, Poole, UK

3`5`-cyclic adenosine monophosphate (cAMP)

Snake venom (*Crotalus atrox*; Western diamondback)

DOWEX MR-3

Supplier: GE Healthcare Ltd, Chalfont St.Giles,UK

[³H] cAMP

2.6 Rap1 activity assay

Supplier: Perbio, Cramlington, UK

EZ-Detect Rap1-activation kit

2.7 Cell cycle analysis

Supplier: Sigma Chemical Co, Poole, UK

Propidium iodide (PI)

5-Bromo-2`-deoxyuridine (BrdU)

Supplier: DAKO, Ely, UK

Anti-BrdU mAb

Supplier: Jackson ImmunoResearch, Luton, UK

FITC labelled sheep anti-mouse IgG

2.8 Annexin-V staining

Supplier: Transduction Laboratories, BD Biosciences, Oxford, UK

Annexin V-FITC Apoptosis detection Kit I

2.9 Immunofluorescence

Supplier: Jackson ImmunoResearch, Luton, UK

FITC labelled sheep anti-mouse IgG

Supplier: Leica UK Ltd, Milton Keynes, UK

Leica SP2MP confocal microscope

Supplier: Transduction Laboratories, BD Biosciences, Oxford, UK

Anti-p85 α mAb

Supplier: Dr. N.R Leslie, University of Dundee

GFP-PH(Akt) construct

Supplier: Sigma Chemical Co, Poole, UK

TRITC phalloidin

Tween 80

Supplier: Vector Laboratories Ltd, Peterborough, UK

Vectashield mounting medium with DAPI

2.10 Western Blotting

Supplier: Amersham International, Little Chalfont, UK

Anti-mouse/horseradish peroxidase conjugate

Anti-rabbit/horseradish peroxidase conjugate

ECL reagent

High molecular weight rainbow markers

Supplier: Biometra, Niedersachsen, Germany

Semi-dry blotting apparatus

Supplier: Chemicon International, Harrow, UK

Re-blot kit

Supplier: Genetic Research Instrumentation, Dunmow, UK

Atto protein electrophoresis apparatus

Supplier: PERBIO, Glasgow, UK

Micro BCA protein assay kit

Supplier: Schleicher and Schuell, London, UK

Nitrocellulose membrane

Supplier: Severn Biotech Ltd, Kidderminster, UK

Design-a-gel 30% (w/v) acrylamide (37.5:1 Acrylamide to Bis-acrylamide)

Design-a-gel 40% (w/v) acrylamide

Design-a-gel 2% (w/v) Bis-acrylamide

Supplier: Sigma Chemical Co, Poole, UK

Ammonium persulphate (APS)

Anti-sheep horse radish peroxidase conjugate

Anti-vinculin mAb

Anti-ERK rAb

Anti-VSV rAb

Anti- α -tubulin mAb
0.1% (v/v) aprotinin
Bovine serum albumin (BSA)
2 mM phenylmethylsulphonyl fluoride
TEMED
Tween 20
Triton X-100
HEPES
Sodium Fluoride (NaF)
Phenylmethanesulphonylfluoride (PMSF)
EGTA
EDTA
Ammoniumpersulphate (APS)

Supplier: Transduction Laboratories, BD Biosciences, Oxford, UK

Anti-p27^{Kip1} mAb
Anti-PTEN mAb
Anti-p85 α mAb
Anti-Rb mAb

Supplier: Santa Cruz Biotechnology, CA, USA

Anti-cyclin A rAb
Anti-cyclin E rAb
Anti-CDK1 rAb
Anti-Skp2 rAb

Supplier: New England Biolabs, Hertfordshire, UK

Anti-pERK1/2 (Thr²⁰²/Tyr²⁰⁴) rAb
Anti-PDK1 rAb
Anti-pAkt (Thr³⁰⁸) rAb
Anti-pAkt (Ser⁴⁷³) rAb
Anti-Akt rAb
Anti-pFKHRL1(Ser²⁵⁶)/pAFX(Ser¹⁹⁵) rAb

Supplier: Thermo Fisher Scientific, Cheshire, UK

Anti-cyclin B1 rAb
Anti-p21^{Cip1/Waf1} rAb

Supplier: Upstate(Millipore), Hampshire, UK

Anti-Epac1 rAb

Supplier: Miles D. Houslay (University of Glasgow)

Anti-pan-PDE4D (sheep polyclonal Ab)

Supplier: Whatman, Maidstone, UK

3MM filter paper

2.11 Reverse transcription (RT)-PCR

Supplier: Qiagen, Crawley, UK

miRNeasy mini RNA extraction kit

Supplier: Applied Biosystems, Warrington, UK

RNA PCR kit

2.12 Stock solutions and buffers

Cell culture solutions

Complete medium for KM12C, KM12SM, KM12L4A, KM12/2C4 and MCF7 cell lines

MEM supplemented with

10% FBS

2 mM L-glutamine

1% MEM NEAA

2% MEM vitamins

1 mM Sodium pyruvate

Complete medium for HT29, A431, WiDr, RKO, A375 and Du145 cell lines

DMEM supplemented with

10% FBS

2 mM L-glutamine

Complete medium for SW480, SW620 and H630 cell lines

RPMI supplemented with

10% FBS

2 mM L-glutamine

Serum free medium

MEM supplemented with

2 mM L-glutamine

1% MEM NEAA

2% MEM vitamins

1 mM Sodium pyruvate

Trypsin

0.25% trypsin in sterile PBS/1mM EDTA

Protein extraction

Lysis buffer (general)

20 mM Tris/HCl, pH 7.4

150 mM NaCl

2 mM EDTA

1% Triton X-100

25 mM NaF

1 mM PMSF

10 µg/ml aprotinin

100 µM sodium orthovanadate

KHEM lysis buffer.

50 mM KCl

50 mM Hepes, pH 7.2

10 mM EGTA

1.92 mM MgCl₂

Cell cycle analysis

70% Ethanol

Saline (0.9g NaCl/100 ml H₂O)

4N HCl (34.5 ml Conc HCl + 65.5 ml H₂O)

PBT (PBS + 0.5% BSA + 0.1% Tween 20)

Western Blotting*Acrylamide gel – 10%*

12 ml Resolving gel buffer

16.7 ml 30% acrylamide (37.5:1 acrylamide/Bis-acrylamide)

20 ml H₂O

400 µl APS

30 µl TEMED

Rb Acrylamide gel – 7%

12 ml Resolving gel buffer

12 ml acrylamide (29.76% acrylamide/0.24% Bis-acrylamide)

24 ml H₂O

400 µl APS

30 µl TEMED

Resolving gel buffer

1.5 M Tris/HCl, pH 8.8

0.4% SDS

Sample buffer – 4x

150 mM Tris pH 6.8

20% SDS

30% Glycerol

15% 2-mercaptoethanol

bromophenol blue to colour

Stacking gel

4.5 ml Stacking gel buffer
2.4 ml 30% acrylamide
11.1 ml H₂O
400 µl APS
30 µl TEMED

Stacking Gel Buffer

0.5 M Tris/HCl, pH 6.8
0.4 % SDS

Tank buffer - 10x

0.52 M Tris
0.52 M glycine
1% SDS

Transfer Buffer – 10x

0.48 M Tris
0.39 M glycine
0.4% SDS
Diluted with H₂O and 20% methanol (v/v)

Antibody dilution and wash buffer (TBST)

50 mM Tris base, pH 7.4
200 mM NaCl
0.25% Tween 20

2.13 Cells and plasmids

KM12C, KM12L4A and KM12SM cells were provided by Professor I Fidler (MD Anderson, TX, USA) and KM12/2C4 cells were derived as previously reported and cultured in complete MEM (MEM, 10% FBS, 2% NEAA, 1% MEM vitamins, 1% L-glutamine, 1% sodium pyruvate) (79). Cell culture media for other cell lines used in this study include: MCF7 as per Fidler model cells; HT29, A431, WiDr, RKO, A375, H630, Du145 were all cultured in DMEM supplemented with 10% FBS and 1% L-glutamine; SW480 and SW620 were cultured in RPMI supplemented with 10% FBS and 1% L-glutamine. MCF7, HT29, A431, WiDr, RKO, A375, H630, Du145, SW480 and SW620 were obtained from the ATCC. All cells were routinely maintained in a humidified incubator at 37°C with 5% CO₂ and sub-cultured prior to reaching confluence. PTEN-GFP (N-terminal tag) expressing cells were generated by retroviral infection of KM12C/2C4 cells with PTEN-GFP in pWZL vector, and single cell clones selected in growth media containing 400 µg/ml hygromycin B (V.G.Brunton).

N-terminally tagged GFP-PH (Akt PH domain) construct was a kind gift from N.R. Leslie (University of Dundee).

A lenti-viral construct containing the sequence AAGAACTTGCCTTGATGTACA, which has previously been shown to specifically silence PDE4D (238), was incorporated into a lenti-viral insert sequence flanked by a 5' BamH I and 3' Xho I restriction sites, the complementary anti-sense sequence and a loop-sequence. The specific sequence was generated on the *Genscript* web-based siRNA construct builder (www.genscript.com). A reverse of this insert was also generated, annealed with the forward sequence and ligated into siRNA expression vector pRNAT-U6.1/lenti (*Genscript Co, USA*) that had previously been cleaved using BamH I and Xho I restriction enzymes. Stocks of the plasmid were generated by transformation of ABLE® C competent cells and selected in ampicillin. The same was

also done for a scrambled PDE4D sequence (PDE4Dscr) as a control (5' - 3' Sequence: GGACCGATTATCTATGAATAC).

PDE4D3-VSV, PDE4D3DN-VSV, PDE4D5-VSV and PDE4D5DN-VSV were kind gifts from M.D. Houslay (University of Glasgow).

Methods

2.14 Routine cell culture

All sub-culturing of adherent cells was achieved by removing the medium was by aspiration, the monolayer rinsed with PBS then with 10% trypsin/PE solution. Upon detachment the cells were resuspended in appropriate media, counted, and then transferred into tissue culture flasks or plates. Cells were generally treated one day after plating (unless otherwise stated).

2.15 Treatment of cells

Cells were treated with the numerous chemical compounds at the concentrations and time points indicated in each figure legend.

2.16 MTT proliferation assay

Cell proliferation and viability was assayed indirectly by a modified MTT assay, based on the enzymatic reduction of 3-(4,5-dimethylthiazol-2-yl)-2,5-diphenyl tetrazolium bromide (MTT; Sigma) to formazan crystal by mitochondria and cellular dehydrogenase enzymes (384). Briefly, 50 μ l of cell suspension containing 500-1000 cells (depending upon cell doubling time) were dispensed into 96-well flat bottomed microplates. Dilutions of pharmacological agents in growth media, were performed in four replicate rows per cell type and per dilution. Plates were then incubated in a humidified incubator in 5% CO₂ at 37°C. At the time points indicated, 50 μ l of MTT solution (5 mg/ml MTT in phosphate buffered saline PBS) was added into a total volume of 150 μ l, and incubated in 5% CO₂ at 37°C for 4 hours. Formazan crystals were dissolved with 100 μ l DMSO and optical density at 570 nm was determined using a plate reader (SpectraMax Plus 384, Molecular Devices, Wokingham, UK).

2.17 PDE activity assay

PDE assays were done by a modification (385) of the two-step method by Thomson and Appleman (386). Cells were lysed in KHEM buffer containing Complete® protease inhibitors (Roche Molecular Biochemicals, Germany) and then subjected to 14,000 *g* for 15 min at 4°C. To 20 µl of the resulting supernatant was added 20mM Tris buffer/inhibitor to achieve a total volume of 50 µl. The tubes were vortexed and 50µl of cAMP mix (1ml 20mM Tris/10mM MgCl₂: 2µl ‘cold’ cAMP: 3µl [³H] cAMP) was added and incubated at 30°C for 10 minutes. Samples were then removed and boiled for 2 minutes. 25 µl of snake venom (1mg/ml in 20mM Tris) was added and incubated for 10 minutes at 30°C and placed on ice. DOWEX mix (400 µl ; 1 part DOWEX: 1 part H₂O: 1 part Ethanol) was added, mixed thoroughly and incubated on ice for 20 minutes and the supernatant (150 µl) was then added to scintillation fluid (1ml) and mixed gently . cAMP mix (50 µl) was also added to separate vials of scintillant fluid as total cAMP controls. Samples were then read on a β-counter (Beckman Coulter LS 6500 TA liquid scintillation counter). Each condition was performed in triplicate and each assay was repeated a minimum of three times. PDE specific activity was calculated as pmol/min/mg protein and data shown is a mean ± SD of n=3 independent experiments. In order to determine the contribution of various PDE family members to the total PDE activity, family specific inhibitors were used at a final concentration that completely inhibited their activities. PDE3 and PDE4 activities were determined using 10 µM cilostamide (PDE3) (223) or 10 µM rolipram (PDE4) (239, 262).

2.18 Preparation of protein extracts

Dishes were transferred directly from the incubator onto ice. The medium was aspirated and cells were washed twice with PBS and lysed in ice-cold lysis buffer for 15 minutes. Cells were then scraped off the tissue culture plastic using a disposable cell scraper and the lysate transferred to a microcentrifuge tube. The lysate was then clarified by

centrifugation at 14,000g for 15 minutes at 4⁰C (Eppendorf chilled centrifuge 5415 D). Protein concentration was determined using the Micro BCATM Protein Assay Kit and light absorbance then measured with a DU® 650 spectrophotometer (Beckman) at a wavelength of 562nm.

2.19 Western blot analysis

To approximately 50-100µg of protein lysate was added sample buffer and then incubated at 99°C for 10 minutes. Protein separation was achieved by running the samples and molecular weight markers on a SDS-PAGE gel consisting of a short stacking gel and a longer resolving gel. The resolving gel contained 7%, 10% or 12% acrylamide depending on the size of the proteins being separated. Retinoblastoma (Rb) protein was separated on a 7% gel with altered ratios of acrylamide:Bis-acrylamide, as detailed in the materials section. Gels were typically run at 40V overnight. Following electrophoresis, the proteins were transferred onto a nitrocellulose membrane, while being buffered by 3MM filter paper saturated in transfer buffer, using semi-dry blotting apparatus at 20V for 1hour 10 minutes. After the proteins had been transferred onto nitrocellulose the membrane was blocked for a minimum of one hour at room temperature in 5% BSA in TBST. The primary antibody in 5% BSA/TBST was then added for 1 hour at room temperature or overnight at 4⁰C. The blots were then washed three times in TBST (10 minutes each) and incubated with horseradish peroxidase conjugated secondary antibodies diluted at 1 in 5000 for 1 hour. The blots were again washed three times in TBST (15 minutes each) and ECL reagent was added for 3 minutes. Bands corresponding to the specific proteins were observed using a Kodak X-OMAT 480 RA film processor. When necessary, blots were stripped using the Re-Blot Plus Strong Antibody Stripping Solution according to manufacturers instruction. The blots shown are representative of experiments which were repeated three times.

Primary antisera dilution for Western Blotting:

All anti-bodies used were diluted 1/1000 in 5% BSA/TBST prior to incubation, unless otherwise stated.

2.20 Rap1 activation assay

Extraction of activated Rap1 (Rap1-GTP) was carried out as per manufacturers instructions. Briefly, approximately 2×10^6 cells were set-up and after treatment cells were washed with ice-cold TBS and 1ml of lysis buffer (supplied in kit) was added and the cells scraped immediately. Cell lysates were incubated on ice prior to centrifugation at 14,000rpm for 15 minutes at 4°C to remove cell debris. Protein concentration was determined and 500µg was added to immobilised glutathione discs in spin columns, which had been equilibrated with 20 µg of GST-RalGDS-RBD (Glutathion-S-transferase tagged-Ras binding domain of the Rap1 interacting protein RalGDS which specifically interacts with GTP bound Rap1) previously. This was then used to purify Rap1-GTP from the lysates by centrifugation. Rap1-GTP was removed from the discs after washing by the addition of sample buffer. As controls, untreated lysates were incubated with either GTPγS (positive control) or GDP (negative control) for 30 minutes at 30°C, prior to the purification of Rap1-GTP. Samples were then subject to SDS-PAGE western blot and purified-active Rap1-GTP was identified using a specific anti-Rap1 polyclonal antibody (supplied with kit). As loading controls, lysates were also run and total Rap1 levels determined by western blot.

2.21 Cell cycle analysis

Cells were treated as indicated, washed in cold PBS (4°C), trypsinised and prior to fixation in 70% ethanol/phosphate-buffered saline (PBS) overnight. For DNA content analysis (including sub-2n DNA), cells were pelleted and resuspended in PBS containing 1 µg/ml RNase (Qiagen Ltd, Crawley, UK) and 10 µg/ml propidium iodide (PI), incubated at

room temperature for 30 min, then analysed using a Beckton Dickinson (Oxford, UK) FACScan flow cytometer. To monitor BrdU incorporation, cells were incubated with 25 μ M BrdU for the final hour of treatment, fixed in ethanol, resuspended in saline (0.9%) and permeabilised using 4N HCl for 15 minutes at room temperature. Cells were centrifuged and washed 3x with PBT and resuspended in 100 μ l PBT/anti-BrdU anti-body and incubated for 30 minutes at room temperature. Cells were then washed once in PBT, centrifuged and resuspended in PBT/ fluorescein isothiocyanate (FITC)-conjugated secondary antibody for 30 minutes in the dark. Cells were again washed, centrifuged and resuspended in PBS containing 5 μ g/ml PI. Samples were immediately analysed by flow cytometry and the cell cycle distribution analysed. Experiments were carried out 3 times and data shown as mean \pm SD.

Antibody dilutions for Brdu/PI analysis:

Antibody	Dilution
Anti-BrdU	1/40
Anti-mouse-FITC conjugate	1/128

2.22 Annexin V detection of apoptosis

Apoptosis was quantified using an Annexin V-FITC detection kit (Beckton Dickinson) and staining was carried out as per manufacturers' instructions. Briefly, KM12C cells were set up at low density and treated for 24 hours, 48 hours or 72 hours with the treatments indicated. At each time point cells were washed with cold PBS, trypsinised and resuspended in binding buffer (100 mM HEPES, 1.4 M NaCl, 25 mM CaCl₂, pH 7.4) at a

concentration of 1×10^6 cells per ml and 100 μ l of resuspended cells were incubated with Annexin V-FITC and 5 μ g/ml PI. Cells were analysed using a Beckton Dickinson (Oxford, UK) FACScan flow cytometer.

2.23 Transient transfection

Cells were plated onto glass cover slips in an eight-well plate and at a density of 1×10^5 per well, twenty four hours prior to transfection. KM12C cells were transfected using Polyfect according to the manufacturers instructions with 1.5 μ g DNA per well. Transfections were incubated at 37°C, 5% CO₂ for 4-5 hours then washed three times with PBS, fresh media added and left overnight in the incubator. Treatments were carried out approximately 24 hours after transfection. Typical transfection efficiencies were around 30%.

2.24 Immunofluorescence

Cells were washed in cold PBS then fixed in 4% paraformaldehyde for 15 minutes. They were then washed 3 times with cold PBS and permeabilised with PBS/0.5% Triton X-100/1% BSA for 15 minutes. Afterwards cells were blocked with PBS/10% FCS, for a minimum of 1 hour cells and then incubated with primary antibodies overnight, at 4°C in the dark. Antibody detection was by reaction with fluorescein isothiocyanate (FITC)-conjugated secondary antibody at 1 in 100 for 1 hour. Cells were then washed and mounted prior to visualisation using a Leica confocal microscope. In the case of GFP-PH transfected cells, these were mounted after blocking stage. These experiments were repeated a minimum of three times and the images shown are representative of the localisation observed in the majority of cells. 100-150 cells under each condition and for each separate experiment were counted and the percentage of cells with the localisation shown under control conditions was calculated. Data shown is a mean \pm SD of n=3 independent experiments.

Primary antibody dilution for IF:

Antibody	Dilution
Anti-p85 α	1/100

2.25 Sub-cellular fractionation

KM12C cells were grown as above and treated as indicated in the figure legend. The medium was aspirated and the cells were washed twice with ice-cold PBS, followed by a wash with ice-cold KHEM buffer (containing Complete™ protease inhibitor cocktail (Roche Molecular Systems)), and then snap-frozen in liquid nitrogen. The frozen cells were thawed on ice and lysed by passing them 10 times through a 26.5-gauge needle. Samples were then centrifuged at 1000 *g* for 10 min (Eppendorf chilled centrifuge 5415 D) to produce a low-speed pellet (P1 fraction) and a low-speed supernatant (S1). S1 was then centrifuged at 100000 *g* for 60 min (Beckman TL-100 ultra centrifuge and TLA-100.3 rotor) to produce a high-speed pellet (P2 fraction). The pellet fractions were resuspended in the same volumes of KHEM buffer. To equal volumes of each fraction was added sample buffer prior to SDS-PAGE/western blot analysis.

2.26 Immunoprecipitation (IP)

The protein concentration of lysates was determined and approximately 1mg total protein was pre-cleared with 20 μ l Protein G-agarose (Sigma, Poole, UK), centrifuged at 14,000 rpm at 4°C and then the supernatant incubated with either 2 μ l of anti-pan-PDE4D anti-sera or pre-immune sera overnight at 4°C. Protein G-agarose was then used to precipitate anti-body/protein complexes, which were then washed three times in lysis buffer and resuspended in 20 μ l of sample buffer prior to SDS-PAGE/western blot analysis. As a control, pre-immune serum was used in place of anti-pan-PDE4D.

2.27 RT-PCR

1x10⁶ cells were used to extract total RNA using the miRNAeasy kit (Qiagen, Crawly, UK) as per the manufacturer's instructions. RNA concentration was determined using UV absorbance and measured with a DU® 650 spectrophotometer (Beckman) at a wavelength of 260nm. 1 µg of RNA was then used to generate cDNA using RNA PCR kit (Applied Biosystems, Warrington, UK) which included the relevant buffers, nucleotides, oligo-d(T)s and MuLV reverse transcriptase. Reverse transcription was carried out at 42°C for 5 minutes and samples were subsequently denatured (99°C for 5 minutes) and cooled. For PCR amplification of specific genes, 5 µl of reverse transcription reaction solution was used. Sense and anti-sense primers of the gene of interest (0.625 µM final concentration) were added to 5 µl of RT reaction as well as sense and anti-sense primers corresponding to GAPDH (0.625 µM final concentration), as an internal control. PCR master mix was then added to the reaction (as per manufacturer's instructions) which included TAQ DNA polymerase. The cycle sequence for each primer set varied and is detailed below. The PCR products were then resolved on a 1.5% agarose gel containing ethidium bromide, and visualised under a UV light source and the image was captured by a SYNGENE gel documentation system. Images shown are representative of experiments carried out at least 3 times.

Sense, anti-sense and cycle condition for genes of interest:

Gene	Sense primer sequence (5' - 3')	Anti-sense primer sequence (5' - 3')	Cycle conditions	Fragment Size(bp)
PDE4D	CCTCTGACTGTTATC- ATGCACACC	GATCCACATCATGTA- TTGCACTGGC	94° 60seconds 50°C 80seconds 72°C 70seconds	262

			30 cycles	
PDE4D3	ATTTTCCGTTTCAGA- AGGCATTCTGG	CCTGGTTGCCAGAC- CGACTCATTCA	94° 60seconds 50°C 80seconds 72°C 70seconds 35 cycles	561
PDE4D5	CTGTTGCAGCATGA- GAAGTCC	CCTGGTTGCCAGAC- CGACTCATTCA	94° 60seconds 52°C 70seconds 72°C 100seconds 35 cycles	685
GAPDH	GTGGATATTGT- GCCCAATGACATC	GGACTCCACGACGTA- CTCAGCGCCAGCA	All above conditions	214

N.B. All PCR reactions are given an initial 1 minute at 94° (denaturing) and a final 7 minutes at 72°C (extension) as additional steps.

2.28 Preparation of DNA

E. coli (ABLE® C) competent cells, stored at -70°C, were thawed on ice and 20µl aliquoted into pre-chilled Eppendorf tubes. Various amounts of DNA, ranging from 0.5 to 2µl, were added to the competent cells and the solution was gently mixed with a pipette tip. The mixture was incubated on ice for 30 minutes, after which the cells were heat-shocked for 45 seconds in a 41°C water bath. After an additional two minutes on ice 80µl of pre-heated L-broth was added and cells were incubated for one hour at 37°C in a shaking incubator (at 225 rpm). The mixture was then spread on agar plates containing 100 µg/ml of ampicillin and incubated overnight at 37°C. DNA extraction was carried out by Maxi prep (Qiagen, Crawley, UK).

2.29 Retroviral infection

Phoenix Eco packaging cells were plated on 60 mm tissue culture dishes for 6 hours prior to the transfection of DNA using DOTAP Liposomal Transfection Reagent. The transfection medium was removed 16 hrs later and replaced with fresh DMEM and 10% FBS. After twenty-four hours the viral supernatant was collected, filtered through a 0.45 μ M membrane and added to KM12C/2C4 cells in the presence of 4 μ g/ml polybrene. Fresh medium was added to the Phoenix Eco cells and a second infection carried out twenty-four hours later. Clones were obtained by the addition of hygromycin.

2.30 Nucleofection

Nucleofection was carried out using Kit V (Amaxa, Koeln, Germany) and a Nucleofector II device (Amaxa, Koeln, Germany) for the efficient transfection of plasmid DNA into KM12C or KM12L4A cell lines. Nucleofection was carried as per the manufacturer's instructions. Briefly, 1×10^6 cells were centrifuged at 1000rpm and resuspended in 100 μ l of supplemented solution V (supplied in kit). To this was added 5 μ g of purified plasmid DNA and transferred into a cuvette (supplied in kit) and subjected to an electrical pulse using programme P-20 on the Nucleofector II. The cell suspension was immediately transferred to a 60mm tissue culture dish containing the appropriate media, allowed to plate overnight and the media replaced and left for a further 24 hours prior to treatment. For the generation of stable cell lines, selection such as Geneticin (G418 sulphate; Invitrogen, Paisley, UK), was added after allowing the cells to plate overnight.

2.31 Stable knockdown of PDE4D in KM12L4A cells

2×10^6 KM12L4A cells were Nucleofected with 5 μ g siRNA constructs containing either PDE4D or PDE4Dscr sequences (as well as containing green fluorescent protein (GFP) under a separate promoter), allowed to plate overnight and then placed in media containing 800 μ g/ml G418 as a selection media. The cells were allowed to grow in the

selection media and when they reached 70-80% confluence, were split and allowed to continue growing. The cells were then FACs sorted for GFP expression and pooled. PDE4 expression was then assessed and the cells were used in subsequent experiments.

2.32 Statistical analysis

Statistical analysis was done using the nonparametric Mann-Whitney test using MiniTab statistical analysis programme. Generation of a P value < 0.05 was considered significant as it corresponded to a $> 95\%$ probability that the two populations being compared are different.

2.33 Densitometry

Analysis of fold expression of a protein was carried out using WCIF image J analysis software, where measurements were taken from western blots of the same exposure, analysed and expressed as fold change.

Chapter 3:
cAMP effects on KM12C proliferation

3. cAMP effects on KM12C proliferation

3.1 Aim

The work presented in this chapter was to test whether or not cAMP could regulate the proliferation of KM12C colorectal cancer cell line which is inherently resistant to common cytotoxic chemotherapeutic agents and signal transduction inhibitors, such as Src tyrosine kinase inhibitors, and, if so, I wished to understand the mechanisms by which cAMP modulated proliferation.

3.2 cAMP inhibits the proliferation of KM12C cells

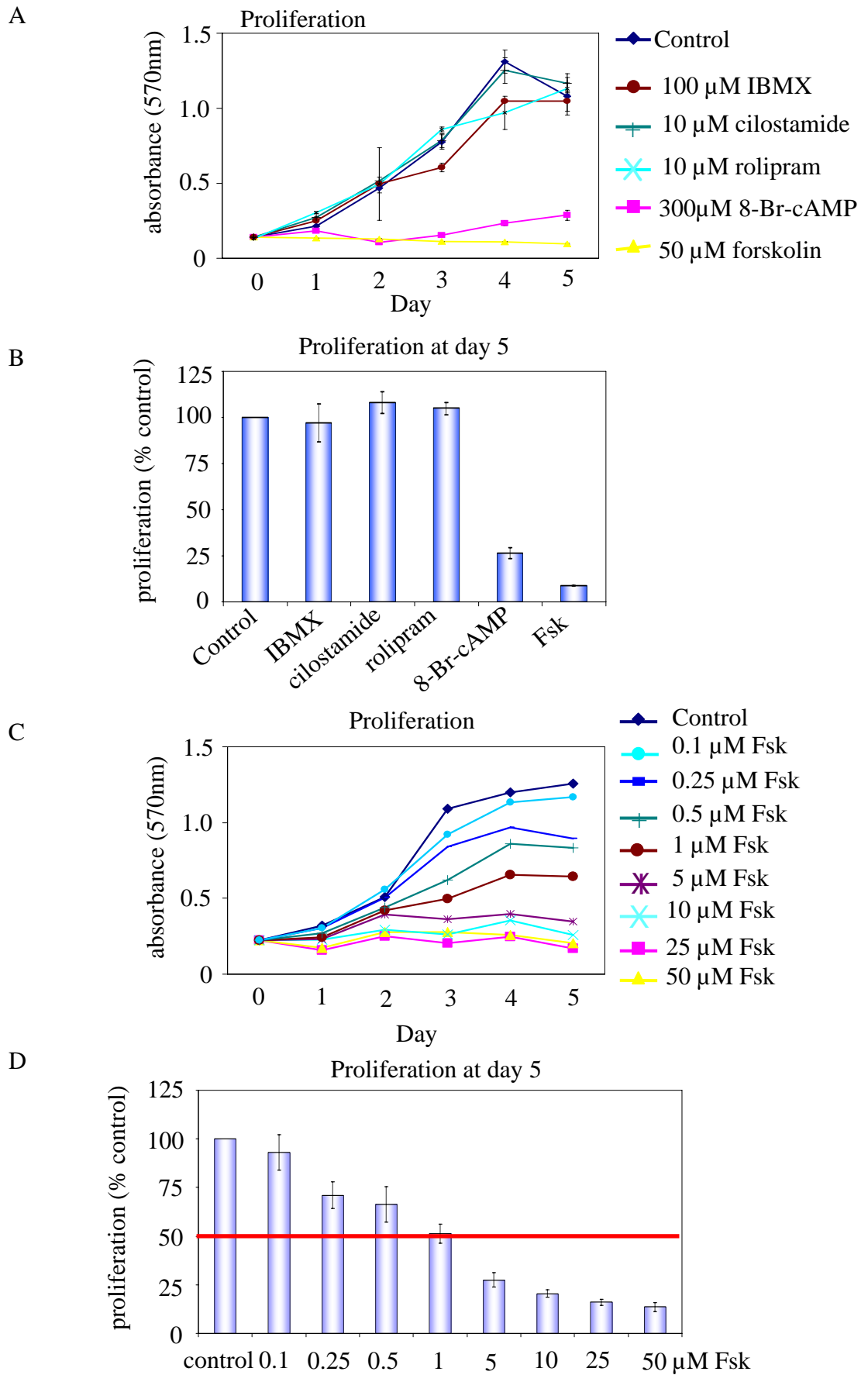
cAMP can have either a positive or negative effect on the proliferation of many cell types (130). However, when I started the work evidence in the literature suggested that the effect cAMP might have is cell type and context specific, and could occur by a variety of mechanisms (375, 387-389). Initial experiments, using an MTT assay to measure proliferation, showed that elevation of cAMP using the adenylyl cyclase activator forskolin (**Fsk**; 50 μ M; yellow line) and the non-hydrolysable cAMP analogue **8-Br-cAMP** (300 μ M; pink line) strongly inhibited the proliferation of KM12C cells over a five day period (Figure 14 A and quantified in Figure 14 B). The anti-proliferative effect of raising intracellular cAMP also occurs in other epithelial cancer cell types including breast (390), ovarian (391) and pancreatic (392). However the mechanism by which cAMP exerts its anti-proliferative effect may not be the same in each case.

Increasing cAMP by phosphodiesterase inhibition alone, using **IBMX** (a non-specific PDE inhibitor), **cilostamide** (a PDE3 specific inhibitor) or **rolipram** (a PDE4 specific inhibitor) at concentrations known to maximally inhibit PDE activity (218, 223, 262, 393), had no effect on the proliferation of KM12C cells (Figure 14 A and quantified in Figure 14 B). This is in contrast to adding the PDE3 and PDE4 inhibitors alone, where these were able to suppress

the proliferation of some normal and cancer cell types (242, 254, 375, 378, 380, 391, 394, 395).

50 μM Fsk completely inhibited the proliferation of KM12C cells (Figures 14 A and B). To define the mechanisms regulating local cAMP concentrations, a lower dose that only exhibited a partial response was required so that we then could modulate pools of cAMP using specific PDE inhibitors. We used **Fsk** at different concentrations and measured the effects on proliferation using the MTT dye based assay over a five day period. This allowed determination of the **Fsk** concentration that gave an approximate 50% inhibition of proliferation. **1 μM Fsk** (Figure 14 C; brown line and Figure 14 D) gave rise to 50% inhibition of proliferation at day 5 of the assay (as indicated by the red line on Figure 14 D). This '**low dose**' concentration of **Fsk** was then used in conjunction with PDE inhibitors to look for potentiation of the anti-proliferative effect.

Figure 14. cAMP inhibits the proliferation of KM12C cells. Proliferation of KM12C cells was monitored over a 5 day period using a MTT dye based assay using the absorbance at 570nm as a readout of viable cells, where increasing A570nm correlates with increased number of viable cells. Data points represent mean A570nm \pm SD of n=3 independent experiments (A) Cells were treated with control (DMSO; dark blue line), 100 μ M IBMX (non-specific PDE inhibitor; brown line), 10 μ M Cilostamide (PDE3 specific inhibitor; dark green line), 10 μ M rolipram (PDE4 specific inhibitor; light blue line), 300 μ M 8-Br-cAMP (non-hydrolysable cAMP analogue; pink line) and 50 μ M forskolin (Fsk, adenylyl cyclase activator; yellow line). (B) Quantification of (A) using proliferation at day 5 (C) A concentration range of Fsk (0.1 μ M – 50 μ M) to establish which concentration (1 μ M; brown line) gave an approximate 50% inhibition of proliferation (D) Quantification of Fsk concentration range in (C) at day 5 time point. Red line indicates 50% of proliferation. Data is expressed as a percentage of control A570nm, mean \pm s.d. (n=3 independent experiments).



3.3 PDE enzymes can regulate the anti-proliferative effects of cAMP

Intracellular signalling by cAMP is a highly compartmentalised process where localised cAMP caused by stimulation of specific receptors via adenylyl cyclase isoforms activates cAMP-binding proteins, such as PKA, Epac and PDEs (130, 143). To test whether or not specific PDE enzymes regulate the pool of cAMP controlling KM12C cell proliferation the 'low dose' (1 μ M) Fsk was used, in combination with PDE inhibitors, to try to potentiate the intermediate effect of the 'low dose' Fsk and so cause a greater inhibition of proliferation.

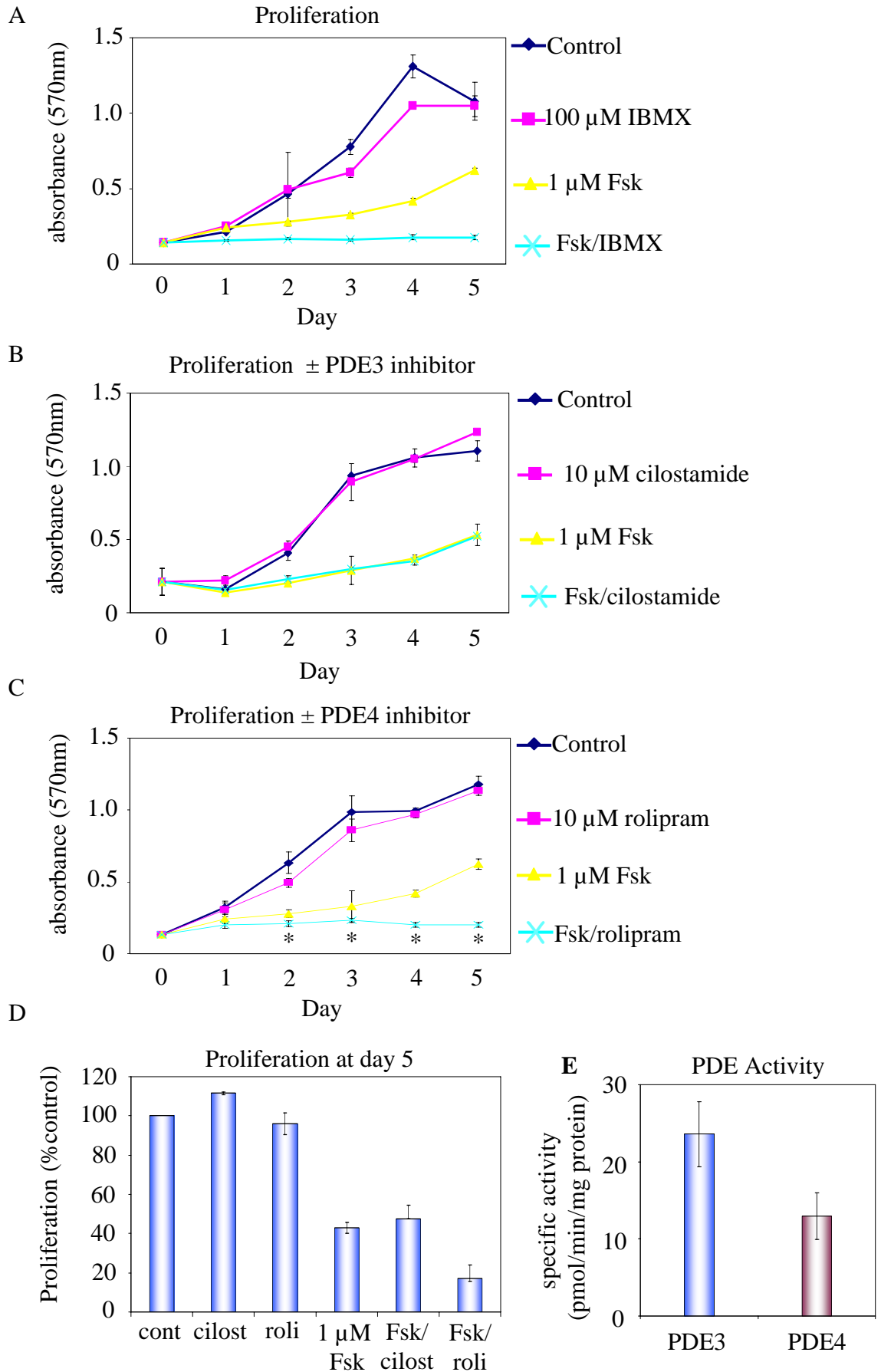
'Low dose' Fsk in combination with the non-specific inhibitor **IBMX** (Figure 15 A, light blue line) induced a complete inhibition of proliferation, where **IBMX** alone (Figure 15 A pink line) had no effect. As before, 'low dose' Fsk (Figure 15 A, yellow line) had only a partial effect (Figure 15 A). This data implied that one or more PDE enzymes was responsible for controlling cAMP regulated proliferation. Since the majority of cAMP hydrolysing activities comes from the PDE3 and PDE4 families (134, 262), it was logical to test whether or not PDE3 or PDE4 inhibitors in combination with 'low dose' Fsk caused growth cessation. The PDE3 inhibitor, **cilostamide**, had no effect on its own at a concentration known to maximally inhibit its activity (10 μ M, ref (223)) (Figure 15 B, pink line). **Cilostamide** did not potentiate the anti-proliferative effects of 'low dose' Fsk when used in combination (Figure 15 B; **Fsk/cilostamide**, light blue line) and 'low dose' Fsk had only an intermediate effect (Figure 15 B, yellow line). In contrast, the PDE4 inhibitor **rolipram**, used at a concentration known to maximally inhibit its activity (10 μ M (262, 393)), enhanced the partial growth suppression induced by 'low dose' Fsk alone (Figure 15 C; **Fsk/rolipram**, light blue line). Statistical analysis of the data in Figure 15 C, showed that there was no significant difference between **control** (vehicle; DMSO) versus **rolipram** alone (Figure 15 C, $P > 0.09$) for all time points. However, for **control** versus 'low dose' Fsk ($P <$

0.03), **'low dose' Fsk** versus **Fsk/rolipram** ($P < 0.02$) and **control** versus **Fsk/rolipram** ($P < 0.02$) the data were statistically significant from day 2 onwards (Figure 15 C) ($P < 0.05$ is statistically significant).

Thus, the above data suggests that under conditions of sub-maximal adenylyl cyclase activation, inhibition of specific cAMP-hydrolysing PDE4 enzymes can suppress the proliferation regulatory machinery in KM12C cells. This is interesting, as under resting conditions PDE3 enzymes have a greater activity (23.6 ± 4 pmol/min/mg protein; Figure 15 E) compared to PDE4 enzymes (13 ± 3 pmol/min/mg protein; Figure 15 E) in KM12C cells. This hints at compartmentalisation of PDE3 and PDE4 enzymes, with PDE4s regulating proliferation and PDE3s having, as yet, an undefined role in KM12C cells.

Figure 15. PDE enzymes regulate the anti-proliferative pool of cAMP. (A) Cells were treated with **control** (DMSO; dark blue line), the non-specific PDE inhibitor **IBMX** (100 μ M; Pink line), '**low dose**' **Fsk** (1 μ M; yellow line) or IBMX in combination with low dose Fsk (1 μ M Fsk +100 μ M IBMX; **Fsk/IBMX**; light blue line). (B) **Fsk/cilostamide** (1 μ M Fsk + 10 μ M cilostamide; light blue line) did not potentiate the partial growth inhibitory effects of Fsk alone (1 μ M Fsk; yellow line) and **cilostamide** alone (10 μ M; pink line) had no effect compared to **control** (DMSO; dark blue line). (C) **Fsk/rolipram** (1 μ M Fsk + 10 μ M rolipram; light blue line) completely inhibited proliferation whereas neither agent alone (**1 μ M Fsk** yellow line; **10 μ M rolipram** pink line) was able to do this. Values shown are mean \pm SD of 3 independent experiments * $P < 0.03$ compared with 1 μ M FSK alone. (D) Quantification of Fsk \pm PDE3/4 inhibitors in (B) and (C) at day 5 time point. Data is expressed as a percentage of control A570nm, mean \pm SD (n=3 independent experiments). (E) PDE activity assays were carried out *in vitro* using 1 μ M cAMP as substrate and the PDE specific inhibitors (cilostamide and rolipram) to calculate the resting activity of the relevant PDE family. The difference between control \pm inhibitor was used to calculate the specific activity. Activities are expressed as a mean \pm SD and were determined in 3 independent assays.

Figure 15. PDE enzymes regulate the anti-proliferative pool of cAMP



3.4 Epac did not mediate the anti-proliferative effects of cAMP

Exchange protein directly activated by cAMP (Epac) is a cAMP binding protein that acts as a guanine nucleotide exchange factor (GEF) for the small GTPases Rap1 and Rap2. Epac can mediate effects of cAMP independently of the main cAMP effector, PKA (132, 396). Rap1 activation by cAMP is one of a number of mechanisms proposed to mediate anti-proliferative effects of cAMP (387). Rap1 mediated inhibition of proliferation is thought to occur via negative regulation of MAP kinase and occurs in both PKA dependent (290, 388) and PKA independent pathways (397, 398). Until recently, there was a lack of biological tools to help distinguish between PKA and Epac dependent activation of Rap1. However, the development of a method for measuring the activation of Rap1 (GTP bound state) (399) and potent and specific Epac agonists which can efficiently activate Rap1 (8-pCPT-2'-O-Me-cAMP and 8-pMeOPT-2'-O-Me-cAMP) (188, 190, 191, 396), allows the efficient measurement of Rap1-GTP loading levels in an Epac specific manner.

50 μ M Fsk (**'high dose' Fsk**) and **'low dose' Fsk** (1 μ M Fsk) in combination with rolipram (**Fsk/rolipram**) induces complete growth cessation in KM12C cells (Figures 14 A and D). Therefore, the question of whether or not Epac/Rap1 is responsible for mediating cAMP-induced inhibition of proliferation observed was addressed.

Firstly, the Epac agonist was tested to ascertain whether or not it was able to induce Rap1 activation. Treatment with 100 μ M Epac agonist (8-pMeOPT-2'-O-Me-cAMP; **8-pMeOPT**) for 24 hours induced Rap1 activation (Figure 16 A) as compared to the control (DMSO; Figure 16 A). Subsequently, several conditions were set-up to test whether PDE4-induced Epac/Rap1 activation caused inhibition of proliferation. Five conditions were used to this end, namely **1) Control** (DMSO vehicle), **2) 'high dose'** (50 μ M) Fsk, which alone blocks cell proliferation, **3) 'low dose'** (**1 μ M**) Fsk (which only suppresses proliferation by around

50%), **4) rolipram** (10 μ M) which does not affect proliferation, and **5) the combination of 'low dose' Fsk** (1 μ M) plus **rolipram** (10 μ M) (**Fsk/rolipram**), which causes complete growth cessation (Figure 15 C). These treatments were used throughout the remainder of this thesis to investigate mechanisms of action. Cells were treated for 24 hours prior to the purification of Rap1-GTP. Lysates from untreated cells were incubated with either GTP γ S (Figure 16 B), a non-hydrolysable GTP analogue which constitutively activates Rap1 (positive control) or GDP (Figure 16 B) as a negative control for Rap1 activation. GTP γ S efficiently activated Rap1 compared to GDP. Total Rap1 and total Epac protein levels were used as loading controls (Figure 16 B). **'High dose' Fsk** and **Fsk/rolipram** induced Rap1 activation consistent with growth inhibition (Figure 16 B). **'Low dose' Fsk** produced only a partial increase in Rap1-GTP and **rolipram** had no effect on Rap1-GTP levels (Figure 16 B). Therefore, PDE4 regulated cAMP can activate Rap1, which could therefore contribute to reduced proliferation.

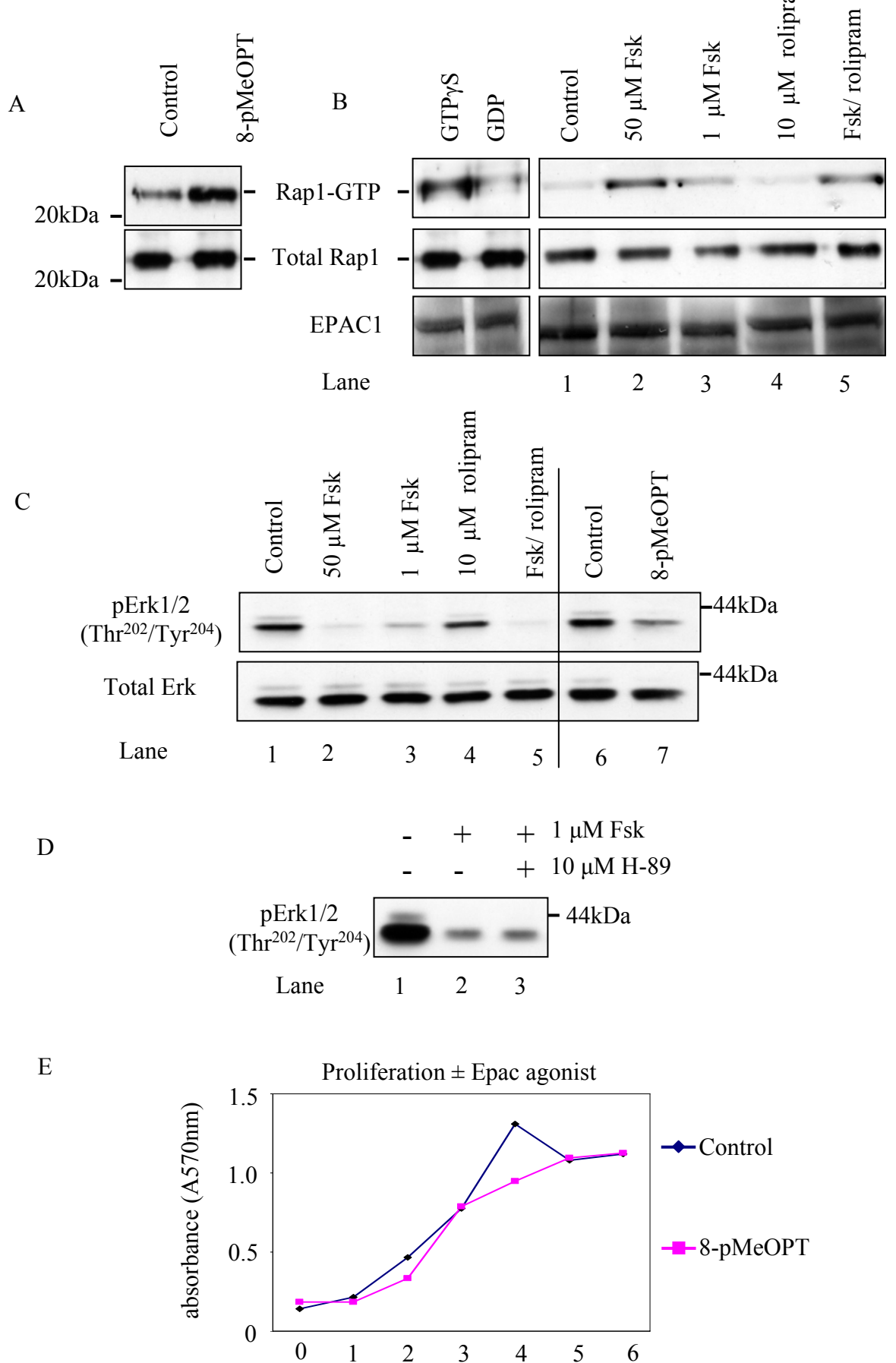
Treatment of cells with the five conditions – the standard treatment set – described above, resulted in both **'high dose Fsk'** and **Fsk/rolipram** suppressing pERK (Thr²⁰²/Tyr²⁰⁴) in a reciprocal manner to Rap1 activation (Figure 16 C). **Control** and **rolipram** treatment had no effect on pERK (Thr²⁰²/Tyr²⁰⁴) and **'low dose Fsk'** had only a partial effect (Figure 16 C). Treatment with the Epac agonist, **8-pMeOPT**, at a concentration known to activate Epac/Rap1, suppressed pERK (Thr²⁰²/Tyr²⁰⁴; Figure 16 C) compared to **control** and using total ERK as a loading control (Figure 16 C). This showed that pErk is suppressed in a reciprocal manner to Rap1 activation and is dependent upon PDE4 inhibition, which may be a mechanism by which proliferation was inhibited.

Treatment of cells with **'low dose' Fsk** alone induced the partial loss of pERK (Thr²⁰²/Tyr²⁰⁴) (Figure 16 D) and the PKA inhibitor H-89, when used in conjunction with **'low dose' Fsk**

had no effect on pERK (Thr²⁰²/Tyr²⁰⁴) status (Figure 16 D). This indicated that suppression of pERK was independent of PKA activity. Cells were then incubated with either **control** (DMSO, dark blue line) or 100 μ M Epac agonist (pink line) and proliferation of KM12C cells was monitored over a six day period (Figure 16 E). Despite the ability of the Epac agonist to activate Rap1 and suppress pERK (Thr²⁰²/Tyr²⁰⁴), there was no inhibition of proliferation observed (Figure 16 E). Thus, PDE4 regulated cAMP-induced activation of Epac/Rap1 and its subsequent suppression of pERK (Thr²⁰²/Tyr²⁰⁴) was not responsible for the inhibition of proliferation in KM12C cells, as the result could not be mimicked by direct activation of Epac/Rap1. Also, inhibition of PKA, in combination with '**low dose**' Fsk, did not negate pERK suppression, indicating that PKA is not involved in the cAMP inhibition of ERK phosphorylation. In fact, a role for PKA in the PDE4/cAMP mediated inhibition of proliferation was not elucidated and the reasons for which are discussed at a later point in this thesis.

Figure 16. Epac/Rap1 did not mediate the anti-proliferative effects of cAMP. The ability of PDE4 regulated cAMP to activate Rap1 via Epac was assessed. (A) Cells were treated with either **control** (DMSO) or 100 μ M Epac agonist (8-pMeOPT-2'-O-Me-cAMP; **8-pMeOPT**) for 24 hours and Rap1-GTP levels assessed. (B) Cells were treated with **control** (DMSO; lane 1), **'high dose' Fsk** (50 μ M; lane 2), **'low dose' Fsk** (1 μ M; lane 3), 10 μ M **rolipram** (lane 4) or **Fsk/rolipram** (1 μ M Fsk + 10 μ M rolipram; lane 5) for 24 hours and Rap1-GTP levels analysed. GTP γ S and GDP treated lysates were used as positive and negative controls for Rap1-GTP respectively. Total Rap1 and total Epac levels were used as loading controls. (C) The effect on pErk (Tyr²⁰²/Thr²⁰⁴) was assessed after treatment with the 5 conditions outlined in (B) and also after **8-pMeOPT** treatment (lane 7) . Total ERK was used as loading control. (D) pERK (Tyr²⁰²/Thr²⁰⁴) status after treatment with **1 μ M Fsk \pm 10 μ M H-89** (PKA inhibitor). (E) Proliferation of cells over a five day period \pm 100 μ M **8-pMeOPT**. All blots are representative of n=3 independent experiments. Proliferation assay points are mean A570nm \pm SD of n=3 independent assays. Molecular weight markers are indicated on blots.

Figure 16. Epac/Rap1 did not mediate the anti-proliferative effects of cAMP 102

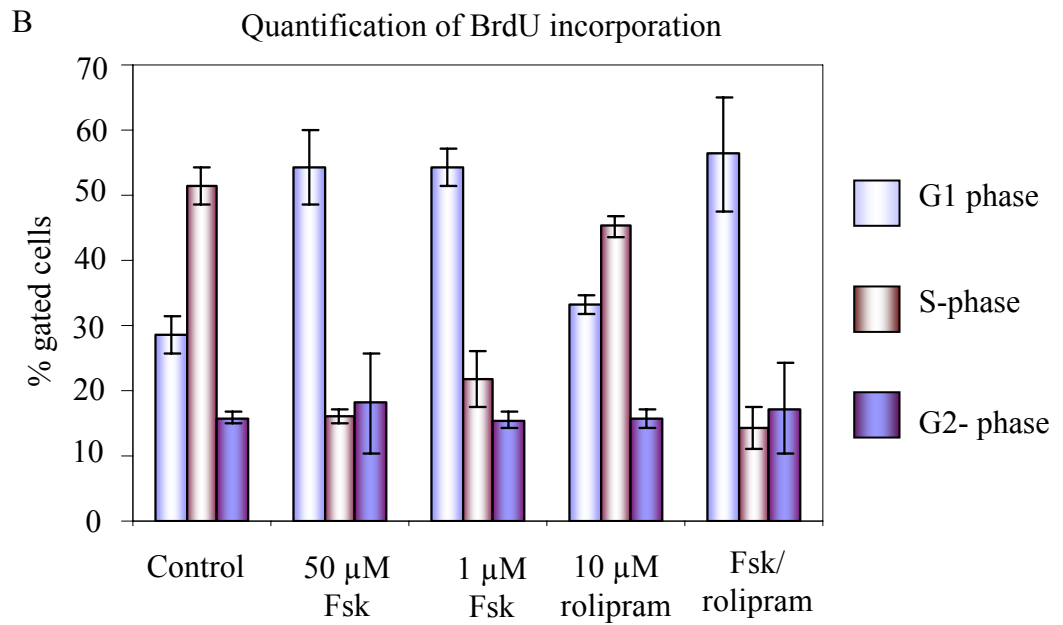
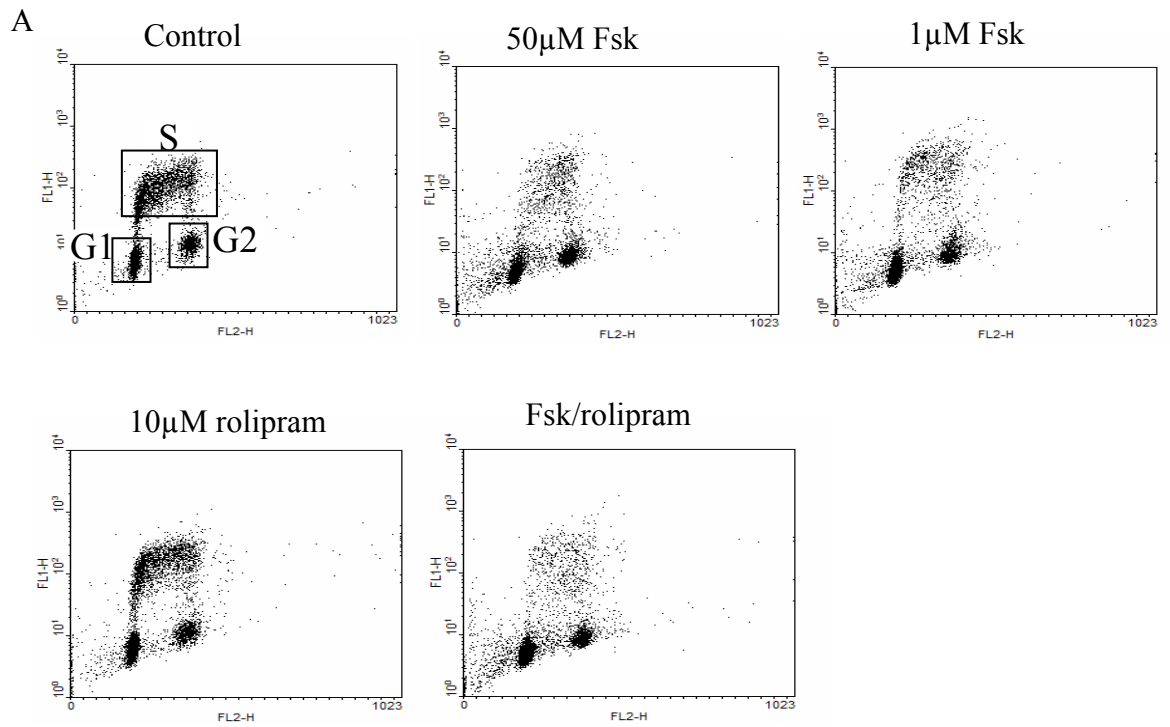


3.5 Fsk/rolipram induces a partial G1/S-phase arrest

In order to better understand the underlying mechanisms by which PDE4 regulated cAMP affects the colon cancer cells used here, KM12C, cell cycle distribution was analysed after treatment with cAMP modulators.

Cells were treated with the standard treatment set outlined in Chapter 3.4 for 24 hours, pulse labeled with 25 μ M bromodeoxyuridine (BrdU) for the final hour of treatment, stained with 10 μ g/ml propidium iodide (PI) and analysed by flow cytometry. Scatter plots were generated for each treatment (Figure 17 A) and analysis (Figure 17 B) of cell cycle stages was carried out using the gates as indicated in Figure 17 A (**control**). In keeping with the anti-proliferative effects observed by MTT assays, quantification of BrdU incorporation showed that **'high dose' Fsk** and **Fsk/rolipram** caused a partial G1 arrest, with around 15-20% of cells still in S-phase (Figure 17 A and B). We found that neither **'high dose' Fsk** nor **Fsk/rolipram** had any effect on G2-phase after 24 hours treatment (Figure 17 A and B). **Rolipram** alone had no effect (Figure 17 A and B) but surprisingly **'low dose' Fsk** caused a similar G1 arrest (Figure 17 A and B) to **Fsk/rolipram**, even although these cultures were still able to proliferate to around 50% of control cells in MTT assays (Figures 14 and 15). This implied that there were other mechanisms in addition to the G1/S-phase arrest which inhibited the proliferation of these cultures. I will come back to the reason for this apparent discrepancy between the proliferation assays and cell cycle analysis in a later chapter. However, next I will assess the effects of the standard treatments on cyclin dependent kinase inhibitor (CKI) proteins, in order to address the mechanisms regulating the G1/S-phase transition.

Figure 17. Fsk/rolipram induces a partial G1/S-phase arrest. Cells were treated with control (DMSO), 50 μ M Fsk (high dose Fsk), 1 μ M Fsk (low dose Fsk), 10 μ M rolipram or Fsk/rolipram (1 μ M Fsk + 10 μ M rolipram) for 24 hours, pulse labelled with BrdU for final hour of treatment and the cell cycle was analysed. (A) Representative scatter plots of BrdU/PI stained cells after treatments of n=3 independent experiments. (B) Quantification of BrdU pulse-labelled cells using gates indicated in control (A). Cell cycle distribution is presented as percentage of gated cells. Bar chart is mean of 3 independent experiments \pm SD.



3.6 Fsk/rolipram induces specific G1/S-phase CKIs

Key regulators of the G1/S-phase transition of the cell cycle are the Cip/Kip family of cyclin dependent kinase inhibitors. Previously, the PDE4 inhibitor rolipram was shown to induce expression of CKIs, p21^{Cip1} and p27^{Kip1}, leading to growth inhibition and differentiation of glioma cells (380). Therefore, we wished to assess the effects of our standard treatments on the expression of the G1/S-phase regulators p21^{Cip1} and p27^{Kip1} after 24 hours.

Firstly, unlike previous reports of Fsk inducing p21^{Cip1} expression (380), we found that neither **'high dose' Fsk** nor **Fsk/rolipram** treatments resulted in a consistent increase in p21^{Cip1} (Figure 18 A). However, **'high dose' Fsk** and **Fsk/rolipram** induced expression of the G1/S-phase inhibitor p27^{Kip1} by approximately 7 fold (Figure 18 A and quantified in Figure 18 B). **'Low dose' Fsk** induced a partial (approx 3.5 fold) increase in p27^{Kip1} expression (Figure 18 A and quantified in Figure 18 B), but had no effect on p21^{Cip1} expression, suggesting that only a small induction of p27^{Kip1} is sufficient for the partial G1/S-phase arrest (Figure 17 B). Neither **rolipram** nor **control (DMSO)** treatments had any effect on the expression of p21^{Cip1} or p27^{Kip1} (Figure 18 A and quantified for p27^{Kip1} in Figure 18 B).

3.7 Fsk/rolipram inhibits Rb/E2F regulated cell cycle proteins

p27^{Kip1} is an important regulator of cell cycle control and negatively regulates the CDK/cyclins responsible for G1/S-phase transition (353).

To help us understand the underlying mechanisms behind the G1/S-phase arrest, expression of Rb protein and Rb/E2F regulated cell cycle proteins was analysed by western blotting. After 24 hours treatment of KM12C cells with the standard treatment set outlined in Chapter 3.4, once again we found that p27^{Kip1} levels were increased under **'high dose' Fsk** and

Fsk/rolipram conditions (Figure 19 A). Induction of p27^{Kip1} by '**high dose**' **Fsk** and **Fsk/rolipram** paralleled an approximate 5-fold reduction in hyper-phosphorylated Rb (ppRb; upper arrow) and a shift to its faster migrating hypo-phosphorylated state (pRb; Figure 19 A). '**Low dose**' **Fsk** reduced the hyper-phosphorylated Rb by approximately 50% (Figure 19 A) which is consistent with the partial inhibition of proliferation observed, while **rolipram** alone had no effect on Rb phosphorylation (Figure 19 A).

'**High dose**' **Fsk** and **Fsk/rolipram** suppressed the expression cyclin A, cyclin B1, cyclin E and CDK1 (Cdc2) proteins to levels 3-4 fold less than control treated cells (Figure 19 A) and all of which are known to be targets of Rb/E2F regulation (364-367). For all the above, vinculin was used as a loading control (Figure 19 A). The induction of p27^{Kip1} and subsequent suppression of ppRb and Rb/E2F regulated cell cycle proteins, paralleled with the reduced G1/S-phase block and the growth inhibitory effects of **Fsk/rolipram**. This was probably contributing to the anti-proliferative effects of **Fsk/rolipram** treatment.

The effects of PDE4 regulated cAMP on the Rb/E2F pathway correlate with increased levels of p27^{Kip1}. One pathway which regulates p27^{Kip1} levels is the SCF (Skp1, Cul1 and F-box protein) ubiquitin ligase degradation pathway. One of the major components of this complex is the F-box adaptor protein Skp2, which targets p27^{Kip1} for ubiquitination and subsequent degradation by the 26S proteasome (400, 401). Skp2 is also overexpressed, and correlates with late stage disease and poor prognosis, in numerous cancers including non-small cell lung carcinoma (372, 402, 403), breast (371, 404), colorectal (373, 405) and ovarian cancer (374). Therefore, we examined whether PDE4 regulated cAMP alters Skp2 levels. Treatment with either '**high dose**' **Fsk** or **Fsk/rolipram** resulted in decreased Skp2 expression by approximately 10 fold in each case (Figure 19 B) and **rolipram** alone had no effect and '**low dose**' **Fsk** had only a partial effect on Skp2 protein expression (Figure 19 B).

Interestingly, Skp2 is a transcriptional target of E2F (406) which could provide an amplification loop for inducing p27^{Kip1} stability and G1/S-phase inhibition.

Figure 18. Fsk/rolipram induces a specific G1/S-phase CKI. Cells were treated with control (DMSO; lane 1), 50 μ M Fsk (high dose Fsk; lane 2), 1 μ M Fsk (low dose Fsk; lane 3), 10 μ M rolipram (lane 4) or Fsk/rolipram (1 μ M Fsk + 10 μ M rolipram; lane 5) for 24 hours and p21^{Cip1} and p27^{Kip1} protein levels were analysed by western blotting using specific anti-bodies as probes. (A) **‘High dose’ Fsk** (lane 2) and **Fsk/rolipram** (lane 5) increases p27^{Kip1} (middle panel) but does not affect p21^{Cip1} levels (top panel) (B) Quantification of change in p27^{Kip1} protein expression in (A). p27^{Kip1} expression is presented as fold-change compared to control in arbitrary units. Bar chart is mean of 3 independent experiments \pm SD.

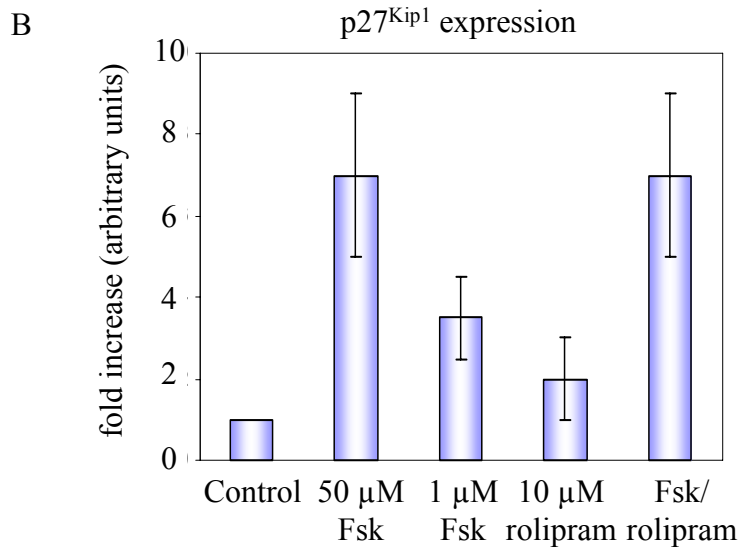
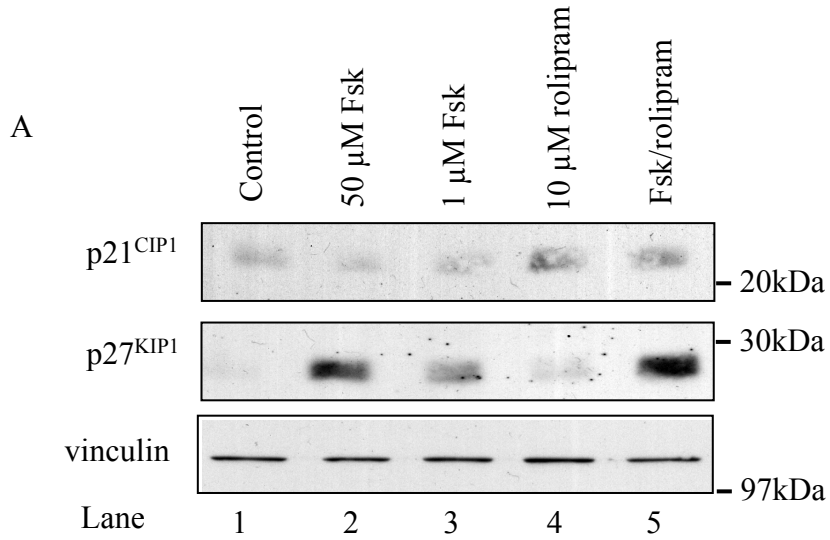
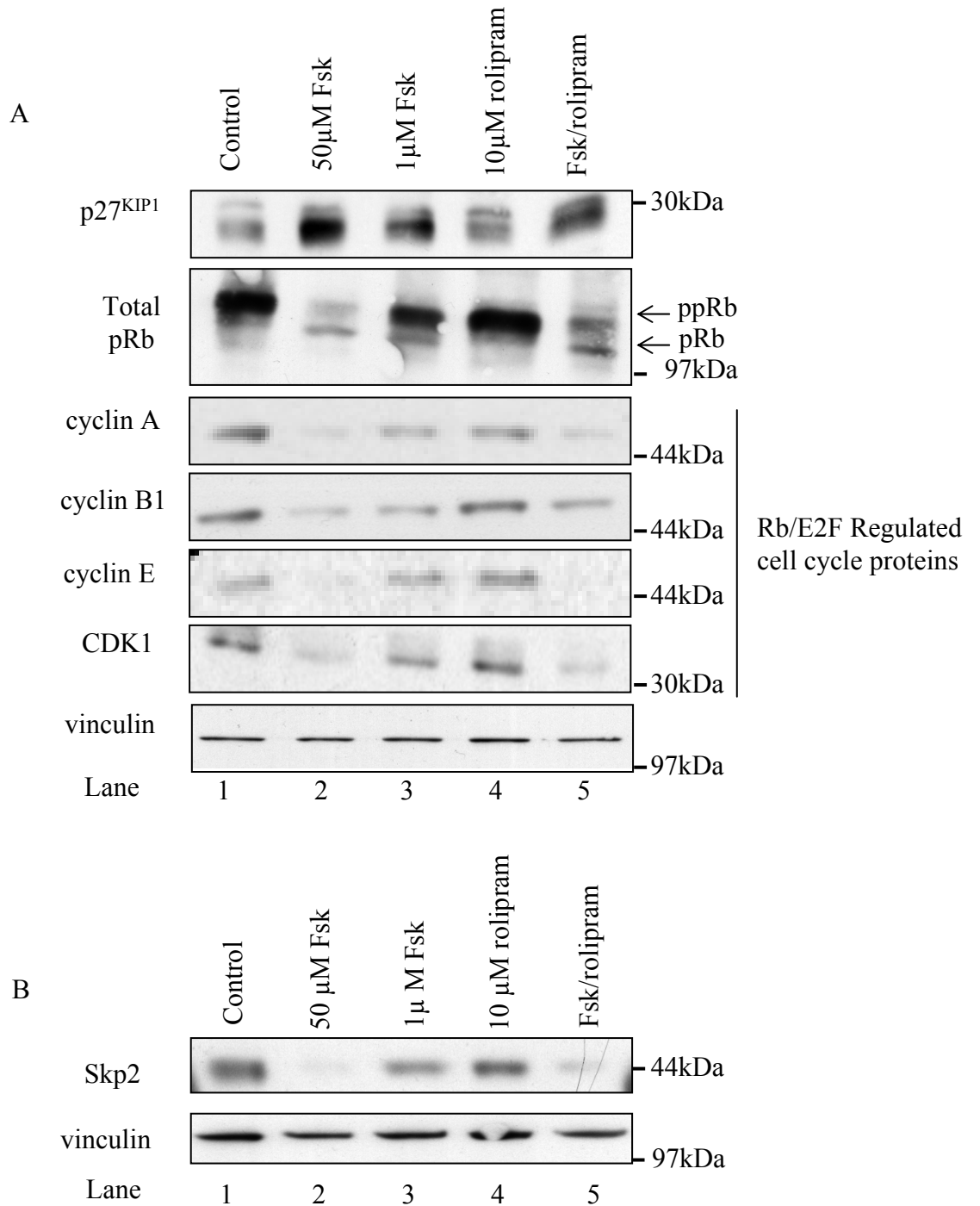


Figure 19. Fsk/rolipram treatment inhibits expression pRb/E2F regulated cell cycle proteins. Cells were treated with **control** (DMSO; lane 1), **'high dose' Fsk** (50 μ M; lane 2), **'low dose' Fsk** (1 μ M; lane 3), 10 μ M **rolipram** (lane 4) or **Fsk/rolipram** (1 μ M Fsk + 10 μ M rolipram; lane 5) for 24 hours and protein levels of Rb and downstream cell cycle regulators were analysed by western blotting using specific antibodies as probes. (A) **'High dose' Fsk** (lane 2) and **Fsk/rolipram** (lane 5) increases p27^{Kip1} (top panel), decreased hyper-phosphorylation of Rb (ppRb) and total Rb (2nd panel), and deregulated Rb/E2F regulated cell cycle proteins cyclin A (3rd panel), cyclin B1 (4th panel), cyclin E (5th panel) and CDK1 (6th panel). Vinculin immunoblotting (bottom panel) was used as a loading control in all of the above. (B) **'High dose' Fsk** (lane 2) and **Fsk/rolipram** (lane 5) caused a decrease in levels of the SCF ubiquitin ligase adapter protein Skp2 (upper panel). Vinculin immunoblotting was used as a loading control in all of the above. All blots are representative of n=3 independent experiments. The relative molecular weight markers are indicated next to blots.

Figure 19. Fsk/rolipram treatment inhibits expression pRb/E2F regulated cell cycle proteins



3.8 Fsk/rolipram induces a cell death morphology

Going back to investigate the apparent differences between the MTT assay versus cell cycle analysis (Figure 14 and Figure 17 respectively) where **'high dose Fsk'** and **Fsk/rolipram** cause complete growth cessation, whilst **'low dose' Fsk**-treated cultures can still proliferate, albeit more slowly, we examined cell viability. Treatment of KM12C cells was extended up to 72 hours and cell viability was then evaluated. Detection and analysis of cell death was exploited by several techniques including light microscopy, PI and Annexin-V staining.

The process of apoptotic cell death is characterised by several morphological and biochemical features that allows identification of dying cells in a population. Morphological features include cell shrinkage, rounding and blebbing of the membrane. Cells were seeded at a density of 5×10^5 cells per 60 mm dish, allowed to adhere overnight and treated with the standard conditions outlined in Chapter 3.4. Phase contrast images were then taken at either 24, 48 or 72 hours and analysed for evidence of cell death. In the control cultures after 48 hours, cells were tightly aggregated (Figure 20). However, **'high dose' Fsk** and **Fsk/rolipram** treatments resulted in fewer of these colonies and the emergence of what appeared to be small, round and shrivelled cells (Figure 20). **'Low dose' Fsk** had only a partial effect and **rolipram** alone had no effect on the morphology of the cells (Figure 20). This data suggested that **'high dose' Fsk** and **Fsk/rolipram** may have been inducing some form of cell death which would account for the differences observed in the proliferation assays (Figures 14-15) even although cell cycle profile of **'high dose' Fsk**, **Fsk/rolipram** and **'low dose' Fsk** were all similarly affected (Figure 17).

3.9 Fsk/rolipram induces DNA fragmentation

To quantify the relative abilities of each standard treatment used to induce cell death, cells were seeded and treated for 24, 48 or 72 hours, fixed in ethanol, stained with PI and analysed by flow cytometry. Fragmented DNA appears as the sub-2n-DNA region of the histograms (arrow indicates regions of interest in Figure 21 A). **Control** or **rolipram** treatments caused no significant increase in fragmented DNA at 24 or 48 hours (Figure 21 A, and quantified in Figure 21 B). An increase in sub-2n DNA content was observed after 72 hours but this was not statistically significant with $P > 0.09$. **'High dose' Fsk** and **Fsk/rolipram** induced more cell death within the cultures than **'low dose' Fsk** alone (Figure 21 A and quantified in Figure 21 B). The difference became statistically significant after 48 hours, with $P < 0.05$ (when compared to **'low dose' Fsk** alone), which was consistent with Figure 15 C, where the inhibition of proliferation became statistically significant after 2 days of treatment (**'low dose' Fsk** alone compared to **Fsk/rolipram**).

3.10 Fsk/rolipram induces apoptosis.

To confirm that **Fsk/rolipram** was inducing apoptotic cell death, Annexin-V staining and analysis by flow cytometry was used to detect early apoptotic cells over a 72 hour period. Cells were trypsinised and resuspended in Annexin-V binding buffer and incubated with Annexin-V FITC conjugate, PI and analysed. Detection of intact cells, early apoptotic and late apoptotic cells were analysed. Scatter plots were generated (Figure 22 A) and the lower right quadrants (corresponding to early apoptotic cells) were quantified (Figure 22 B). Cells treated with either **'high dose' Fsk** or **Fsk/rolipram** were induced to die by apoptosis (26% and 27% of gated cells respectively at 72 hours). This became statistically significant at 48 hours ($P < 0.05$) when compared to **'low dose' Fsk** alone (Figure 22 A, and quantified in Figure 22 B). **Control** (7%) and **rolipram** (10%) treated cells did not show a significant induction of apoptosis after 72 hours (Figure 22 A and quantified in Figure 22 B).

Importantly, **'low dose' Fsk** produced only a partial induction of early apoptotic cells (Figure 22 A and quantified in Figure 22 B).

Using PI and Annexin-V/FITC staining of cells, we found that both **'high dose' Fsk** and **Fsk/rolipram** treatments induced apoptosis in a manner that was statistically significant after 48 hours compared to **'low dose' Fsk** alone. This data indicates that **'low dose' Fsk** not only causes G1 arrest but also primes KM12C cells to die, presumably from the G1 arrested population, on addition of the PDE4 inhibitor rolipram and challenge with **rolipram** alone did not cause apoptosis (Figures 21 and 22).

Figure 20. Fsk/rolipram induces a cell-death like morphology. Cells were treated with **control** (DMSO), **'high dose' Fsk** (50 μ M), **'low dose' Fsk** (1 μ M), 10 μ M **rolipram** or **Fsk/rolipram** (1 μ M Fsk + 10 μ M rolipram for 48 hours and phase contrast images taken and alterations in cell shape and morphology was examined. **'High dose' Fsk** and Fsk/rolipram appear to induce altered cell morphology where more detached, rounded cells were visible compared to control (arrows indicate cells that were representative of those observed).

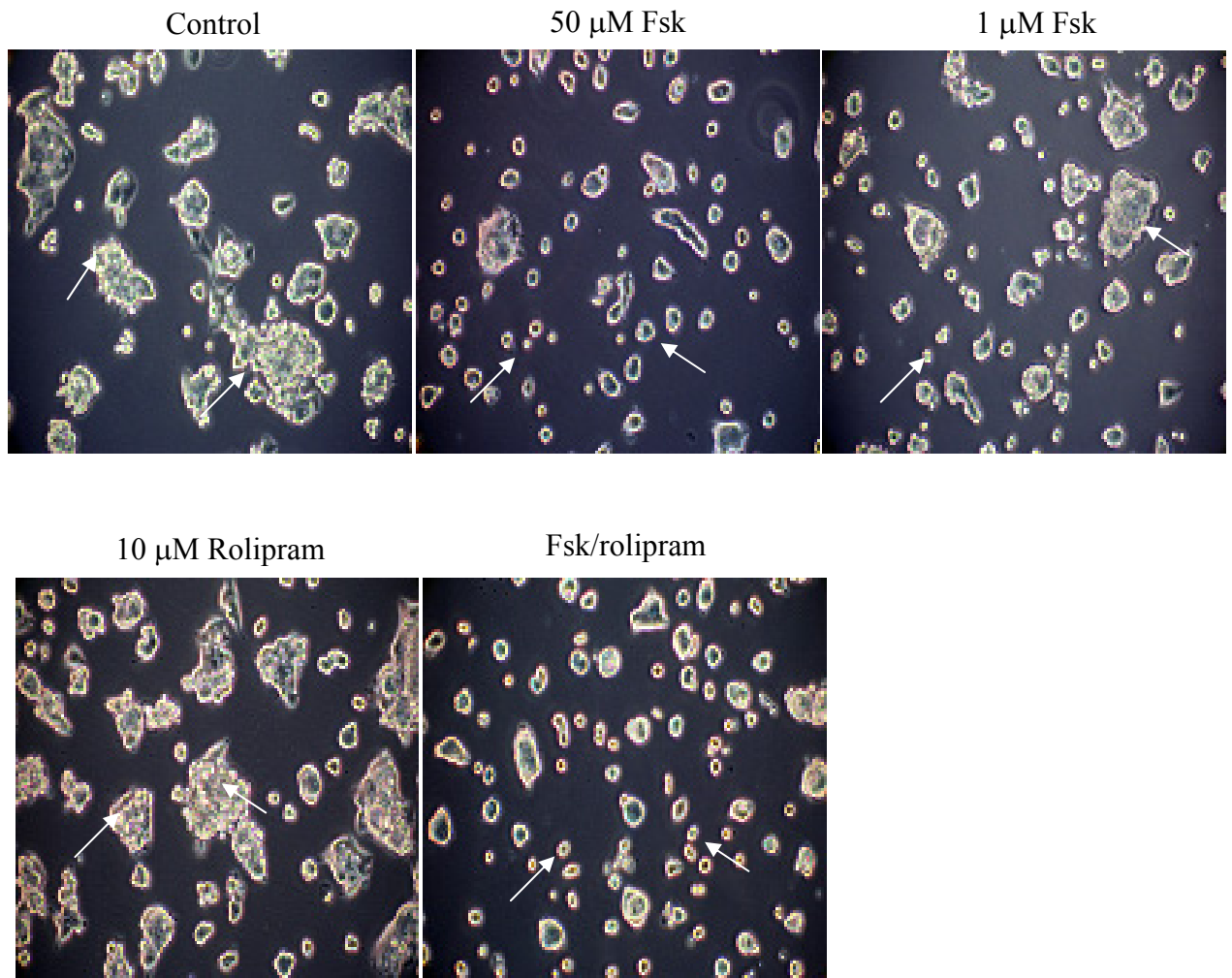
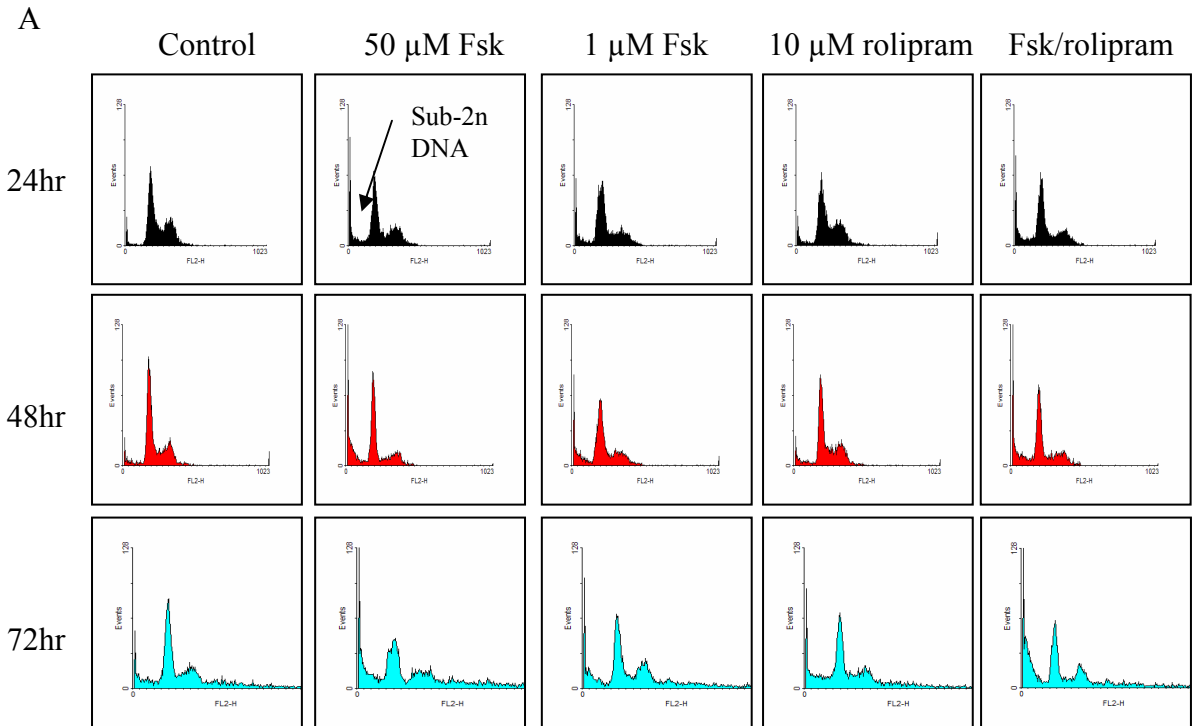


Figure 21. Fsk/rolipram induced DNA fragmentation. The effects on cell viability were examined by treatment with **control** (DMSO), 50 μ M Fsk (**'high dose' Fsk**), 1 μ M Fsk (**'low dose' Fsk**), 10 μ M **rolipram** or **Fsk/rolipram** (1 μ M Fsk + 10 μ M rolipram) for 24, 48 and 72 hours. Cells were then washed, trypsinised and incubated with propidium iodide (PI) and analysed by FACs for the detection of sub-2n DNA. (A) Representative histograms for all time points and treatments are shown, with the sub-2n region indicated by arrow. (B) Quantification of sub-2n DNA regions of the histograms and data is expressed as percentage of gated cells shown as a mean \pm SD of 3 independent experiments. * $P < 0.05$ compared to 1 μ M Fsk alone.

Figure 21. Fsk/rolipram induces DNA fragmentation



B Quantification of PI staining – sub-2n DNA content

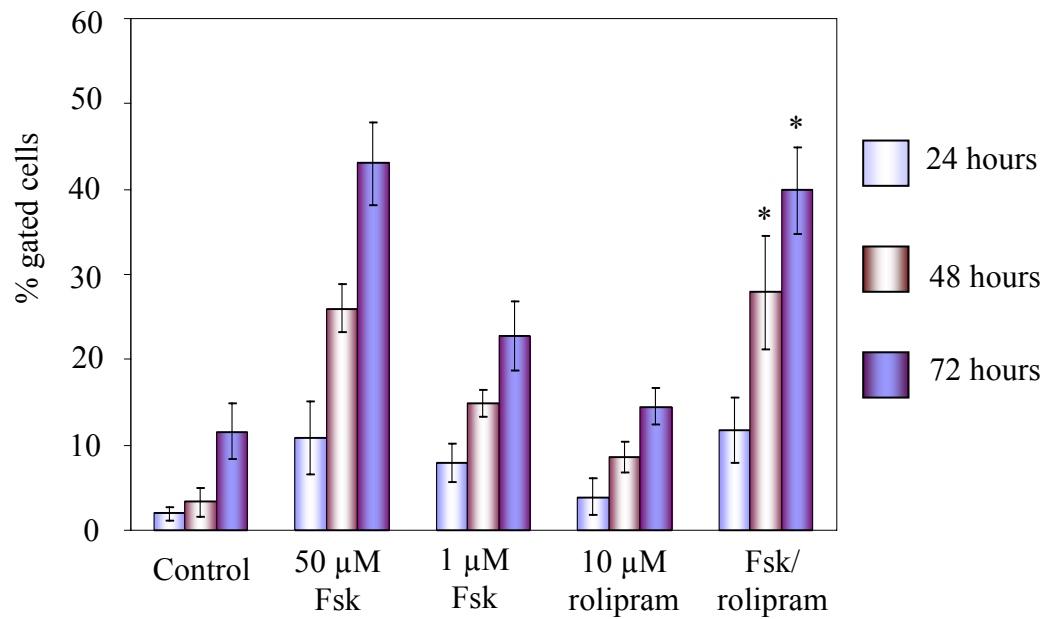
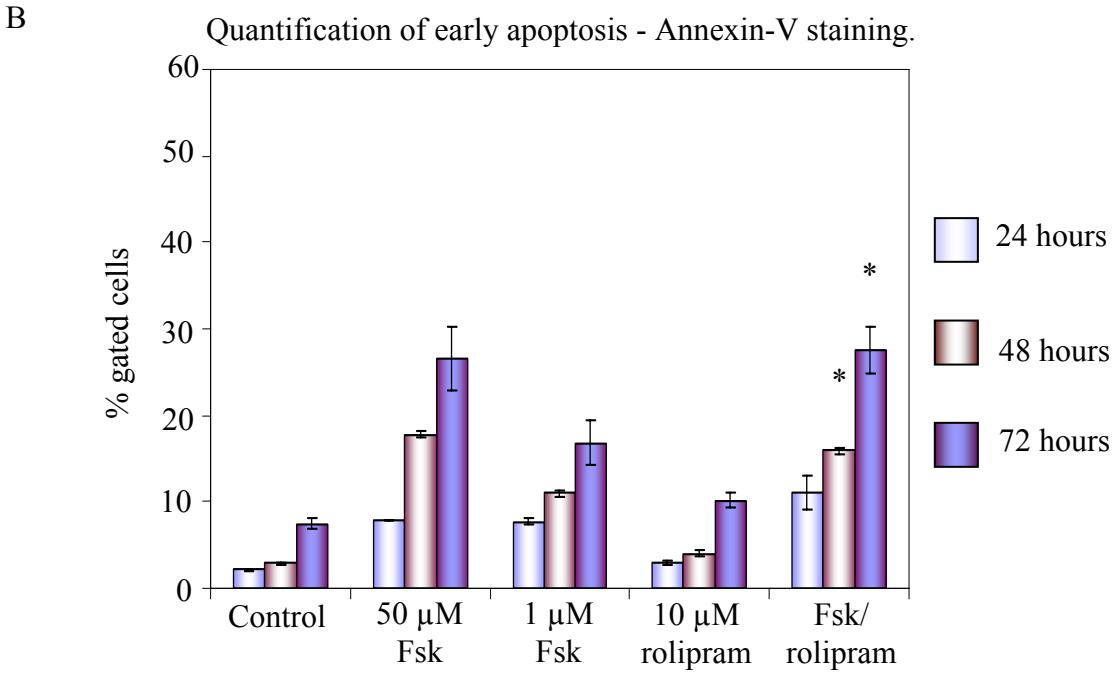
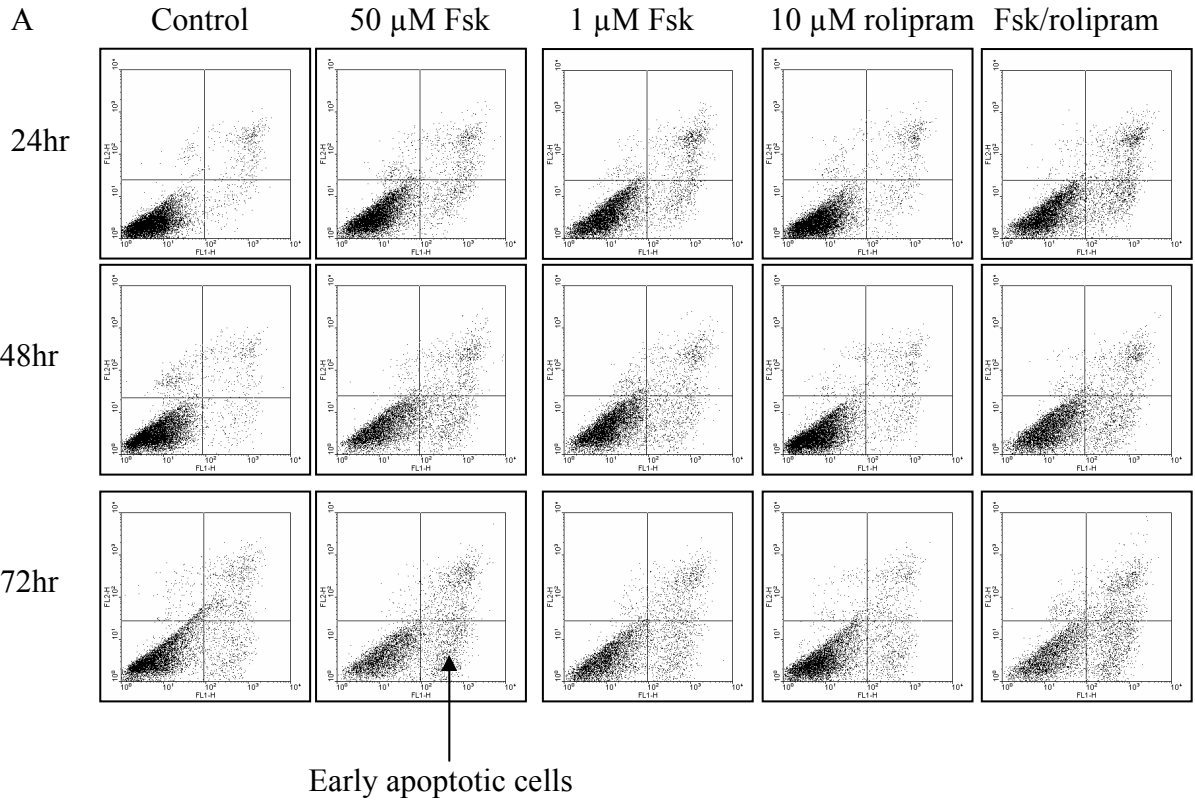


Figure 22. Fsk/rolipram induces apoptosis. To confirm the type of cell death induced cells were treated with with control (DMSO), 50 μ M Fsk (high dose Fsk), 1 μ M Fsk (low dose Fsk), 10 μ M rolipram or Fsk/rolipram (1 μ M Fsk + 10 μ M rolipram) for 24, 48 and 72 hours Cells were then washed, trypsinised and incubated with Annexin-V FITC conjugate, PI and analysed by FACs for the detection of early apoptotic cells. (A) Representative scatter plots for all time points and treatments are shown, with the lower right quadrant (corresponding to early apoptotic cells) indicated by arrow. (B) Quantification of lower right quadrants of the dot plots for the detection of Annexin-V positive early apoptotic cells. Data expressed as percentage of gated cells shown as a mean \pm s.d. of 3 independent experiments. * $P < 0.05$ compared to 1 μ M FSK alone.

Figure 22. Fsk/rolipram induces apoptosis



Discussion

3.11 Inhibition of chemo-resistant colon cancer cells by cAMP

Since their isolation, KM12C cells have been used for many studies, including the characterisation of the v-Src oncoprotein and its cellular homologue c-Src where its role in mediating cell-cell and cell-matrix adhesions was elucidated (77, 79-81). Proliferation of these cells, *in vitro* and *in vivo*, is unaffected by Src tyrosine kinase activity and expression (77, 79-81) and they are also resistant to cell death induced by common chemo-therapeutic agents such as 5-fluourouracil (5-FU) and cis-platin (V.G. Brunton, unpublished data). This increased tolerance to first-line therapeutics is a trait indicative of some advanced cancer cells, including colorectal cancer, and is therefore perhaps the major problem in colorectal cancer treatment (31, 407). This study used the KM12C colon cancer cells from the Fidler model of colorectal metastasis (40) to examine whether modulators of intracellular cAMP may provide means to kill chemo-resistant tumour cells, and ultimately colorectal cancer, thereby providing novel mechanisms by which these tumours may be treated.

Numerous studies have shown that cAMP can have either a positive or negative effects on proliferation, which is both cell type and context specific (387, 388). However, in the majority of cases cAMP appears to have an anti-proliferative effect. The inhibition of proliferation by cAMP occurs by a variety of mechanisms that can lead to either cell cycle arrest and/or apoptosis. For example, as I was carrying out my work Naderi *et al* published that by using cAMP elevating agents such as forskolin, IBMX and PGE₂, a S-phase arrest and an inhibition of DNA replication was induced (408). This correlated with increased p21^{Cip1} levels and subsequent binding to (and inhibition of Cdk2-cyclin complexes), leading to dephosphorylation of Rb and dissociation of PCNA (Proliferating Cell Nuclear Antigen) from chromatin in S-phase cells. cAMP has also been shown to induce apoptosis as a means of inhibiting cancer cell proliferation. This has been shown in A-172 glioma cells, where

elevation of cAMP using 8-Br-cAMP, forskolin or IBMX resulted in the activation of PKA and subsequent decreased proliferation and increased apoptosis (409).

In the work presented in this thesis, we used chemical agents that have previously been shown to directly increase cAMP, such as forskolin and 8-Br-cAMP, as well as indirectly by modulating the breakdown of cAMP to the inactive 5'AMP. We found that only forskolin (at relatively high doses) and 8-Br-cAMP had significant effects on KM12C cells and that using the PDE inhibitors IBMX, cilostamide or rolipram on their own was insufficient to suppress proliferation. This indicated that the adenylyl cyclase (AC) molecules were in a 'low' activity state, which can be the result of reduced endogenous activation by GPCR/ $G\alpha_s$ proteins, inhibition by $G\alpha_i$ proteins or low levels of signalling by other molecules known to activate ACs (410). We also investigated whether or not rolipram, in combination with GPCR agonists, such as PGE2 and isoproterenol (β_2 -adrenergic receptor agonist), could synergise and inhibit KM12C proliferation. We have some preliminary evidence that PGE2, and not isoproterenol, can synergise with rolipram and inhibit KM12C proliferation (data not shown), indicating that natural agonists that are often overexpressed by colorectal tumours (reviewed in (156)), may be utilised to inhibit their proliferation.

Thus, we have shown that in cells, refractory to Src kinase inhibitors and common chemotherapeutics such as Cis-platin and 5-FU, cAMP can robustly inhibit their proliferation when its production is exogenously stimulated.

3.12 Is Epac or PKA regulating KM12C proliferation?

cAMP-induced inhibition of proliferation can occur by a number of mechanisms, one of which is the inhibition of the ERK pathway (411). Both of the major cAMP effectors, PKA and Epac, have been shown to inhibit the ERK pathway in a context specific manner, but both can do so by the inhibition of the upstream kinase Raf-1. PKA can phosphorylate and inactivate Raf-1 on a number of residues, including Ser²⁵⁹, and cAMP mediated activation of Epac induces Rap1 association with Raf-1 and prevents its activation by Ras (283, 290, 387).

We have shown that under conditions which inhibit proliferation, namely **'high dose' Fsk** and **Fsk/rolipram**, Rap1 is activated (presumably by Epac) and correlates with a suppression of ERK phosphorylation. Moreover, the suppression of pERK appears to be mediated by Epac activated Rap1 as use of the Epac specific agonist, 8-pMeOPT, suppresses pERK and also, use of the PKA inhibitor H-89 does not counter the effects of Fsk on pERK suppression, indicating that is occurring in a manner independent of PKA. However, the Epac/Rap1 mediated suppression of pERK does not appear to be responsible for inhibiting the proliferation of KM12C cells, as 8-pMeOPT did not inhibit the proliferation of these cells.

Despite the inhibition of PKA not having an effect of pERK, we have not fully ruled out the possibility of it having a role in the PDE4/cAMP mediated inhibition of proliferation. We examined PKA activity after our standard treatment set (as outlined in Chapter 3.4) and PKA activity was elevated under all conditions compared to control treatment (data not shown). However, we were hampered in our efforts to assess whether or not inhibition of PKA, using either H-89 or the more potent and specific inhibitor KT5720 (412), in conjunction with Fsk/rolipram was able to counteract the anti-proliferative effects as PKA inhibition alone was sufficient to inhibit the proliferation of KM12C cells (data not shown). If time permitted,

further investigation could make use of RNAi depletion of PKA types I and II, as well as using the Ht31 peptides which disrupts anchoring of PKA type II to AKAPs (237) to elucidate the mechanisms by which PKA can regulate KM12C proliferation and also whether or not PKA activity is required for Fsk/rolipram mediated inhibition of proliferation.

3.13 PDE3 vs PDE4 induced inhibition of proliferation

Modulation of specific ‘pools’ of cAMP that was regulated by specific PDE enzymes, was achieved using the ‘**low dose**’ Fsk, which caused a partial inhibition of proliferation, in combination with PDE inhibitors, which in the cases of IBMX (non-specific PDE inhibitor) and **rolipram** (PDE4 specific), resulted in a synergistic inhibition of proliferation. The PDE inhibitors, when used alone, were unable to elicit any effect on the proliferation of KM12C cells. This approach allowed us to determine which PDE family was responsible for regulating the anti-proliferative intracellular pool of cAMP. This was in contrast with previous research which showed that, at least in the same context, PDE inhibition alone was sufficient to prevent the proliferation of several cell types (378, 380, 394, 413). Presumably, in their situation adenylyl cyclase was in a ‘high’ activity state, and inhibition of cAMP breakdown caused a larger accumulation of cAMP in those cells.

The combination of Fsk plus the non-specific PDE inhibitor IBMX has been used extensively to elicit the maximum cAMP response of cells. When we used IBMX in combination with low dose Fsk we observed an inhibition of proliferation, indicating that one or more PDEs are controlling the ant-proliferative pool of cAMP. Since PDE3s and PDE4s constitute the major cAMP hydrolyzing machinery in the cell (134, 262), we used specific inhibitors of these enzymes in conjunction with low dose Fsk. Intriguingly, we showed that KM12C cells can be efficiently growth arrested by a low dose combination of the adenylyl cyclase activator forskolin, and the PDE4 selective inhibitor rolipram (Figures 15, 17, 21 and 22), but not by forskolin plus the PDE3 selective inhibitor cilostamide. Such selectivity is consistent with the

now well-established notion that cAMP signalling is compartmentalised in cells, with PDE3 and PDE4 activities contributing to distinct functional compartments (218, 262, 414). The ability of PDE4 enzymes to negatively regulate proliferation of cells, including cancer cell lines, is now becoming clear. For example, in chronic lymphocytic leukaemia (CLL) and B-cell CLL (B-CLL), the PDE4 inhibitor rolipram, alone and in combination with Fsk, was shown to inhibit the proliferation of these cell lines (375, 377). This is consistent with other reports highlighting cAMP and PDE4 enzymes as critical regulators of proliferation in numerous other cell lines (242, 339, 378, 380).

In contrast to PDE4 inhibitors, PDE3 inhibitors in combination with **'low dose' Fsk** did not potentiate the anti-proliferative effect of Fsk in the KM12C cells. Such distinct compartmentalisation of PDE3 and PDE4 enzymes regulating separate intracellular pools of cAMP in the same cell type has been previously reported. For example, in rat mesangial cells inhibition of PDE3 enzymes results in an inhibition of DNA synthesis, whereas PDE4s in the same cell type regulates the generation of reactive oxygen metabolites (394). Also, using real-time imaging of cAMP generation in situ, PDE4 enzymes were shown to be responsible for regulating the duration and amplitude of rat cardiac myocytes response to the β -agonist, norepinephrine (218). PDE3 enzymes are also localised to distinct compartments but had no role in the response to β -agonists. In addition, it has recently emerged that PDE3 enzymes regulate cAMP concentrations in sarcoplasmic reticulum, resulting in increased Ca^{2+} -ATPase pumping in PI 3-kinase- γ deficient cardiac myocytes (415). Also, loss of PI 3-kinase- γ expression selectively abolishes PDE4, but not PDE3, activity (415). In KM12C cells, the role of PDE3 enzymes, if any, has still to be explored. However, our results further underpin the compartmentalisation of cAMP signalling and show that specific pools of cAMP can regulate precise cellular outcomes.

3.14 PDE4/cAMP controlled cell cycle arrest

One of the first studies that linked cAMP to cell cycle regulation, and in particular an inhibition of G1/S-phase, was carried out by Kato *et al* (416). These authors showed that by modulating cAMP, they could induce a G1/S-phase arrest by induction of p27^{Kip1}. Following on from this, several groups have noted that cAMP, and in particular PDE4 regulated cAMP, can induce the CKIs p21^{Cip1} and p27^{Kip1}. For example, in malignant glioma cells rolipram mediated inhibition of proliferation occurs via the induction of both p21^{Cip1} and p27^{Kip1} CKIs resulting in differentiation and eventually apoptosis (380). Rolipram has also been shown to induce p21^{Cip1} in lymphoblastic leukaemia cells (378) and p27^{Kip1} in corneal epithelial cells (336). In our study, we showed that inhibiting PDE4s, in combination with low dose forskolin treatment, induced p27^{Kip1}. This provides further evidence that PDE4 regulated cAMP can control the expression of G1/S-phase CKIs and that PDE4s may be useful therapeutic targets for several human malignancies.

We have shown that under conditions that inhibited the proliferation of KM12C cells, namely **‘high dose’ Fsk** and **Fsk/rolipram**, levels of the SCF adaptor protein Skp2 were substantially decreased (Figure 19 B). This suggests that the mechanism by which p27^{Kip1} accumulates during cell cycle withdrawal may be due, at least in part, to loss of Skp2-mediated degradation. It has also been reported that targeting of p27^{Kip1} for degradation requires phosphorylation on its Thr¹⁸⁷ by the cyclin E/CDK2 complex (355) which acts as a substrate recognition motif for Skp2 (360, 361). Here, we monitored p27^{Kip1} levels using an antibody against total protein, but we were unsuccessful in observing the phosphorylation status at Thr¹⁸⁷ using a phospho-specific antibody due to a lack of specificity and high background noise (data not shown). Previously, there has been only one report of cAMP mediated down-regulation of Skp2 protein levels (362) and we have provided the first link

between PDE4 inhibition and the suppression of Skp2, an important regulator of p27^{Kip1} stability and cell cycle progression.

3.15 Rolipram mediated apoptosis

Apoptosis is the protective mechanism by which cells undergo programmed cell death in response to signals such as DNA damage, growth factor withdrawal and activation of death receptors and is functionally distinct from autophagy and necrosis. The apoptotic program itself is characterized by certain morphologic features, including loss of plasma membrane asymmetry and attachment, condensation of the cytoplasm and nucleus, and internucleosomal cleavage of DNA. Previous work in a number of cell types has implicated PDE4 enzymes as regulators of apoptotic pathways. For example, treatment of B-CLL cells with the PDE4 specific inhibitor rolipram induces apoptosis of the B-CLL cell population but not T-cells in a manner that requires PP2A (protein-phosphatase 2A) but not the cAMP effector Epac/Rap1 (291, 375, 377, 417). Indeed, rolipram has also been shown to induce apoptosis in other haematological malignancies including acute lymphoblastic leukaemia (378) and diffuse large B-cell lymphoma (DLBCL) (339). Also, rolipram can induce apoptosis in malignant glioma cells after extended treatment (greater than 48 hours) (380). The data available for the effects of rolipram on haematological malignancies has led to the idea that PDE4 inhibitors may be useful anti-cancer agents in the clinic (254).

In the context of breast cancer, resveratrol (RSVL) is a naturally occurring, biologically active, phytoalexin commonly found in grapes and berries (418, 419) and is proposed to be a chemo-protective agent in breast cancer models (420). Treatment of MCF7 cells (breast epithelial cancer cell line) with RSVL selectively activated adenylyl cyclase (and not guanylyl cyclase) and inhibited the proliferation of the breast cancer cells (421). Moreover, a combination of RSVL and rolipram significantly augmented the inhibition of proliferation by

cAMP, indicating that PDE4 enzymes were regulating the anti-proliferative pool of cAMP in MCF7 breast cancer cells (421).

Our work has provided further evidence that PDE4 regulated cAMP can inhibit proliferation and induce apoptosis in a colorectal cancer cell line that is difficult to kill. This may offer a potential therapeutic opportunity to combine PDE inhibitors with low concentrations of adenylyl cyclase activators, as we have mimicked here, although with non-physiologically relevant Fsk, as novel anti-cancer therapeutic approach.

3.16 Summary

In KM12C cells, elevation of cAMP by high dose Fsk or treatment with a non-hydrolysable cAMP analogue, resulted in complete growth cessation. A combination of low dose Fsk plus PDE4 (but not PDE3) recapitulated these results, where neither alone had any effect. Fsk/rolipram induced a G1/S-phase arrest, presumably, as a result of increased p27^{Kip1}, decreased ppRb and inhibition of Rb/E2F regulated cell cycle proteins including cyclins A, B1 and E and CDK1 as well as the SCF ubiquitin ligase adaptor protein, Skp2. This resulted in complete deregulation of the cell cycle and sustained treatment (>24 hours) with Fsk/rolipram induced apoptosis more effectively than low dose Fsk alone, contributing to the anti-proliferative effect of cAMP on chemo-resistant KM12C cells.

Together with my work, these observations raise the exciting possibility of cAMP modulation as a novel anti-cancer therapy that may attack some chemo-resistant cancers. I will address the generality of my findings in a number of solid cancers later (Chapter 6.2) and discuss how we might utilise this *in vivo* (Chapter 7.1). This further highlights the importance for developing PDE4 inhibitors as novel anti-cancer agents for the treatment of the disease.

Chapter 4:
cAMP interference with oncogene addiction

4. cAMP interference with oncogene addiction

4.1 Aim

We showed that PDE4 regulated cAMP inhibits the proliferation of KM12C cells. In this chapter, we describe the mechanisms by which PDE4/cAMP inhibits a pathway critical for KM12C proliferation and survival. We also describe the alterations that lead to oncogene addiction and how exogenous reconstitution of a key component of the pathway alters proliferation and sensitises the cells to further inhibition by modulation of cAMP.

4.2 Loss of pAkt (Ser⁴⁷³) is an early event in PDE4/cAMP inhibition of proliferation

Using a 36 hour time course of **Fsk/rolipram** (1 μ M Fsk + 10 μ M rolipram) treatment of KM12C cells to monitor the changes of cell cycle regulators (as detailed in the previous chapter), we determined the order, and timing, of some events important for PDE4/cAMP mediated inhibition of proliferation. The induction of p27^{Kip1} (Figure 23), observed at 6 hours, occurs at approximately the same time as loss of hyperphosphorylated Rb (ppRb) (Figure 23) and loss of Skp2, but precedes the loss of CDK1 which occurs at between 20 to 22 hours after start of treatment (Figure 23). The induction of p27^{Kip1} is probably brought about, at least in part, by stabilisation of the protein, due to a partial loss of Skp2 expression at approximately the same time (6 hours) (Figure 23). This is likely to result in the binding of p27^{Kip1} to CDK/cyclin complexes and suppression of hyperphosphorylated Rb.

The early events governing induction of p27^{Kip1} are unknown. To help understand the early events by which PDE4 regulated cAMP inhibited proliferation, the PI 3-kinase pathway was examined, since it has a major role in regulating cell growth and survival (300). As an initial readout of PI 3-kinase activity, the phosphorylation status of the major downstream effector, Akt at Serine 473 (pAkt (Ser⁴⁷³)) was used. Treatment with **Fsk/rolipram** resulted in the

loss of pAkt (Ser⁴⁷³) between 0 and 3 hours of treatment (Figure 23). Total Akt was used to ensure equal loading in each lane (Figure 23). The reduction in pAkt (Ser⁴⁷³) at such an early time point, and prior to the induction of p27^{Kip1}, loss of hyperphosphorylated Rb or Rb/E2F regulated cell cycle proteins, suggests that this may lie upstream of cell cycle withdrawal. This implies that PDE4 regulated cAMP may be impeding throughput of the PI 3-kinase/Akt pathway.

4.3 Fsk/rolipram perturbs PtdIns(3,4,5)P₃ localisation

Phosphatidylinositol (3,4,5)-trisphosphate (PtdIns(3,4,5)P₃) is a second messenger and the product of class I PI 3-kinase enzymes that phosphorylate phosphatidylinositol (4,5)-biphosphate (PtdIns(4,5)P₂) on the 3 position of the inositol ring structure. PtdIns(3,4,5)P₃ recruits and activates kinases with a lipid-protein interaction, PH, domain (300). To assess any effects **Fsk/rolipram** may have on PI 3-kinase activity, we used the PH domain of Akt fused to GFP (PH-GFP) as a reporter of PtdIns(3,4,5)P₃ localisation (422). Under **control** (DMSO) and **rolipram** conditions, PH-GFP was constitutively localised to the plasma membrane in a uniformly distributed manner (Figure 24 A). Under conditions that inhibited proliferation (namely '**high dose**' **Fsk** and **Fsk/rolipram**) displacement of PH-GFP from the plasma membrane was observed (Figure 24 A). Localisation of PH-GFP was quantified by counting 100 transfected cells under each condition in 3 independent experiments and statistical analysis of the differences was carried out. Both '**high dose**' **Fsk** and **Fsk/rolipram** had less than 20% of cells with PH-GFP localised at the plasma membrane (quantified in Figure 24 B) and the differences were statistically significant ($P < 0.05$ '**high dose**' **Fsk** versus **control** and $P < 0.05$ **Fsk/rolipram** versus '**low dose**' **Fsk**). '**Low dose**' **Fsk**, which caused a partial inhibition of proliferation, displayed an intermediate phenotype, where both membrane localisation and internalised PH-GFP was evident. Approximately 50 % of cells analysed showed uniform distribution of the PH-GFP reporter at the plasma membrane, similar to that of both **control** and **rolipram** treatments (Figure 24 A and quantified in Figure 24 B). Thus, under conditions that inhibited the proliferation of KM12C cells, namely '**high dose**' **Fsk** and **Fsk/rolipram**, a loss of PH-GFP, and presumably therefore PtdIns(3,4,5)P₃, from the plasma membrane correlated with the growth suppressive effects of these treatments.

4.4 Fsk/rolipram displaces PI 3-kinase p85 α subunit from the cell periphery

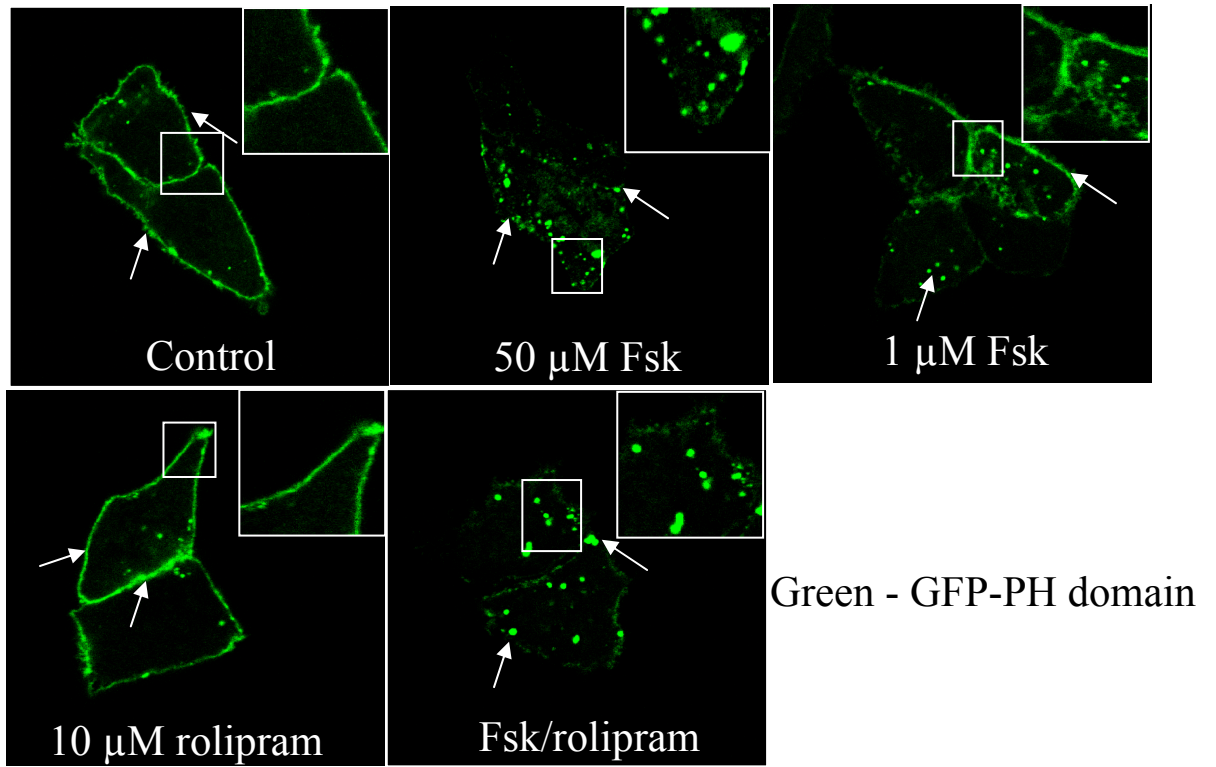
PI 3-kinase is recruited to the plasma membrane by the SH2 domain of the p85 (regulatory) subunit interacting with phospho-tyrosine residues on activated receptors. This localises the catalytic subunit in the vicinity of its substrate, PtdIns(4,5)P₂, and catalyses PtdIns(3,4,5)P₃ production. Therefore, PI 3-kinase requires to be correctly localised at the plasma membrane, where it is in close proximity to its substrate, to be fully functional.

We next analysed the distribution of the p85 α subunit of PI 3-kinase in response to **Fsk/rolipram**. Distribution of PI 3-kinase p85 α was monitored using a specific antibody and immunofluorescence after treatment with the standard conditions outlined in Chapter 3.4. Cells were treated for 3 hours, fixed and incubated with anti-p85 α anti-body overnight. Under **control** and **rolipram** treated conditions, p85 α (green) was located proximal to the cortical actin structure (red; Figure 25 A). In contrast to **control** and **rolipram** treatments, p85 α was displaced from its normal membrane-proximal localisation in cells treated with **'high dose' Fsk** or **Fsk/rolipram** (compare proximity of green staining (p85 α) with red staining; Figure 25 A). **'Low dose' Fsk** gave an intermediate phenotype with approximately 45% of treated cells with membrane-proximal localisation of p85 α (Figures 25 A and B). Quantification (as in Chapter 4.3) and statistical analysis of the data shows that under growth inhibitory cAMP-elevating conditions, the loss of p85 α at the cell periphery is statistically significant ($P < 0.05$; control versus **'high dose' Fsk**; **'low dose' Fsk** versus **Fsk/rolipram**) (Figure 25 B), in keeping with the loss of PH-GFP from the plasma membrane (Figure 24). Thus, displacement of p85 α localisation, and therefore its activity, could explain loss of PH-GFP localisation from the plasma membrane (Figure 24) as well as the suppression of pAkt (Ser⁴⁷³) (Figure 23) after **Fsk/rolipram** treatment.

To confirm the loss of p85 α from the plasma membrane, sub-cellular fractionation was carried out after treatment with either **control** (DMSO) or **Fsk/rolipram** and p85 α distribution analysed by western blotting. Three fractions per sample were generated by this method: cytosolic (S2), plasma membranes (P2) and nuclear (P1). In **control** samples, p85 α distribution appears to be mainly cytosolic; however, there was also a significant association with both the membrane (P2; fractions marked with *) and the nuclear fractions (P1) (Figure 25 C). Treatment with **Fsk/rolipram** resulted in a loss of p85 α from the membrane fraction (Figure 25 C). Interestingly, the same pattern of regulation was observed with PDK1, which contains a PH domain and is responsive to PI 3-kinase activity (Figure 25 C). This data suggests that cAMP elevation caused the PI 3-kinase p85 α regulatory subunit to dissociate from its normal membrane localisation in KM12C cells with an associated loss of activity. This, in turn, may cause the delocalisation of PDK1, an important effector of PI 3-kinase, and presumably a decrease in its activity. Therefore, cAMP elevation interferes with the localisation of PH-GFP, p85 α and PDK1 and their mis-localisation may be critical events in loss of signalling to pAkt and decreased proliferation.

Figure 24. Fsk/rolipram perturbs PtdIns(3,4,5)P₃ localisation. (A) A PH-GFP-expressing plasmid was transiently transfected into KM12C cells to monitor PtdIns(3,4,5)P₃ distribution. Its localisation after 3 hours treatment with **control** (DMSO), **'high dose' Fsk** (50 µM), **'low dose' Fsk** (1 µM), 10 µM **rolipram** or **Fsk/rolipram** (1 µM Fsk + 10 µM rolipram) was visualised using confocal microscopy. Arrows show distribution of the PtdIns(3,4,5)P₃ reporter. (B) Quantification of membrane-localised PH-GFP was carried out by counting 100 transfected cells under each condition. The number of cells is presented as percentage ± SD of 3 independent experiments. * $P < 0.05$ compared to control, **, $P < 0.05$ compared to 1 µM Fsk alone.

A



B

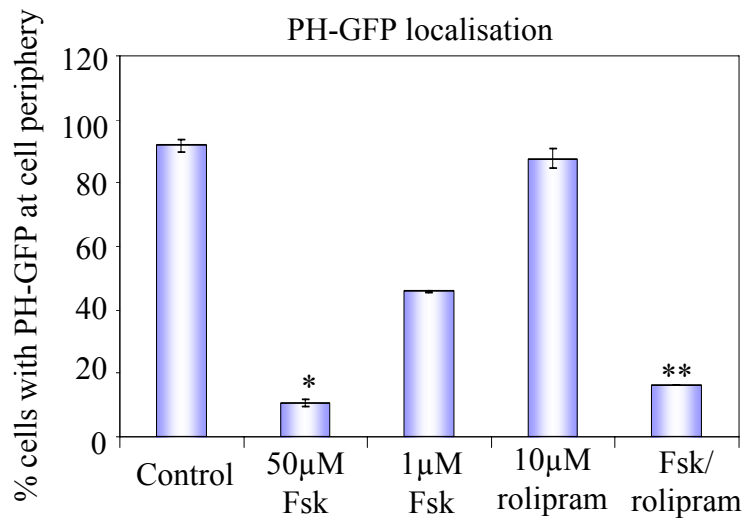
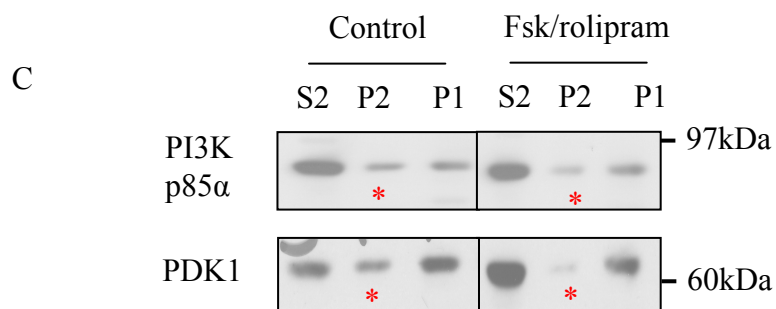
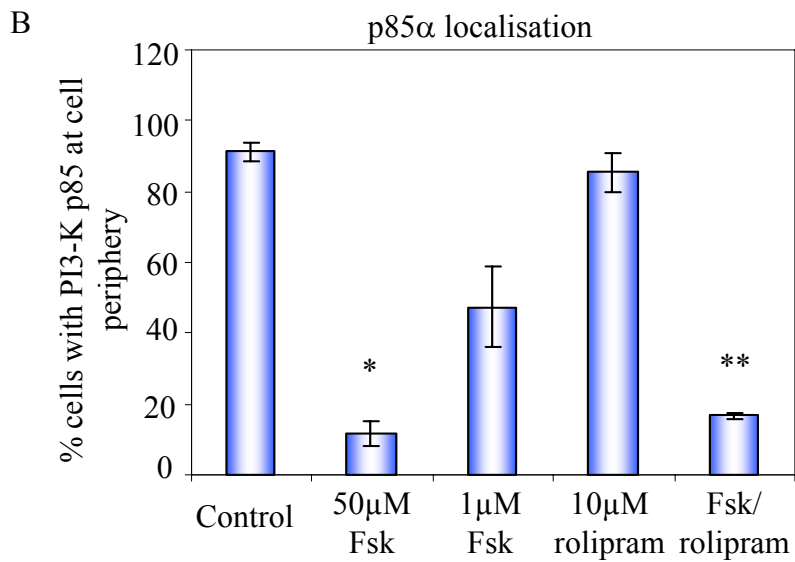
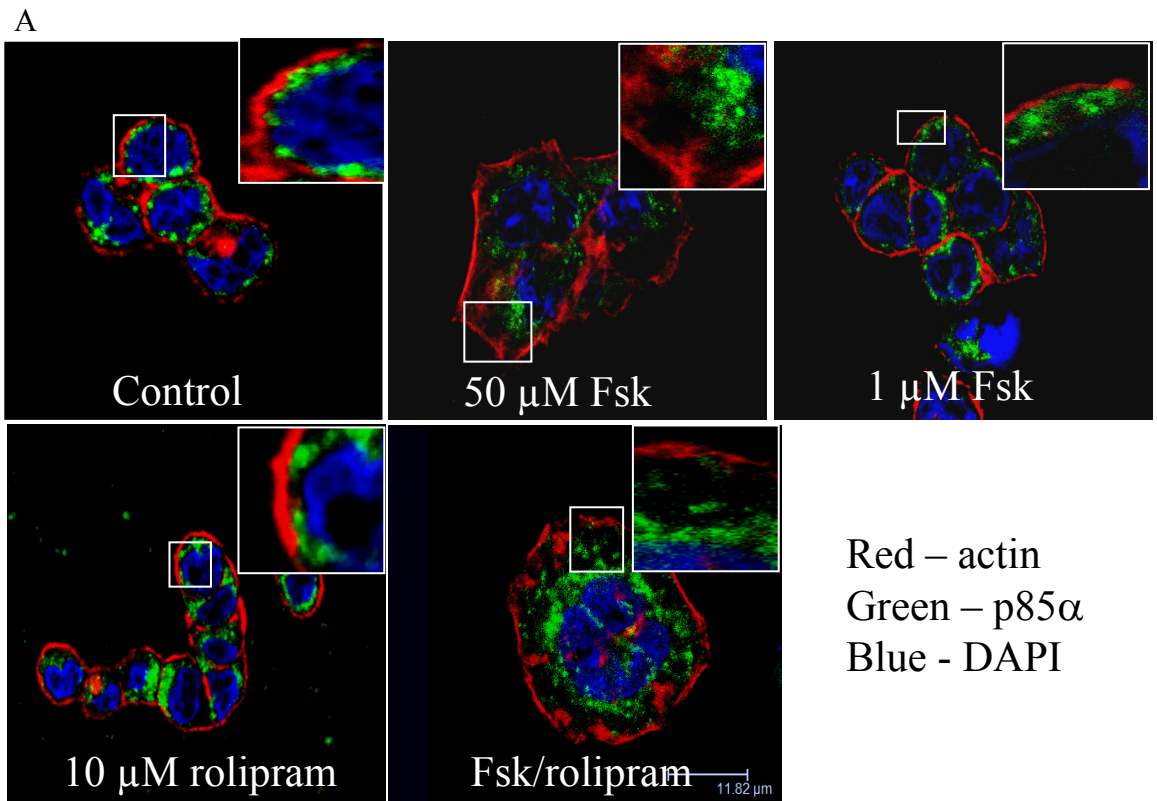


Figure 25. Fsk/rolipram displaces PI 3-kinase p85 α from the cell periphery. Immunofluorescence using anti-p85 α antibody (green), TRITC-phalloidin (actin; red) and DAPI (nucleus; blue) was carried out to determine if PDE4-regulated cAMP altered the localisation of PI 3-kinase after standard treatment set outlined in Chapter 3.4 (A) 3 hours treatment with either '**high dose**' Fsk (50 μ M) or **Fsk/rolipram** (1 μ M FSK + 10 μ M rolipram) resulted in p85 α (green) being displaced and was no-longer proximal to the cortical actin (red) structure. Visualisation was achieved using confocal microscopy (B) Quantification of membrane-localised p85 α and was carried out by counting 100 cells under each condition. The number of cells is presented as percentage \pm SD of 3 independent experiments. * $P < 0.05$ compared to control, **, $P < 0.05$ compared to 1 μ M FSK alone. (C) Sub-cellular fractionation and western blotting revealed that both p85 α (upper panel) and the phosphoinositide dependent protein kinase (PDK1; bottom panel) were displaced from the membrane fraction (P2; marked by *) after **Fsk/rolipram** treatment, compared to control (DMSO) treated cells.



4.5 PDE4/cAMP inhibits downstream effectors of the PI 3-kinase pathway

Akt phosphorylation on Ser⁴⁷³ and Thr³⁰⁸ can be used as a readout of both PI 3-kinase and Akt activity. Phosphorylation at Thr³⁰⁸, is sufficient for Akt activity, but Akt also requires Ser⁴⁷³ phosphorylation for maximal activity (320). When activated, Akt can phosphorylate its target substrates and promote cell survival, growth and proliferation. Therefore, in light of the effects on GFP-PH and p85 α localisation, we decided to assess the timing of pAkt suppression and to confirm the long term effects our standard treatments have on pAkt status.

Loss of pAkt (Ser⁴⁷³) occurred within 3 hours of **Fsk/rolipram** treatment and this loss of pAkt was sustained throughout the period of treatment (Figure 23). To define how early the loss of pAkt (Ser⁴⁷³) occurred, a shorter, more precise time course of Fsk/rolipram treatment was used, with time points between 0 and 60 minutes. The phosphorylation status of Ser⁴⁷³, as well as Thr³⁰⁸, was monitored by western blot. Between 5 to 10 minutes, phosphorylation was lost at both Ser⁴⁷³ and Thr³⁰⁸ (Figure 26 A) and total Akt levels were judged not to be altered by **Fsk/rolipram** treatment (Figure 26 A). Continuous treatment up to 24 hours with **'high dose' Fsk** and **Fsk/rolipram** suppressed pAkt at both sites (Figure 26 B). **Rolipram** alone had no effect and **'low dose' Fsk** had only a partial effect on pAkt (Ser⁴⁷³ and Thr³⁰⁸; Figure 26 B). Loss of pAkt is both rapid and sustained and correlated with the anti-proliferative conditions, namely **'high dose' Fsk** and **Fsk/rolipram**. Moreover, this loss of pAkt, and presumably its activity, was mirrored by a partial suppression of Akt-mediated phosphorylation of two of its downstream substrates, namely FKHRL1 (Ser²⁵⁶) and AFX (Ser¹⁹³) after both **'high dose' Fsk** and **Fsk/rolipram** (Figure 26 C).

Figure 26. PDE4/cAMP inhibits downstream effectors of the PI 3-kinase pathway. (A) Phosphorylated Akt (pAkt) (Ser⁴⁷³ and Thr³⁰⁸) was monitored by western blot of lysates prepared from cells treated for time points up to 60 minutes after **Fsk/rolipram** (1 μ M Fsk + 10 μ M rolipram) treatment, and compared to total Akt. (B) Cells were treated continuously for 24 hours with the standard treatment set outlined in Chapter 3.4. **'High dose' Fsk** and **Fsk/rolipram** treatments (lanes 2 and 5, respectively) resulted in loss of pAkt (at both Ser⁴⁷³ and Thr³⁰⁸). (C) The effects on downstream signalling of Akt was addressed using western blotting with phospho-specific antibodies against two Akt substrates, namely FKHRL1 (Ser²⁵⁶) and AFX (Ser¹⁹³). Both **'high dose' Fsk** and **Fsk/rolipram** inhibited the phosphorylation of both of these Akt target substrates at the sites indicated after 24 hour treatment. Blots shown for all of the above are representative of n=3 independent experiments.

Both FKHRL1 and AFX are Forkhead transcription factors and have been implicated in Akt regulation of p27^{Kip1} (423-425). However, since the loss of phosphorylation is not complete, there may be other mechanisms involved in the regulation of p27^{Kip1} levels and proliferation.

4.6 LY294002 induces similar effects to Fsk/rolipram

We next sought to test whether or not KM12C cells were dependent on the PI 3-kinase/Akt pathway for continued proliferation and survival, by using the PI 3-kinase inhibitor, **LY294002**.

We first titrated **LY294002** to find a relatively low concentration of the PI 3-kinase inhibitor that caused suppression of Akt phosphorylation. We established that a concentration of 20 μ M was sufficient and this was used throughout the study (data not shown).

Cells were treated with either **control** (DMSO) or 20 μ M **LY294002** for 24 hours, pulse labeled with 25 μ M BrdU for the final hour, fixed and stained with PI and FITC conjugated anti-BrdU antibody and the cell cycle was analysed. Scatter plots were generated for each treatment (Figure 27 A) and analysis (Figure 27 B) was carried out using the gates (as described for Figure 17 A). Under **control** conditions, there were approximately 30% of cells in G1 phase (light blue column), 55% in S-phase (dark red column) and 20% in G2 phase (blue/purple column) of the cell cycle (Figures 27 A and B). After treatment with **LY294002** the G1 content of the cells increased (55 %) and the number of cells in S-phase decreased to 15% (Figures 27 A and B). No significant change in G2 phase was observed after LY294002 treatment (Figures 27 A and B). Thus, treatment of KM12C cells with **LY294002** induced a partial G1/S-phase arrest similar to that induced by **Fsk/rolipram**.

Next, the effects on cell cycle proteins examined in Chapters 3.6 and 3.7 were assessed after 24 hours treatment with either **control** (DMSO) or **LY294002**. **LY294002** induced the expression of the G1/S-phase inhibitor p27^{Kip1} (Figure 27 C). This may account for the

ability of LY294002 to induce a G1/S-phase arrest. Also, **LY294002** treatment resulted in reduced Skp2 expression as well as a loss of hyperphosphorylated Rb (Figure 27 C). Expression of the Rb/E2F controlled cell cycle proteins cyclin A, cyclin B1, cyclin E and CDK1 were also reduced (Figure 4.6 C). As a control, pAkt (Ser⁴⁷³) was used to confirm the inhibition of the PI 3-kinase pathway by **LY294002** and total Akt was also analysed (Figure 27 C). Interestingly, treatment with **LY294002** also resulted in the loss of phosphorylation of both Forkhead proteins, FKHLR1 (Ser²⁵⁶) and AFX (Ser¹⁹³) at sites specific for Akt phosphorylation (Figure 27 D). Reduced phosphorylation at these sites may lead to increased Forkhead transcriptional activity, and could provide another mechanism by which p27^{Kip1} levels were elevated. Taken together, these results demonstrate inhibiting the PI 3-kinase/Akt pathway in KM12C cells induces a partial G1/S-phase arrest, most likely, by an increase in p27^{Kip1} levels, loss of hyperphosphorylated Rb and inhibition of Rb/E2F cell cycle proteins. These effects were all similar to PDE4 regulated cAMP mediated inhibition of proliferation, supporting the idea that PDE4 regulated cAMP is acting by inhibiting the PI 3-kinase/Akt pathway to suppress proliferation.

4.7 LY294002 induces apoptosis and inhibits proliferation

The effect of sustained PI 3-kinase suppression on long term survival of KM12C cells was also examined. Inhibiting the PI 3-kinase/Akt pathway for greater than 24 hours was assessed by analysis of sub-2n DNA content and an MTT proliferation assay. **LY294002** induced sub-2n DNA content over a 72 hour period compared to **control** (DMSO) treated cells when analysed by PI staining (Figure 28 A and quantified in 28 B). Also, extended treatment of cells with **LY294002** resulted in complete cessation of proliferation over a five day period, as measured by an MTT assay (Figure 28 C).

Figure 27. LY294002 induces similar effects to Fsk/rolipram. The effects on cell cycle proteins was assessed using the PI 3-kinase specific inhibitor **LY294002**. (A) Cells were treated with either **control** (DMSO) or 20 μ M **LY294002** for 24 hours, and BrdU analysis was carried out as described in Figure 3.5. (A) Scatter plots were generated and cells were gated as previously (Figure 3.5) indicated. (B) Quantification of BrdU incorporation after 24 hours of **LY294002** treatment. Data shown is mean \pm SD of n=3 independent experiments and scatter plots are representative results. (C) Sub-confluent KM12C cells were treated with **control** (DMSO) or 20 μ M **LY294002** for 24 hours and western blot analysis of cell cycle regulators was carried out using specific antibodies. LY294002 induced p27^{Kip1} and loss of Skp2, cyclin A, cyclin B1, cyclin E and CDK1. pAkt (Ser⁴⁷³) was used as a readout of PI 3-kinase inhibition and total Akt was used as a loading control in all of the above (D) Sub-confluent KM12C cells were treated with either **control** (DMSO) or 20 μ M **LY294002** and western blot analysis of pFKHRL1 (Ser²⁵⁶) and pAFX (Ser¹⁹³) levels was carried out using specific antibodies. Total FKHRL1 and vinculin were used as loading controls.

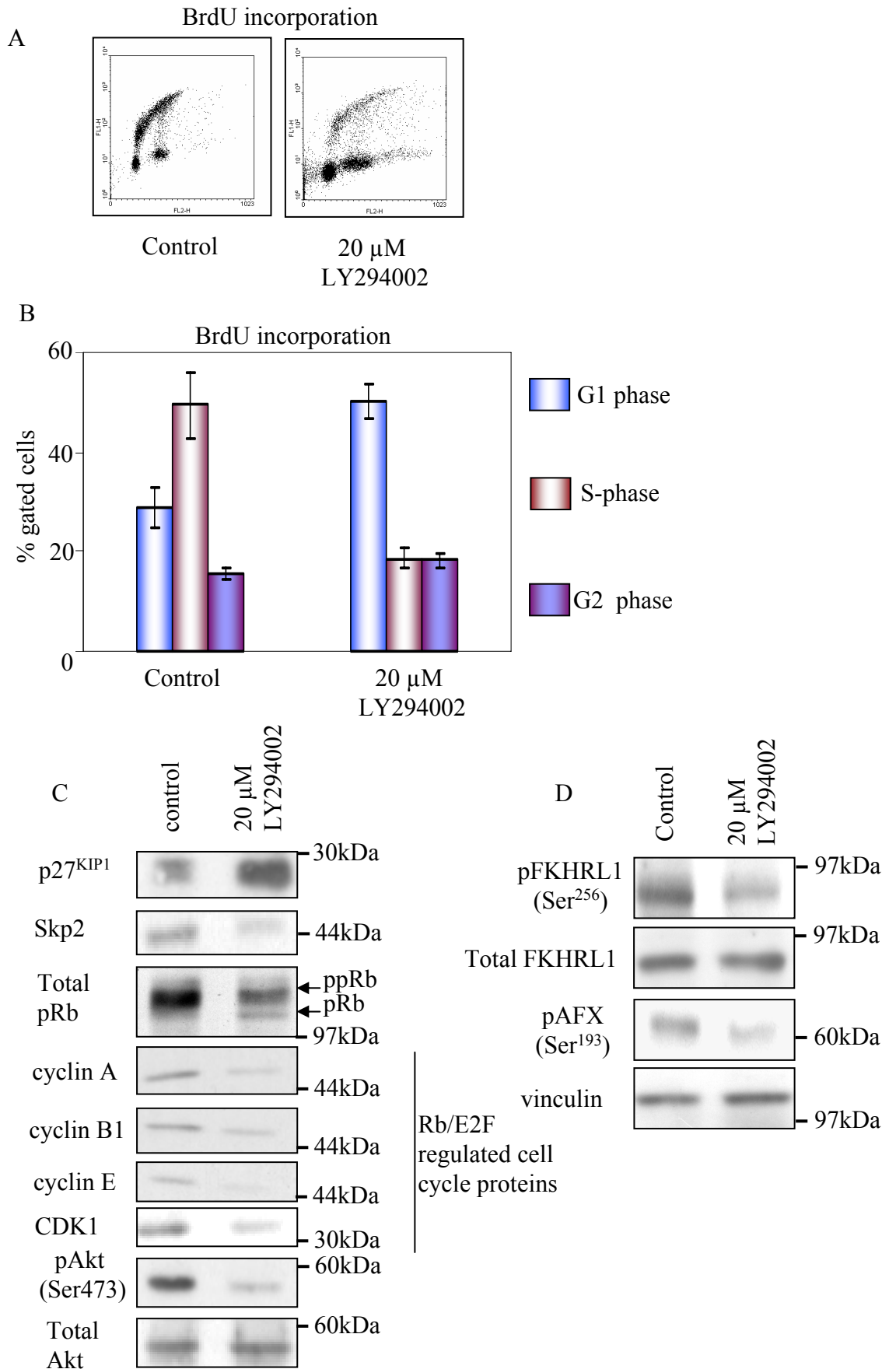
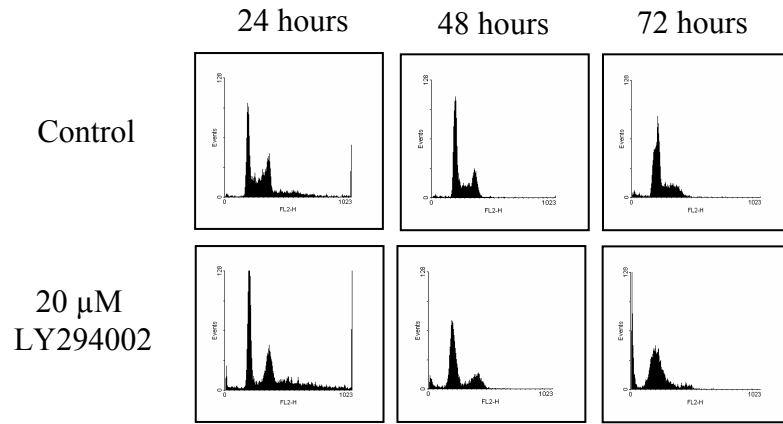
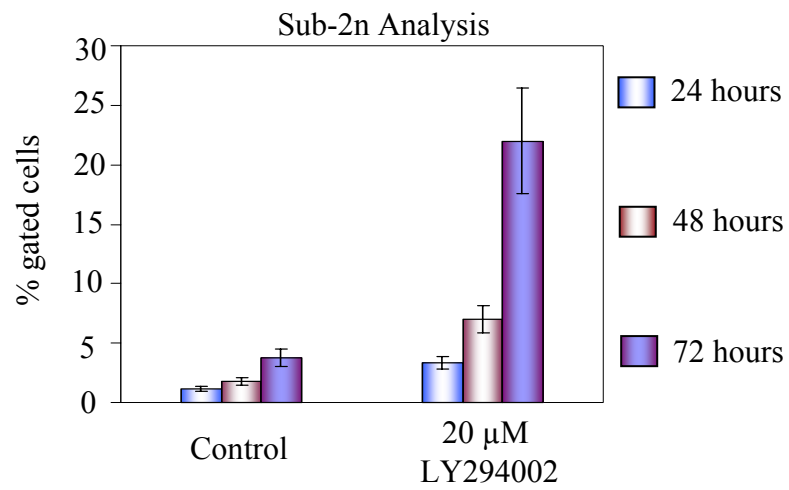


Figure 28. LY294002 induces apoptosis and inhibits proliferation. PI analysis (A) and quantification (B) of sub-2n DNA content of KM12C cells treated with **control** (DMSO) or **LY294002** for 24 hours, 48 hours or 72 hours was (as performed for Figure 21, for n=3 independent experiments \pm SD). (C) Proliferation of KM12C cells was monitored by MTT assay over a 5 day period in the presence of control (DMSO), 50 μ M Fsk or 20 μ M LY294002 and values shown are mean \pm SD of n=3 independent experiments.

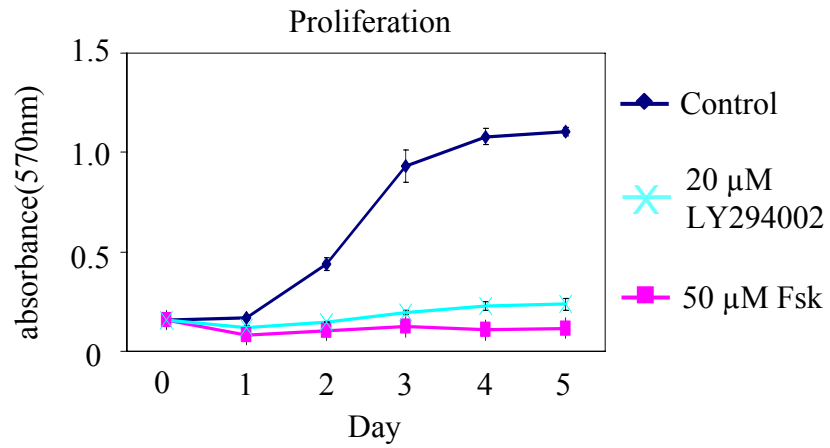
A



B



C



Overall, these results indicate that treatment of KM12C cells with a small molecule inhibitor of the PI 3-kinase/Akt pathway induces cell cycle arrest, induction of p27^{Kip1}, inhibition of the Rb/E2F pathway and the stimulation of apoptosis in a manner similar to that induced by PDE4-regulated cAMP. KM12C cells are critically dependent on the PI 3-kinase/Akt pathway for their proliferation and survival and are therefore ‘addicted’ to this oncogenic pathway for proliferation. Moreover, elevated cAMP, in a compartment regulated by PDE4 enzymes, feeds in to the PI 3-kinase pathway causing displacement of components of the pathway and suppression of signalling. This provides a mechanism by which compartmentalised PDE4s block cancer cell proliferation.

4.8 Exogenous expression of PTEN inhibits Akt phosphorylation and sensitises KM12C cells to Fsk

The tumour suppressor gene *PTEN* (phosphatase with tensin homology, which is located on chromosome 10) is a lipid phosphatase that negatively regulates PI 3-kinase signalling by dephosphorylation of PtdIns(3,4,5) P_3 (302). Mutation or deletion of the *PTEN* gene results in an inactive protein being transcribed and consequently, constitutive PI 3-kinase signalling to downstream effectors, such as the survival kinase Akt. Alterations in *PTEN* are common in sporadic tumours and can also predispose to Cowden disease, a rare autosomal dominant syndrome where patients have increased risk of developing skin, thyroid, bowel, and in the case of females, breast cancer (331).

To assess whether or not known oncogenic or tumour suppressor regulators of the PI 3-kinase pathway influenced KM12C proliferation, cells in which either PTEN or Src proteins had been modulated by exogenous expression were analysed at low densities. Src, which positively regulates PI 3-kinase (426) is occasionally activated, and commonly over-expressed, in late stage colon cancer cells (427, 428), while PTEN is commonly lost or

mutated (300, 331). The expression of PTEN in KM12C cells is lost (personal communication, V.G. Brunton). We therefore reconstituted KM12C cells with PTEN-GFP by retroviral infection. Endogenous PTEN protein was retained in HT29 colon cancer cells (Figure 29 A), while, as expected, no expression of PTEN was detected by western blot in KM12C, or in KM12C cells over-expressing SrcY527F (constitutively active Src (77); KM12C/2C4) (Figure 29 A). Exogenous expression of PTEN-GFP was detected as a slower migrating species compared to endogenous PTEN (HT29 cells; Figure 29 A). Endogenous PTEN protein expression in HT29 and PTEN-GFP in KM12C/2C4 cells correlated with decreased pAkt (Ser⁴⁷³) levels (Figure 29 A). However, expression of SrcY527F had no further activating effect on pAkt (Ser⁴⁷³; Figure 29 A).

The proliferation of KM12C, KM12C/2C4 and KM12C/2C4 +PTEN-GFP cells was analysed over a 6 day period. Over-expression of SrcY527F had no effect on the proliferation of KM12C cells (Figure 29 B) and was consistent with what had previously reported (77). However, re-expression of PTEN-GFP (Figure 29 B) resulted in decreased proliferation but did not cause complete growth cessation as observed when cells were treated with **LY294002** or **Fsk/rolipram**.

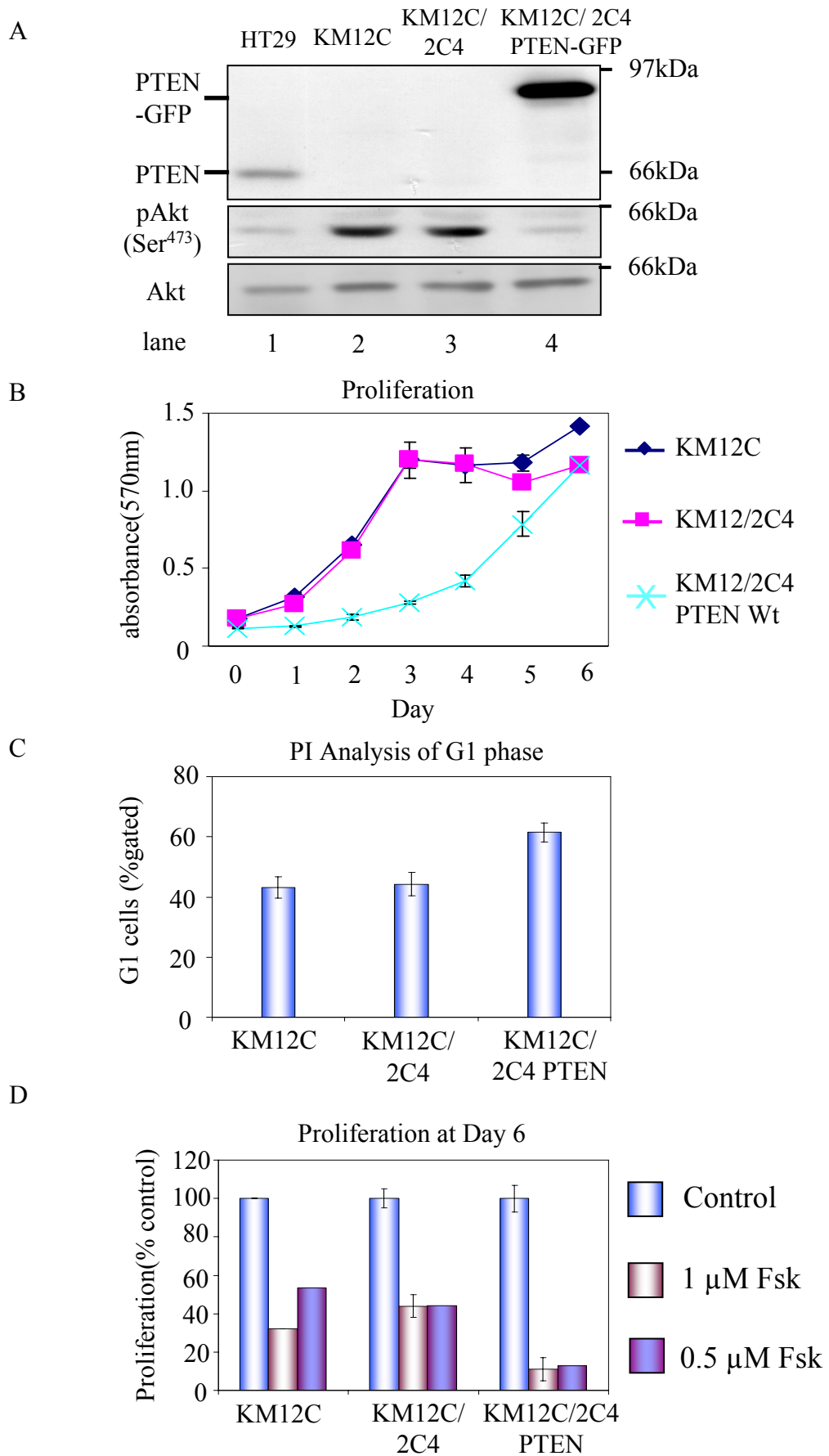
KM12C and KM12C/2C4 cells both had approximately 40% of gated cells in G1 (Figure 29 C). KM12C/2C4 + PTEN-GFP showed a 20% increase, with approximately 60% of gated cells in G1 compared to KM12C and KM12C/2C4 cell lines (Figure 29 C). This accumulation of cells in G1 may be responsible for the reduced proliferation of KM12C/2C4 + PTEN-GFP cells, compared to KM12C and KM12C/2C4 cells. Furthermore, the re-expression of PTEN-GFP in KM12C/2C4 cells sensitized the cells to increased inhibition of proliferation by 'low doses' (1 or 0.5 μ M) of **Fsk** when grown continuously in its presence

(Figure 29 D). Proliferation, when measured at day 6, was reduced by approximately 80% by **'low dose' Fsk** (1 μ M) treatment of KM12C/2C4 + PTEN cells (Figure 29 D).

Re-expression of PTEN resulted in reduced pAkt (Ser⁴⁷³; Figure 29 A) and although some PTEN-mediated control of the PI 3-kinase/Akt pathway was restored, this did not result in complete growth cessation or cell death (Figure 29 B). The re-expression of PTEN may result in a finely balanced PI 3-kinase/Akt signalling pathway, whereby treatment with **'low doses' of Fsk** is sufficient to elicit anti-proliferative effects on PTEN expressing cells more effectively than control cells (Figure 29 D). Together, these data provide support for a critical role for the PI 3-kinase pathway in KM12C proliferation, presumably mediated, at least in part, by PTEN loss and is possibly a point of intersection between cAMP and PI 3-kinase pathways.

Figure 29. Exogenous expression of PTEN inhibits Akt phosphorylation and sensitises KM12C cells to Fsk. Cells were plated at low density (5×10^5 cells in 60 mm dish). (A) KM12C cells do not express PTEN and re-introduction reduces pAkt (Ser⁴⁷³). Expression of endogenous PTEN protein in HT29 colon cancer cells and PTEN-GFP in KM12C/2C4 (upper panel) correlates with reduced pAkt (Ser⁴⁷³), whereas lack of PTEN protein in KM12C and KM12C/2C4 cells correlates with raised pAkt. Immunoblots were carried out using the specific PTEN and pAkt antibodies as probes. Total Akt was used as a loading control in all of the above. (B) Re-introduction of PTEN affects low density growth of KM12C cells. Proliferation of KM12C, KM12C/2C4 and KM12C/2C4 PTEN-GFP cells was monitored using an MTT assay over a 6 day period and (C) Re-expression of PTEN in KM12C cells increases the percentage of cells in G1 phase as analysed by PI staining. (D) Proliferation of KM12C, KM12C/2C4 and KM12C/2C4 PTEN-GFP cells in the presence of **control** (DMSO), **1 μ M** and **0.5 μ M Fsk** and was monitored over a 6 day period and the percentage proliferation of **control** (DMSO) at day 6 was calculated for the mean \pm SD of 3 independent experiments. All blots are representative of n=3 independent experiments.

Figure 29. Exogenous expression of PTEN inhibits Akt phosphorylation and sensitises KM12C cells to Fsk



Discussion

4.9 PI 3-kinase localisation

One common method for detecting the production and localisation of specific phosphoinositides is through the use of a PH domain fused to a reporter protein such as GFP (PH-GFP). Previous studies have utilised the PH domains of various proteins including Akt/PKB and GRP1 (General Receptor for Phosphoinositides-1) and have shown that both overlap in their abilities to bind PtdIns(3,4,5)P₃ (the product of PI 3-kinase) (422).

In our study, we used the PH domain of Akt fused to GFP as a reporter of PtdIns(3,4,5)P₃. Under normal conditions, PH-GFP constitutively localised to the plasma membrane in KM12C cells. This suggests that PI 3-kinase is continuously producing PtdIns(3,4,5)P₃ and that a gradient or localised concentration is not established. Therefore, this continuous production of PtdIns(3,4,5)P₃ has implications for downstream signalling of PI 3-kinase, including events regulated by the downstream kinase Akt. Under anti-proliferative conditions of increased cAMP, namely **'high dose' Fsk** or **Fsk/rolipram** treatment, PH-GFP was mis-localised from its peripheral membrane position. The data presented here implies that PI 3-kinase signalling is disrupted under conditions that inhibited proliferation and induced apoptosis. This constitutive localisation of PH-GFP was in contrast to what was reported by Gray *et al* where, in their study, they required stimulation of the cells with growth factors, such as PDGF, in order to obtain membrane localisation of the reporter (422) and which may be a difference between normal and cancer cells.

Key to the production of 3' phosphoinositides by PI 3-kinase and successful downstream signalling events, is the localisation of PI 3-kinase subunits to regions of high substrate concentration, namely at cell membranes. In conjunction with our studies using the PH-GFP reporter for analysis of the spatial distribution of PtdIns(3,4,5)P₃, we analysed the

localisation of the regulatory subunit of PI 3-kinase, p85 α using both immunofluorescence and sub-cellular fractionation techniques. We found that the PI 3-kinase subunit p85 α was displaced from its membrane-proximal localisation under anti-proliferative conditions, similar to the regulation of PH-GFP localisation in KM12C cells. Interestingly, a recent study of the p85 α regulatory subunit of PI 3-kinase has revealed the presence of a PKA phosphorylation site at Ser⁸³. Phosphorylation of this site by PKA is critical for cAMP induced G1 arrest in Swiss 3T3 mouse fibroblasts (175). In addition, the same site on p85 α was also implied to play a positive role in oestrogen and TSH stimulated cAMP production with respect to PI 3-kinase activity (175, 176). Thus, PI 3-kinase regulation by cAMP is context specific.

4.10 PDE4/cAMP induced loss of Akt/PKB phosphorylation

Activation of PI 3-kinase by growth factors and the subsequent generation of PtdIns(3,4,5)P₃ has been shown to have key roles in regulating key aspects of cellular processes such as control of cell growth, proliferation, survival, glucose metabolism and genome stability (reviewed in (429, 430)). One major down-stream effector of PI 3-kinase signalling is the serine/threonine kinase Akt which was one of the first proteins to be discovered that contained a PH domain (431-433).

In our study, treatment of KM12C cells with either **‘high dose’ Fsk** or **Fsk/rolipram** resulted in the rapid and sustained dephosphorylation of Akt at both Thr³⁰⁸ and Ser⁴⁷³. We believe that this is the result of an inhibition/delocalisation of PI 3-kinase and hence loss of PtdIns(3,4,5)P₃ from the plasma membrane. Previous studies have identified a role for cAMP in the inhibition of Akt phosphorylation by several mechanisms. One of which is the cAMP/Fsk induced dephosphorylation of both Thr³⁰⁸ and Ser⁴⁷³ sites on Akt. Most notably, PDK1 localisation at the plasma membrane was shown to be disrupted upon

cAMP elevation resulting in loss of pAkt (Thr³⁰⁸) (333), although PDE4 enzymes were not investigated. In the same study, cAMP/Fsk treatment resulted in the *in vivo* loss of PtdIns(3,4,5)P₃ and PI 3-kinase/Akt activity, which was probably responsible for PDK1 mislocalisation. In our study, the localisation of PDK1 was not studied in detail although we were able to show that upon treatment with **Fsk/rolipram**, PDK1s distribution was lost from the membrane fraction. Therefore, this may contribute to the loss of pAkt (Thr³⁰⁸) in our study.

Regarding the regulation of pAkt (Ser⁴⁷³) phosphorylation, there are currently no reports linking PDE4s with regulation of the two widely accepted ‘PDK2s’ – mTOR and DNA-PK. Interestingly, one report does highlight the ability of cAMP to attenuate insulin mediated activation of mTOR by an undefined mechanism (434). This may provide a way by which cAMP can suppress pAkt (Ser⁴⁷³) in KM12C cells when treated with **Fsk/rolipram**. However, Smith *et al* showed that PDE4 inhibition in diffuse large B-cell lymphoma results in the inhibition of Akt phosphorylation (339).

In addition, the protein phosphatase PP2A can dephosphorylate Akt (435) and that cAMP and, more specifically PDE4 regulated cAMP, can activate PP2A (377, 436). However, inhibition of PP2A using okadaic acid and subsequent treatment with **Fsk/rolipram** did not alleviate the suppression of pAkt at either site indicating that the cAMP dependent inhibition of Akt is independent of PP2A activation (not shown).

Taken together, our data that describes that ability of PDE4 regulated cAMP to inhibit the phosphorylation of Akt at both Ser⁴⁷³ and Thr³⁰⁸ supports evidence that PDE4s may be present at a critical intersection point between two second messenger pathways, namely those regulated by PtdIns(3,4,5)P₃ and cAMP.

4.11 PI 3-kinase/Akt regulation of proliferation

The regulation of cell proliferation by PI 3-kinase/Akt can occur at the G1/S-phase transition, where inhibition of PI 3-kinase/Akt causes accumulation in G1 (424, 437). One mechanism by which this might occur is Akts' ability to govern p27^{Kip1} localisation, degradation and expression by phosphorylation at multiple sites on p27^{Kip1} including Ser¹⁰ (356) Thr¹⁵⁷ (359, 438), Thr¹⁸⁷ and Thr¹⁹⁸ (358). Phosphorylation of Ser¹⁰ regulates the stability and nuclear export of p27^{Kip1} at the G0/G1 transition (439, 440). Phosphorylation of Thr¹⁸⁷ regulates Skp2 binding and recruitment to SCF/E3 ubiquitin ligase complex (361) and phosphorylation of both Thr¹⁵⁷ and Thr¹⁹⁸ both increase binding to 14-3-3 proteins resulting in nuclear exclusion and cytoplasmic retention (356, 357).

Here we found that, loss of pAkt after '**high dose**' Fsk treatment, **Fsk/rolipram** combination or inhibition of PI 3-kinase/Akt directly (**LY294002**) resulted in induction and/or stabilisation of p27^{Kip1}. We could not detect any alterations in the phosphorylation status of p27^{Kip1} at any of the reported sites (data not shown). However, cAMP mediated suppression of pAkt may induce loss of phosphorylation at one of the sites on p27^{Kip1} and could be a contributing factor to the G1/S-phase block.

The PI 3-kinase/Akt pathway also regulates the expression of Skp2 (441, 442), the adaptor protein responsible for targeting p27^{Kip1} for degradation (360). Direct inhibition of PI 3-kinase using **LY294002** in KM12C cells resulted in an increase in p27^{Kip1} and a decrease in Skp2. This was similar to the effects of **Fsk/rolipram** treatment, indicating that the inhibition of the PI 3-kinase/Akt pathway, either directly or indirectly, is responsible for the decrease in Skp2 levels, increase in p27^{Kip1} levels and, presumably, the subsequent G1/S-phase block. However, Skp2 is also a target for E2F transcription (406). Therefore, further work would be required to completely understand how Skp2 expression is controlled in response to cAMP elevation in.

Another way by which PI 3-kinase/Akt can control p27^{Kip1} levels is by regulation of its transcription by the activity of Forkhead transcription factors (TFs) such as, FKHRL1 (FOXO3) and AFX (FOXO4) (363, 424). We examined both pFKHRL1 (Ser²⁵⁶) and pAFX (Ser¹⁹³) levels after treatment with **Fsk/rolipram** and **LY294002**, both of which suppressed phosphorylation at these sites. However, we were unable to visualise any translocation of these TFs from the cytoplasm to the nucleus due to a high background signal. Therefore we cannot directly attribute the loss of phosphorylated Forkhead TFs to the increased expression of p27^{Kip1}. However, it is likely that decreased targeting for degradation (by loss of Skp2) and increased transcription (by Forkhead mediated mechanisms) after either **Fsk/rolipram** or **LY294002** treatment were both responsible for elevated p27^{Kip1} levels, and the induction of the G1/S-phase arrest in KM12C cells.

Long-term inhibition of the PI 3-kinase/Akt pathway induces apoptosis and complete inhibition of proliferation of KM12C cells over a 5 day period (Figure 28). Although the precise mechanism by which either direct (**LY294002**) or indirect (**Fsk/rolipram**) inhibition of the PI 3-kinase/Akt pathway induced apoptosis was not elucidated, several candidate pathways exist. These include phosphorylation and inhibition of Caspase 9 (443), the pro-apoptotic protein Bad (444) and FKHRL1 (445), all of which regulate apoptosis in a PI 3-kinase/Akt dependent manner. In the case of Bad, it is a phosphorylation target of both Akt and PKA, and both have the ability to inhibit its pro-apoptotic action by increasing interaction with 14-3-3 proteins and decreasing its ability to bind Bcl-2/Bcl-X_L (172-174, 444, 446, 447). Attempts at analysing the phosphorylation status of Bad and caspase activation were inconclusive and the manner in which PDE4 regulated cAMP induces apoptosis in KM12C cells is as yet, undefined.

4.12 Effects of PTEN expression

PTEN loss can result in constitutive activation of PI 3-kinase signalling and increased survival and proliferation of cancer cells. In KM12C cells, PTEN expression is lost and this could contribute to the constitutive localisation of the PH-GFP reporter to the plasma membrane, by ensuring the PI 3-kinase/Akt pathway is highly active. When both PTEN protein expression and pAkt levels were compared in HT29 colon cancer cells, PTEN was expressed and levels of pAkt (Ser⁴⁷³) was low. When re-expressed PTEN in the KM12/2C4 cells we were able to increase their G1 cell content, slow their proliferation at low cell densities and sensitised them to low concentrations of Fsk mediated growth inhibition (Figure 29).

Because of its tumour suppressor activities, there has been much interest in evaluating the effects of re-expression of PTEN in cancer cells as a possible gene therapy approach. For example, adenovirus mediated gene transfer of wild type (Wt) *PTEN* into colon cancer cells resulted in suppression of PI 3-kinase/Akt signalling, a G2/M cell cycle arrest and an induction of apoptosis (448). The same study also identified that over-expression of PTEN in two of the cell lines (HT-29 and SW480) resulted in a significant inhibition of tumour growth in tumour xenografts (448). Moreover, exogenous expression of PTEN in numerous glioblastoma cell lines results in an inhibition of the G1/S-phase transition by inducing p27^{Kip1}, reducing cyclinE/CDK2 activity and dephosphorylation of Rb but no apoptosis (449). PTEN re-expression in MCF-7 breast cancer cells results in a G1 arrest and subsequent apoptosis, which was dependent on inhibition of PI 3-kinase/Akt (450).

Our results correspond with some aspects of what has previously been reported, but PTEN re-expression did not recapitulate the complete growth cessation and cell death associated with direct PI 3-kinase inhibition using **LY294002**. Therefore, re-expression of PTEN may not be sufficient to induce apoptosis or during the process of establishing a cell line that

stably expresses PTEN, selective pressure has removed those cells in which PTEN did induce apoptosis.

A dual strategy of re-introducing PTEN into cells and treatment with either chemotherapy or radiotherapy of prostate cancer cell lines or xenografts is an effective approach to inhibit their growth (451, 452). Interestingly, combinational therapy using caffeine, a known phosphodiesterase inhibitor, and adenovirus-mediated gene transfer of PTEN results in a synergistic suppression of colorectal cancer cell growth by the inhibition of the PI 3-kinase/Akt pathway and arrest in G2/M (453). These studies, in combination with our own data, raise the exciting possibility that combination therapy combining the re-introduction of wild type PTEN and treatment with cAMP modulators, such as the adenylyl cyclase activator Fsk or PDE inhibitors, may provide a novel therapeutic strategy for combating some human malignancies.

4.13 Oncogene addiction and its inhibition

Cancer cells, despite having many genetic, epigenetic and chromosomal abnormalities, are often ‘addicted’ to one or two oncogenic changes for continued proliferation and survival (454). Therapeutic advances now come from determining oncogenic addictions of individual tumours. This would, in turn, allow tailored therapy to be more widely applied. There are now a number of examples of agents that target critical molecular events having therapeutic benefit. For example, in non-small cell lung cancer, a subset of patients with activating mutations in the kinase domain of the epidermal growth factor receptor (EGFR), exhibit impressive clinical responses to the EGFR inhibitor gefitinib (455). In this case, oncogene addiction is a result of mutation, not simply over-expression or inappropriate cellular activation, and it is thought addiction may be mediated by constitutive activation of the pro-survival Akt pathway downstream of activated EGFR (456). Other clear examples of clinical benefit arising from the targeting of critical oncogenes have come

from treatment of breast cancers, in which the HER2 receptor tyrosine kinase is over-expressed, with the monoclonal antibody trastuzumab (Herceptin®) (457). A further example is imatinib (Gleevec®) which is used to treat chronic myeloid leukaemia and gastrointestinal stromal tumours that are driven by the oncogenic BCR-Abl and c-Kit proteins, respectively (458). It is likely that identification of tumour oncogene addiction will thus provide a key part of delivering effective cancer treatments in the future.

4.14 Summary

Here we establish for the first time that KM12C colon cancer cells, which are resistant to cell death induced by DNA damaging or other cytotoxic agents commonly used to treat colorectal cancers (our unpublished data), are critically dependent upon the PI 3-kinase pathway for their continued proliferation and survival. In cancer cells which are addicted to the PI 3-kinase pathway, there is an urgent need to devise effective, yet relatively non-toxic, ways to inhibit tumour cell growth and survival. In this regard, inhibitors of PI 3-kinase have been developed with against various classes of PI 3-kinase (459), although these drugs are not particularly specific (460). Although there is optimism that on-going efforts will lead to selective isoform-specific PI 3-kinase inhibitors as therapeutic agents, these are neither readily available nor at an advanced stage of clinical development (461). Thus, the need for novel therapeutics to exploit such oncogenic addictions is required and therefore this raises the exciting possibility that the adenylyl cyclase/PDE4 combinational treatment we have defined here may be exploited for therapeutic benefit.

Chapter 5:

**PDE4 expression and activity is altered in
metastatic cells – consequences for Fsk
sensitivity**

5. PDE4 expression and activity is altered in metastatic cells - consequences for Fsk sensitivity

5.1 Aim

The aims of this chapter were to assess the activity and expression of PDE4 enzymes in the metastatic derivatives of the KM12C cells, namely KM12L4A and KM12SM, and to address whether or not modulation of PDE4 expression altered Fsk sensitivity to cAMP modulation.

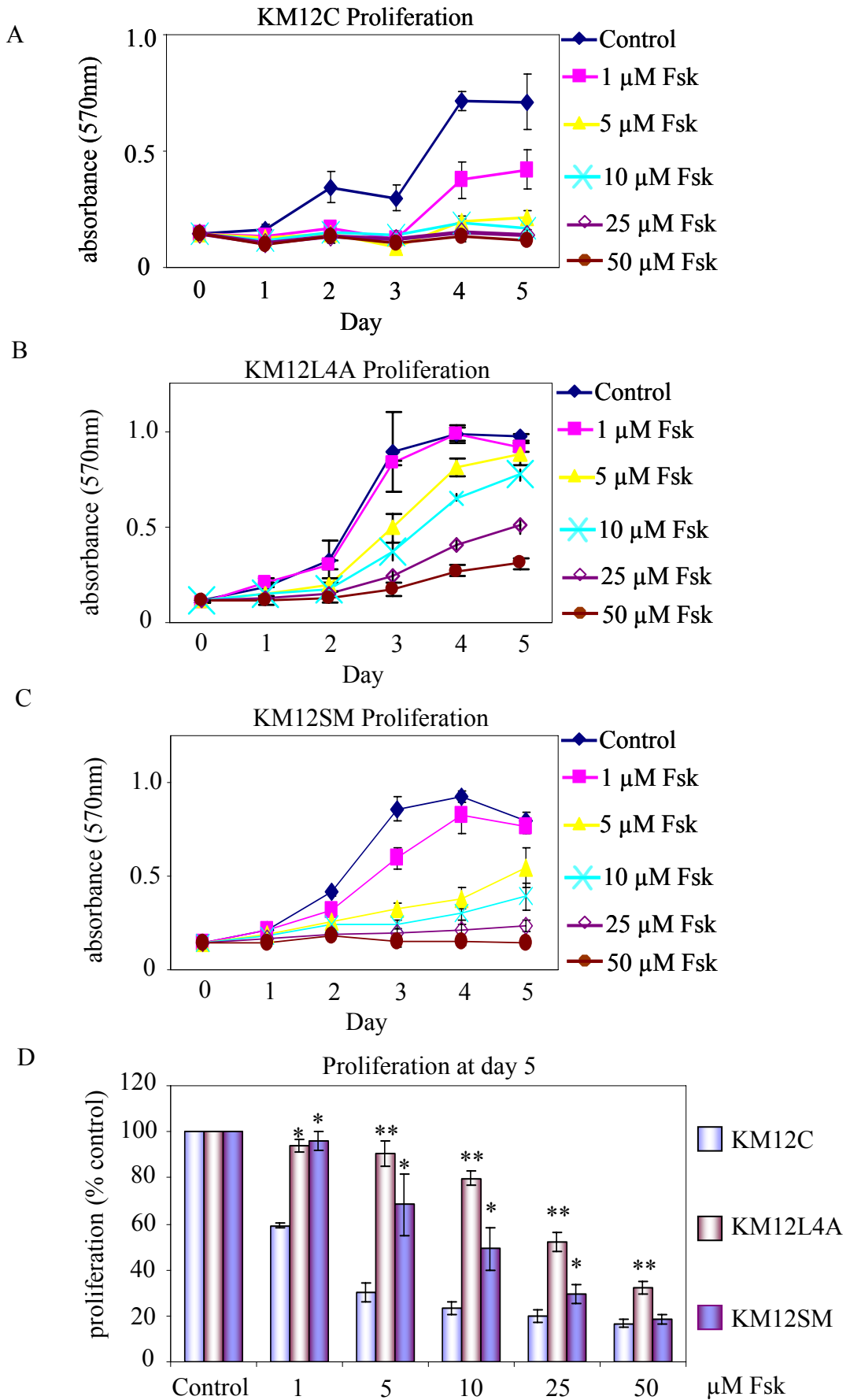
5.2 Metastatic cells have increased resistance to Fsk mediated inhibition of proliferation

Treatment of KM12C cells with the adenylyl cyclase activator, Fsk (50 μ M), completely inhibits their proliferation whilst treatment with 1 μ M Fsk results in approximate 50 % inhibition of their proliferation (Figures 14 C and 30 A). A number of variants of this cell line have been described (40) that differ in their abilities to metastasise to the liver of nude mice following intrasplenic injection (40, 41). Here we set out to evaluate the KM12L4A and KM12SM metastatic variants of the KM12C cells for their abilities to proliferate in the presence of Fsk. KM12L4A cells exhibited increased tolerance to Fsk-mediated growth inhibition (Figure 30 B) compared to the non-metastatic KM12C parental cell line (Figure 30 A). Indeed, KM12L4A cells were resistant to growth inhibition up to a concentration of 25 μ M Fsk, which gave an approximate 50% inhibition of proliferation at day 5 of the assay and was statistically significant ($P < 0.01$; Figure 30 D). Interestingly, KM12SM cells, also a metastatic variant of KM12Cs, exhibited increased tolerance to Fsk mediated inhibition of proliferation (Figure 30 C) with 10 μ M Fsk giving an approximate 50% inhibition (Figure 30 D). This was also statistically significant ($P < 0.05$) compared to 10 μ M Fsk treated KM12C cells at day 5.

Thus, we have shown that the experimentally derived KM12L4A metastatic derivative cell line, and, to a lesser extent, KM12SM (which arose as a spontaneous metastasis (41) of KM12C cells), appear to have evolved an ability to resist the anti-proliferative effects of cAMP elevation by Fsk.

Figure 30. Metastatic cells have increased resistance to Fsk. Proliferation of KM12C (poorly-metastatic), KM12L4A (highly metastatic) and KM12SM (highly metastatic) cells were assessed over a five day period in the presence of either control (DMSO), 1 μ M, 5 μ M, 10 μ M, 25 μ M or 50 μ M Fsk using an MTT assay. (A) KM12C cells are strongly inhibited by concentrations of Fsk > 1 μ M. (B) KM12L4A cells are less sensitive to Fsk mediated inhibition of proliferation. (C) KM12SM cells are less sensitive to Fsk inhibition of proliferation compared to KM12C cells. (D) Quantification (percentage of control at day 5) of treatments shows a statistically significant difference between KM12L4A (upto 50 μ M Fsk) and KM12SM (up to 25 μ M Fsk) compared to KM12C cells. Data shown is mean \pm SD of n=3 independent experiments. (*) $P < 0.05$; (**) $P < 0.01$.

Figure 30. Metastatic cells have increased resistance to Fsk

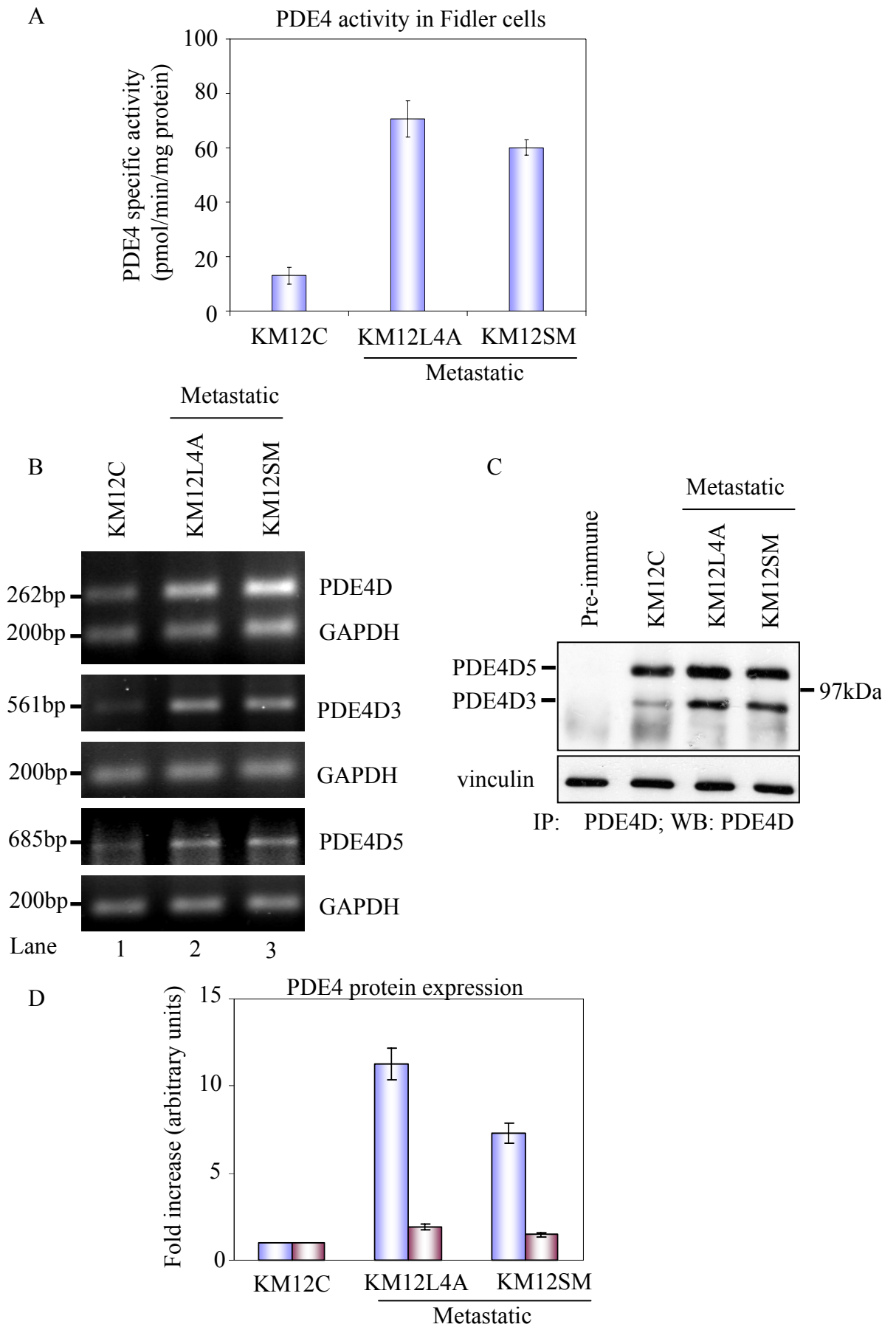


5.3 Metastatic cells have increased PDE4 activity and expression

One mechanism by which the metastatic cell lines might evade the anti-proliferative effects of Fsk is through increased activity and/or expression of PDEs which serve to cause the breakdown of cAMP. We showed that PDE4 actively regulates the anti-proliferative effects of cAMP in KM12C cells (Chapters 3 and 4). Therefore, we decided to examine the activity and expression of PDE4 isoforms in the metastatic cell lines to assess any alterations in this pathway which might account for the acquired resistance to cAMP elevation. Firstly, we examined the cAMP specific PDE activity of all three cell lines under resting conditions and found that while KM12C cells had relatively low PDE4 activity (13 ± 3 pmol/min/mg protein; Figure 15 E and Figure 31 A), KM12L4A metastatic cells had a 4 to 5 fold increase in PDE4 specific activity (70 ± 3 pmol/min/mg protein; Figure 31 A). The KM12SM cells had a similar increase in PDE4 specific activity (60 ± 7 pmol/min/mg protein; Figure 31 A). We next analysed PDE4 subfamily expression using semi-quantitative RT-PCR, showing that mRNA corresponding to PDE4A and PDE4C sub-families was not present in any of the cell lines (data not shown), and that PDE4B mRNA was present but no protein could be detected (data not shown). For PDE4D, mRNA was increased in both the KM12L4A and KM12SM cells (Figure 31 B). In particular, PDE4D3 and PDE4D5 isoforms had increased mRNA expression in both of the metastatic cell lines, compared to the poorly metastatic KM12C cell line (Figure 31 B). This was confirmed by immunoprecipitation and immunoblotting with a pan-PDE4D antibody (Figure 31 C). In KM12C cells, the predominant PDE4 isoform was the 108 kDa PDE4D5, with very little PDE4D3 detected (Figure 31 C). However, in KM12L4A cells, we found that PDE4D3 expression was increased approximately 12 fold and PDE4D5 expression by approximately 1.5-2 fold compared to KM12C cells (Figure 31 C and quantified in 31 D). KM12SM cells also exhibited increased expression of PDE4D3 and PDE4D5 but to a lesser extent

(approximately 7 fold and 1.5 fold respectively; Figure 31 C and quantified in 31 D). These data suggests that during the multi-step process of tumourigenesis, there was selection for increased PDE4D expression, presumably contributing to the reduced sensitivity to cAMP-mediated growth suppression in these cells.

Figure 31. Metastatic cells have altered PDE4 expression and activity. (A) PDE4 specific activity in KM12C, KM12SM and KM12L4A cells was assessed *in vitro* using 1 μ M cAMP as substrate in the presence and absence of rolipram to calculate resting PDE4 activity. The difference between untreated \pm rolipram was used to calculate the specific activity. Activities are expressed as a mean \pm SD of n=3 independent assays. Both metastatic cell lines have a 5-6 fold increase in PDE4 activity compared to KM12C cells. (B) Semi-quantitative Reverse-transcription polymerase chain reaction (RT-PCR) using cDNA derived from mRNA as template and PDE4 sub-family specific primers as probes, showed elevated levels of PDE4D transcript were present in both KM12L4A and KM12SM cell lines (upper panel; lanes 2 and 3). Using isoform specific primers as probes, both PDE4D3 and PDE4D5 isoforms were also shown to have increased levels of transcript present. Primers for GAPDH were used as an internal loading control in all of the above. Gels shown are representative of n=3 independent experiments. (C) Immunoprecipitation with either pre-immune serum or a pan-PDE4D sub-family specific anti-body using KM12C, KM12L4A and KM12SM lysates and probing with the same antibody in a western blot indicated that PDE4D3 and PDE4D5 protein levels were also increased in the metastatic cell lines. Blot is representative of n=3 independent experiments. (D) Densitometry quantification of PDE4 expression (fold increase compared to control (KM12C); arbitrary units) showed a 1.5-2 fold increase in PDE4D5 protein and an approximate 12 fold increase in PDE4D3 levels. Quantification is mean \pm SD of n=3 independent experiments.



5.4 PDE4D RNAi sensitises metastatic cells to Fsk

Next, we set out to generate a stable knockdown of PDE4D sub-family in KM12L4A cells, using an RNAi sequence directed against PDE4D family enzymes (238) cloned into a short hairpin vector (shRNA). This was used to determine the role of the PDE4D enzymes in regulating key proliferation pathways in these late stage metastatic tumour cell lines. Therefore, KM12L4A were transfected with PDE4D shRNA (L4 4Di) or scrambled 4D sequence as a control (L4A 4D_{cont}). Analysis of PDE4D expression by western blotting, in the L4A 4D_{cont} and L4A 4Di cell lines showed an approximate 80% reduction in PDE4D3 and 50% reduction in PDE4D5 protein expression (Figures 32 A and B).

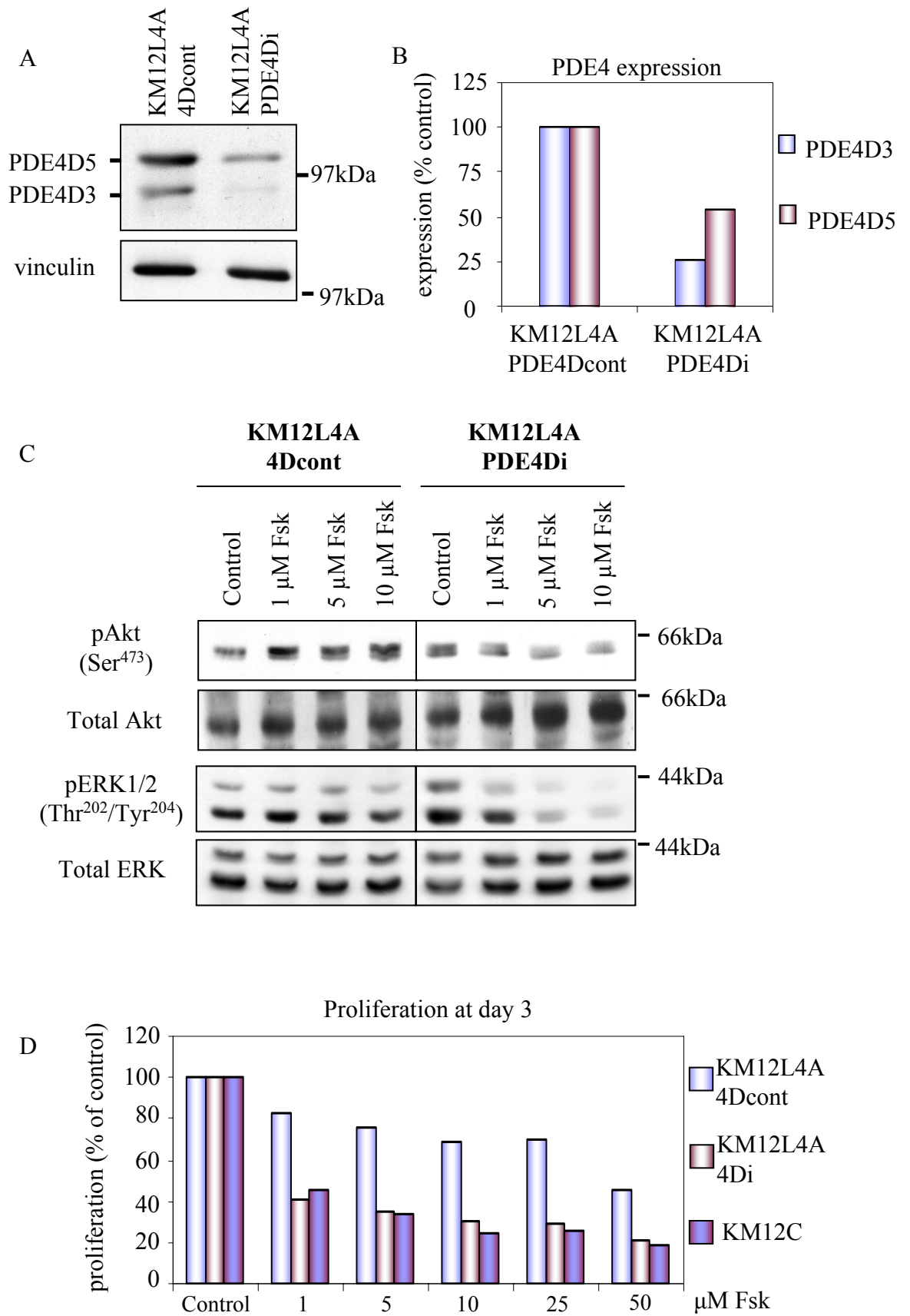
We then tested whether or not reduced expression of PDE4D isoforms in the L4A 4Di metastatic cell line had any effect on the ability of these cells to respond to the effects of Fsk and signaling to the ERK and PI 3-kinase/Akt pathways. Potentially, this would offer insight into the roles of PDE4D3 and PDE4D5 in the metastatic Fidler cells.

L4A 4D_{cont} and L4A 4Di cells were challenged with increasing Fsk concentrations and pAkt (Ser⁴⁷³) and pERK (Thr²⁰²/Tyr²⁰⁴) levels were monitored by western blotting. Although there was a decrease in pAkt (Ser⁴⁷³; Figure 32 C), a larger decrease in the levels of pERK (Thr²⁰²/Tyr²⁰⁴) was observed (Figure 32 C). Interestingly, treatment of L4A 4Di cells with increasing concentrations of Fsk, resulted in a partial inhibition of proliferation, as measured by MTT assay (Figure 32 D). This greater sensitivity to Fsk in the metastatic Fidler cells when PDE4D proteins reduced was similar to the inhibition of proliferation achieved in the poorly-metastatic KM12C cells (Figure 32 D). These data imply that increased expression of PDE4D isoforms, and in particular PDE4D3, was contributing to the increased resistance to Fsk mediated inhibition of proliferation in the metastatic cells. The metastatic cells may have used this mechanism to counter the strong anti-proliferative effects cAMP in PDE4

regulated compartments to which the poorly-metastatic parental cell line, KM12C, is sensitive (Chapters 3-4).

Figure 32. PDE4D RNAi sensitises KM12L4A cells to Fsk. (A) Partial knockdown of PDE4D protein levels was achieved using a lenti-viral vector containing a sequence specific for PDE4D sub-family. KM12L4A cells were infected with either PDE4D RNAi (KM12L4A4Di) or PDE4D scrambled sequence as a control (KM12L4A4D_{cont}), grown in selection media, FACs sorted for GFP-positive cells and pooled. PDE4D protein expression was analysed by immunoprecipitation and western-blotting using a pan-PDE4D antibody. Blot shown is representative of n=3 independent experiments. As a loading control, lysates were also subject to SDS-PAGE and vinculin expression was analysed using a specific antibody. (B) Densitometry quantification of PDE4D knockdown of both isoforms of n=3 independent experiments. PDE4D3 protein expression was reduced by approximately 80% and PDE4D5 by approximately 50%. (C) KM12L4A4D_{cont} and KM12L4A4Di cells were treated with increasing concentrations of Fsk and pAkt(Ser⁴⁷³) and pERK (Thr²⁰²/Tyr²⁰⁴) levels were analysed by western blotting. (D) Proliferation of KM12L4A4D_{cont}, KM12L4A4Di and KM12C cells were analysed after 3 days continuous growth in the presence of increasing concentrations of Fsk. All blots are representative of n=3 independent experiments. Proliferation assays are the mean \pm SD calculated as a percentage of control of n=3 independent experiments.

Figure 32. PDE4D RNAi sensitises KM12L4A cells to Fsk



5.5 PDE4D3 does not regulate the apoptosis in KM12C cells

Next, we individually expressed both PDE4D3 and PDE4D5 isoforms in KM12C cells and challenged them with Fsk in order to ascertain which isoform is involved in the regulation of the apoptotic pool of cAMP in these cancer cells. Therefore, cells were treated in the presence or absence of 1 μ M Fsk for 24 hours (which only produces a small increase apoptosis; Figure 21 B). The PDE4 proteins expressed were either wild type or dominant negative full length proteins with a VSV tag, to aid identification. The dominant negative (DN) isoforms were generated by a point mutation in the codon corresponding to the aspartate residue in the catalytic domain (D556A in PDE4D5), rendering the enzyme catalytically inactive (237, 238, 273). The VSV epitope tag is a stretch of 10 amino acids that is located within amino acids 501-511 of the Vesicular Stomatitis virus glycoprotein and contains the sequence YTDIEMNRLGK (462) and has previously been used as a tag by numerous groups, including the Houslay group, from whom I received the tagged PDE4 constructs (145).

KM12C cells were either mock transfected, transfected with VSV-PDE4D3 Wt (4D3 Wt) or VSV-PDE4D3 DN (4D3 DN) constructs, allowed to recover for 48 hours and incubated in the presence or absence of 1 μ M Fsk for 24 hours. We found that over-expression of 4D3 Wt alone was sufficient to prevent the Fsk/cAMP mediated loss of pAkt (Ser⁴⁷³ and Thr³⁰⁸) and pERK (Thr²⁰²/Tyr²⁰⁴) (Figure 33 A). Also, expression of 4D3 Wt and treatment with Fsk does not lead to a statistically significant increase in apoptosis ($P > 0.05$), as measured by PI staining and when compared to 4D3 Wt transfected, untreated cells (Figure 33 B). This suggests that PDE4D3 may have a protective role against Fsk mediated apoptosis in KM12C cells. Expression of PDE4D3 DN resulted in suppression of pAkt (Ser⁴⁷³ and Thr³⁰⁸) and pERK (Thr²⁰²/Tyr²⁰⁴) after Fsk treatment (Figure 33 A) as well as restoration of Fsk mediated apoptosis (Figure 33 B). However, this effect was not enhanced over mock-transfected, Fsk

treated cells and was not statistically different ($P > 0.05$). This indicates that although expression of PDE4D3 dominant negative restored Fsk mediated suppression of pAkt (Ser⁴⁷³ and Thr³⁰⁸) and pERK (Thr²⁰²/Tyr²⁰⁴), it did not enhance apoptosis. Therefore, if PDE4D3 was regulating the cAMP pool which controls apoptosis in KM12C cells, displacement of the endogenous enzyme would have enhanced the apoptotic effect of increasing cAMP in compartments regulated by PDE4D3. Thus, PDE4D3 may not be responsible for controlling the apoptotic pool of cAMP in KM12C cells.

5.6 PDE4D5 may regulate KM12C apoptotic response to cAMP

Next, PDE4D5 Wt (4D5Wt) and PDE4D5 DN (4D5DN) were individually expressed in KM12C cells and pAkt (Ser⁴⁷³ and Thr³⁰⁸), pERK (Thr²⁰²/Tyr²⁰⁴) and apoptosis were analysed after 24 hours treatment with 1 μ M Fsk. Over-expression of PDE4D5, which is the major PDE4 isoform expressed in KM12C cells (Figure 31), resulted in a rescue of Fsk mediated suppression of pAkt (Ser⁴⁷³ and Thr³⁰⁸) and pERK (Thr²⁰²/Tyr²⁰⁴) (Figure 34 A) when compared to Fsk treated, mock transfected cells (Figure 34 A). Although expression of PDE4D5 in KM12C cells resulted in an increase in basal apoptosis, the overall increase in apoptosis was only 3% when challenged with 1 μ M Fsk, implying that PDE4D5 may also be playing some protective role in these cells (Figure 34 B). However, expression of PDE4D5 DN and Fsk treatment resulted in the suppression of pAkt (Ser⁴⁷³ and Thr³⁰⁸) as well as pERK (Thr²⁰²/Tyr²⁰⁴) (Figure 34 A). In contrast to the results obtained when PDE4D3 DN was over-expressed, the combination of 4D5DN and Fsk treatment resulted in a large increase in apoptosis (20% gated cells had sub-2n DNA; Figure 34 B) which was statistically significant ($P < 0.05$) compared to Fsk treated, mock transfected cells. Thus, it is possible that PDE4D5, and not PDE4D3, regulates specific sub-cellular pools of cAMP which controls downstream signalling and, when inhibited, causes cell death. Potentially, we have identified a new role for PDE4D5 and which may be important in controlling cancer cell death/survival pathways and that could be utilised for therapeutic benefit.

Figure 33. PDE4D3 does not regulate apoptosis in KM12C cells. (A) KM12C cells were either mock transfected, transfected with PDE3D3-VSV or PDE4D3 (dominant negative; DN)-VSV, left for 48 hours and treated with either control (DMSO) or 1 μ M Fsk for 3 hours. Cells were lysed and pAkt (Ser⁴⁷³ and Thr³⁰⁸) or pERK (Thr²⁰²/Tyr²⁰⁴) levels were analysed by western blotting. Total Akt and total ERK levels were used as loading controls and an anti-VSV antibody was used to monitor PDE4D3 expression. (B) Propidium iodide (PI) analysis of sub-2n DNA content in cells transfected as above, treated with 1 μ M Fsk for 24 hours. Data is expressed as mean percentage gated cells \pm SD. ** $P > 0.05$.

Figure 33. PDE4D3 does not regulate apoptosis in KM12C cells

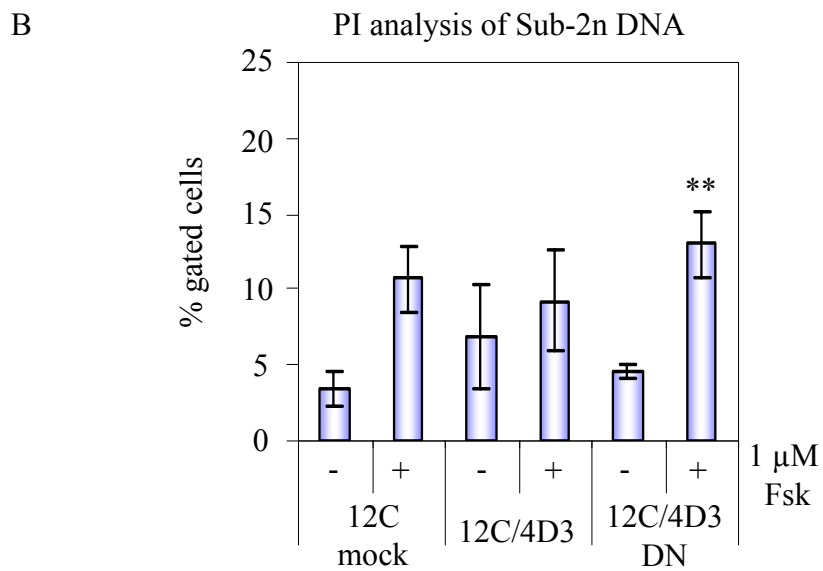
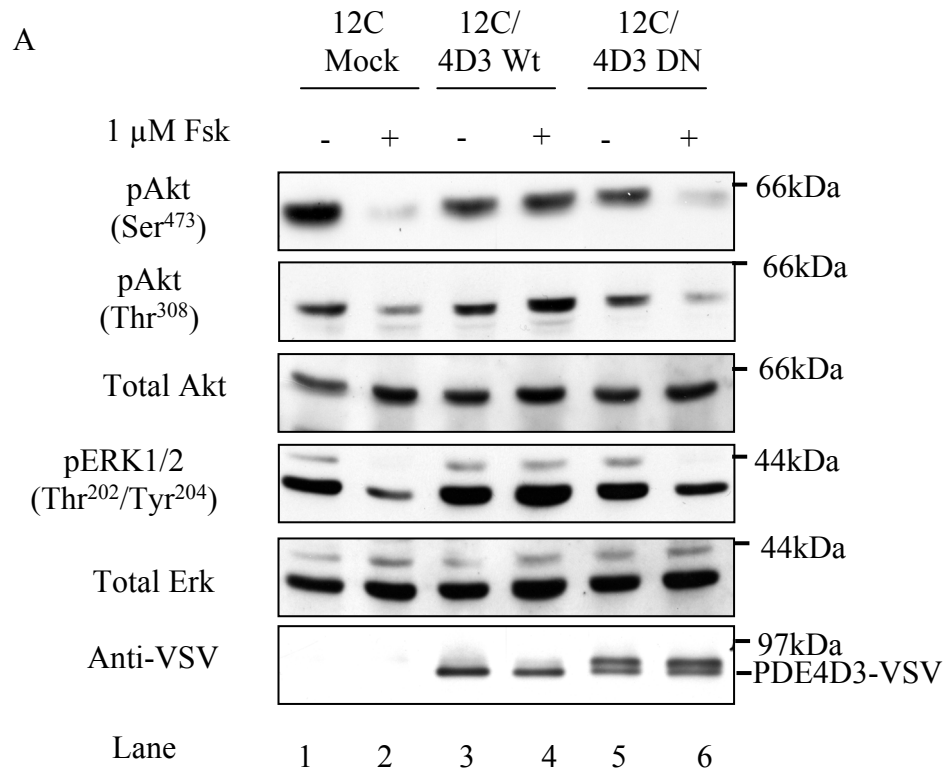
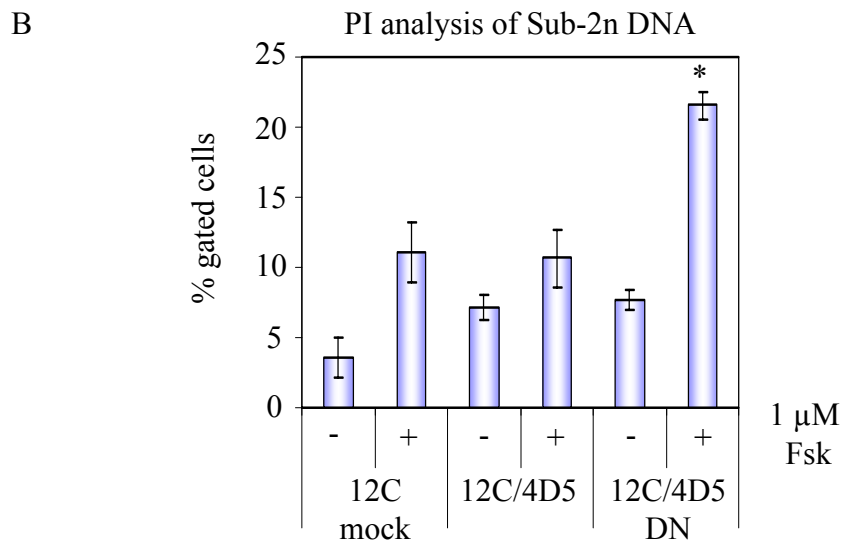
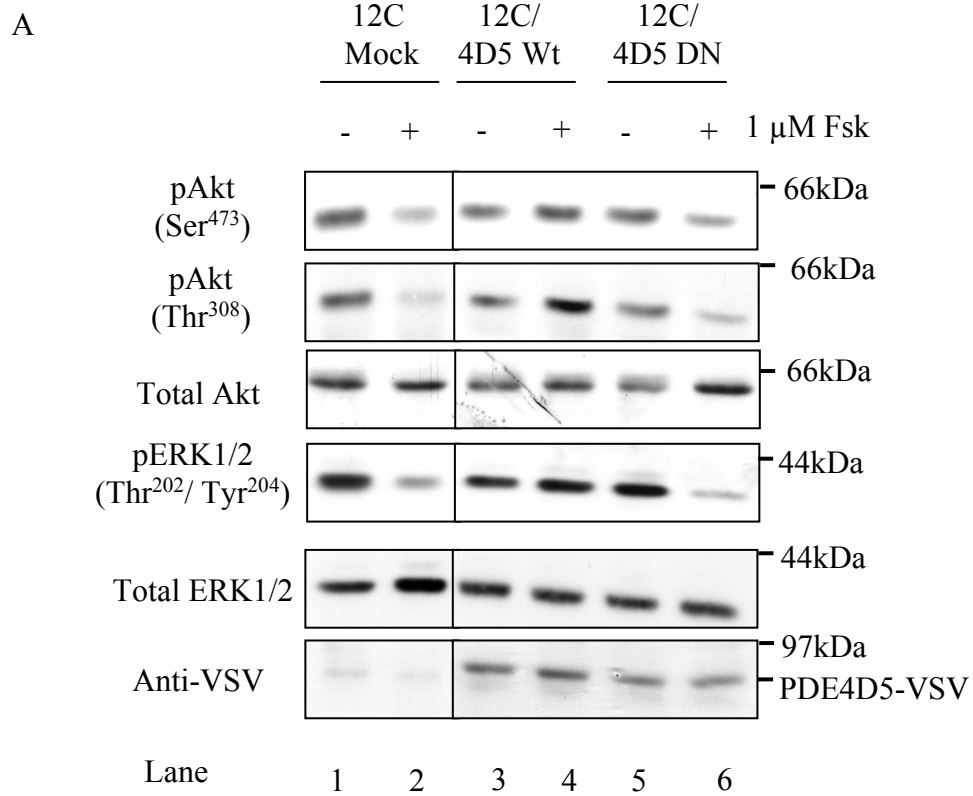


Figure 34. PDE4D5 may regulate KM12C apoptotic response to cAMP. (A) KM12C cells were either mock transfected, transfected with PDE3D5-VSV or PDE4D5 DN-VSV, left for 48 hours and treated with either control (DMSO) or 1 μ M Fsk for 3 hours. Cells were lysed and pAkt (Ser⁴⁷³ and Thr³⁰⁸) or pERK (Thr²⁰²/Tyr²⁰⁴) levels were analysed by western-blotting. Total Akt and total ERK levels were used as loading controls and an anti-VSV antibody was used to monitor PDE4D5 expression. (B) Propidium iodide (PI) analysis of sub-2n DNA content in cells transfected as above, treated with 1 μ M Fsk for 24 hours. PDE4D5 protects KM12C cells from apoptosis and PDE4D3DN enhanced the effect of Fsk with an increase in cells with sub-2n DNA compared to mock transfected, Fsk treated cells. Data is expressed as mean percentage gated cells \pm SD. * $P < 0.05$.



Discussion

5.7 Metastatic resistance to Fsk inhibition of proliferation

Increased resistance to chemotherapeutic agents is a key theme in advanced cancer and even now examples of resistance to new molecularly targeted therapies are emerging. For example, resistance against the BCR-Abl tyrosine kinase inhibitor imatinib, which is used extensively in the treatment of CML and gastrointestinal stromal tumours (GIST), occurs by mutation of several key residues in the Abl tyrosine kinase domain (463). These mutations frequently resulted in outgrowth of clones with imatinib-resistant BCR-Abl mutations and subsequent patient relapse. To combat this, dasatinib, the dual Src/BCR-Abl kinase inhibitor, is used to overcome imatinib-resistant BCR-Abl mutations, at least in all but one of the mutations (464). It is reported that dasatinib is 300 times more selective for BCR-Abl than imatinib and may eventually become the frontline treatment for CML (465, 466). This highlights the need to understand molecular mechanisms by which drug resistance emerges and the requirement to further develop more effective treatments.

In our study, we found that the metastatic derivatives of KM12C cells, namely the experimentally derived KM12L4A and spontaneous metastatic cell line KM12SM, have increased resistance to cAMP induced inhibition of proliferation. It appears that a hierarchical correlation exists between increasing metastatic potential and decreased sensitivity to Fsk, where Fsk resistance is ordered as such $KM12C < KM12SM < KM12L4A$; with KM12C cells being least metastatic (and most sensitive to Fsk) and KM12L4A cells being producing the greatest frequency of liver metastases (and being least sensitive to Fsk) when injected into the spleens of nude mice (40, 41). There are several mechanisms by which cells could evade the anti-proliferative effects of Fsk, including alterations in the cell death pathways, increased PDE expression and/or activity as well as alterations in the adenylyl cyclase proteins that produce cAMP. Interestingly, alterations in Fsk sensitivity in adrenocortical

tumour cells arises through loss of expression of adenylyl cyclase-4 (AC4) enzymes, which renders these resistant to stimulation of cAMP production and therefore inhibition of proliferation (467-470). However, due to time constraints we were unable to examine these proteins in this study, which was concentrating on PDEs, but nevertheless investigation into other components of the cAMP pathway may provide further ideas as to how it may be exploited for therapeutic benefit.

These observations may have implications for future therapies designed to exploit cAMP-mediated inhibition of proliferation and, in particular, for the metastatic diseases that are often difficult to treat.

5.8 Increased PDE4 expression and activity in metastatic cell lines

Under conditions of normal cell proliferation and differentiation, PDE4 expression and activity changes in a cell-type and -context manner. For example, in the monocyte to macrophage differentiation process, there is a dramatic reduction in PDE4-activity and this is associated with a marked down-regulation of both PDE4D3 and PDE4D5 isoforms (471). Also, PDE4 expression is altered in inflammatory cells of smokers with COPD, when compared to smokers without COPD and non-smokers (472). PDE4 expression can also be regulated by changes in intracellular cAMP. For example, increasing intracellular cAMP in smooth muscle cells can induce expression of PDE4D5 and site directed mutagenesis identified a cAMP responsive element (CRE) present in its promoter sequence(244). Also, the short PDE4D1 and super-short PDE4D2 isoforms are also expressed in response to increased cAMP, which allows for the attenuation of cAMP signalling in cells (265).

In metastatic derivatives of the KM12C cells, we found a robust up-regulation of PDE4 specific cAMP hydrolysing activity that correlates with increased expression of PDE4D, in particular PDE4D3 and PDE4D5 enzymes (Figure 31). This led us to propose that elevated

PDE4D3 and/or PDE4D5 were primarily responsible for the reduced sensitivity of metastatic cells to Fsk. Metastatic cells appear to have selected for an up-regulation of PDE4s which enhances their ability to proliferate under conditions of increased cAMP. When we depleted PDE4D using a sub-family specific RNAi sequence, we sensitised these cells to Fsk inhibition of proliferation making them respond in a similar way to the poorly-metastatic KM12C cells (Figure 32). This underlines the importance of PDE4 regulation of proliferation in cancer cells from the Fidler model of colorectal metastasis. A similar increase in PDE4D expression has been reported in thyroid tumours with activating mutations in either the thyroid stimulating hormone receptor (TSHR) or the $G_s\alpha$ subunit of the G-proteins (473). This raises the exciting possibility that PDE4 expression may be generally associated with late stage metastatic tumours, and that this may be a result of increased cAMP signalling occurring during tumour progression.

The role of PDE4D sub-family enzymes in regulating proliferation of epithelial cells has not been widely studied. However, it has been reported that PDE4D plays a non-redundant role in regulating interleukin-2 (IL-2) production as well as proliferation in T-cells, as RNAi depletion of PDE4D resulted in decreased IL-2 production and inhibited proliferation, similar to what was seen when using a pan-PDE4 inhibitor (474). It appears to be PDE4B that is primarily responsible for regulating the PDE4-mediated inhibition of proliferation in other cell types, such as lymphocytes (339, 417, 475). The emerging role of PDE4 enzymes as critical regulators of proliferation in tumour cells has wide ranging implications for the development of future therapeutics where further development of PDE4 sub-family specific inhibitors may be clinically important in the treatment of cancer (discussed in detail later).

5.9 PDE4D3 versus PDE4D5 regulation of proliferation and cell death

Spatial and temporal regulation of cyclic AMP signalling is a well studied phenomenon (130). Highly compartmentalised signalling is achieved mainly by the scaffolding of both cAMP degradation and effector machinery, often close to a particular receptor, or the localisation with a particular adenylyl cyclase isoform. This allows specific activation of downstream pathways as well as regulating the duration and amplitude of the signal (137, 414). This is especially true for PDE4 regulated cAMP signalling, where interaction with scaffolding proteins such as AKAPs, RACK1 and β -arrestins can influence the effects of cAMP in a context specific manner (137, 143, 262, 414). The two main PDE4 enzymes identified in this study, namely PDE4D3 and PDE4D5, have completely different binding partners which can either act to recruit (as in the case of PDE4D5 and β -arrestin and RACK1) or anchor (as with PDE4D3 and mAKAP) the enzymes to different sub-cellular locations (144, 145, 271, 275-278).

We have found that over-expression of either PDE4D3 or PDE4D5 enzymes protects KM12C cells from Fsk mediated reduction in pAkt, pERK and induction of apoptosis (Figures 33 and 34). Overexpression of dominant-negative, catalytically inactive, versions of PDE4D5 and PDE4D3 and subsequent challenge with Fsk resulted in both suppression of pAkt and pERK as well as increased cell death (Figures 33 and 34). Using the Mann-Whitney two-sample test of PI stained cells to compare mock transfected, Fsk treated and DN, Fsk treated populations, indicated that transfection with PDE4D5 DN (and not PDE4D3 DN) and subsequent treatment with Fsk resulted in a statistically significant increase in cell death. This data implies that is potentially PDE4D5 (and not PDE4D3) which is regulating the intracellular pool of cAMP responsible for inducing cell death, despite both isoforms seemingly able to regulate both pAkt and pERK (Figures 33 and 34). Therefore, we propose

that it is the spatial regulation of cAMP and its influences on specific sub-cellular pools of pAkt/pERK that is important for the induction apoptosis. However, due to time constraints, we were not able to investigate this further using techniques such as confocal microscopy (for analysing pAkt/pERK/PDE4 localisation) or FRET (spatial generation of cAMP) which would have given us further insights into the precise mechanisms governing PDE4-mediated regulation of proliferation and apoptosis in KM12C cells. Also, over-expression of PDE4D enzymes may not be the ideal experiment, as we may have been effectively ‘forcing’ the PDE4s into compartments that they would not be in at endogenous expression levels. More refined approaches to take the work forward will be required, and will be discussed later.

5.10 Summary

We have found that PDE4 activity is 4 to 5-fold higher in two highly-metastatic variant cell lines, namely KM12L4A and KM12SM, compared to their poorly-metastatic parental cell line KM12C. This increase in PDE4-specific activity strongly correlated with increased expression of PDE4D3 and PDE4D5 isoforms at both mRNA and protein levels, as well as reduced sensitivity to Fsk mediated inhibition of proliferation. Partial depletion of PDE4D enzymes using RNAi resulted in re-sensitisation of these cells to Fsk mediated inhibition of proliferation, which appeared to be dependent mainly on the PDE4D3 isoform. In contrast, we found that over-expression of PDE4D3 and PDE4D5 separately in KM12C cells was sufficient to protect from Fsk mediated apoptosis. Using dominant negative forms of the enzymes, we identified PDE4D5 as the principal contributor to altered proliferation of these cells.

The important role of PDE4s in the Fidler model of colorectal cancer cell line in regulating proliferation raises the exciting prospect that a Fsk/rolipram-type of treatment may be exploited as a therapeutic strategy for epithelial cancers. However, at this stage it is unclear whether this is a unique feature of this cell line and if it can be more widely applicable to

other cancer cell types. The next chapter will address the generality of Fsk/rolipram-induced inhibition of cancer cell lines of different origins as well as the effects of a Fsk analogue which is water soluble and has been used in a number of animal and clinical studies.

Chapter 6:
**NKH477: A potentially clinically relevant
Fsk analogue**

6. Effects of Fsk/rolipram and Fsk analogues on cancer cell proliferation

6.1 Aim

To address the generality of Fsk/rolipram treatment to inhibit proliferation we used of cancer cell lines of different origin. Also, we tested the effects of a more clinically relevant Fsk analogue, NKH477 (colforsin daropate) in its ability to inhibit KM12C proliferation, effects on downstream signalling and also the effects NKH477 has on the proliferation of the panel of cancer cell lines.

6.2 Sensitivity to growth inhibition by cAMP modulation is not restricted to KM12C cells

In considering the potential therapeutic benefit of any new strategy, for example combinations of cAMP modulators, it is important to test whether the observed effects are not particular to one cell line, in this case KM12C cells. Therefore, we examined a number of different cell lines for their ability to proliferate in the presence of Fsk/rolipram using the MTT dye based assay to measure the proliferation. Of the 11 cell lines were selected from various tissues of origin, these were 7 colon cancer cell lines (KM12C, HT29, WiDr, RKO, H630, SW480 and SW620), 1 breast (MCF7), 1 squamous cell carcinoma (SCC; A431), 1 prostate (Du145) and 1 melanoma (A375) cell line. All cell lines differed in their doubling times and the assay was optimised by assessing which starting cell number gave a non-saturated A570nm absorbance after 3 days. All cell lines were plated at their optimised density, allowed to adhere overnight and then treated continuously with **control** (DMSO) or **Fsk/rolipram** for 3 days continuously prior to MTT analysis.

After Fsk/rolipram treatment, the cell lines segregated into three distinct groups; highly sensitive (red), intermediately sensitive (blue) and resistant (green). In conjunction with

proliferation assays, each cell line was also analysed for their endogenous levels of PTEN, pAkt (Ser⁴⁷³) and pERK (Thr²⁰²/Tyr²⁰⁴) with tubulin used as a loading control. As a readout of PTEN activity, pAkt (Thr³⁰⁸) was used as this site is dependent on PDK1 activity, which, in turn requires PtdIns(3,4,5)P3 and therefore active PI 3-kinase.

3 out of the 11 cancer cell lines tested (KM12C, MCF7 and HT29) were sensitive to Fsk/rolipram-induced inhibition of proliferation, displaying approximately 80% inhibition of proliferation (Figure 35 A). Analysis of the PI 3-kinase/Akt and ERK pathways showed that KM12C cells completely lack PTEN expression and have relatively high pAkt (Thr³⁰⁸ and Ser⁴⁷³; Figure 35 B). In contrast, both MCF7 and HT29 cells appear to express functional PTEN protein, due to the presence of pAkt (Thr³⁰⁸) (Figure 35 B). Also, MCF7 and HT29 cells displayed almost undetectable levels of pAkt (Ser⁴⁷³) and only modest levels of pERK (Thr²⁰²/Tyr²⁰⁴) (Figure 35 B).

5 out of the 11 cell lines (A431, WiDr, RKO, A375 and H630; blue) showed a partial sensitivity to Fsk/rolipram treatment, displaying between 40% and 60% inhibition of proliferation (Fig. 35 A). Interestingly, all five cell lines had PTEN protein present, but in A431 and RKO cells, pAkt(Thr³⁰⁸) levels were relatively high which did not correlate with PTEN status when compared to the other cell lines (Fig. 35 B). In contrast, A375 and H630 cell lines appeared to retain functional PTEN protein due to decreased levels of pAkt (Thr³⁰⁸) but both showed elevated levels of pAkt (Ser⁴⁷³), indicating that this is possibly regulated independently from PI 3-kinase activity (Fig. 35 B). Also, it was interesting to note that the more Fsk/rolipram resistant cell lines have increased levels of pERK (Thr²⁰²/Tyr²⁰⁴), indicating that perhaps their survival is dependent on other signalling pathways and not solely on the PI 3-kinase/Akt pathway (Fig. 35 B).

Du145, SW480 and SW620 cell lines were all insensitive (green), as their proliferation was only inhibited by approximately 20% upon Fsk/rolipram treatment (Figure 35 A). Both

PTEN and pAkt status varied between each cell type, with Du145 displaying active PTEN (through lack of pAkt (Thr³⁰⁸)), which did not correlate with pAkt (Ser⁴⁷³) status and also had moderate to high levels of pERK (Thr²⁰²/Tyr²⁰⁴) compared with the other cell lines (Figure 35 B). SW480 cell line showed a correlative expression of PTEN and decreased levels of pAkt (Thr³⁰⁸ and Ser⁴⁷³) whereas SW620 showed a similar pattern to that of Du145, but with greatly decreased levels of pERK (Thr²⁰²/Tyr²⁰⁴) (Fig. 35 B). Thus, there are a sub-set of cancer cells that respond to a greater or lesser extent to the Fsk/rolipram combination (8 out of 11 in our study), implying that a proportion of cancer cells may be sensitive to this type of growth modulation.

Figure 35. Fsk/rolipram inhibits a number of cancer cell lines. (A) Cancer cell lines of varying origins were treated with either control (DMSO) or Fsk/rolipram (100 μ M Fsk + 10 μ M rolipram) for 3 days and their proliferation assessed using an MTT assay, and expressed as a percentage of control. Response to Fsk/rolipram treatment of the 11 cancer cell lines placed them into three distinct groups: Sensitive (>60% inhibition; red writing), intermediately sensitive (40-60% inhibition; blue) and insensitive (<20% inhibition; green). Data shown is mean \pm SD of n=3 independent experiments. Red dotted line represents cut-off for sensitive cell lines (30% control) and blue dotted line represents cut-off for intermediately sensitive cell lines (60% of control). (B) Protein levels of PTEN, pAkt (Thr³⁰⁸ and Ser⁴⁷³) and pERK (Thr²⁰²/Tyr²⁰⁴) was assessed in Fsk/rolipram sensitive (red text), intermediately sensitive (blue text) and insensitive (green text) cell lines. Tubulin was used as a loading control for all of the above. Blots shown are representative of n=3 independent experiments.

6.3 NKH477 induces p27^{Kip1} and loss of pAkt in KM12C cells.

We now know that compounds that elevate intracellular cAMP can effectively kill cancer cell lines of various origins by multiple mechanisms (380, 392, 408, 476). Despite these potent anti-tumour effects, substances such as Fsk and 8-Br-cAMP cannot be used as anti-cancer agents due to their poor solubility and their high toxicity *in vivo*. However, the orally available, water soluble, adenylyl cyclase activator and Fsk analogue 6-(3-dimethylaminopropionyl)-Forskolin (NKH477 or colforsin daropate hydrochloride) has been used in a wide range of animal models, as well as in humans, to treat a variety of conditions (477-482). We therefore tested whether or not NKH477 inhibited KM12C proliferation by similar mechanisms to Fsk, whether rolipram also potentiated the effects of low concentrations of this adenylyl cyclase activator.

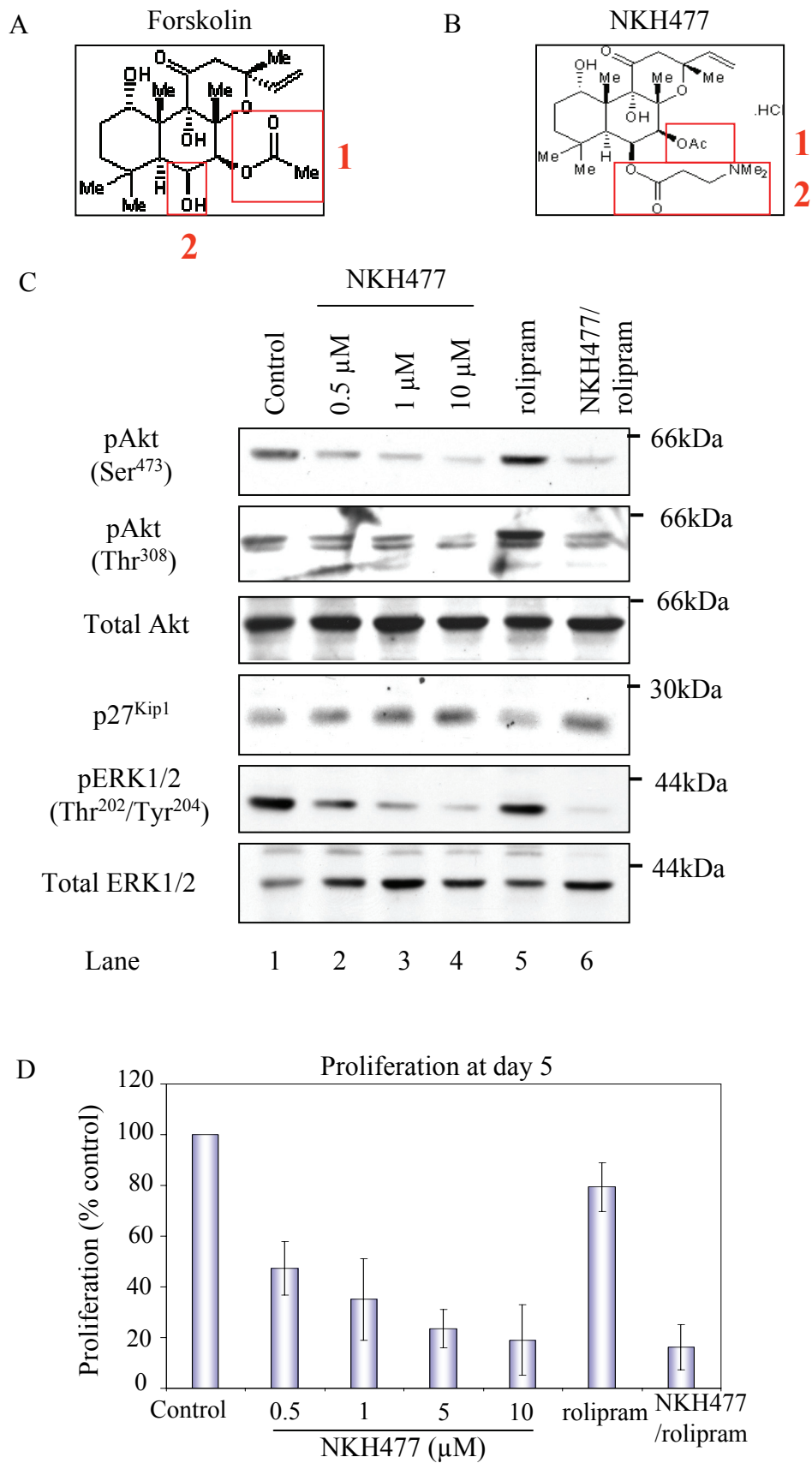
Both **Fsk** (Figure 36 A) and **NKH477** (Figure 36 B) are structurally similar, with only two side chain modifications altered (red boxes 1 and 2). Using increasing concentrations of **NKH477** (0.5, 1 and 10 μ M; Figure 36 C), 10 μ M **rolipram** alone (Figure 36 C) and a combination of 0.5 μ M NKH477 + 10 μ M rolipram (**NKH477/rolipram**; Figure 36 C) we examined the effects of these combinations on pAkt and pERK in KM12C cells. Treatment of KM12C cells with increasing concentrations of **NKH477** alone for 24 hours resulted in the dose dependent loss of pAkt (Ser⁴⁷³ and Thr³⁰⁸; Figure 36 C) compared to **control** cells. Increases in p27^{Kip1} and a decrease in pERK (Thr²⁰²/Tyr²⁰⁴) was also observed with increasing concentrations of **NKH477** when compared to **control** cells (Figure 36 C). Total ERK was used as a loading control (Figure 36 C). **NKH477/rolipram** treatment resulted in potentiation of low dose NKH477 (0.5 μ M) treatment causing a suppression of pAkt (Ser⁴⁷³ and Thr³⁰⁸), an increase in p27^{Kip1} and loss of pERK (Thr²⁰²/Tyr²⁰⁴) compared to **rolipram** treated KM12C cells (Figure 36 C). Also, using an MTT assay to assess the effect on proliferation after 5 days of treatment, we can see that the increasing concentrations of

NKH477 correlate with decreased proliferation (Figure 36 D). In addition, **NKH477/rolipram** can potentiate the inhibition of proliferation, where neither agent alone, at the concentrations used, can do so (Figure 36 D). This implied that **NKH477** and **Fsk** may be acting through similar pathways in KM12C cells despite the small structural differences.

6.4 NKH477 inhibits the proliferation of numerous cancer cell lines

We next assessed the effects of the Fsk analogue NKH477 on proliferation of the cancer cell lines described previously (Figure 35). In this case, treatment with either 100 or 50 μ M NKH477 alone induced approximately 70% (or greater) inhibition in all of the 10 cell lines tested (Figure 37). Thus, all 10 cell cancer cell lines tested were highly sensitive to NKH477. This is in contrast to Fsk/rolipram treatment, where only three cell lines were highly sensitive. This raises the exciting possibility of using NKH477, a compound which has extensively been tested in a variety of animal and human conditions with no adverse effects, as a potent anti-cancer agent. Further work to elucidate the mechanisms by which NKH477 so potently inhibits such a wide variety of cancer cell lines is required if any potential anti-cancer therapies based around this drug are to be realised. At this point we do not know why it has a more general effect on inhibiting cancer cell proliferation, but the mechanism of action cannot be identical to that of Fsk.

Figure 36. NKH477 suppresses pAkt, pERK and KM12C proliferation. (A) Chemical structure of Fsk, and (B) NKH 477, with the altered side chains highlighted (red boxes, 1 and 2). (C) KM12C cells were treated with control (DMSO), increasing concentrations of NKH477, 10 μ M rolipram or 0.5 μ M NKH477 + 10 μ M rolipram (NKH477/rolipram) and levels of pAkt (Thr³⁰⁸ and Ser⁴⁷³), p27^{Kip1} and pERK1/2 (Thr²⁰²/Tyr²⁰⁴) were analysed by western blotting. NKH477/rolipram synergise to suppress both pAkt (both sites) and pERK as well as inducing p27^{Kip1}. (D) NKH477, both alone, and in combination with rolipram, suppressed the proliferation of KM12C cells. All blots are representative of n=3 independent experiments. Proliferation is expressed as a percentage of control and is mean \pm SD of n=3 independent assays.



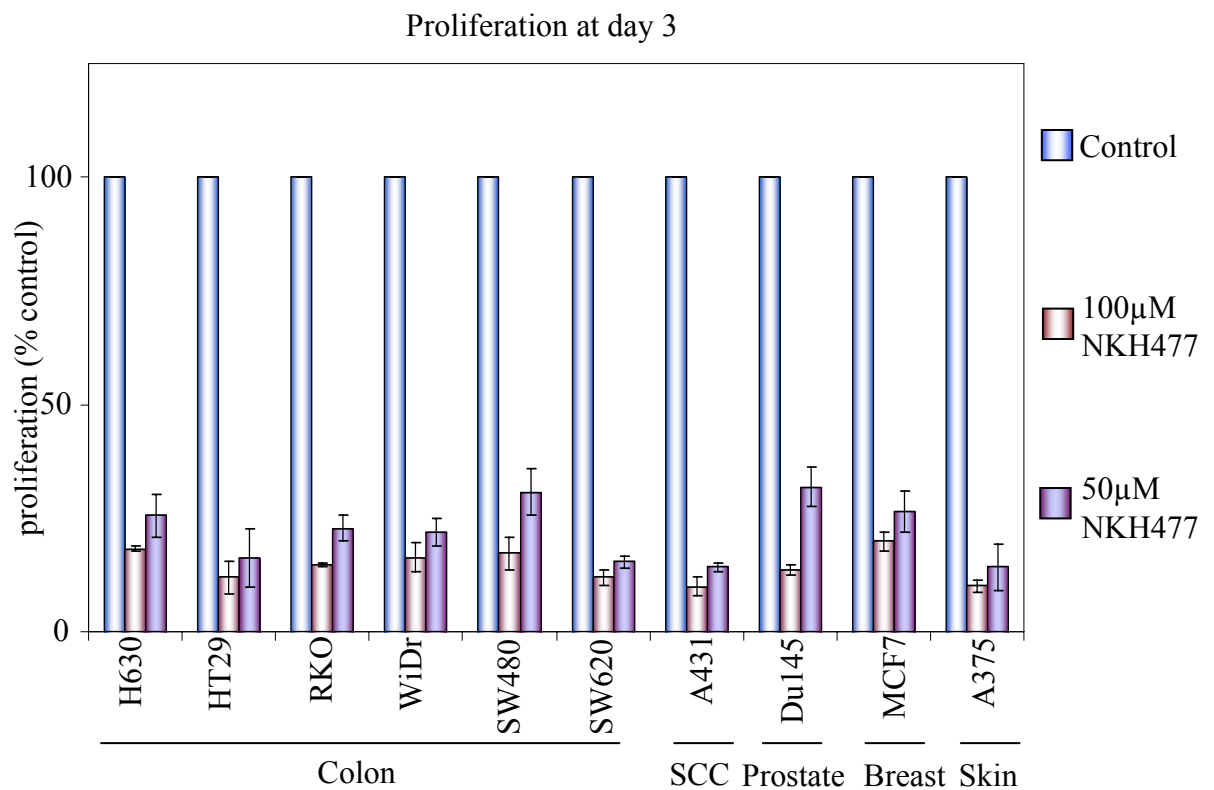


Figure 37. NKH477 inhibits the proliferation of all cancer cell lines. Proliferation of colon cancer cell lines (H630, HT29, RKO, WiDr, SW480 and SW620), squamous cell carcinoma (SCC; A431), prostate (Du145), breast (MCF7) and skin melanoma (A375) cell lines was assessed after 72 hours treatment with either control (DMSO), 100 µM NKH477 or 50 µM NKH477 using an MTT assay and was expressed as a percentage of control. Both concentration of NKH477 inhibited all the cell lines to >70% of control, where Fsk alone was unable to do so (data not shown).

Discussion

6.5 Cell lines sensitivity to Fsk/rolipram

Advanced cancer cells carry a unique set of mutated or inactivated genes that contribute to defining the nature and aggressiveness of individual tumours. For example, in lung cancer EGFR is frequently overexpressed leading to hyper activation of both ERK and PI 3-kinase pathways and in colon cancer mutations in the PI 3-kinase pathway, such as inactivation of PTEN or activating mutations in p85 or p110, as well as loss of APC are also common (7). In skin cancer, B-Raf V600E is a common, activating mutation that leads to hyperactivation of the ERK pathway (483).

In our study, we assessed the sensitivity of a variety of cancer cell lines to Fsk/rolipram mediated inhibition of proliferation and found that there were distinct variations in their sensitivities. Moreover, the sensitive and insensitive cell lines, when treated with LY294002, exhibited proliferation profiles similar to Fsk/rolipram treatment, indicating a possible correlation between Fsk/rolipram sensitivity and PI 3-kinase dependence (data not shown). However, despite our best efforts in analysing the PTEN/pAkt status of these cells, we could not define any distinct pattern that related PTEN/pAkt with Fsk/rolipram sensitivity (Figure 35). This could be attributed to a number of factors including mutations in PTEN that render it catalytically inactive but the cells still retain PTEN expression. This could explain why some cell lines exhibited relatively high levels of pAkt (Thr³⁰⁸) in the face of PTEN expression, for example A431 and RKO cell lines. However, in the case of A431 cells, EGFR is over expressed which may lead to hyperactivation of the PI 3-kinase/Akt pathway and therefore could account for the increased levels of pAkt observed (484). In the case of the RKO cell line, expression of wild type PTEN inhibited the activation of Akt as well as downstream signalling to β -catenin, indicating that the PTEN expressed in RKO cells is non-

functional (485). However, overall we could not correlate PTEN status with sensitivity to Fsk/rolipram-induced inhibition of proliferation.

In spite of this, this data does highlight the potential of pharmacological activators of adenylyl cyclase and PDE4 inhibitors, to have therapeutic benefit in the treatment of numerous cancers of different origins.

6.6 NKH477 as an anti-cancer therapy

Chemical compounds that often used in the laboratory setting are, more often than not, unsuitable for use in animal models or for the treatment of human diseases. Therefore, it is important to produce small molecules that overcome problems such as toxicity, insolubility, and increase their bioavailability. Forskolin is unsuitable for some of these reasons and so NKH477 (or colforsin daropate hydrochloride) was developed as a water soluble analogue that may be more suitable for *in vivo* use (477). It has been used in a wide variety of animal models for research topics including immuno-modulation in mice (480), canine ischemia (486), canine arrhythmia (478) and as an anti-depressant in a rat model (487). It has also been used in humans as a bronchodilator (488, 489) and as both an immune-suppressant and vasodilator during cardiac surgery (481). However, at present there are no reports of this compound being used as an anti-cancer drug either in cells or animal based studies.

In our study, we showed that NKH477 suppressed the proliferation of all 11 cell lines tested (Figures 36 and 37), where Fsk/rolipram was only able to inhibit 8 out of the 11 cell lines tested. We have also shown that NKH477 suppresses the proliferation of KM12C cells in a manner similar to that of Fsk and a low concentration of NKH477 was also able to synergise with rolipram (Figures 36). The mechanisms involved in NKH477 mediated inhibition of proliferation in the panel of cell lines remain unsolved, but clearly there are some differences to Fsk. Further work is required to elucidate whether or not NKH477 is inducing cell cycle

block and/or apoptosis in all the cell lines tested, which may provide useful information about potential uses. It has been reported that NKH477 is more selective for adenylyl cyclase-V isoform (490) and that could be the AC isoform important in the regulation of the anti-proliferative effects of cAMP in cancer cells. These data suggests the exciting possibility that this orally available, water soluble compound may be useful as an anti-cancer therapy. Further, work using both tissue culture and animal models is being undertaken to fully explore NKH477s potential as an anti-tumour agent.

6.7 Summary

We have found that a combination of Fsk/rolipram inhibits the proliferation of 8 out of 11 cancer cell lines of differing origins. Also, we addressed the effects of a more clinically relevant Fsk analogue, NKH477, on the same panel of cell lines. We found that NKH477 inhibited the proliferation of KM12C cells in a manner similar to that of Fsk and also that NKH477 potentiated the effects of a ‘low dose’ of NKH477 on pAkt, pERK and proliferation. Most surprising of all was the inhibition of proliferation observed in all cancer cell lines tested. The final chapter of my thesis will now discuss the potential of using PDE4 inhibitors and NKH477 as an anti-tumour therapy.

Chapter 7:
**Concluding remarks and future
perspectives**

7. Concluding remarks and future perspectives

7.1 cAMP, PDE4s and their therapeutic potential in cancer

We showed that a colorectal cancer cell line (KM12C), which is resistant to common chemotherapeutic agents such as 5-FU, can be inhibited from proliferating, and killed, by increasing cAMP in compartments regulated by PDE4 enzymes. We can also interfere with and inhibit the PI 3-kinase/Akt pathway as a result of modulating cAMP in PDE4-regulated compartments. Thus, KM12C cells are critically ‘addicted’ to the PI 3-kinase/Akt pathway, and use of a PI 3-kinase inhibitor, LY294002, recapitulated the effects of PDE4/cAMP modulation on proliferation and apoptosis. In retrospect, we could have stumbled upon this ‘addiction’ to the PI 3-kinase/Akt pathway by simply testing a range of inhibitors, including LY294002 (and potentially wortmannin). However, by approaching the inhibition of proliferation from the angle of modulating cAMP, we were able to identify a further ‘addiction’, namely that of keeping low levels of cAMP in PDE4-regulated sub-cellular compartments. We identified a new intersection between cAMP regulation and the PI 3-kinase/Akt pathway. We propose that cAMP-regulation of events may offer a new potential ‘Achilles heel’ for the treatment of some tumours that are resistant to conventional therapies.

Identification of ‘new’ addictions (such as keeping low cAMP in compartments controlled by PDE4s) that could be exploited to combat cancer may provide another therapeutic option for a tumour in advanced stage disease. Identification of patients that may benefit from a cAMP-based, or other molecularly targeted therapy, would ideally allow the tailoring of a patient’s treatment to their specific genetic drivers and oncogene addictions, hopefully providing a better long-term outcome.

Also, we have shown that in at least one model of colon cancer PDE4 expression and activity are elevated in metastatic cells, which confers a proliferative advantage to these cells in the presence of cAMP agonists.

The work presented in this thesis raises several important questions with regards to exploiting PDE4s and cAMP based therapeutics for the treatment of cancers which are otherwise difficult to kill:

- 1. Does PDE4 expression and/or activity correlate more evidently with tumour grade and/or survival?**
- 2. Can PDE4s and/or cAMP pathways be exploited as potential anti-cancer therapies?**
- 3. Can this work be translated from cell-based models of cancer to more relevant animal-based models of cancer, including colorectal?**

I will now address each of these important issues.

7.2 Does PDE4s elevation correlate with disease stage?

In terms of the clinical value, PDE4 expression may be a good prognostic marker for some late stage tumours and potentially could give an indication as to whether or not a cAMP/PDE4 based treatment may be effective for a particular individual, if expression was analysed in a tumour biopsy sample. This seems to be the case for diffuse B-cell lymphocytic leukaemia (DLBCL), where increased PDE4 expression was highlighted during analysis of a large number of genes from clinical DLBCL samples and which also correlated with the cells ability to be growth inhibited by PDE4-specific inhibitors (339, 379). This work has potentially opened the door for PDE4 based therapies for the treatment of some leukaemia's, and my work suggests this may also be applicable to other cancer types.

PDE4 expression and/or activity in epithelial cancer cells, or in tumours samples, is still not widely studied. Here we have considered several lines of investigation that would address the generality of PDE4 expression in tumours and, whether or not, elevated expression correlates with tumour grade. Firstly, a tissue micro-array (TMA) of tumour biopsy samples that are fixed and mounted ready for immunohistochemical (IHC) staining. This type of TMA study would, in principal, allow analysis of a large quantity of tumour samples, and from a variety of origins and multiple tumour stages. Often good TMAs are available from cancer centres where the samples are linked to clinical outcome, enabling inferences to be drawn about protein expression and disease progression. Equally in clinical setting, IHC analysis of PDE4 expression in a patient tumour biopsy could provide valuable insight as to whether not PDE4s are altered in cancer, and whether PDE4 inhibitor-based therapy might be employed. However, one major problem associated with PDE4 expression analysis by IHC is the limited availability of good, specific anti-human PDE4 antibodies, for all isoforms identified thus far. Due to the limited availability of antibodies, and coupled with time constraints, a TMA study would be technically difficult at the present time.

Another alternative to immunostaining is genetic profiling of tumour samples to define PDE4 isoform RNA levels. For example, RT-PCR or the more accurate quantitative-PCR (q-PCR), would tell us which PDE4 enzymes, both sub-family and specific isoforms, are expressed and whether or not their expression is altered relative to the surrounding tissue. This would be particularly useful for screening a number of tumour tissues as well as primary and metastatic cancer cell lines. This could also, in principal, provide a prognostic indicator of disease advancement, which may be useful information in a clinical setting. PCR-based analysis would counter the disadvantages of a lack of antibodies; however, it would not give any indication as to whether or not the activity of the enzymes was altered.

PDE4 activity would have to be investigated by biochemical means, as unlike cases of increased kinase activity/expression, there are no direct downstream readouts that could act as surrogate markers. Using anti-cAMP antibodies, its levels could potentially be observed by some IHC techniques, but this would have limitations, as it is most likely that PDE4s would be regulating distinct pools of cAMP, and perhaps not 'global' cAMP within the cell.

The relationship, if any, between PDE4 expression and aggressiveness of a particular tumour type, for example colon cancer, requires further investigation. Although difficult, as discussed above, this could potentially be rewarding in terms of identifying late stage tumours and potentially recognizing particular patient sub-groups who may benefit from therapeutic strategies based around PDE4 enzyme inhibition.

7.3 Can PDE4s be exploited as therapeutic targets for cancer?

PDE4s have been long-standing therapeutic targets for diseases such as asthma and COPD, where it is postulated that specific inhibitors will have both anti-inflammatory and smooth muscle relaxant properties. In recently completed phase III trials, the PDE4-selective inhibitor cilomilast decreased inflammatory responses and has subsequently been approved for the treatment of COPD (259). Another PDE4-selective inhibitor, roflumilast, also potently inhibits inflammatory responses (even more so than cilomilast), is active in models of bronchoconstriction and lung inflammation and is orally active (259). As a result, it too has been approved for the treatment of both COPD and asthma. There are also other PDE4 inhibitors undergoing phase I and Phase II trials for the treatment of asthma, COPD and neurological disorders (239). Therefore, there is great scope to utilise these compounds for clinical application in other disease areas that have also been shown to be dependent upon PDE4 activity. In addition, because these have undergone pre-clinical and clinical evaluation, such agents may be developed more rapidly as anti-cancer therapies.

Despite some tantalising reports suggesting PDE4s may be critical regulators of key cancer cell processes, they have not been fully exploited as potential anti-cancer therapeutics yet. However, during the period of my PhD, several reports have been published which highlighted PDE4-regulated cAMP elevation as a potent growth inhibitory event, especially in the case of haematological malignancies. Together with my work, these reports lend further credence to the potential of cAMP modulation as an anti-cancer therapeutic strategy (254, 291, 339, 377, 417).

My studies have focused on a potential role for PDE4 enzymes in the regulation of colorectal cancer cell proliferation and survival. However, we were aware that the effects observed by modulating PDE4/cAMP in the Fidler model of colorectal metastasis may not have been widely applicable to other cancer cell types. Nevertheless, despite not having a broad range study on PDE4 expression and/or activity in numerous cancer cell lines, we showed that using a combination of Fsk/rolipram, we could inhibit the proliferation of 8 out of 11 cancer cell lines of varying origin. This highlights the exciting possibility that there are potentially a number of cancers that may respond to a PDE4/cAMP based therapy. At this stage it is not clear whether, and if so how, Fsk/rolipram-induced apoptosis and/or cell cycle arrest in those 8 cell lines. However, it may be of value to carry out more extensive tests of other cancer cell types that were not represented, particularly chemoresistant and difficult to treat cancer cells (such as pancreatic), and attempt to identify common features that may define susceptibility to a cAMP-modulation based therapy.

Potentially, one of the major problems associated with PDE4-based therapy would be targeting specific PDE4 isoforms or even sub-families involved in specific disease states. This is due to the high degree of structural similarity between all of the PDE4 active sites. However, differential effects of abolishing specific PDE4 sub-family activities are an effective strategy in other disease contexts. For example, the PDE4-selective inhibitor

rolipram failed in early clinical trials due to adverse side effects that limited its use. The adverse side effects, such as nausea and emesis, were eventually related to inhibition of PDE4D, while the desired anti-inflammatory effects were related to PDE4B inhibition (235, 259). Therefore, it may be worthwhile pursuing the generation of sub-family specific rather than isoform specific inhibitors. This has already been exemplified by the generation of PDE4D selective inhibitors (491). However, another problem associated with generating PDE4 sub-family selective inhibitors is the conformation of the catalytic domain. It is believed that the PDE4 catalytic site of all four sub-families can adopt either a high-affinity rolipram binding site (HARBS) or a low affinity rolipram binding site (LARBS) (492). In fact, it was initially thought that the emesis and nausea caused by PDE4 inhibitor was due to the binding to PDE4s in the HARBS conformation (492). Currently, all PDE4 crystal structures of their catalytic domains bound to rolipram, are in the LARBS state. One of the biggest challenges for PDE4 inhibitor design is crystallisation of full-length protein and understanding the mechanisms involved in the switching of the active site to the HARBS conformation which will enable the design of more potent PDE4-selective inhibitors.

One compounding problem is that it may be difficult to generate specific small molecule inhibitors of specific PDE4 isoform active sites. Therefore, more likely PDE4 isoform targeting would involve the sub-cellular distribution of the enzymes, rather than their catalytic activity. This ‘displacement’ of PDE4 isoforms from their particular signalling complexes may be achieved by using small interfering peptides that compete with the native PDE4 enzymes for binding on specific scaffolding proteins. This is exemplified in ‘dominant-negative’ strategies where overexpression of a catalytically inactive PDE4 most likely displaces the endogenous enzyme, thereby preventing the regulation of cAMP in that particular sub-cellular compartment. Use of a specific interfering peptide that consisting of

38 amino acids that is identical to a portion of PDE4D5s unique amino-terminal region, disrupts the endogenous PDE4D5 interaction with both RACK1 and β -arrestin scaffolding proteins causing enhanced PKA phosphorylation of β 2-adrenergic receptor(493). This strategy itself offers yet more technical challenges, such as effective delivery of peptides to all cells in a tumour as well as limiting adverse side effects. A disruption based therapy for PDE4D3 would have to consider adverse effects on the heart, due to PDE4D3s prominent role in regulating contraction of the heart muscle (268). However, despite these obvious imperfections in designing an ideal strategy at this point, it is promising potential area of drug discovery to disrupt specific PDE enzyme isoform signalling.

In terms of metastatic cancer cells, we showed that in least one model PDE4 expression and activity were increased, hinting at a potential role for PDE4s in the metastatic process. To investigate this, we stably depleted PDE4D3 and PDE4D5 using a sub-family specific RNAi sequence. This depletion apparently sensitised the metastatic cells to inhibition of proliferation by low doses of Fsk alone. In addition, we showed that in KM12C cells PDE4D5 was the more likely regulator of the cAMP pool that controlled apoptosis. However, due to time constraints I was unable to fully investigate the roles of PDE4D3 and PDE4D5 in the metastatic cells, although we could infer that PDE4D3 was responsible for the metastatic cells increase tolerance to Fsk. If time permitted, in order to investigate the role of each enzyme further I would have liked to generate cells with stable knockdowns of both PDE4D isoforms individually and assess the effects on downstream signalling pathways. It would also have been exciting to use the stable knockdown cells in the *in vivo* metastasis assay that for which the Fidler cell lines are valuable i.e. the intrasplenic to liver metastasis assay, assaying both tumour growth at the site of injection and at site of ectopic metastatic growth, in this case the liver. This work would again further our knowledge of

how specific PDE4 isoforms regulate aspects of late stage colon cancer behaviour, including potentially how their activity may influence the metastatic process.

PDE4 research in cancer is an exciting new field which, as mentioned, may offer some therapeutic potential for some advanced cancers resistant to conventional therapies. With selective PDE4 inhibitors in advanced stages of clinical development, for other diseases advancing PDE4 based therapies for cancer treatment could occur fairly rapidly than completely new drug discovery programmes, since toxicology issues have already been dealt with.

7.4 Future work

Perhaps one of the most exciting aspects to come out of my study is the potential anti-cancer applications of the Fsk analogue, NKH477. NKH477 (or colforsin daropate) has been used in several small patient studies and acts as an anti inflammatory agent (481), a bronchodilator (488, 489) and also a vasodilator (482). Trials using this agent have focused on the cardiovascular and anti-inflammatory effects of NKH477, a common theme for agents that increase intracellular cAMP. Towards the end of my study I examined the effect of NKH477 treatment on a variety of cancer cell lines because it was a potentially more clinically relevant agent. NKH477 inhibited the proliferation of KM12C cells in a manner similar to that of Fsk (as far as was examined) and low concentrations of NKH477 could synergise with rolipram to inhibit proliferation. Also, when we tested the panel of cell lines used to assess the generality of Fsk/rolipram-induced inhibition of proliferation, I found that NKH477 alone was sufficient to inhibit the proliferation of all cancer cell lines tested. This was a remarkable result as Fsk alone was not sufficient to elicit such a universal and strong response, and even the Fsk/rolipram combination only inhibited 8 out of 11 cell lines. Clearly then there are other mechanisms by which NKH477 inhibits proliferation or NKH477 is activating specific adenylyl cyclase isoforms to a greater extent

than Fsk alone. In this regard, NKH477 can activate adenylyl cyclase-V more potently than other isoforms (490). Again, due to time constraints I was unable to investigate the mechanism of action of NKH477 fully but this should be done now by determining if NKH477 more potently stimulates the production of cAMP by directly measuring cAMP in the cells using either a biochemical cAMP assay, an ELISA (Enzyme linked immunosorbent assay) based method or by either using PKA or Epac FRET sensors (185, 218).

Finally, perhaps one of the most exciting areas of work to progress this research would be to use NKH477 into an animal model of colorectal cancer. We have now begun a collaboration with Dr. Owen Sansom at the Beatson Institute to address the long-term effects of NKH477 on tumour formation in the APC^{MIN} (multiple intestinal neoplasias) transgenic mouse model of colon cancer (68, 69). By analysing the number of intestinal polyps as well as the survival time of the mice (by Kaplan-Meiers survival curve) we can assess whether or not NKH477 can be used as a chemo-preventative treatment for colorectal cancer. We will also utilise the APC^{flox} model, which has been crossed with $PTEN^{flox}$ mice, in order to generate $APC^{flox}/PTEN^{flox}$ mice; the tumours generated in this model are both highly invasive and metastatic and the mice can be treated with NKH477 after tumour initiation. Thus, in light of our results with the KM12C cells, this model will allow us to address the whether or not NKH477 treatment has any effect on aggressive, metastatic tumours which have alterations in tumour suppressor genes that are common in colorectal cancer. In this instance, we intend to look at markers for apoptosis (such as activated caspase 3), alterations in cell cycle (for example phospho-histone H3, a marker for G2/M) and differentiation. Indeed, preliminary results using the $APC^{flox}/PTEN^{flox}$ have been encouraging, and although it is very preliminary, NKH477 does appear to have a

substantial effect on the tumours, with a first experiment suggesting increased differentiation and apoptosis in mice treated with NKH477 (Figure 38).

In addition to the *APC*-deletion models of colorectal cancer, there are now a growing number of other genetically engineered mouse models of cancer that more closely mimic the human disease. Also, the advent of new imaging technologies, such as the knocking-in of GFP or luciferase, allows for the *in vivo* imaging of fluorescent tumours such that the effects of any treatments, like NKH477, can be monitored in live animals and tumour volume as well as metastasis can be accurately visualised.

In conclusion, I believe that the work presented in this thesis adds to the growing body of evidence that PDE4 and cAMP pathways could potentially be utilised as anti-cancer therapies. NKH477, which we are now beginning to test *in vivo* in animal models of cancer looks to provide a promising start to test this proof of principal.

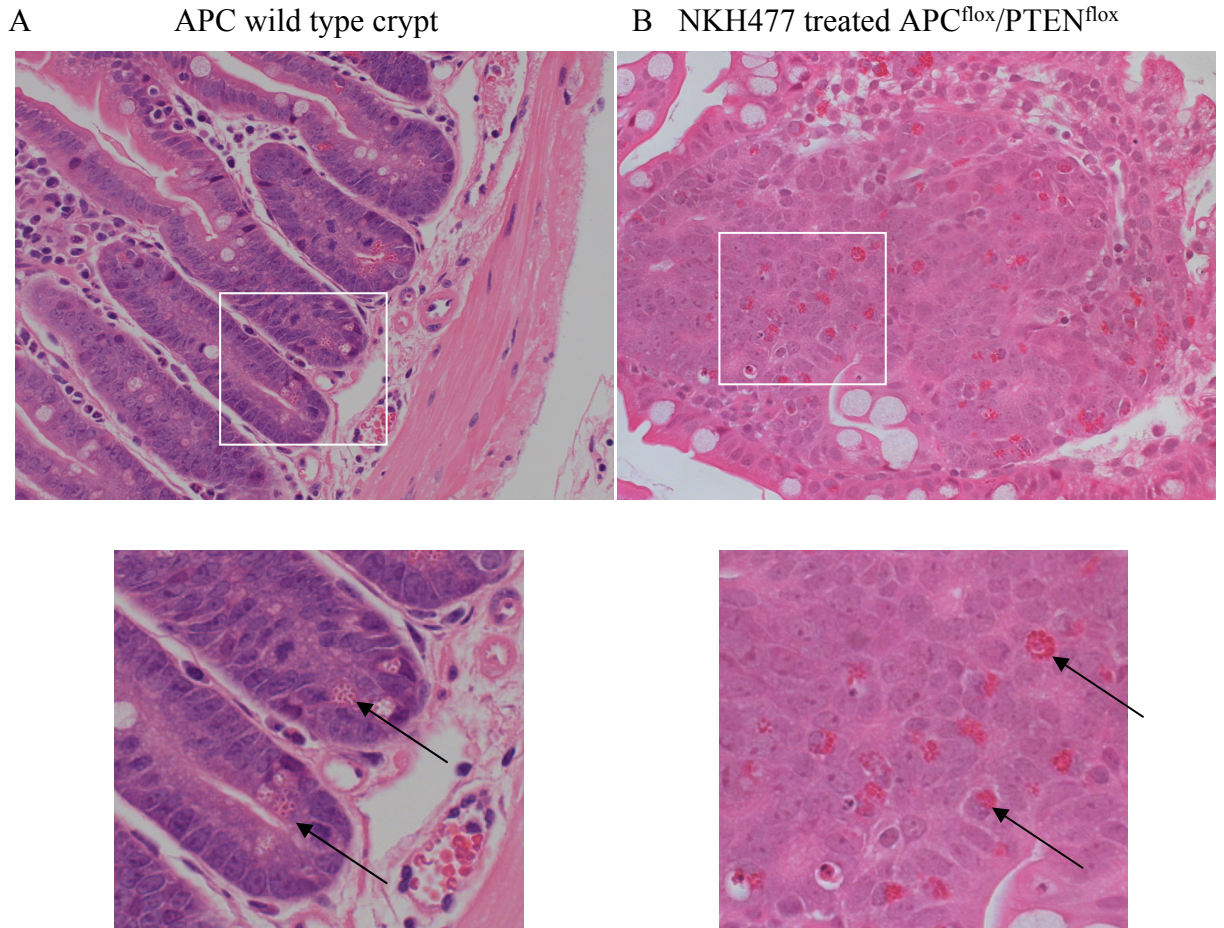


Figure 38. NKH477 treatment of *APC^{fllox}/PTEN^{fllox}* mice. Hematoxylin and eosin (H&E) staining of intestine sections of (A) *APC* wild type crypt (top) showing enlargement (below) and arrows indicate presence of paneth cells. (B) *APC^{fllox}/PTEN^{fllox}* adenoma. Note the number of paneth cells (indicated by arrow in the bottom panel) which are not normally present at during this stage of tumourigenesis. NKH477 treatment may be inducing differentiation in these tumours.

8. References

1. Campbell NC, Elliott AM, Sharp L, Ritchie LD, Cassidy J, Little J. Rural and urban differences in stage at diagnosis of colorectal and lung cancers. *Br J Cancer*. 2001 Apr 6;84(7):910-4.
2. AJCC cancer staging manual. 5th ed. / American Joint Committee on Cancer ... ed. Philadelphia: Lippincott-Raven; 1997.
3. Sobin LH, Wittekind C. TNM classification of malignant tumours. 6th ed. / edited by L.H. Sobin and Ch. Wittekind. ed. New York ; [Chichester]: Wiley-Liss; 2002.
4. Wittekind C. TNM atlas : illustrated guide to the TNM/pTNM classification of malignant tumours. 5th ed. / edited by Ch. Wittekind .. [et al.]. ed. Berlin ; [London]: Springer; 2004.
5. Winawer SJ, Fletcher RH, Miller L, Godlee F, Stolar MH, Mulrow CD, et al. Colorectal cancer screening: clinical guidelines and rationale. *Gastroenterology*. 1997 Feb;112(2):594-642.
6. Fearon ER, Vogelstein B. A genetic model for colorectal tumorigenesis. *Cell*. 1990 Jun 1;61(5):759-67.
7. Vogelstein B, Kinzler KW. Cancer genes and the pathways they control. *Nat Med*. 2004 Aug;10(8):789-99.
8. Hanahan D, Weinberg RA. The hallmarks of cancer. *Cell*. 2000 Jan 7;100(1):57-70.
9. Weinstein IB, Joe AK. Mechanisms of disease: Oncogene addiction--a rationale for molecular targeting in cancer therapy. *Nat Clin Pract Oncol*. 2006 Aug;3(8):448-57.
10. Felsher DW, Bishop JM. Reversible tumorigenesis by MYC in hematopoietic lineages. *Mol Cell*. 1999 Aug;4(2):199-207.
11. Guerin M, Barrois M, Terrier MJ, Spielmann M, Riou G. Overexpression of either c-myc or c-erbB-2/neu proto-oncogenes in human breast carcinomas: correlation with poor prognosis. *Oncogene Res*. 1988;3(1):21-31.
12. D'Cruz CM, Gunther EJ, Boxer RB, Hartman JL, Sintasath L, Moody SE, et al. c-MYC induces mammary tumorigenesis by means of a preferred pathway involving spontaneous Kras2 mutations. *Nat Med*. 2001 Feb;7(2):235-9.
13. Pelengaris S, Khan M, Evan GI. Suppression of Myc-induced apoptosis in beta cells exposes multiple oncogenic properties of Myc and triggers carcinogenic progression. *Cell*. 2002 May 3;109(3):321-34.

14. Jain M, Arvanitis C, Chu K, Dewey W, Leonhardt E, Trinh M, et al. Sustained loss of a neoplastic phenotype by brief inactivation of MYC. *Science*. 2002 Jul 5;297(5578):102-4.
15. Colomer R, Lupu R, Bacus SS, Gelmann EP. erbB-2 antisense oligonucleotides inhibit the proliferation of breast carcinoma cells with erbB-2 oncogene amplification. *Br J Cancer*. 1994 Nov;70(5):819-25.
16. Arber N, Doki Y, Han EK, Sgambato A, Zhou P, Kim NH, et al. Antisense to cyclin D1 inhibits the growth and tumorigenicity of human colon cancer cells. *Cancer Res*. 1997 Apr 15;57(8):1569-74.
17. Aoki K, Yoshida T, Matsumoto N, Ide H, Sugimura T, Terada M. Suppression of Ki-ras p21 levels leading to growth inhibition of pancreatic cancer cell lines with Ki-ras mutation but not those without Ki-ras mutation. *Mol Carcinog*. 1997 Oct;20(2):251-8.
18. Verma UN, Surabhi RM, Schmaltieg A, Becerra C, Gaynor RB. Small interfering RNAs directed against beta-catenin inhibit the in vitro and in vivo growth of colon cancer cells. *Clin Cancer Res*. 2003 Apr;9(4):1291-300.
19. Li K, Lin SY, Brunnicardi FC, Seu P. Use of RNA interference to target cyclin E-overexpressing hepatocellular carcinoma. *Cancer Res*. 2003 Jul 1;63(13):3593-7.
20. Sharma A, Trivedi NR, Zimmerman MA, Tuveson DA, Smith CD, Robertson GP. Mutant V599EB-Raf regulates growth and vascular development of malignant melanoma tumors. *Cancer Res*. 2005 Mar 15;65(6):2412-21.
21. Kantarjian H, Sawyers C, Hochhaus A, Guilhot F, Schiffer C, Gambacorti-Passerini C, et al. Hematologic and cytogenetic responses to imatinib mesylate in chronic myelogenous leukemia. *N Engl J Med*. 2002 Feb 28;346(9):645-52.
22. Sawyers CL, Hochhaus A, Feldman E, Goldman JM, Miller CB, Ottmann OG, et al. Imatinib induces hematologic and cytogenetic responses in patients with chronic myelogenous leukemia in myeloid blast crisis: results of a phase II study. *Blood*. 2002 May 15;99(10):3530-9.
23. Talpaz M, Silver RT, Druker BJ, Goldman JM, Gambacorti-Passerini C, Guilhot F, et al. Imatinib induces durable hematologic and cytogenetic responses in patients with accelerated phase chronic myeloid leukemia: results of a phase 2 study. *Blood*. 2002 Mar 15;99(6):1928-37.
24. Nahta R, Esteva FJ. HER-2-targeted therapy: lessons learned and future directions. *Clin Cancer Res*. 2003 Nov 1;9(14):5078-84.
25. Tan AR, Swain SM. Ongoing adjuvant trials with trastuzumab in breast cancer. *Semin Oncol*. 2003 Oct;30(5 Suppl 16):54-64.
26. McArdle C. ABC of colorectal cancer: effectiveness of follow up. *Bmj*. 2000 Nov 25;321(7272):1332-5.

27. Gelmann A, Desnoyers R, Cagir B, Weinberg D, Boman BM, Waldman SA. Colorectal cancer staging and adjuvant chemotherapy. *Expert Opin Pharmacother*. 2000 May;1(4):737-55.
28. Longley DB, Harkin DP, Johnston PG. 5-fluorouracil: mechanisms of action and clinical strategies. *Nat Rev Cancer*. 2003 May;3(5):330-8.
29. Modulation of fluorouracil by leucovorin in patients with advanced colorectal cancer: evidence in terms of response rate. Advanced Colorectal Cancer Meta-Analysis Project. *J Clin Oncol*. 1992 Jun;10(6):896-903.
30. Miwa M, Ura M, Nishida M, Sawada N, Ishikawa T, Mori K, et al. Design of a novel oral fluoropyrimidine carbamate, capecitabine, which generates 5-fluorouracil selectively in tumours by enzymes concentrated in human liver and cancer tissue. *Eur J Cancer*. 1998 Jul;34(8):1274-81.
31. Tebbutt NC, Cattell E, Midgley R, Cunningham D, Kerr D. Systemic treatment of colorectal cancer. *Eur J Cancer*. 2002 May;38(7):1000-15.
32. Longley DB, Johnston PG. Molecular mechanisms of drug resistance. *J Pathol*. 2005 Jan;205(2):275-92.
33. Chu E, Koeller DM, Johnston PG, Zinn S, Allegra CJ. Regulation of thymidylate synthase in human colon cancer cells treated with 5-fluorouracil and interferon-gamma. *Mol Pharmacol*. 1993 Apr;43(4):527-33.
34. Swain SM, Lippman ME, Egan EF, Drake JC, Steinberg SM, Allegra CJ. Fluorouracil and high-dose leucovorin in previously treated patients with metastatic breast cancer. *J Clin Oncol*. 1989 Jul;7(7):890-9.
35. Chu E, Voeller D, Koeller DM, Drake JC, Takimoto CH, Maley GF, et al. Identification of an RNA binding site for human thymidylate synthase. *Proc Natl Acad Sci U S A*. 1993 Jan 15;90(2):517-21.
36. Longley DB, Boyer J, Allen WL, Latif T, Ferguson PR, Maxwell PJ, et al. The role of thymidylate synthase induction in modulating p53-regulated gene expression in response to 5-fluorouracil and antifolates. *Cancer Res*. 2002 May 1;62(9):2644-9.
37. Longley DB, Ferguson PR, Boyer J, Latif T, Lynch M, Maxwell P, et al. Characterization of a thymidylate synthase (TS)-inducible cell line: a model system for studying sensitivity to TS- and non-TS-targeted chemotherapies. *Clin Cancer Res*. 2001 Nov;7(11):3533-9.
38. Takebe N, Zhao SC, Ural AU, Johnson MR, Banerjee D, Diasio RB, et al. Retroviral transduction of human dihydropyrimidine dehydrogenase cDNA confers resistance to 5-fluorouracil in murine hematopoietic progenitor cells and human CD34+-enriched peripheral blood progenitor cells. *Cancer Gene Ther*. 2001 Dec;8(12):966-73.
39. Shirota Y, Stoehlmacher J, Brabender J, Xiong YP, Uetake H, Danenberg KD, et al. ERCC1 and thymidylate synthase mRNA levels predict survival for

colorectal cancer patients receiving combination oxaliplatin and fluorouracil chemotherapy. *J Clin Oncol*. 2001 Dec 1;19(23):4298-304.

40. Morikawa K, Walker SM, Jessup JM, Fidler IJ. In vivo selection of highly metastatic cells from surgical specimens of different primary human colon carcinomas implanted into nude mice. *Cancer Res*. 1988 Apr 1;48(7):1943-8.

41. Morikawa K, Walker SM, Nakajima M, Pathak S, Jessup JM, Fidler IJ. Influence of organ environment on the growth, selection, and metastasis of human colon carcinoma cells in nude mice. *Cancer Res*. 1988 Dec 1;48(23):6863-71.

42. Fodde R, Smits R, Clevers H. APC, signal transduction and genetic instability in colorectal cancer. *Nat Rev Cancer*. 2001 Oct;1(1):55-67.

43. Golas JM, Lucas J, Etienne C, Golas J, Discafani C, Sridharan L, et al. SKI-606, a Src/Abl inhibitor with in vivo activity in colon tumor xenograft models. *Cancer Res*. 2005 Jun 15;65(12):5358-64.

44. Ninomiya I, Terada I, Yoshizumi T, Takino T, Nagai N, Morita A, et al. Anti-metastatic effect of capecitabine on human colon cancer xenografts in nude mouse rectum. *Int J Cancer*. 2004 Oct 20;112(1):135-42.

45. Yao M, Zhou W, Sangha S, Albert A, Chang AJ, Liu TC, et al. Effects of nonselective cyclooxygenase inhibition with low-dose ibuprofen on tumor growth, angiogenesis, metastasis, and survival in a mouse model of colorectal cancer. *Clin Cancer Res*. 2005 Feb 15;11(4):1618-28.

46. Biscardi JS, Tice DA, Parsons SJ. c-Src, receptor tyrosine kinases, and human cancer. *Adv Cancer Res*. 1999;76:61-119.

47. Cartwright CA, Coad CA, Egbert BM. Elevated c-Src tyrosine kinase activity in premalignant epithelia of ulcerative colitis. *J Clin Invest*. 1994 Feb;93(2):509-15.

48. Talamonti MS, Roh MS, Curley SA, Gallick GE. Increase in activity and level of pp60c-src in progressive stages of human colorectal cancer. *J Clin Invest*. 1993 Jan;91(1):53-60.

49. Staley CA, Parikh NU, Gallick GE. Decreased tumorigenicity of a human colon adenocarcinoma cell line by an antisense expression vector specific for c-Src. *Cell Growth Differ*. 1997 Mar;8(3):269-74.

50. Chen TR, Drabkowski D, Hay RJ, Macy M, Peterson W, Jr. WiDr is a derivative of another colon adenocarcinoma cell line, HT-29. *Cancer Genet Cytogenet*. 1987 Jul;27(1):125-34.

51. Leibovitz A, Stinson JC, McCombs WB, 3rd, McCoy CE, Mazur KC, Mabry ND. Classification of human colorectal adenocarcinoma cell lines. *Cancer Res*. 1976 Dec;36(12):4562-9.

52. de Vries JE, Dinjens WN, De Bruyne GK, Verspaget HW, van der Linden EP, de Bruine AP, et al. In vivo and in vitro invasion in relation to phenotypic

characteristics of human colorectal carcinoma cells. *Br J Cancer*. 1995 Feb;71(2):271-7.

53. Hewitt RE, McMarlin A, Kleiner D, Wersto R, Martin P, Tsokos M, et al. Validation of a model of colon cancer progression. *J Pathol*. 2000 Dec;192(4):446-54.

54. Witty JP, McDonnell S, Newell KJ, Cannon P, Navre M, Tressler RJ, et al. Modulation of matrilysin levels in colon carcinoma cell lines affects tumorigenicity in vivo. *Cancer Res*. 1994 Sep 1;54(17):4805-12.

55. Kinzler KW, Vogelstein B. Lessons from hereditary colorectal cancer. *Cell*. 1996 Oct 18;87(2):159-70.

56. Powell SM, Zilz N, Beazer-Barclay Y, Bryan TM, Hamilton SR, Thibodeau SN, et al. APC mutations occur early during colorectal tumorigenesis. *Nature*. 1992 Sep 17;359(6392):235-7.

57. Kikuchi A. Tumor formation by genetic mutations in the components of the Wnt signaling pathway. *Cancer Sci*. 2003 Mar;94(3):225-9.

58. Ikeda S, Kishida M, Matsuura Y, Usui H, Kikuchi A. GSK-3beta-dependent phosphorylation of adenomatous polyposis coli gene product can be modulated by beta-catenin and protein phosphatase 2A complexed with Axin. *Oncogene*. 2000 Jan 27;19(4):537-45.

59. Bommer GT, Fearon ER. Role of c-Myc in Apc mutant intestinal phenotype: case closed or time for a new beginning? *Cancer Cell*. 2007 May;11(5):391-4.

60. Sansom OJ, Meniel VS, Muncan V, Pheese TJ, Wilkins JA, Reed KR, et al. Myc deletion rescues Apc deficiency in the small intestine. *Nature*. 2007 Apr 5;446(7136):676-9.

61. Sansom OJ, Reed KR, van de Wetering M, Muncan V, Winton DJ, Clevers H, et al. Cyclin D1 is not an immediate target of beta-catenin following Apc loss in the intestine. *J Biol Chem*. 2005 Aug 5;280(31):28463-7.

62. Aoki K, Taketo MM. Adenomatous polyposis coli (APC): a multi-functional tumor suppressor gene. *J Cell Sci*. 2007 Oct 1;120(Pt 19):3327-35.

63. Faux MC, Ross JL, Meeker C, Johns T, Ji H, Simpson RJ, et al. Restoration of full-length adenomatous polyposis coli (APC) protein in a colon cancer cell line enhances cell adhesion. *J Cell Sci*. 2004 Jan 26;117(Pt 3):427-39.

64. Akiyama T, Kawasaki Y. Wnt signalling and the actin cytoskeleton. *Oncogene*. 2006 Dec 4;25(57):7538-44.

65. Kawasaki Y, Sato R, Akiyama T. Mutated APC and Asef are involved in the migration of colorectal tumour cells. *Nat Cell Biol*. 2003 Mar;5(3):211-5.

66. Tighe A, Johnson VL, Taylor SS. Truncating APC mutations have dominant effects on proliferation, spindle checkpoint control, survival and chromosome stability. *J Cell Sci.* 2004 Dec 15;117(Pt 26):6339-53.
67. Morin PJ, Sparks AB, Korinek V, Barker N, Clevers H, Vogelstein B, et al. Activation of beta-catenin-Tcf signaling in colon cancer by mutations in beta-catenin or APC. *Science.* 1997 Mar 21;275(5307):1787-90.
68. Moser AR, Pitot HC, Dove WF. A dominant mutation that predisposes to multiple intestinal neoplasia in the mouse. *Science.* 1990 Jan 19;247(4940):322-4.
69. Su LK, Kinzler KW, Vogelstein B, Preisinger AC, Moser AR, Luongo C, et al. Multiple intestinal neoplasia caused by a mutation in the murine homolog of the APC gene. *Science.* 1992 May 1;256(5057):668-70.
70. Sansom OJ, Reed KR, Hayes AJ, Ireland H, Brinkmann H, Newton IP, et al. Loss of Apc in vivo immediately perturbs Wnt signaling, differentiation, and migration. *Genes Dev.* 2004 Jun 15;18(12):1385-90.
71. Jacobs C, Rubsamen H. Expression of pp60c-src protein kinase in adult and fetal human tissue: high activities in some sarcomas and mammary carcinomas. *Cancer Res.* 1983 Apr;43(4):1696-702.
72. Ottenhoff-Kalff AE, Rijksen G, van Beurden EA, Hennipman A, Michels AA, Staal GE. Characterization of protein tyrosine kinases from human breast cancer: involvement of the c-src oncogene product. *Cancer Res.* 1992 Sep 1;52(17):4773-8.
73. Verbeek BS, Vroom TM, Adriaansen-Slot SS, Ottenhoff-Kalff AE, Geertzema JG, Hennipman A, et al. c-Src protein expression is increased in human breast cancer. An immunohistochemical and biochemical analysis. *J Pathol.* 1996 Dec;180(4):383-8.
74. Budde RJ, Ke S, Levin VA. Activity of pp60c-src in 60 different cell lines derived from human tumors. *Cancer Biochem Biophys.* 1994 Oct;14(3):171-5.
75. Mazurenko NN, Kogan EA, Zborovskaya IB, Kissel'jov FL. Expression of pp60c-src in human small cell and non-small cell lung carcinomas. *Eur J Cancer.* 1992;28(2-3):372-7.
76. van Oijen MG, Rijksen G, ten Broek FW, Slootweg PJ. Overexpression of c-Src in areas of hyperproliferation in head and neck cancer, premalignant lesions and benign mucosal disorders. *J Oral Pathol Med.* 1998 Apr;27(4):147-52.
77. Jones RJ, Avizienyte E, Wyke AW, Owens DW, Brunton VG, Frame MC. Elevated c-Src is linked to altered cell-matrix adhesion rather than proliferation in KM12C human colorectal cancer cells. *Br J Cancer.* 2002 Nov 4;87(10):1128-35.
78. Frame MC. Src in cancer: deregulation and consequences for cell behaviour. *Biochim Biophys Acta.* 2002 Jun 21;1602(2):114-30.

79. Avizienyte E, Wyke AW, Jones RJ, McLean GW, Westhoff MA, Brunton VG, et al. Src-induced de-regulation of E-cadherin in colon cancer cells requires integrin signalling. *Nat Cell Biol.* 2002 Aug;4(8):632-8.
80. Avizienyte E, Fincham VJ, Brunton VG, Frame MC. Src SH3/2 domain-mediated peripheral accumulation of Src and phospho-myosin is linked to deregulation of E-cadherin and the epithelial-mesenchymal transition. *Mol Biol Cell.* 2004 Jun;15(6):2794-803.
81. Brunton VG, Avizienyte E, Fincham VJ, Serrels B, Metcalf CA, 3rd, Sawyer TK, et al. Identification of Src-specific phosphorylation site on focal adhesion kinase: dissection of the role of Src SH2 and catalytic functions and their consequences for tumor cell behavior. *Cancer Res.* 2005 Feb 15;65(4):1335-42.
82. Hernandez A, Smith F, Wang Q, Wang X, Evers BM. Assessment of differential gene expression patterns in human colon cancers. *Ann Surg.* 2000 Oct;232(4):576-85.
83. De Lange R, Burtscher H, Jarsch M, Weidle UH. Identification of metastasis-associated genes by transcriptional profiling of metastatic versus non-metastatic colon cancer cell lines. *Anticancer Res.* 2001 Jul-Aug;21(4A):2329-39.
84. Hegde P, Qi R, Gaspard R, Abernathy K, Dharap S, Earle-Hughes J, et al. Identification of tumor markers in models of human colorectal cancer using a 19,200-element complementary DNA microarray. *Cancer Res.* 2001 Nov 1;61(21):7792-7.
85. Lengauer C, Kinzler KW, Vogelstein B. Genetic instabilities in human cancers. *Nature.* 1998 Dec 17;396(6712):643-9.
86. Boland CR, Thibodeau SN, Hamilton SR, Sidransky D, Eshleman JR, Burt RW, et al. A National Cancer Institute Workshop on Microsatellite Instability for cancer detection and familial predisposition: development of international criteria for the determination of microsatellite instability in colorectal cancer. *Cancer Res.* 1998 Nov 15;58(22):5248-57.
87. Gryfe R, Kim H, Hsieh ET, Aronson MD, Holowaty EJ, Bull SB, et al. Tumor microsatellite instability and clinical outcome in young patients with colorectal cancer. *N Engl J Med.* 2000 Jan 13;342(2):69-77.
88. Camps J, Morales C, Prat E, Ribas M, Capella G, Egozcue J, et al. Genetic evolution in colon cancer KM12 cells and metastatic derivatives. *Int J Cancer.* 2004 Jul 20;110(6):869-74.
89. Elsaleh H, Shannon B, Iacopetta B. Microsatellite instability as a molecular marker for very good survival in colorectal cancer patients receiving adjuvant chemotherapy. *Gastroenterology.* 2001 Apr;120(5):1309-10.
90. Hemminki A, Mecklin JP, Jarvinen H, Aaltonen LA, Joensuu H. Microsatellite instability is a favorable prognostic indicator in patients with colorectal cancer receiving chemotherapy. *Gastroenterology.* 2000 Oct;119(4):921-8.

91. Lanza G, Gafa R, Santini A, Maestri I, Guerzoni L, Cavazzini L. Immunohistochemical test for MLH1 and MSH2 expression predicts clinical outcome in stage II and III colorectal cancer patients. *J Clin Oncol*. 2006 May 20;24(15):2359-67.
92. de Vos tot Nederveen Cappel WH, Meulenbeld HJ, Kleibeuker JH, Nagengast FM, Menko FH, Griffioen G, et al. Survival after adjuvant 5-FU treatment for stage III colon cancer in hereditary nonpolyposis colorectal cancer. *Int J Cancer*. 2004 Apr 10;109(3):468-71.
93. Lamberti C, Lundin S, Bogdanow M, Pagenstecher C, Friedrichs N, Buttner R, et al. Microsatellite instability did not predict individual survival of unselected patients with colorectal cancer. *Int J Colorectal Dis*. 2007 Feb;22(2):145-52.
94. Ribic CM, Sargent DJ, Moore MJ, Thibodeau SN, French AJ, Goldberg RM, et al. Tumor microsatellite-instability status as a predictor of benefit from fluorouracil-based adjuvant chemotherapy for colon cancer. *N Engl J Med*. 2003 Jul 17;349(3):247-57.
95. Warusavitarne J, Ramanathan P, Kaufman A, Robinson BG, Schnitzler M. 5-fluorouracil (5FU) treatment does not influence invasion and metastasis in microsatellite unstable (MSI-H) colorectal cancer. *Int J Colorectal Dis*. 2006 Oct;21(7):625-31.
96. Spano JP, Lagorce C, Atlan D, Milano G, Domont J, Benamouzig R, et al. Impact of EGFR expression on colorectal cancer patient prognosis and survival. *Ann Oncol*. 2005 Jan;16(1):102-8.
97. Zhang W, Gordon M, Lenz HJ. Novel approaches to treatment of advanced colorectal cancer with anti-EGFR monoclonal antibodies. *Ann Med*. 2006;38(8):545-51.
98. Baselga J. The EGFR as a target for anticancer therapy--focus on cetuximab. *Eur J Cancer*. 2001 Sep;37 Suppl 4:S16-22.
99. Yang XD, Jia XC, Corvalan JR, Wang P, Davis CG. Development of ABX-EGF, a fully human anti-EGF receptor monoclonal antibody, for cancer therapy. *Crit Rev Oncol Hematol*. 2001 Apr;38(1):17-23.
100. Yang XD, Jia XC, Corvalan JR, Wang P, Davis CG, Jakobovits A. Eradication of established tumors by a fully human monoclonal antibody to the epidermal growth factor receptor without concomitant chemotherapy. *Cancer Res*. 1999 Mar 15;59(6):1236-43.
101. Goldberg RM. Cetuximab. *Nat Rev Drug Discov*. 2005 May;Suppl:S10-1.
102. Saltz L, Easley C, Kirkpatrick P. Panitumumab. *Nat Rev Drug Discov*. 2006 Dec;5(12):987-8.
103. Sharma SV, Bell DW, Settleman J, Haber DA. Epidermal growth factor receptor mutations in lung cancer. *Nat Rev Cancer*. 2007 Mar;7(3):169-81.

104. Blackhall F, Ranson M, Thatcher N. Where next for gefitinib in patients with lung cancer? *Lancet Oncol*. 2006 Jun;7(6):499-507.
105. Wakeling AE, Guy SP, Woodburn JR, Ashton SE, Curry BJ, Barker AJ, et al. ZD1839 (Iressa): an orally active inhibitor of epidermal growth factor signaling with potential for cancer therapy. *Cancer Res*. 2002 Oct 15;62(20):5749-54.
106. Fukuoka M, Yano S, Giaccone G, Tamura T, Nakagawa K, Douillard JY, et al. Multi-institutional randomized phase II trial of gefitinib for previously treated patients with advanced non-small-cell lung cancer (The IDEAL 1 Trial) [corrected]. *J Clin Oncol*. 2003 Jun 15;21(12):2237-46.
107. Kris MG, Natale RB, Herbst RS, Lynch TJ, Jr., Prager D, Belani CP, et al. Efficacy of gefitinib, an inhibitor of the epidermal growth factor receptor tyrosine kinase, in symptomatic patients with non-small cell lung cancer: a randomized trial. *Jama*. 2003 Oct 22;290(16):2149-58.
108. Perez-Soler R. Phase II clinical trial data with the epidermal growth factor receptor tyrosine kinase inhibitor erlotinib (OSI-774) in non-small-cell lung cancer. *Clin Lung Cancer*. 2004 Dec;6 Suppl 1:S20-3.
109. Perez-Soler R, Chachoua A, Hammond LA, Rowinsky EK, Huberman M, Karp D, et al. Determinants of tumor response and survival with erlotinib in patients with non--small-cell lung cancer. *J Clin Oncol*. 2004 Aug 15;22(16):3238-47.
110. Ferrara N, Hillan KJ, Gerber HP, Novotny W. Discovery and development of bevacizumab, an anti-VEGF antibody for treating cancer. *Nat Rev Drug Discov*. 2004 May;3(5):391-400.
111. Kim KJ, Li B, Winer J, Armanini M, Gillett N, Phillips HS, et al. Inhibition of vascular endothelial growth factor-induced angiogenesis suppresses tumour growth in vivo. *Nature*. 1993 Apr 29;362(6423):841-4.
112. Hurwitz H, Fehrenbacher L, Novotny W, Cartwright T, Hainsworth J, Heim W, et al. Bevacizumab plus irinotecan, fluorouracil, and leucovorin for metastatic colorectal cancer. *N Engl J Med*. 2004 Jun 3;350(23):2335-42.
113. Caprioni F, Fornarini G. Bevacizumab in the treatment of metastatic colorectal cancer. *Future Oncol*. 2007 Apr;3(2):141-8.
114. de Gramont A, Tournigand C, Andre T, Larsen AK, Louvet C. Adjuvant therapy for stage II and III colorectal cancer. *Semin Oncol*. 2007 Apr;34(2 Suppl 1):S37-40.
115. Zucker S, Vacirca J. Role of matrix metalloproteinases (MMPs) in colorectal cancer. *Cancer Metastasis Rev*. 2004 Jan-Jun;23(1-2):101-17.
116. Pavlaki M, Zucker S. Matrix metalloproteinase inhibitors (MMPi): the beginning of phase I or the termination of phase III clinical trials. *Cancer Metastasis Rev*. 2003 Jun-Sep;22(2-3):177-203.

117. Clevers H. Colon cancer--understanding how NSAIDs work. *N Engl J Med.* 2006 Feb 16;354(7):761-3.
118. Brown JR, DuBois RN. COX-2: a molecular target for colorectal cancer prevention. *J Clin Oncol.* 2005 Apr 20;23(12):2840-55.
119. Eberhart CE, Coffey RJ, Radhika A, Giardiello FM, Ferrenbach S, DuBois RN. Up-regulation of cyclooxygenase 2 gene expression in human colorectal adenomas and adenocarcinomas. *Gastroenterology.* 1994 Oct;107(4):1183-8.
120. Kargman SL, O'Neill GP, Vickers PJ, Evans JF, Mancini JA, Jothy S. Expression of prostaglandin G/H synthase-1 and -2 protein in human colon cancer. *Cancer Res.* 1995 Jun 15;55(12):2556-9.
121. Sano H, Kawahito Y, Wilder RL, Hashiramoto A, Mukai S, Asai K, et al. Expression of cyclooxygenase-1 and -2 in human colorectal cancer. *Cancer Res.* 1995 Sep 1;55(17):3785-9.
122. Williams CS, DuBois RN. Prostaglandin endoperoxide synthase: why two isoforms? *Am J Physiol.* 1996 Mar;270(3 Pt 1):G393-400.
123. Oshima M, Dinchuk JE, Kargman SL, Oshima H, Hancock B, Kwong E, et al. Suppression of intestinal polyposis in Apc delta716 knockout mice by inhibition of cyclooxygenase 2 (COX-2). *Cell.* 1996 Nov 29;87(5):803-9.
124. Bresalier RS, Sandler RS, Quan H, Bolognese JA, Oxenius B, Horgan K, et al. Cardiovascular events associated with rofecoxib in a colorectal adenoma chemoprevention trial. *N Engl J Med.* 2005 Mar 17;352(11):1092-102.
125. Kerr DJ, Dunn JA, Langman MJ, Smith JL, Midgley RS, Stanley A, et al. Rofecoxib and cardiovascular adverse events in adjuvant treatment of colorectal cancer. *N Engl J Med.* 2007 Jul 26;357(4):360-9.
126. Drazen JM. COX-2 inhibitors--a lesson in unexpected problems. *N Engl J Med.* 2005 Mar 17;352(11):1131-2.
127. Rall TW, Sutherland EW. Formation of a cyclic adenine ribonucleotide by tissue particles. *J Biol Chem.* 1958 Jun;232(2):1065-76.
128. Sutherland EW, Rall TW. Fractionation and characterization of a cyclic adenine ribonucleotide formed by tissue particles. *J Biol Chem.* 1958 Jun;232(2):1077-91.
129. Neves SR, Ram PT, Iyengar R. G protein pathways. *Science.* 2002 May 31;296(5573):1636-9.
130. Beavo JA, Brunton LL. Cyclic nucleotide research -- still expanding after half a century. *Nat Rev Mol Cell Biol.* 2002 Sep;3(9):710-8.
131. Houslay MD, Milligan G. Tailoring cAMP-signalling responses through isoform multiplicity. *Trends Biochem Sci.* 1997 Jun;22(6):217-24.

132. de Rooij J, Zwartkruis FJ, Verheijen MH, Cool RH, Nijman SM, Wittinghofer A, et al. Epac is a Rap1 guanine-nucleotide-exchange factor directly activated by cyclic AMP. *Nature*. 1998 Dec 3;396(6710):474-7.
133. Kawasaki H, Springett GM, Mochizuki N, Toki S, Nakaya M, Matsuda M, et al. A family of cAMP-binding proteins that directly activate Rap1. *Science*. 1998 Dec 18;282(5397):2275-9.
134. Conti M, Jin SL. The molecular biology of cyclic nucleotide phosphodiesterases. *Prog Nucleic Acid Res Mol Biol*. 1999;63:1-38.
135. Manganiello VC, Degerman E. Cyclic nucleotide phosphodiesterases (PDEs): diverse regulators of cyclic nucleotide signals and inviting molecular targets for novel therapeutic agents. *Thromb Haemost*. 1999 Aug;82(2):407-11.
136. Soderling SH, Beavo JA. Regulation of cAMP and cGMP signaling: new phosphodiesterases and new functions. *Curr Opin Cell Biol*. 2000 Apr;12(2):174-9.
137. Baillie GS, Houslay MD. Arrestin tines for compartmentalised cAMP signalling and phosphodiesterase-4 enzymes. *Curr Opin Cell Biol*. 2005 Apr;17(2):129-34.
138. Buxton IL, Brunton LL. Compartments of cyclic AMP and protein kinase in mammalian cardiomyocytes. *J Biol Chem*. 1983 Sep 10;258(17):10233-9.
139. Hayes JS, Brunton LL. Functional compartments in cyclic nucleotide action. *J Cyclic Nucleotide Res*. 1982;8(1):1-16.
140. Bacskai BJ, Hochner B, Mahaut-Smith M, Adams SR, Kaang BK, Kandel ER, et al. Spatially resolved dynamics of cAMP and protein kinase A subunits in *Aplysia* sensory neurons. *Science*. 1993 Apr 9;260(5105):222-6.
141. Hempel CM, Vincent P, Adams SR, Tsien RY, Selverston AI. Spatio-temporal dynamics of cyclic AMP signals in an intact neural circuit. *Nature*. 1996 Nov 14;384(6605):166-9.
142. Zaccolo M, Pozzan T. Discrete microdomains with high concentration of cAMP in stimulated rat neonatal cardiac myocytes. *Science*. 2002 Mar 1;295(5560):1711-5.
143. Wong W, Scott JD. AKAP signalling complexes: focal points in space and time. *Nat Rev Mol Cell Biol*. 2004 Dec;5(12):959-70.
144. Bolger GB, Baillie GS, Li X, Lynch MJ, Herzyk P, Mohamed A, et al. Scanning peptide array analyses identify overlapping binding sites for the signalling scaffold proteins, beta-arrestin and RACK1, in cAMP-specific phosphodiesterase PDE4D5. *Biochem J*. 2006 Aug 15;398(1):23-36.
145. Yarwood SJ, Steele MR, Scotland G, Houslay MD, Bolger GB. The RACK1 signaling scaffold protein selectively interacts with the cAMP-specific phosphodiesterase PDE4D5 isoform. *J Biol Chem*. 1999 May 21;274(21):14909-17.

146. Nauert JB, Rigas JD, Lester LB. Identification of an IQGAP1/AKAP79 complex in beta-cells. *J Cell Biochem.* 2003 Sep 1;90(1):97-108.
147. Spiegel AM. Defects in G protein-coupled signal transduction in human disease. *Annu Rev Physiol.* 1996;58:143-70.
148. Spiegel AM. Mutations in G proteins and G protein-coupled receptors in endocrine disease. *J Clin Endocrinol Metab.* 1996 Jul;81(7):2434-42.
149. Spiegel AM, Weinstein LS. Inherited diseases involving g proteins and g protein-coupled receptors. *Annu Rev Med.* 2004;55:27-39.
150. Young D, Waitches G, Birchmeier C, Fasano O, Wigler M. Isolation and characterization of a new cellular oncogene encoding a protein with multiple potential transmembrane domains. *Cell.* 1986 Jun 6;45(5):711-9.
151. Coughlin SR. Thrombin signalling and protease-activated receptors. *Nature.* 2000 Sep 14;407(6801):258-64.
152. Even-Ram S, Uziely B, Cohen P, Grisaru-Granovsky S, Maoz M, Ginzburg Y, et al. Thrombin receptor overexpression in malignant and physiological invasion processes. *Nat Med.* 1998 Aug;4(8):909-14.
153. Liu Y, Gilcrease MZ, Henderson Y, Yuan XH, Clayman GL, Chen Z. Expression of protease-activated receptor 1 in oral squamous cell carcinoma. *Cancer Lett.* 2001 Aug 28;169(2):173-80.
154. Daaka Y. G proteins in cancer: the prostate cancer paradigm. *Sci STKE.* 2004 Jan 20;2004(216):re2.
155. Hansen-Petrik MB, McEntee MF, Jull B, Shi H, Zemel MB, Whelan J. Prostaglandin E(2) protects intestinal tumors from nonsteroidal anti-inflammatory drug-induced regression in Apc(Min/+) mice. *Cancer Res.* 2002 Jan 15;62(2):403-8.
156. Hull MA, Ko SC, Hawcroft G. Prostaglandin EP receptors: targets for treatment and prevention of colorectal cancer? *Mol Cancer Ther.* 2004 Aug;3(8):1031-9.
157. Sonoshita M, Takaku K, Sasaki N, Sugimoto Y, Ushikubi F, Narumiya S, et al. Acceleration of intestinal polyposis through prostaglandin receptor EP2 in Apc(Delta 716) knockout mice. *Nat Med.* 2001 Sep;7(9):1048-51.
158. Castellone MD, Teramoto H, Williams BO, Druey KM, Gutkind JS. Prostaglandin E2 promotes colon cancer cell growth through a Gs-axin-beta-catenin signaling axis. *Science.* 2005 Dec 2;310(5753):1504-10.
159. Landis CA, Masters SB, Spada A, Pace AM, Bourne HR, Vallar L. GTPase inhibiting mutations activate the alpha chain of Gs and stimulate adenylyl cyclase in human pituitary tumours. *Nature.* 1989 Aug 31;340(6236):692-6.

160. Lyons J, Landis CA, Harsh G, Vallar L, Grunewald K, Feichtinger H, et al. Two G protein oncogenes in human endocrine tumors. *Science*. 1990 Aug 10;249(4969):655-9.
161. Skalhegg BS, Tasken K. Specificity in the cAMP/PKA signaling pathway. Differential expression, regulation, and subcellular localization of subunits of PKA. *Front Biosci*. 2000 Aug 1;5:D678-93.
162. Tasken K, Skalhegg BS, Tasken KA, Solberg R, Knutsen HK, Levy FO, et al. Structure, function, and regulation of human cAMP-dependent protein kinases. *Adv Second Messenger Phosphoprotein Res*. 1997;31:191-204.
163. Taylor SS, Yang J, Wu J, Haste NM, Radzio-Andzelm E, Anand G. PKA: a portrait of protein kinase dynamics. *Biochim Biophys Acta*. 2004 Mar 11;1697(1-2):259-69.
164. Tasken K, Aandahl EM. Localized effects of cAMP mediated by distinct routes of protein kinase A. *Physiol Rev*. 2004 Jan;84(1):137-67.
165. Moffett S, Adam L, Bonin H, Loisel TP, Bouvier M, Mouillac B. Palmitoylated cysteine 341 modulates phosphorylation of the beta2-adrenergic receptor by the cAMP-dependent protein kinase. *J Biol Chem*. 1996 Aug 30;271(35):21490-7.
166. Yuan N, Friedman J, Whaley BS, Clark RB. cAMP-dependent protein kinase and protein kinase C consensus site mutations of the beta-adrenergic receptor. Effect on desensitization and stimulation of adenylylcyclase. *J Biol Chem*. 1994 Sep 16;269(37):23032-8.
167. Hoffmann R, Wilkinson IR, McCallum JF, Engels P, Houslay MD. cAMP-specific phosphodiesterase HSPDE4D3 mutants which mimic activation and changes in rolipram inhibition triggered by protein kinase A phosphorylation of Ser-54: generation of a molecular model. *Biochem J*. 1998 Jul 1;333 (Pt 1):139-49.
168. Sette C, Conti M. Phosphorylation and activation of a cAMP-specific phosphodiesterase by the cAMP-dependent protein kinase. Involvement of serine 54 in the enzyme activation. *J Biol Chem*. 1996 Jul 12;271(28):16526-34.
169. Sidovar MF, Kozlowski P, Lee JW, Collins MA, He Y, Graves LM. Phosphorylation of serine 43 is not required for inhibition of c-Raf kinase by the cAMP-dependent protein kinase. *J Biol Chem*. 2000 Sep 15;275(37):28688-94.
170. Wu J, Dent P, Jelinek T, Wolfman A, Weber MJ, Sturgill TW. Inhibition of the EGF-activated MAP kinase signaling pathway by adenosine 3',5'-monophosphate. *Science*. 1993 Nov 12;262(5136):1065-9.
171. Yamamoto KK, Gonzalez GA, Biggs WH, 3rd, Montminy MR. Phosphorylation-induced binding and transcriptional efficacy of nuclear factor CREB. *Nature*. 1988 Aug 11;334(6182):494-8.

172. Harada H, Becknell B, Wilm M, Mann M, Huang LJ, Taylor SS, et al. Phosphorylation and inactivation of BAD by mitochondria-anchored protein kinase A. *Mol Cell*. 1999 Apr;3(4):413-22.
173. Virdee K, Parone PA, Tolkovsky AM. Phosphorylation of the pro-apoptotic protein BAD on serine 155, a novel site, contributes to cell survival. *Curr Biol*. 2000 Sep 21;10(18):1151-4.
174. Lizcano JM, Morrice N, Cohen P. Regulation of BAD by cAMP-dependent protein kinase is mediated via phosphorylation of a novel site, Ser155. *Biochem J*. 2000 Jul 15;349(Pt 2):547-57.
175. Cosentino C, Di Domenico M, Porcellini A, Cuozzo C, De Gregorio G, Santillo MR, et al. p85 regulatory subunit of PI3K mediates cAMP-PKA and estrogens biological effects on growth and survival. *Oncogene*. 2006 Oct 2.
176. De Gregorio G, Coppa A, Cosentino C, Ucci S, Messina S, Nicolussi A, et al. The p85 regulatory subunit of PI3K mediates TSH-cAMP-PKA growth and survival signals. *Oncogene*. 2006 Oct 9.
177. McKnight GS, Clegg CH, Uhler MD, Chrivia JC, Cadd GG, Correll LA, et al. Analysis of the cAMP-dependent protein kinase system using molecular genetic approaches. *Recent Prog Horm Res*. 1988;44:307-35.
178. Scott JD. Cyclic nucleotide-dependent protein kinases. *Pharmacol Ther*. 1991;50(1):123-45.
179. Dostmann WR, Taylor SS. Identifying the molecular switches that determine whether (Rp)-cAMPS functions as an antagonist or an agonist in the activation of cAMP-dependent protein kinase I. *Biochemistry*. 1991 Sep 3;30(35):8710-6.
180. Lohmann SM, DeCamilli P, Einig I, Walter U. High-affinity binding of the regulatory subunit (RII) of cAMP-dependent protein kinase to microtubule-associated and other cellular proteins. *Proc Natl Acad Sci U S A*. 1984 Nov;81(21):6723-7.
181. Sarkar D, Erlichman J, Rubin CS. Identification of a calmodulin-binding protein that co-purifies with the regulatory subunit of brain protein kinase II. *J Biol Chem*. 1984 Aug 10;259(15):9840-6.
182. Theurkauf WE, Vallee RB. Molecular characterization of the cAMP-dependent protein kinase bound to microtubule-associated protein 2. *J Biol Chem*. 1982 Mar 25;257(6):3284-90.
183. de Rooij J, Rehmann H, van Triest M, Cool RH, Wittinghofer A, Bos JL. Mechanism of regulation of the Epac family of cAMP-dependent RapGEFs. *J Biol Chem*. 2000 Jul 7;275(27):20829-36.
184. Rehmann H, Das J, Knipscheer P, Wittinghofer A, Bos JL. Structure of the cyclic-AMP-responsive exchange factor Epac2 in its auto-inhibited state. *Nature*. 2006 Feb 2;439(7076):625-8.

185. Ponsioen B, Zhao J, Riedl J, Zwartkruis F, van der Krogt G, Zaccolo M, et al. Detecting cAMP-induced Epac activation by fluorescence resonance energy transfer: Epac as a novel cAMP indicator. *EMBO Rep.* 2004 Dec;5(12):1176-80.
186. Kitayama H, Matsuzaki T, Ikawa Y, Noda M. Genetic analysis of the Kirsten-ras-revertant 1 gene: potentiation of its tumor suppressor activity by specific point mutations. *Proc Natl Acad Sci U S A.* 1990 Jun;87(11):4284-8.
187. Knox AL, Brown NH. Rap1 GTPase regulation of adherens junction positioning and cell adhesion. *Science.* 2002 Feb 15;295(5558):1285-8.
188. Enserink JM, Christensen AE, de Rooij J, van Triest M, Schwede F, Genieser HG, et al. A novel Epac-specific cAMP analogue demonstrates independent regulation of Rap1 and ERK. *Nat Cell Biol.* 2002 Nov;4(11):901-6.
189. Su Y, Dostmann WR, Herberg FW, Durick K, Xuong NH, Ten Eyck L, et al. Regulatory subunit of protein kinase A: structure of deletion mutant with cAMP binding domains. *Science.* 1995 Aug 11;269(5225):807-13.
190. Holz GG, Kang G, Harbeck M, Roe MW, Chepurny OG. Cell physiology of cAMP sensor Epac. *J Physiol.* 2006 Nov 15;577(Pt 1):5-15.
191. Christensen AE, Selheim F, de Rooij J, Dremier S, Schwede F, Dao KK, et al. cAMP analog mapping of Epac1 and cAMP kinase. Discriminating analogs demonstrate that Epac and cAMP kinase act synergistically to promote PC-12 cell neurite extension. *J Biol Chem.* 2003 Sep 12;278(37):35394-402.
192. Rangarajan S, Enserink JM, Kuiperij HB, de Rooij J, Price LS, Schwede F, et al. Cyclic AMP induces integrin-mediated cell adhesion through Epac and Rap1 upon stimulation of the beta 2-adrenergic receptor. *J Cell Biol.* 2003 Feb 17;160(4):487-93.
193. Enserink JM, Price LS, Methi T, Mahic M, Sonnenberg A, Bos JL, et al. The cAMP-Epac-Rap1 pathway regulates cell spreading and cell adhesion to laminin-5 through the alpha3beta1 integrin but not the alpha6beta4 integrin. *J Biol Chem.* 2004 Oct 22;279(43):44889-96.
194. Fukuhara S, Sakurai A, Sano H, Yamagishi A, Somekawa S, Takakura N, et al. Cyclic AMP potentiates vascular endothelial cadherin-mediated cell-cell contact to enhance endothelial barrier function through an Epac-Rap1 signaling pathway. *Mol Cell Biol.* 2005 Jan;25(1):136-46.
195. Okada S, Matsuda M, Anafi M, Pawson T, Pessin JE. Insulin regulates the dynamic balance between Ras and Rap1 signaling by coordinating the assembly states of the Grb2-SOS and CrkII-C3G complexes. *Embo J.* 1998 May 1;17(9):2554-65.
196. Boussiotis VA, Freeman GJ, Berezovskaya A, Barber DL, Nadler LM. Maintenance of human T cell anergy: blocking of IL-2 gene transcription by activated Rap1. *Science.* 1997 Oct 3;278(5335):124-8.
197. Carey KD, Dillon TJ, Schmitt JM, Baird AM, Holdorf AD, Straus DB, et al. CD28 and the tyrosine kinase lck stimulate mitogen-activated protein kinase

activity in T cells via inhibition of the small G protein Rap1. *Mol Cell Biol.* 2000 Nov;20(22):8409-19.

198. Cook SJ, Rubinfeld B, Albert I, McCormick F. RapV12 antagonizes Ras-dependent activation of ERK1 and ERK2 by LPA and EGF in Rat-1 fibroblasts. *Embo J.* 1993 Sep;12(9):3475-85.

199. Zwartkruis FJ, Wolthuis RM, Nabben NM, Franke B, Bos JL. Extracellular signal-regulated activation of Rap1 fails to interfere in Ras effector signalling. *Embo J.* 1998 Oct 15;17(20):5905-12.

200. Ohtsuka T, Shimizu K, Yamamori B, Kuroda S, Takai Y. Activation of brain B-Raf protein kinase by Rap1B small GTP-binding protein. *J Biol Chem.* 1996 Jan 19;271(3):1258-61.

201. York RD, Yao H, Dillon T, Ellig CL, Eckert SP, McCleskey EW, et al. Rap1 mediates sustained MAP kinase activation induced by nerve growth factor. *Nature.* 1998 Apr 9;392(6676):622-6.

202. Vossler MR, Yao H, York RD, Pan MG, Rim CS, Stork PJ. cAMP activates MAP kinase and Elk-1 through a B-Raf- and Rap1-dependent pathway. *Cell.* 1997 Apr 4;89(1):73-82.

203. Wang Z, Dillon TJ, Pokala V, Mishra S, Labudda K, Hunter B, et al. Rap1-mediated activation of extracellular signal-regulated kinases by cyclic AMP is dependent on the mode of Rap1 activation. *Mol Cell Biol.* 2006 Mar;26(6):2130-45.

204. Cho-Chung YS, Pepe S, Clair T, Budillon A, Nesterova M. cAMP-dependent protein kinase: role in normal and malignant growth. *Crit Rev Oncol Hematol.* 1995 Nov;21(1-3):33-61.

205. Miller WR. Regulatory subunits of PKA and breast cancer. *Ann N Y Acad Sci.* 2002 Jun;968:37-48.

206. Bold RJ, Warren RE, Ishizuka J, Cho-Chung YS, Townsend CM, Jr., Thompson JC. Experimental gene therapy of human colon cancer. *Surgery.* 1994 Aug;116(2):189-95; discussion 95-6.

207. Srivastava RK, Srivastava AR, Park YG, Agrawal S, Cho-Chung YS. Antisense depletion of RIalpha subunit of protein kinase A induces apoptosis and growth arrest in human breast cancer cells. *Breast Cancer Res Treat.* 1998 May;49(2):97-107.

208. Srivastava RK, Srivastava AR, Seth P, Agrawal S, Cho-Chung YS. Growth arrest and induction of apoptosis in breast cancer cells by antisense depletion of protein kinase A-RI alpha subunit: p53-independent mechanism of action. *Mol Cell Biochem.* 1999 May;195(1-2):25-36.

209. Nesterova M, Cho-Chung YS. Oligonucleotide sequence-specific inhibition of gene expression, tumor growth inhibition, and modulation of cAMP signaling by an RNA-DNA hybrid antisense targeted to protein kinase A RIalpha subunit. *Antisense Nucleic Acid Drug Dev.* 2000 Dec;10(6):423-33.

210. Nesterova M, Yokozaki H, McDuffie E, Cho-Chung YS. Overexpression of RII beta regulatory subunit of protein kinase A in human colon carcinoma cell induces growth arrest and phenotypic changes that are abolished by site-directed mutation of RII beta. *Eur J Biochem.* 1996 Feb 1;235(3):486-94.
211. Cho-Chung YS, Nesterova MV. Tumor reversion: protein kinase A isozyme switching. *Ann N Y Acad Sci.* 2005 Nov;1058:76-86.
212. Verthelyi D, Ishii KJ, Gursel M, Takeshita F, Klinman DM. Human peripheral blood cells differentially recognize and respond to two distinct CPG motifs. *J Immunol.* 2001 Feb 15;166(4):2372-7.
213. Nesterova MV, Johnson NR, Stewart T, Abrams S, Cho-Chung YS. CpG immunomer DNA enhances antisense protein kinase A RIalpha inhibition of multidrug-resistant colon carcinoma growth in nude mice: molecular basis for combinatorial therapy. *Clin Cancer Res.* 2005 Aug 15;11(16):5950-5.
214. Itoh M, Nelson CM, Myers CA, Bissell MJ. Rap1 integrates tissue polarity, lumen formation, and tumorigenic potential in human breast epithelial cells. *Cancer Res.* 2007 May 15;67(10):4759-66.
215. Gao L, Feng Y, Bowers R, Becker-Hapak M, Gardner J, Council L, et al. Ras-associated protein-1 regulates extracellular signal-regulated kinase activation and migration in melanoma cells: two processes important to melanoma tumorigenesis and metastasis. *Cancer Res.* 2006 Aug 15;66(16):7880-8.
216. Vanvooren V, Allgeier A, Nguyen M, Massart C, Parma J, Dumont JE, et al. Mutation analysis of the Epac--Rap1 signaling pathway in cold thyroid follicular adenomas. *Eur J Endocrinol.* 2001 Jun;144(6):605-10.
217. Bender AT, Beavo JA. Cyclic nucleotide phosphodiesterases: molecular regulation to clinical use. *Pharmacol Rev.* 2006 Sep;58(3):488-520.
218. Mongillo M, McSorley T, Evellin S, Sood A, Lissandron V, Terrin A, et al. Fluorescence resonance energy transfer-based analysis of cAMP dynamics in live neonatal rat cardiac myocytes reveals distinct functions of compartmentalized phosphodiesterases. *Circ Res.* 2004 Jul 9;95(1):67-75.
219. Maurice DH, Haslam RJ. Molecular basis of the synergistic inhibition of platelet function by nitrovasodilators and activators of adenylate cyclase: inhibition of cyclic AMP breakdown by cyclic GMP. *Mol Pharmacol.* 1990 May;37(5):671-81.
220. Wechsler J, Choi YH, Krall J, Ahmad F, Manganiello VC, Movsesian MA. Isoforms of cyclic nucleotide phosphodiesterase PDE3A in cardiac myocytes. *J Biol Chem.* 2002 Oct 11;277(41):38072-8.
221. Shakur Y, Holst LS, Landstrom TR, Movsesian M, Degerman E, Manganiello V. Regulation and function of the cyclic nucleotide phosphodiesterase (PDE3) gene family. *Prog Nucleic Acid Res Mol Biol.* 2001;66:241-77.

222. Murata T, Taira M, Manganiello VC. Differential expression of cGMP-inhibited cyclic nucleotide phosphodiesterases in human hepatoma cell lines. *FEBS Lett.* 1996 Jul 15;390(1):29-33.
223. Manganiello VC, Taira M, Degerman E, Belfrage P. Type III cGMP-inhibited cyclic nucleotide phosphodiesterases (PDE3 gene family). *Cell Signal.* 1995 Jul;7(5):445-55.
224. Shimizu K, Murata T, Okumura K, Manganiello VC, Tagawa T. Expression and role of phosphodiesterase 3 in human squamous cell carcinoma KB cells. *Anticancer Drugs.* 2002 Sep;13(8):875-80.
225. Murata T, Shimizu K, Narita M, Manganiello VC, Tagawa T. Characterization of phosphodiesterase 3 in human malignant melanoma cell line. *Anticancer Res.* 2002 Nov-Dec;22(6A):3171-4.
226. Murata T, Sugatani T, Shimizu K, Manganiello VC, Tagawa T. Phosphodiesterase 3 as a potential target for therapy of malignant tumors in the submandibular gland. *Anticancer Drugs.* 2001 Jan;12(1):79-83.
227. Murata K, Kameyama M, Fukui F, Ohigashi H, Hiratsuka M, Sasaki Y, et al. Phosphodiesterase type III inhibitor, cilostazol, inhibits colon cancer cell motility. *Clin Exp Metastasis.* 1999;17(6):525-30.
228. Sun B, Li H, Shakur Y, Hensley J, Hockman S, Kambayashi J, et al. Role of phosphodiesterase type 3A and 3B in regulating platelet and cardiac function using subtype-selective knockout mice. *Cell Signal.* 2007 Aug;19(8):1765-71.
229. Boswell-Smith V, Spina D, Page CP. Phosphodiesterase inhibitors. *Br J Pharmacol.* 2006 Jan;147 Suppl 1:S252-7.
230. Castro A, Jerez MJ, Gil C, Martinez A. Cyclic nucleotide phosphodiesterases and their role in immunomodulatory responses: advances in the development of specific phosphodiesterase inhibitors. *Med Res Rev.* 2005 Mar;25(2):229-44.
231. Ariga M, Neitzert B, Nakae S, Mottin G, Bertrand C, Pruniaux MP, et al. Nonredundant function of phosphodiesterases 4D and 4B in neutrophil recruitment to the site of inflammation. *J Immunol.* 2004 Dec 15;173(12):7531-8.
232. Jin SL, Conti M. Induction of the cyclic nucleotide phosphodiesterase PDE4B is essential for LPS-activated TNF-alpha responses. *Proc Natl Acad Sci U S A.* 2002 May 28;99(11):7628-33.
233. Jin SL, Richard FJ, Kuo WP, D'Ercole AJ, Conti M. Impaired growth and fertility of cAMP-specific phosphodiesterase PDE4D-deficient mice. *Proc Natl Acad Sci U S A.* 1999 Oct 12;96(21):11998-2003.
234. Mehats C, Jin SL, Wahlstrom J, Law E, Umetsu DT, Conti M. PDE4D plays a critical role in the control of airway smooth muscle contraction. *Faseb J.* 2003 Oct;17(13):1831-41.

235. Robichaud A, Stamatiou PB, Jin SL, Lachance N, MacDonald D, Laliberte F, et al. Deletion of phosphodiesterase 4D in mice shortens alpha(2)-adrenoceptor-mediated anesthesia, a behavioral correlate of emesis. *J Clin Invest*. 2002 Oct;110(7):1045-52.
236. Zhang HT, Huang Y, Jin SL, Frith SA, Suvarna N, Conti M, et al. Antidepressant-like profile and reduced sensitivity to rolipram in mice deficient in the PDE4D phosphodiesterase enzyme. *Neuropsychopharmacology*. 2002 Oct;27(4):587-95.
237. McCahill A, McSorley T, Huston E, Hill EV, Lynch MJ, Gall I, et al. In resting COS1 cells a dominant negative approach shows that specific, anchored PDE4 cAMP phosphodiesterase isoforms gate the activation, by basal cyclic AMP production, of AKAP-tethered protein kinase A type II located in the centrosomal region. *Cell Signal*. 2005 Sep;17(9):1158-73.
238. Lynch MJ, Baillie GS, Mohamed A, Li X, Maisonneuve C, Klussmann E, et al. RNA silencing identifies PDE4D5 as the functionally relevant cAMP phosphodiesterase interacting with beta arrestin to control the protein kinase A/AKAP79-mediated switching of the beta2-adrenergic receptor to activation of ERK in HEK293B2 cells. *J Biol Chem*. 2005 Sep 30;280(39):33178-89.
239. Houslay MD, Schafer P, Zhang KY. Keynote review: phosphodiesterase-4 as a therapeutic target. *Drug Discov Today*. 2005 Nov 15;10(22):1503-19.
240. Draheim R, Egerland U, Rundfeldt C. Anti-inflammatory potential of the selective phosphodiesterase 4 inhibitor N-(3,5-dichloro-pyrid-4-yl)-[1-(4-fluorobenzyl)-5-hydroxy-indole-3-yl]-glyoxylic acid amide (AWD 12-281), in human cell preparations. *J Pharmacol Exp Ther*. 2004 Feb;308(2):555-63.
241. Banner KH, Trevethick MA. PDE4 inhibition: a novel approach for the treatment of inflammatory bowel disease. *Trends Pharmacol Sci*. 2004 Aug;25(8):430-6.
242. Banner KH, Houlst JR, Taylor MN, Landells LJ, Page CP. Possible Contribution of Prostaglandin E2 to the antiproliferative effect of phosphodiesterase 4 inhibitors in human mononuclear cells. *Biochem Pharmacol*. 1999 Nov 1;58(9):1487-95.
243. Fan Chung K. Phosphodiesterase inhibitors in airways disease. *European Journal of Pharmacology*. 2006;533(1-3):110-7.
244. Le Jeune IR, Shepherd M, Van Heeke G, Houslay MD, Hall IP. Cyclic AMP-dependent transcriptional up-regulation of phosphodiesterase 4D5 in human airway smooth muscle cells. Identification and characterization of a novel PDE4D5 promoter. *J Biol Chem*. 2002 Sep 27;277(39):35980-9.
245. Favot L, Keravis T, Lugnier C. Modulation of VEGF-induced endothelial cell cycle protein expression through cyclic AMP hydrolysis by PDE2 and PDE4. *Thromb Haemost*. 2004 Sep;92(3):634-45.
246. Bolger GB, Peden AH, Steele MR, MacKenzie C, McEwan DG, Wallace DA, et al. Attenuation of the activity of the cAMP-specific phosphodiesterase

PDE4A5 by interaction with the immunophilin XAP2. *J Biol Chem.* 2003 Aug 29;278(35):33351-63.

247. Bolger GB, Erdogan S, Jones RE, Loughney K, Scotland G, Hoffmann R, et al. Characterization of five different proteins produced by alternatively spliced mRNAs from the human cAMP-specific phosphodiesterase PDE4D gene. *Biochem J.* 1997 Dec 1;328 (Pt 2):539-48.

248. Jeffery P. Phosphodiesterase 4-selective inhibition: novel therapy for the inflammation of COPD. *Pulm Pharmacol Ther.* 2005;18(1):9-17.

249. Soto FJ, Hanania NA. Selective phosphodiesterase-4 inhibitors in chronic obstructive lung disease. *Curr Opin Pulm Med.* 2005 Mar;11(2):129-34.

250. Hajjhussein H, Suvarna NU, Gremillion C, Chandler LJ, O'Donnell JM. Changes in NMDA receptor-induced cyclic nucleotide synthesis regulate the age-dependent increase in PDE4A expression in primary cortical cultures. *Brain Res.* 2007 May 29;1149:58-68.

251. Wang SJ. An investigation into the effect of the type IV phosphodiesterase inhibitor rolipram in the modulation of glutamate release from rat prefrontocortical nerve terminals. *Synapse.* 2006 Jan;59(1):41-50.

252. Zhao Y, Zhang HT, O'Donnell JM. Antidepressant-induced increase in high-affinity rolipram binding sites in rat brain: dependence on noradrenergic and serotonergic function. *J Pharmacol Exp Ther.* 2003 Oct;307(1):246-53.

253. Miro X, Perez-Torres S, Puigdomenech P, Palacios JM, Mengod G. Differential distribution of PDE4D splice variant mRNAs in rat brain suggests association with specific pathways and presynaptical localization. *Synapse.* 2002 Sep 15;45(4):259-69.

254. Lerner A, Epstein PM. Cyclic nucleotide phosphodiesterases as targets for treatment of haematological malignancies. *Biochem J.* 2006 Jan 1;393(Pt 1):21-41.

255. O'Donnell JM, Zhang HT. Antidepressant effects of inhibitors of cAMP phosphodiesterase (PDE4). *Trends Pharmacol Sci.* 2004 Mar;25(3):158-63.

256. Spina D. The potential of PDE4 inhibitors in respiratory disease. *Curr Drug Targets Inflamm Allergy.* 2004 Sep;3(3):231-6.

257. Smith D. Rolipram: antidepressant used in Europe and Japan might have promise against TNF, HIV. *AIDS Treat News.* 1996 Mar 1(no 242):3-4.

258. Zeller E, Stief HJ, Pflug B, Sastre-y-Hernandez M. Results of a phase II study of the antidepressant effect of rolipram. *Pharmacopsychiatry.* 1984 Nov;17(6):188-90.

259. Lipworth BJ. Phosphodiesterase-4 inhibitors for asthma and chronic obstructive pulmonary disease. *Lancet.* 2005 Jan 8-14;365(9454):167-75.

260. Lugnier C, Stierle A, Beretz A, Schoeffter P, Lebec A, Wermuth CG, et al. Tissue and substrate specificity of inhibition by alkoxy-aryl-lactams of platelet and arterial smooth muscle cyclic nucleotide phosphodiesterases relationship to pharmacological activity. *Biochem Biophys Res Commun.* 1983 Jun 29;113(3):954-9.
261. Wachtel H. Potential antidepressant activity of rolipram and other selective cyclic adenosine 3',5'-monophosphate phosphodiesterase inhibitors. *Neuropharmacology.* 1983 Mar;22(3):267-72.
262. Houslay MD, Adams DR. PDE4 cAMP phosphodiesterases: modular enzymes that orchestrate signalling cross-talk, desensitization and compartmentalization. *Biochem J.* 2003 Feb 15;370(Pt 1):1-18.
263. Conti M, Richter W, Mehats C, Livera G, Park JY, Jin C. Cyclic AMP-specific PDE4 phosphodiesterases as critical components of cyclic AMP signaling. *J Biol Chem.* 2003 Feb 21;278(8):5493-6.
264. Rena G, Begg F, Ross A, MacKenzie C, McPhee I, Campbell L, et al. Molecular cloning, genomic positioning, promoter identification, and characterization of the novel cyclic amp-specific phosphodiesterase PDE4A10. *Mol Pharmacol.* 2001 May;59(5):996-1011.
265. Vicini E, Conti M. Characterization of an intronic promoter of a cyclic adenosine 3',5'-monophosphate (cAMP)-specific phosphodiesterase gene that confers hormone and cAMP inducibility. *Mol Endocrinol.* 1997 Jun;11(7):839-50.
266. Jin SL, Latour AM, Conti M. Generation of PDE4 knockout mice by gene targeting. *Methods Mol Biol.* 2005;307:191-210.
267. Xiang Y, Naro F, Zoudilova M, Jin SL, Conti M, Kobilka B. Phosphodiesterase 4D is required for beta2 adrenoceptor subtype-specific signaling in cardiac myocytes. *Proc Natl Acad Sci U S A.* 2005 Jan 18;102(3):909-14.
268. Lehnart SE, Wehrens XH, Reiken S, Warriar S, Belevych AE, Harvey RD, et al. Phosphodiesterase 4D deficiency in the ryanodine-receptor complex promotes heart failure and arrhythmias. *Cell.* 2005 Oct 7;123(1):25-35.
269. Jin SL, Lan L, Zoudilova M, Conti M. Specific role of phosphodiesterase 4B in lipopolysaccharide-induced signaling in mouse macrophages. *J Immunol.* 2005 Aug 1;175(3):1523-31.
270. Siuciak JA, Chapin DS, McCarthy SA, Martin AN. Antipsychotic profile of rolipram: efficacy in rats and reduced sensitivity in mice deficient in the phosphodiesterase-4B (PDE4B) enzyme. *Psychopharmacology (Berl).* 2007 Jun;192(3):415-24.
271. Baillie GS, Sood A, McPhee I, Gall I, Perry SJ, Lefkowitz RJ, et al. beta-Arrestin-mediated PDE4 cAMP phosphodiesterase recruitment regulates beta-adrenoceptor switching from Gs to Gi. *Proc Natl Acad Sci U S A.* 2003 Feb 4;100(3):940-5.

272. Perry SJ, Baillie GS, Kohout TA, McPhee I, Magiera MM, Ang KL, et al. Targeting of cyclic AMP degradation to beta 2-adrenergic receptors by beta-arrestins. *Science*. 2002 Oct 25;298(5594):834-6.
273. Houslay MD, Baillie GS, Maurice DH. cAMP-Specific phosphodiesterase-4 enzymes in the cardiovascular system: a molecular toolbox for generating compartmentalized cAMP signaling. *Circ Res*. 2007 Apr 13;100(7):950-66.
274. MacKenzie SJ, Baillie GS, McPhee I, MacKenzie C, Seamons R, McSorley T, et al. Long PDE4 cAMP specific phosphodiesterases are activated by protein kinase A-mediated phosphorylation of a single serine residue in Upstream Conserved Region 1 (UCR1). *Br J Pharmacol*. 2002 Jun;136(3):421-33.
275. Baillie GS, Adams DR, Bhari N, Houslay TM, Vadrevu S, Meng D, et al. Mapping binding sites for the PDE4D5 cAMP-specific phosphodiesterase to the N- and C-domains of beta-arrestin using spot-immobilized peptide arrays. *Biochem J*. 2007 May 15;404(1):71-80.
276. Bolger GB, McCahill A, Huston E, Cheung YF, McSorley T, Baillie GS, et al. The unique amino-terminal region of the PDE4D5 cAMP phosphodiesterase isoform confers preferential interaction with beta-arrestins. *J Biol Chem*. 2003 Dec 5;278(49):49230-8.
277. Carlisle Michel JJ, Dodge KL, Wong W, Mayer NC, Langeberg LK, Scott JD. PKA-phosphorylation of PDE4D3 facilitates recruitment of the mAKAP signalling complex. *Biochem J*. 2004 Aug 1;381(Pt 3):587-92.
278. Dodge KL, Khouangsathiene S, Kapiloff MS, Mouton R, Hill EV, Houslay MD, et al. mAKAP assembles a protein kinase A/PDE4 phosphodiesterase cAMP signaling module. *Embo J*. 2001 Apr 17;20(8):1921-30.
279. Shakur Y, Pryde JG, Houslay MD. Engineered deletion of the unique N-terminal domain of the cyclic AMP-specific phosphodiesterase RD1 prevents plasma membrane association and the attainment of enhanced thermostability without altering its sensitivity to inhibition by rolipram. *Biochem J*. 1993 Jun 15;292 (Pt 3):677-86.
280. Baillie GS, MacKenzie SJ, McPhee I, Houslay MD. Sub-family selective actions in the ability of Erk2 MAP kinase to phosphorylate and regulate the activity of PDE4 cyclic AMP-specific phosphodiesterases. *Br J Pharmacol*. 2000 Oct;131(4):811-9.
281. Hoffmann R, Baillie GS, MacKenzie SJ, Yarwood SJ, Houslay MD. The MAP kinase ERK2 inhibits the cyclic AMP-specific phosphodiesterase HSPDE4D3 by phosphorylating it at Ser579. *Embo J*. 1999 Feb 15;18(4):893-903.
282. MacKenzie SJ, Baillie GS, McPhee I, Bolger GB, Houslay MD. ERK2 mitogen-activated protein kinase binding, phosphorylation, and regulation of the PDE4D cAMP-specific phosphodiesterases. The involvement of COOH-terminal docking sites and NH2-terminal UCR regions. *J Biol Chem*. 2000 Jun 2;275(22):16609-17.

283. Dhillon AS, Pollock C, Steen H, Shaw PE, Mischak H, Kolch W. Cyclic AMP-dependent kinase regulates Raf-1 kinase mainly by phosphorylation of serine 259. *Mol Cell Biol.* 2002 May;22(10):3237-46.
284. Hafner S, Adler HS, Mischak H, Janosch P, Heidecker G, Wolfman A, et al. Mechanism of inhibition of Raf-1 by protein kinase A. *Mol Cell Biol.* 1994 Oct;14(10):6696-703.
285. Dumaz N, Marais R. Protein kinase A blocks Raf-1 activity by stimulating 14-3-3 binding and blocking Raf-1 interaction with Ras. *J Biol Chem.* 2003 Aug 8;278(32):29819-23.
286. MacNicol MC, MacNicol AM. Nerve growth factor-stimulated B-Raf catalytic activity is refractory to inhibition by cAMP-dependent protein kinase. *J Biol Chem.* 1999 May 7;274(19):13193-7.
287. Calipel A, Mouriaux F, Glotin AL, Malecaze F, Faussat AM, Mascarelli F. Extracellular signal-regulated kinase-dependent proliferation is mediated through the protein kinase A/B-Raf pathway in human uveal melanoma cells. *J Biol Chem.* 2006 Apr 7;281(14):9238-50.
288. Yamaguchi T, Nagao S, Wallace DP, Belibi FA, Cowley BD, Pelling JC, et al. Cyclic AMP activates B-Raf and ERK in cyst epithelial cells from autosomal-dominant polycystic kidneys. *Kidney Int.* 2003 Jun;63(6):1983-94.
289. Duca L, Lambert E, Debret R, Rothhut B, Blanchevoye C, Delacoux F, et al. Elastin peptides activate extracellular signal-regulated kinase 1/2 via a Ras-independent mechanism requiring both p110gamma/Raf-1 and protein kinase A/B-Raf signaling in human skin fibroblasts. *Mol Pharmacol.* 2005 Apr;67(4):1315-24.
290. Schmitt JM, Stork PJ. Cyclic AMP-mediated inhibition of cell growth requires the small G protein Rap1. *Mol Cell Biol.* 2001 Jun;21(11):3671-83.
291. Tiwari S, Felekakis K, Moon EY, Flies A, Sherr DH, Lerner A. Among circulating hematopoietic cells, B-CLL uniquely expresses functional EPAC1, but EPAC1-mediated Rap1 activation does not account for PDE4 inhibitor-induced apoptosis. *Blood.* 2004 Apr 1;103(7):2661-7.
292. Cantley LC. The phosphoinositide 3-kinase pathway. *Science.* 2002 May 31;296(5573):1655-7.
293. Otsu M, Hiles I, Gout I, Fry MJ, Ruiz-Larrea F, Panayotou G, et al. Characterization of two 85 kd proteins that associate with receptor tyrosine kinases, middle-T/pp60c-src complexes, and PI3-kinase. *Cell.* 1991 Apr 5;65(1):91-104.
294. Yu J, Zhang Y, McIlroy J, Rordorf-Nikolic T, Orr GA, Backer JM. Regulation of the p85/p110 phosphatidylinositol 3'-kinase: stabilization and inhibition of the p110alpha catalytic subunit by the p85 regulatory subunit. *Mol Cell Biol.* 1998 Mar;18(3):1379-87.

295. Inukai K, Anai M, Van Breda E, Hosaka T, Katagiri H, Funaki M, et al. A novel 55-kDa regulatory subunit for phosphatidylinositol 3-kinase structurally similar to p55PIK Is generated by alternative splicing of the p85alpha gene. *J Biol Chem*. 1996 Mar 8;271(10):5317-20.
296. Vanhaesebroeck B, Welham MJ, Kotani K, Stein R, Warne PH, Zvelebil MJ, et al. P110delta, a novel phosphoinositide 3-kinase in leukocytes. *Proc Natl Acad Sci U S A*. 1997 Apr 29;94(9):4330-5.
297. Gaidarov I, Smith ME, Domin J, Keen JH. The class II phosphoinositide 3-kinase C2alpha is activated by clathrin and regulates clathrin-mediated membrane trafficking. *Mol Cell*. 2001 Feb;7(2):443-9.
298. DiNitto JP, Cronin TC, Lambright DG. Membrane recognition and targeting by lipid-binding domains. *Sci STKE*. 2003 Dec 16;2003(213):re16.
299. Simonsen A, Wurmser AE, Emr SD, Stenmark H. The role of phosphoinositides in membrane transport. *Curr Opin Cell Biol*. 2001 Aug;13(4):485-92.
300. Vivanco I, Sawyers CL. The phosphatidylinositol 3-Kinase AKT pathway in human cancer. *Nat Rev Cancer*. 2002 Jul;2(7):489-501.
301. Hawkins PT, Anderson KE, Davidson K, Stephens LR. Signalling through Class I PI3Ks in mammalian cells. *Biochem Soc Trans*. 2006 Nov;34(Pt 5):647-62.
302. Stambolic V, Suzuki A, de la Pompa JL, Brothers GM, Mirtsos C, Sasaki T, et al. Negative regulation of PKB/Akt-dependent cell survival by the tumor suppressor PTEN. *Cell*. 1998 Oct 2;95(1):29-39.
303. Lee JO, Yang H, Georgescu MM, Di Cristofano A, Maehama T, Shi Y, et al. Crystal structure of the PTEN tumor suppressor: implications for its phosphoinositide phosphatase activity and membrane association. *Cell*. 1999 Oct 29;99(3):323-34.
304. Tolkacheva T, Boddapati M, Sanfiz A, Tsuchida K, Kimmelman AC, Chan AM. Regulation of PTEN binding to MAGI-2 by two putative phosphorylation sites at threonine 382 and 383. *Cancer Res*. 2001 Jul 1;61(13):4985-9.
305. Torres J, Pulido R. The tumor suppressor PTEN is phosphorylated by the protein kinase CK2 at its C terminus. Implications for PTEN stability to proteasome-mediated degradation. *J Biol Chem*. 2001 Jan 12;276(2):993-8.
306. Vazquez F, Ramaswamy S, Nakamura N, Sellers WR. Phosphorylation of the PTEN tail regulates protein stability and function. *Mol Cell Biol*. 2000 Jul;20(14):5010-8.
307. Birle D, Bottini N, Williams S, Huynh H, deBelle I, Adamson E, et al. Negative feedback regulation of the tumor suppressor PTEN by phosphoinositide-induced serine phosphorylation. *J Immunol*. 2002 Jul 1;169(1):286-91.

308. Vazquez F, Grossman SR, Takahashi Y, Rokas MV, Nakamura N, Sellers WR. Phosphorylation of the PTEN tail acts as an inhibitory switch by preventing its recruitment into a protein complex. *J Biol Chem*. 2001 Dec 28;276(52):48627-30.
309. Miller SJ, Lou DY, Seldin DC, Lane WS, Neel BG. Direct identification of PTEN phosphorylation sites. *FEBS Lett*. 2002 Sep 25;528(1-3):145-53.
310. Koul D, Jasser SA, Lu Y, Davies MA, Shen R, Shi Y, et al. Motif analysis of the tumor suppressor gene MMAC/PTEN identifies tyrosines critical for tumor suppression and lipid phosphatase activity. *Oncogene*. 2002 Apr 4;21(15):2357-64.
311. Lu Y, Yu Q, Liu JH, Zhang J, Wang H, Koul D, et al. Src family protein-tyrosine kinases alter the function of PTEN to regulate phosphatidylinositol 3-kinase/AKT cascades. *J Biol Chem*. 2003 Oct 10;278(41):40057-66.
312. Leslie NR, Downes CP. PTEN function: how normal cells control it and tumour cells lose it. *Biochem J*. 2004 Aug 15;382(Pt 1):1-11.
313. Lee SR, Yang KS, Kwon J, Lee C, Jeong W, Rhee SG. Reversible inactivation of the tumor suppressor PTEN by H₂O₂. *J Biol Chem*. 2002 Jun 7;277(23):20336-42.
314. Leslie NR, Bennett D, Lindsay YE, Stewart H, Gray A, Downes CP. Redox regulation of PI 3-kinase signalling via inactivation of PTEN. *Embo J*. 2003 Oct 15;22(20):5501-10.
315. Aman MJ, Lamkin TD, Okada H, Kurosaki T, Ravichandran KS. The inositol phosphatase SHIP inhibits Akt/PKB activation in B cells. *J Biol Chem*. 1998 Dec 18;273(51):33922-8.
316. Bruhns P, Vely F, Malbec O, Fridman WH, Vivier E, Daron M. Molecular basis of the recruitment of the SH2 domain-containing inositol 5-phosphatases SHIP1 and SHIP2 by fcgamma RIIB. *J Biol Chem*. 2000 Dec 1;275(48):37357-64.
317. Helgason CD, Kalberer CP, Damen JE, Chappel SM, Pineault N, Krystal G, et al. A dual role for Src homology 2 domain-containing inositol-5-phosphatase (SHIP) in immunity: aberrant development and enhanced function of B lymphocytes in ship ^{-/-} mice. *J Exp Med*. 2000 Mar 6;191(5):781-94.
318. Liu Q, Sasaki T, Kozieradzki I, Wakeham A, Itie A, Dumont DJ, et al. SHIP is a negative regulator of growth factor receptor-mediated PKB/Akt activation and myeloid cell survival. *Genes Dev*. 1999 Apr 1;13(7):786-91.
319. Myers MP, Pass I, Batty IH, Van der Kaay J, Stolarov JP, Hemmings BA, et al. The lipid phosphatase activity of PTEN is critical for its tumor suppressor function. *Proc Natl Acad Sci U S A*. 1998 Nov 10;95(23):13513-8.
320. Alessi DR, Andjelkovic M, Caudwell B, Cron P, Morrice N, Cohen P, et al. Mechanism of activation of protein kinase B by insulin and IGF-1. *Embo J*. 1996 Dec 2;15(23):6541-51.

321. Feng J, Park J, Cron P, Hess D, Hemmings BA. Identification of a PKB/Akt hydrophobic motif Ser-473 kinase as DNA-dependent protein kinase. *J Biol Chem*. 2004 Sep 24;279(39):41189-96.
322. Hresko RC, Mueckler M. mTOR.RICTOR is the Ser473 kinase for Akt/protein kinase B in 3T3-L1 adipocytes. *J Biol Chem*. 2005 Dec 9;280(49):40406-16.
323. Luo J, Manning BD, Cantley LC. Targeting the PI3K-Akt pathway in human cancer: rationale and promise. *Cancer Cell*. 2003 Oct;4(4):257-62.
324. Bader AG, Kang S, Zhao L, Vogt PK. Oncogenic PI3K deregulates transcription and translation. *Nat Rev Cancer*. 2005 Dec;5(12):921-9.
325. Samuels Y, Velculescu VE. Oncogenic mutations of PIK3CA in human cancers. *Cell Cycle*. 2004 Oct;3(10):1221-4.
326. Janssen JW, Schleithoff L, Bartram CR, Schulz AS. An oncogenic fusion product of the phosphatidylinositol 3-kinase p85beta subunit and HUMORF8, a putative deubiquitinating enzyme. *Oncogene*. 1998 Apr 2;16(13):1767-72.
327. Jimenez C, Jones DR, Rodriguez-Viciana P, Gonzalez-Garcia A, Leonardo E, Wennstrom S, et al. Identification and characterization of a new oncogene derived from the regulatory subunit of phosphoinositide 3-kinase. *Embo J*. 1998 Feb 2;17(3):743-53.
328. Jucker M, Sudel K, Horn S, Sickel M, Wegner W, Fiedler W, et al. Expression of a mutated form of the p85alpha regulatory subunit of phosphatidylinositol 3-kinase in a Hodgkin's lymphoma-derived cell line (CO). *Leukemia*. 2002 May;16(5):894-901.
329. Borlado LR, Redondo C, Alvarez B, Jimenez C, Criado LM, Flores J, et al. Increased phosphoinositide 3-kinase activity induces a lymphoproliferative disorder and contributes to tumor generation in vivo. *Faseb J*. 2000 May;14(7):895-903.
330. Philp AJ, Campbell IG, Leet C, Vincan E, Rockman SP, Whitehead RH, et al. The phosphatidylinositol 3'-kinase p85alpha gene is an oncogene in human ovarian and colon tumors. *Cancer Res*. 2001 Oct 15;61(20):7426-9.
331. Sansal I, Sellers WR. The biology and clinical relevance of the PTEN tumor suppressor pathway. *J Clin Oncol*. 2004 Jul 15;22(14):2954-63.
332. Cantley LC, Neel BG. New insights into tumor suppression: PTEN suppresses tumor formation by restraining the phosphoinositide 3-kinase/AKT pathway. *Proc Natl Acad Sci U S A*. 1999 Apr 13;96(8):4240-5.
333. Kim S, Jee K, Kim D, Koh H, Chung J. Cyclic AMP inhibits Akt activity by blocking the membrane localization of PDK1. *J Biol Chem*. 2001 Apr 20;276(16):12864-70.

334. Liu L, Xie Y, Lou L. Cyclic AMP inhibition of proliferation of hepatocellular carcinoma cells is mediated by Akt. *Cancer Biol Ther.* 2005 Nov;4(11):1240-7.
335. Kuiperij HB, van der Horst A, Raaijmakers J, Weijzen S, Medema RH, Bos JL, et al. Activation of FoxO transcription factors contributes to the antiproliferative effect of cAMP. *Oncogene.* 2005 Mar 17;24(12):2087-95.
336. Lee HT, Kay EP. Regulatory role of cAMP on expression of Cdk4 and p27(Kip1) by inhibiting phosphatidylinositol 3-kinase in corneal endothelial cells. *Invest Ophthalmol Vis Sci.* 2003 Sep;44(9):3816-25.
337. Filippa N, Sable CL, Filloux C, Hemmings B, Van Obberghen E. Mechanism of protein kinase B activation by cyclic AMP-dependent protein kinase. *Mol Cell Biol.* 1999 Jul;19(7):4989-5000.
338. Sable CL, Filippa N, Hemmings B, Van Obberghen E. cAMP stimulates protein kinase B in a Wortmannin-insensitive manner. *FEBS Lett.* 1997 Jun 9;409(2):253-7.
339. Smith PG, Wang F, Wilkinson KN, Savage KJ, Klein U, Neuberg DS, et al. The phosphodiesterase PDE4B limits cAMP-associated PI3K/AKT-dependent apoptosis in diffuse large B-cell lymphoma. *Blood.* 2005 Jan 1;105(1):308-16.
340. Zmuda-Trzebiatowska E, Manganiello V, Degerman E. Novel mechanisms of the regulation of protein kinase B in adipocytes; implications for protein kinase A, Epac, phosphodiesterases 3 and 4. *Cell Signal.* 2007 Jan;19(1):81-6.
341. Vermeulen K, Berneman ZN, Van Bockstaele DR. Cell cycle and apoptosis. *Cell Prolif.* 2003 Jun;36(3):165-75.
342. Vermeulen K, Van Bockstaele DR, Berneman ZN. The cell cycle: a review of regulation, deregulation and therapeutic targets in cancer. *Cell Prolif.* 2003 Jun;36(3):131-49.
343. Sherr CJ. G1 phase progression: cycling on cue. *Cell.* 1994 Nov 18;79(4):551-5.
344. Arellano M, Moreno S. Regulation of CDK/cyclin complexes during the cell cycle. *Int J Biochem Cell Biol.* 1997 Apr;29(4):559-73.
345. Girard F, Strausfeld U, Fernandez A, Lamb NJ. Cyclin A is required for the onset of DNA replication in mammalian fibroblasts. *Cell.* 1991 Dec 20;67(6):1169-79.
346. King RW, Jackson PK, Kirschner MW. Mitosis in transition. *Cell.* 1994 Nov 18;79(4):563-71.
347. Ohtsubo M, Theodoras AM, Schumacher J, Roberts JM, Pagano M. Human cyclin E, a nuclear protein essential for the G1-to-S phase transition. *Mol Cell Biol.* 1995 May;15(5):2612-24.

348. Glotzer M, Murray AW, Kirschner MW. Cyclin is degraded by the ubiquitin pathway. *Nature*. 1991 Jan 10;349(6305):132-8.
349. Sherr CJ, Roberts JM. Inhibitors of mammalian G1 cyclin-dependent kinases. *Genes Dev*. 1995 May 15;9(10):1149-63.
350. Harper JW, Elledge SJ, Keyomarsi K, Dynlacht B, Tsai LH, Zhang P, et al. Inhibition of cyclin-dependent kinases by p21. *Mol Biol Cell*. 1995 Apr;6(4):387-400.
351. Lee MH, Reynisdottir I, Massague J. Cloning of p57KIP2, a cyclin-dependent kinase inhibitor with unique domain structure and tissue distribution. *Genes Dev*. 1995 Mar 15;9(6):639-49.
352. Polyak K, Kato JY, Solomon MJ, Sherr CJ, Massague J, Roberts JM, et al. p27Kip1, a cyclin-Cdk inhibitor, links transforming growth factor-beta and contact inhibition to cell cycle arrest. *Genes Dev*. 1994 Jan;8(1):9-22.
353. Polyak K, Lee MH, Erdjument-Bromage H, Koff A, Roberts JM, Tempst P, et al. Cloning of p27Kip1, a cyclin-dependent kinase inhibitor and a potential mediator of extracellular antimitogenic signals. *Cell*. 1994 Jul 15;78(1):59-66.
354. el-Deiry WS, Tokino T, Velculescu VE, Levy DB, Parsons R, Trent JM, et al. WAF1, a potential mediator of p53 tumor suppression. *Cell*. 1993 Nov 19;75(4):817-25.
355. Sheaff RJ, Groudine M, Gordon M, Roberts JM, Clurman BE. Cyclin E-CDK2 is a regulator of p27Kip1. *Genes Dev*. 1997 Jun 1;11(11):1464-78.
356. Fujita N, Sato S, Katayama K, Tsuruo T. Akt-dependent phosphorylation of p27Kip1 promotes binding to 14-3-3 and cytoplasmic localization. *J Biol Chem*. 2002 Aug 9;277(32):28706-13.
357. Sekimoto T, Fukumoto M, Yoneda Y. 14-3-3 suppresses the nuclear localization of threonine 157-phosphorylated p27(Kip1). *Embo J*. 2004 May 5;23(9):1934-42.
358. Motti ML, De Marco C, Califano D, Fusco A, Viglietto G. Akt-dependent T198 phosphorylation of cyclin-dependent kinase inhibitor p27kip1 in breast cancer. *Cell Cycle*. 2004 Aug;3(8):1074-80.
359. Liang J, Zubovitz J, Petrocelli T, Kotchetkov R, Connor MK, Han K, et al. PKB/Akt phosphorylates p27, impairs nuclear import of p27 and opposes p27-mediated G1 arrest. *Nat Med*. 2002 Oct;8(10):1153-60.
360. Carrano AC, Eytan E, Hershko A, Pagano M. SKP2 is required for ubiquitin-mediated degradation of the CDK inhibitor p27. *Nat Cell Biol*. 1999 Aug;1(4):193-9.
361. Tsvetkov LM, Yeh KH, Lee SJ, Sun H, Zhang H. p27(Kip1) ubiquitination and degradation is regulated by the SCF(Skp2) complex through phosphorylated Thr187 in p27. *Curr Biol*. 1999 Jun 17;9(12):661-4.

362. Wu YJ, Bond M, Sala-Newby GB, Newby AC. Altered S-phase kinase-associated protein-2 levels are a major mediator of cyclic nucleotide-induced inhibition of vascular smooth muscle cell proliferation. *Circ Res*. 2006 May 12;98(9):1141-50.
363. Dijkers PF, Medema RH, Pals C, Banerji L, Thomas NS, Lam EW, et al. Forkhead transcription factor FKHR-L1 modulates cytokine-dependent transcriptional regulation of p27(KIP1). *Mol Cell Biol*. 2000 Dec;20(24):9138-48.
364. Ohtani K, DeGregori J, Nevins JR. Regulation of the cyclin E gene by transcription factor E2F1. *Proc Natl Acad Sci U S A*. 1995 Dec 19;92(26):12146-50.
365. Dalton S. Cell cycle regulation of the human cdc2 gene. *Embo J*. 1992 May;11(5):1797-804.
366. Knudsen KE, Fribourg AF, Strobeck MW, Blanchard JM, Knudsen ES. Cyclin A is a functional target of retinoblastoma tumor suppressor protein-mediated cell cycle arrest. *J Biol Chem*. 1999 Sep 24;274(39):27632-41.
367. Zhu W, Giangrande PH, Nevins JR. E2Fs link the control of G1/S and G2/M transcription. *Embo J*. 2004 Nov 24;23(23):4615-26.
368. Vousden KH, Lane DP. p53 in health and disease. *Nat Rev Mol Cell Biol*. 2007 Apr;8(4):275-83.
369. Alao JP. The regulation of cyclin D1 degradation: roles in cancer development and the potential for therapeutic invention. *Mol Cancer*. 2007;6:24.
370. Classon M, Harlow E. The retinoblastoma tumour suppressor in development and cancer. *Nat Rev Cancer*. 2002 Dec;2(12):910-7.
371. Traub F, Mengel M, Luck HJ, Kreipe HH, von Wasielewski R. Prognostic impact of Skp2 and p27 in human breast cancer. *Breast Cancer Res Treat*. 2006 Sep;99(2):185-91.
372. Takanami I. The prognostic value of overexpression of Skp2 mRNA in non-small cell lung cancer. *Oncol Rep*. 2005 Apr;13(4):727-31.
373. Shapira M, Ben-Izhak O, Linn S, Futerman B, Minkov I, Hershko DD. The prognostic impact of the ubiquitin ligase subunits Skp2 and Cks1 in colorectal carcinoma. *Cancer*. 2005 Apr 1;103(7):1336-46.
374. Shigemasa K, Gu L, O'Brien TJ, Ohama K. Skp2 overexpression is a prognostic factor in patients with ovarian adenocarcinoma. *Clin Cancer Res*. 2003 May;9(5):1756-63.
375. Kim DH, Lerner A. Type 4 cyclic adenosine monophosphate phosphodiesterase as a therapeutic target in chronic lymphocytic leukemia. *Blood*. 1998 Oct 1;92(7):2484-94.
376. Lerner A, Kim DH, Lee R. The cAMP signaling pathway as a therapeutic target in lymphoid malignancies. *Leuk Lymphoma*. 2000 Mar;37(1-2):39-51.

377. Moon EY, Lerner A. PDE4 inhibitors activate a mitochondrial apoptotic pathway in chronic lymphocytic leukemia cells that is regulated by protein phosphatase 2A. *Blood*. 2003 May 15;101(10):4122-30.
378. Ogawa R, Streiff MB, Bugayenko A, Kato GJ. Inhibition of PDE4 phosphodiesterase activity induces growth suppression, apoptosis, glucocorticoid sensitivity, p53, and p21(WAF1/CIP1) proteins in human acute lymphoblastic leukemia cells. *Blood*. 2002 May 1;99(9):3390-7.
379. Shipp MA, Ross KN, Tamayo P, Weng AP, Kutok JL, Aguiar RC, et al. Diffuse large B-cell lymphoma outcome prediction by gene-expression profiling and supervised machine learning. *Nat Med*. 2002 Jan;8(1):68-74.
380. Chen TC, Wadsten P, Su S, Rawlinson N, Hofman FM, Hill CK, et al. The type IV phosphodiesterase inhibitor rolipram induces expression of the cell cycle inhibitors p21(Cip1) and p27(Kip1), resulting in growth inhibition, increased differentiation, and subsequent apoptosis of malignant A-172 glioma cells. *Cancer Biol Ther*. 2002 May-Jun;1(3):268-76.
381. Narita M, Murata T, Shimizu K, Sugiyama T, Nakagawa T, Manganiello VC, et al. Phosphodiesterase 4 in osteoblastic osteosarcoma cells as a potential target for growth inhibition. *Anticancer Drugs*. 2003 Jun;14(5):377-81.
382. Netherton SJ, Maurice DH. Vascular endothelial cell cyclic nucleotide phosphodiesterases and regulated cell migration: implications in angiogenesis. *Mol Pharmacol*. 2005 Jan;67(1):263-72.
383. Fleming YM, Frame MC, Houslay MD. PDE4-regulated cAMP degradation controls the assembly of integrin-dependent actin adhesion structures and REF52 cell migration. *J Cell Sci*. 2004 May 1;117(Pt 11):2377-88.
384. Mosmann T. Rapid colorimetric assay for cellular growth and survival: application to proliferation and cytotoxicity assays. *J Immunol Methods*. 1983 Dec 16;65(1-2):55-63.
385. Marchmont RJ, Houslay MD. A peripheral and an intrinsic enzyme constitute the cyclic AMP phosphodiesterase activity of rat liver plasma membranes. *Biochem J*. 1980 May 1;187(2):381-92.
386. Thompson WJ, Appleman MM. Multiple cyclic nucleotide phosphodiesterase activities from rat brain. *Biochemistry*. 1971 Jan 19;10(2):311-6.
387. Stork PJ, Schmitt JM. Crosstalk between cAMP and MAP kinase signaling in the regulation of cell proliferation. *Trends Cell Biol*. 2002 Jun;12(6):258-66.
388. Dugan LL, Kim JS, Zhang Y, Bart RD, Sun Y, Holtzman DM, et al. Differential effects of cAMP in neurons and astrocytes. Role of B-raf. *J Biol Chem*. 1999 Sep 3;274(36):25842-8.
389. Blomhoff HK, Blomhoff R, Stokke T, deLange Davies C, Brevik K, Smeland EB, et al. cAMP-mediated growth inhibition of a B-lymphoid precursor

cell line Reh is associated with an early transient delay in G2/M, followed by an accumulation of cells in G1. *J Cell Physiol.* 1988 Dec;137(3):583-7.

390. Melck D, Rueda D, Galve-Roperh I, De Petrocellis L, Guzman M, Di Marzo V. Involvement of the cAMP/protein kinase A pathway and of mitogen-activated protein kinase in the anti-proliferative effects of anandamide in human breast cancer cells. *FEBS Lett.* 1999 Dec 17;463(3):235-40.

391. Shaw TJ, Keszthelyi EJ, Tonary AM, Cada M, Vanderhyden BC. Cyclic AMP in ovarian cancer cells both inhibits proliferation and increases c-KIT expression. *Exp Cell Res.* 2002 Feb 1;273(1):95-106.

392. Ohmura E, Wakai K, Isozaki O, Murakami H, Onoda N, Emoto N, et al. Inhibition of human pancreatic cancer cell (MIA PaCa-2) growth by cholera toxin and 8-chloro-cAMP in vitro. *Br J Cancer.* 1993 Feb;67(2):279-83.

393. Lugnier C. Cyclic nucleotide phosphodiesterase (PDE) superfamily: a new target for the development of specific therapeutic agents. *Pharmacol Ther.* 2006 Mar;109(3):366-98.

394. Chini CC, Grande JP, Chini EN, Dousa TP. Compartmentalization of cAMP signaling in mesangial cells by phosphodiesterase isozymes PDE3 and PDE4. Regulation of superoxidation and mitogenesis. *J Biol Chem.* 1997 Apr 11;272(15):9854-9.

395. Osinski MT, Schror K. Inhibition of platelet-derived growth factor-induced mitogenesis by phosphodiesterase 3 inhibitors: role of protein kinase A in vascular smooth muscle cell mitogenesis. *Biochem Pharmacol.* 2000 Aug 1;60(3):381-7.

396. Bos JL. Epac: a new cAMP target and new avenues in cAMP research. *Nat Rev Mol Cell Biol.* 2003 Sep;4(9):733-8.

397. Fujita T, Meguro T, Fukuyama R, Nakamuta H, Koida M. New signaling pathway for parathyroid hormone and cyclic AMP action on extracellular-regulated kinase and cell proliferation in bone cells. Checkpoint of modulation by cyclic AMP. *J Biol Chem.* 2002 Jun 21;277(25):22191-200.

398. Hecquet C, Lefevre G, Valtink M, Engelmann K, Mascarelli F. cAMP inhibits the proliferation of retinal pigmented epithelial cells through the inhibition of ERK1/2 in a PKA-independent manner. *Oncogene.* 2002 Sep 5;21(39):6101-12.

399. Franke B, Akkerman JW, Bos JL. Rapid Ca²⁺-mediated activation of Rap1 in human platelets. *Embo J.* 1997 Jan 15;16(2):252-9.

400. Pagano M. Control of DNA synthesis and mitosis by the Skp2-p27-Cdk1/2 axis. *Mol Cell.* 2004 May 21;14(4):414-6.

401. Nakayama KI, Hatakeyama S, Nakayama K. Regulation of the cell cycle at the G1-S transition by proteolysis of cyclin E and p27Kip1. *Biochem Biophys Res Commun.* 2001 Apr 13;282(4):853-60.

402. Zhu CQ, Blackhall FH, Pintilie M, Iyengar P, Liu N, Ho J, et al. Skp2 gene copy number aberrations are common in non-small cell lung carcinoma, and its overexpression in tumors with ras mutation is a poor prognostic marker. *Clin Cancer Res.* 2004 Mar 15;10(6):1984-91.
403. Yokoi S, Yasui K, Mori M, Iizasa T, Fujisawa T, Inazawa J. Amplification and overexpression of SKP2 are associated with metastasis of non-small-cell lung cancers to lymph nodes. *Am J Pathol.* 2004 Jul;165(1):175-80.
404. Radke S, Pirkmaier A, Germain D. Differential expression of the F-box proteins Skp2 and Skp2B in breast cancer. *Oncogene.* 2005 May 12;24(21):3448-58.
405. Li JQ, Wu F, Masaki T, Kubo A, Fujita J, Dixon DA, et al. Correlation of Skp2 with carcinogenesis, invasion, metastasis, and prognosis in colorectal tumors. *Int J Oncol.* 2004 Jul;25(1):87-95.
406. Zhang L, Wang C. F-box protein Skp2: a novel transcriptional target of E2F. *Oncogene.* 2006 Apr 27;25(18):2615-27.
407. Folprecht G, Kohne CH. The role of new agents in the treatment of colorectal cancer. *Oncology.* 2004;66(1):1-17.
408. Naderi S, Wang JY, Chen TT, Gutzkow KB, Blomhoff HK. cAMP-mediated inhibition of DNA replication and S phase progression: involvement of Rb, p21Cip1, and PCNA. *Mol Biol Cell.* 2005 Mar;16(3):1527-42.
409. Chen TC, Hinton DR, Zidovetzki R, Hofman FM. Up-regulation of the cAMP/PKA pathway inhibits proliferation, induces differentiation, and leads to apoptosis in malignant gliomas. *Lab Invest.* 1998 Feb;78(2):165-74.
410. Cooper DM. Regulation and organization of adenylyl cyclases and cAMP. *Biochem J.* 2003 Nov 1;375(Pt 3):517-29.
411. Houslay MD, Kolch W. Cell-type specific integration of cross-talk between extracellular signal-regulated kinase and cAMP signaling. *Mol Pharmacol.* 2000 Oct;58(4):659-68.
412. Kase H, Iwahashi K, Nakanishi S, Matsuda Y, Yamada K, Takahashi M, et al. K-252 compounds, novel and potent inhibitors of protein kinase C and cyclic nucleotide-dependent protein kinases. *Biochem Biophys Res Commun.* 1987 Jan 30;142(2):436-40.
413. Zurbonsen K, Michel A, Vittet D, Bonnet PA, Chevillard C. Dissociation between phosphodiesterase inhibition and antiproliferative effects of phosphodiesterase inhibitors on the Dami cell line. *Biochem Pharmacol.* 1997 Apr 25;53(8):1141-7.
414. Baillie GS, Scott JD, Houslay MD. Compartmentalisation of phosphodiesterases and protein kinase A: opposites attract. *FEBS Lett.* 2005 Jun 13;579(15):3264-70.

415. sKerfant BG, Zhao D, Lorenzen-Schmidt I, Wilson LS, Cai S, Chen SR, et al. PI3Kgamma is required for PDE4, not PDE3, activity in subcellular microdomains containing the sarcoplasmic reticular calcium ATPase in cardiomyocytes. *Circ Res*. 2007 Aug 17;101(4):400-8.
416. Kato JY, Matsuoka M, Polyak K, Massague J, Sherr CJ. Cyclic AMP-induced G1 phase arrest mediated by an inhibitor (p27Kip1) of cyclin-dependent kinase 4 activation. *Cell*. 1994 Nov 4;79(3):487-96.
417. Tiwari S, Dong H, Kim EJ, Weintraub L, Epstein PM, Lerner A. Type 4 cAMP phosphodiesterase (PDE4) inhibitors augment glucocorticoid-mediated apoptosis in B cell chronic lymphocytic leukemia (B-CLL) in the absence of exogenous adenylyl cyclase stimulation. *Biochem Pharmacol*. 2005 Feb 1;69(3):473-83.
418. El-Mowafy AM. Resveratrol activates membrane-bound guanylyl cyclase in coronary arterial smooth muscle: a novel signaling mechanism in support of coronary protection. *Biochem Biophys Res Commun*. 2002 Mar 15;291(5):1218-24.
419. Savouret JF, Quesne M. Resveratrol and cancer: a review. *Biomed Pharmacother*. 2002 Mar;56(2):84-7.
420. Gusman J, Malonne H, Atassi G. A reappraisal of the potential chemopreventive and chemotherapeutic properties of resveratrol. *Carcinogenesis*. 2001 Aug;22(8):1111-7.
421. El-Mowafy AM, Alkhalaf M. Resveratrol activates adenylyl-cyclase in human breast cancer cells: a novel, estrogen receptor-independent cytostatic mechanism. *Carcinogenesis*. 2003 May;24(5):869-73.
422. Gray A, Van Der Kaay J, Downes CP. The pleckstrin homology domains of protein kinase B and GRP1 (general receptor for phosphoinositides-1) are sensitive and selective probes for the cellular detection of phosphatidylinositol 3,4-bisphosphate and/or phosphatidylinositol 3,4,5-trisphosphate in vivo. *Biochem J*. 1999 Dec 15;344 Pt 3:929-36.
423. Takaishi H, Konishi H, Matsuzaki H, Ono Y, Shirai Y, Saito N, et al. Regulation of nuclear translocation of forkhead transcription factor AFX by protein kinase B. *Proc Natl Acad Sci U S A*. 1999 Oct 12;96(21):11836-41.
424. Medema RH, Kops GJ, Bos JL, Burgering BM. AFX-like Forkhead transcription factors mediate cell-cycle regulation by Ras and PKB through p27kip1. *Nature*. 2000 Apr 13;404(6779):782-7.
425. Kops GJ, de Ruiter ND, De Vries-Smits AM, Powell DR, Bos JL, Burgering BM. Direct control of the Forkhead transcription factor AFX by protein kinase B. *Nature*. 1999 Apr 15;398(6728):630-4.
426. Haefner B, Frame MC. Distinctive regulation of v-Src-associated phosphatidylinositol 3-kinase during PC12 cell differentiation. *Biochem J*. 1997 Dec 1;328 (Pt 2):649-55.

427. Bolen JB, Veillette A, Schwartz AM, Deseau V, Rosen N. Analysis of pp60c-src in human colon carcinoma and normal human colon mucosal cells. *Oncogene Res.* 1987 Jul;1(2):149-68.
428. Cartwright CA, Kamps MP, Meisler AI, Pipas JM, Eckhart W. pp60c-src activation in human colon carcinoma. *J Clin Invest.* 1989 Jun;83(6):2025-33.
429. Bellacosa A, Kumar CC, Di Cristofano A, Testa JR. Activation of AKT kinases in cancer: implications for therapeutic targeting. *Adv Cancer Res.* 2005;94:29-86.
430. Lawlor MA, Alessi DR. PKB/Akt: a key mediator of cell proliferation, survival and insulin responses? *J Cell Sci.* 2001 Aug;114(Pt 16):2903-10.
431. Burgering BM, Coffey PJ. Protein kinase B (c-Akt) in phosphatidylinositol-3-OH kinase signal transduction. *Nature.* 1995 Aug 17;376(6541):599-602.
432. Franke TF, Yang SI, Chan TO, Datta K, Kazlauskas A, Morrison DK, et al. The protein kinase encoded by the Akt proto-oncogene is a target of the PDGF-activated phosphatidylinositol 3-kinase. *Cell.* 1995 Jun 2;81(5):727-36.
433. Kohn AD, Kovacina KS, Roth RA. Insulin stimulates the kinase activity of RAC-PK, a pleckstrin homology domain containing ser/thr kinase. *Embo J.* 1995 Sep 1;14(17):4288-95.
434. Scott PH, Lawrence JC, Jr. Attenuation of mammalian target of rapamycin activity by increased cAMP in 3T3-L1 adipocytes. *J Biol Chem.* 1998 Dec 18;273(51):34496-501.
435. Liu W, Akhand AA, Takeda K, Kawamoto Y, Itoigawa M, Kato M, et al. Protein phosphatase 2A-linked and -unlinked caspase-dependent pathways for downregulation of Akt kinase triggered by 4-hydroxynonenal. *Cell Death Differ.* 2003 Jul;10(7):772-81.
436. Feschenko MS, Stevenson E, Nairn AC, Sweadner KJ. A novel cAMP-stimulated pathway in protein phosphatase 2A activation. *J Pharmacol Exp Ther.* 2002 Jul;302(1):111-8.
437. Sun H, Lesche R, Li DM, Liliental J, Zhang H, Gao J, et al. PTEN modulates cell cycle progression and cell survival by regulating phosphatidylinositol 3,4,5,-trisphosphate and Akt/protein kinase B signaling pathway. *Proc Natl Acad Sci U S A.* 1999 May 25;96(11):6199-204.
438. Viglietto G, Motti ML, Bruni P, Melillo RM, D'Alessio A, Califano D, et al. Cytoplasmic relocalization and inhibition of the cyclin-dependent kinase inhibitor p27(Kip1) by PKB/Akt-mediated phosphorylation in breast cancer. *Nat Med.* 2002 Oct;8(10):1136-44.
439. Ishida N, Hara T, Kamura T, Yoshida M, Nakayama K, Nakayama KI. Phosphorylation of p27Kip1 on serine 10 is required for its binding to CRM1 and nuclear export. *J Biol Chem.* 2002 Apr 26;277(17):14355-8.

440. Ishida N, Kitagawa M, Hatakeyama S, Nakayama K. Phosphorylation at serine 10, a major phosphorylation site of p27(Kip1), increases its protein stability. *J Biol Chem.* 2000 Aug 18;275(33):25146-54.
441. Andreu EJ, Lledo E, Poch E, Ivorra C, Albero MP, Martinez-Climent JA, et al. BCR-ABL induces the expression of Skp2 through the PI3K pathway to promote p27Kip1 degradation and proliferation of chronic myelogenous leukemia cells. *Cancer Res.* 2005 Apr 15;65(8):3264-72.
442. Mamillapalli R, Gavrilova N, Mihaylova VT, Tsvetkov LM, Wu H, Zhang H, et al. PTEN regulates the ubiquitin-dependent degradation of the CDK inhibitor p27(KIP1) through the ubiquitin E3 ligase SCF(SKP2). *Curr Biol.* 2001 Feb 20;11(4):263-7.
443. Cardone MH, Roy N, Stennicke HR, Salvesen GS, Franke TF, Stanbridge E, et al. Regulation of cell death protease caspase-9 by phosphorylation. *Science.* 1998 Nov 13;282(5392):1318-21.
444. Datta SR, Dudek H, Tao X, Masters S, Fu H, Gotoh Y, et al. Akt phosphorylation of BAD couples survival signals to the cell-intrinsic death machinery. *Cell.* 1997 Oct 17;91(2):231-41.
445. Brunet A, Bonni A, Zigmond MJ, Lin MZ, Juo P, Hu LS, et al. Akt promotes cell survival by phosphorylating and inhibiting a Forkhead transcription factor. *Cell.* 1999 Mar 19;96(6):857-68.
446. del Peso L, Gonzalez-Garcia M, Page C, Herrera R, Nunez G. Interleukin-3-induced phosphorylation of BAD through the protein kinase Akt. *Science.* 1997 Oct 24;278(5338):687-9.
447. Blume-Jensen P, Janknecht R, Hunter T. The kit receptor promotes cell survival via activation of PI 3-kinase and subsequent Akt-mediated phosphorylation of Bad on Ser136. *Curr Biol.* 1998 Jun 18;8(13):779-82.
448. Saito Y, Swanson X, Mhashilkar AM, Oida Y, Schrock R, Branch CD, et al. Adenovirus-mediated transfer of the PTEN gene inhibits human colorectal cancer growth in vitro and in vivo. *Gene Ther.* 2003 Nov;10(23):1961-9.
449. Cheney IW, Neuteboom ST, Vaillancourt MT, Ramachandra M, Bookstein R. Adenovirus-mediated gene transfer of MMAC1/PTEN to glioblastoma cells inhibits S phase entry by the recruitment of p27Kip1 into cyclin E/CDK2 complexes. *Cancer Res.* 1999 May 15;59(10):2318-23.
450. Weng LP, Smith WM, Dahia PL, Ziebold U, Gil E, Lees JA, et al. PTEN suppresses breast cancer cell growth by phosphatase activity-dependent G1 arrest followed by cell death. *Cancer Res.* 1999 Nov 15;59(22):5808-14.
451. Anai S, Goodison S, Shiverick K, Iczkowski K, Tanaka M, Rosser CJ. Combination of PTEN gene therapy and radiation inhibits the growth of human prostate cancer xenografts. *Hum Gene Ther.* 2006 Oct;17(10):975-84.

452. Tanaka M, Rosser CJ, Grossman HB. PTEN gene therapy induces growth inhibition and increases efficacy of chemotherapy in prostate cancer. *Cancer Detect Prev.* 2005;29(2):170-4.
453. Saito Y, Gopalan B, Mhashilkar AM, Roth JA, Chada S, Zumstein L, et al. Adenovirus-mediated PTEN treatment combined with caffeine produces a synergistic therapeutic effect in colorectal cancer cells. *Cancer Gene Ther.* 2003 Nov;10(11):803-13.
454. Weinstein IB. Cancer. Addiction to oncogenes--the Achilles heel of cancer. *Science.* 2002 Jul 5;297(5578):63-4.
455. Lynch TJ, Bell DW, Sordella R, Gurubhagavatula S, Okimoto RA, Brannigan BW, et al. Activating mutations in the epidermal growth factor receptor underlying responsiveness of non-small-cell lung cancer to gefitinib. *N Engl J Med.* 2004 May 20;350(21):2129-39.
456. Sordella R, Bell DW, Haber DA, Settleman J. Gefitinib-sensitizing EGFR mutations in lung cancer activate anti-apoptotic pathways. *Science.* 2004 Aug 20;305(5687):1163-7.
457. Slamon DJ, Leyland-Jones B, Shak S, Fuchs H, Paton V, Bajamonde A, et al. Use of chemotherapy plus a monoclonal antibody against HER2 for metastatic breast cancer that overexpresses HER2. *N Engl J Med.* 2001 Mar 15;344(11):783-92.
458. Hughes TP, Kaeda J, Branford S, Rudzki Z, Hochhaus A, Hensley ML, et al. Frequency of major molecular responses to imatinib or interferon alfa plus cytarabine in newly diagnosed chronic myeloid leukemia. *N Engl J Med.* 2003 Oct 9;349(15):1423-32.
459. Knight ZA, Gonzalez B, Feldman ME, Zunder ER, Goldenberg DD, Williams O, et al. A pharmacological map of the PI3-K family defines a role for p110alpha in insulin signaling. *Cell.* 2006 May 19;125(4):733-47.
460. Jacobs MD, Black J, Futer O, Swenson L, Hare B, Fleming M, et al. Pim-1 ligand-bound structures reveal the mechanism of serine/threonine kinase inhibition by LY294002. *J Biol Chem.* 2005 Apr 8;280(14):13728-34.
461. Ward SG, Finan P. Isoform-specific phosphoinositide 3-kinase inhibitors as therapeutic agents. *Curr Opin Pharmacol.* 2003 Aug;3(4):426-34.
462. Kreis TE. Microinjected antibodies against the cytoplasmic domain of vesicular stomatitis virus glycoprotein block its transport to the cell surface. *Embo J.* 1986 May;5(5):931-41.
463. Shah NP, Nicoll JM, Nagar B, Gorre ME, Paquette RL, Kuriyan J, et al. Multiple BCR-ABL kinase domain mutations confer polyclonal resistance to the tyrosine kinase inhibitor imatinib (STI571) in chronic phase and blast crisis chronic myeloid leukemia. *Cancer Cell.* 2002 Aug;2(2):117-25.

464. Talpaz M, Shah NP, Kantarjian H, Donato N, Nicoll J, Paquette R, et al. Dasatinib in imatinib-resistant Philadelphia chromosome-positive leukemias. *N Engl J Med*. 2006 Jun 15;354(24):2531-41.
465. Fausel CA. Novel treatment strategies for chronic myeloid leukemia. *Am J Health Syst Pharm*. 2006 Dec 1;63(23 Suppl 8):S15-20; quiz S1-2.
466. Quintas-Cardama A, Kantarjian H, Cortes J. Targeting ABL and SRC kinases in chronic myeloid leukemia: experience with dasatinib. *Future Oncol*. 2006 Dec;2(6):655-65.
467. Al-Hakim A, Rui X, Tsao J, Albert PR, Schimmer BP. Forskolin-resistant Y1 adrenal cell mutants are deficient in adenylyl cyclase type 4. *Mol Cell Endocrinol*. 2004 Feb 12;214(1-2):155-65.
468. Rui X, Al-Hakim A, Tsao J, Albert PR, Schimmer BP. Expression of adenylyl cyclase-4 (AC-4) in Y1 and forskolin-resistant adrenal cells. *Mol Cell Endocrinol*. 2004 Feb 27;215(1-2):101-8.
469. Schimmer BP, Tsao J. Isolation of forskolin-resistant adrenal cells defective in the adenylate cyclase system. *J Biol Chem*. 1984 May 10;259(9):5376-9.
470. Schimmer BP, Tsao J, Collie G, Wong M, Schulz P. Analysis of the mutation to forskolin-resistance in Y1 adrenocortical tumor cells. *Endocr Res*. 1984;10(3-4):365-86.
471. Shepherd MC, Baillie GS, Stirling DI, Houslay MD. Remodelling of the PDE4 cAMP phosphodiesterase isoform profile upon monocyte-macrophage differentiation of human U937 cells. *Br J Pharmacol*. 2004 May;142(2):339-51.
472. Barber R, Baillie GS, Bergmann R, Shepherd MC, Sepper R, Houslay MD, et al. Differential expression of PDE4 cAMP phosphodiesterase isoforms in inflammatory cells of smokers with COPD, smokers without COPD, and nonsmokers. *Am J Physiol Lung Cell Mol Physiol*. 2004 Aug;287(2):L332-43.
473. Persani L, Lania A, Alberti L, Romoli R, Mantovani G, Filetti S, et al. Induction of specific phosphodiesterase isoforms by constitutive activation of the cAMP pathway in autonomous thyroid adenomas. *J Clin Endocrinol Metab*. 2000 Aug;85(8):2872-8.
474. Peter D, Jin SL, Conti M, Hatzelmann A, Zitt C. Differential expression and function of phosphodiesterase 4 (PDE4) subtypes in human primary CD4+ T cells: predominant role of PDE4D. *J Immunol*. 2007 Apr 15;178(8):4820-31.
475. Moon E, Lee R, Near R, Weintraub L, Wolda S, Lerner A. Inhibition of PDE3B augments PDE4 inhibitor-induced apoptosis in a subset of patients with chronic lymphocytic leukemia. *Clin Cancer Res*. 2002 Feb;8(2):589-95.
476. McEwan DG, Brunton VG, Baillie GS, Leslie NR, Houslay MD, Frame MC. Chemoresistant KM12C Colon Cancer Cells Are Addicted to Low Cyclic AMP Levels in a Phosphodiesterase 4-Regulated Compartment via Effects on Phosphoinositide 3-Kinase. *Cancer Res*. 2007 Jun 1;67(11):5248-57.

477. Hosono M, Takahira T, Fujita A, Fujihara R, Ishizuka O, Tatee T, et al. Cardiovascular and adenylate cyclase stimulant properties of NKH477, a novel water-soluble forskolin derivative. *J Cardiovasc Pharmacol.* 1992 Apr;19(4):625-34.
478. Hirasawa A, Awaji T, Hosono M, Haruno A, Hashimoto K. Effects of a new forskolin derivative, NKH477, on canine ventricular arrhythmia models. *J Cardiovasc Pharmacol.* 1993 Dec;22(6):847-51.
479. Mori M, Takeuchi M, Takaoka H, Hata K, Hayashi Y, Yokoyama M. Effect of NKH477, a new water-soluble forskolin derivative, on arterial-ventricular coupling and mechanical energy transduction in patients with left ventricular systolic dysfunction: comparison with dobutamine. *J Cardiovasc Pharmacol.* 1994 Aug;24(2):310-6.
480. Furukawa Y, Matsumori A, Hirozane T, Matsui S, Sato Y, Ono K, et al. Immunomodulation by an adenylate cyclase activator, NKH477, in vivo and vitro. *Clin Immunol Immunopathol.* 1996 Apr;79(1):25-35.
481. Hayashida N, Chihara S, Tayama E, Takaseya T, Enomoto N, Kawara T, et al. Antiinflammatory effects of colforsin daropate hydrochloride, a novel water-soluble forskolin derivative. *Ann Thorac Surg.* 2001 Jun;71(6):1931-8.
482. Kikura M, Morita K, Sato S. Pharmacokinetics and a simulation model of colforsin daropate, new forskolin derivative inotropic vasodilator, in patients undergoing coronary artery bypass grafting. *Pharmacol Res.* 2004 Mar;49(3):275-81.
483. Wellbrock C, Karasarides M, Marais R. The RAF proteins take centre stage. *Nat Rev Mol Cell Biol.* 2004 Nov;5(11):875-85.
484. Merlino GT, Xu YH, Ishii S, Clark AJ, Semba K, Toyoshima K, et al. Amplification and enhanced expression of the epidermal growth factor receptor gene in A431 human carcinoma cells. *Science.* 1984 Apr 27;224(4647):417-9.
485. Agarwal A, Das K, Lerner N, Sathe S, Cicek M, Casey G, et al. The AKT/I kappa B kinase pathway promotes angiogenic/metastatic gene expression in colorectal cancer by activating nuclear factor-kappa B and beta-catenin. *Oncogene.* 2005 Feb 3;24(6):1021-31.
486. Ishikawa H, Jin MB, Ogata T, Taniguchi M, Suzuki T, Shimamura T, et al. Role of cyclic nucleotides in ischemia and reperfusion injury of canine livers. *Transplantation.* 2002 Apr 15;73(7):1041-8.
487. Maeda H, Ozawa H, Saito T, Irie T, Takahata N. Potential antidepressant properties of forskolin and a novel water-soluble forskolin (NKH477) in the forced swimming test. *Life Sci.* 1997;61(25):2435-42.
488. Wajima Z, Shiga T, Yoshikawa T, Ogura A, Imanaga K, Inoue T, et al. Effect of prophylactic bronchodilator treatment with intravenous colforsin daropate, a water-soluble forskolin derivative, on airway resistance after tracheal intubation. *Anesthesiology.* 2003 Jul;99(1):18-26.

489. Wajima Z, Yoshikawa T, Ogura A, Imanaga K, Shiga T, Inoue T, et al. Intravenous colforsin daropate, a water-soluble forskolin derivative, prevents thiamylal-fentanyl-induced bronchoconstriction in humans. *Crit Care Med*. 2002 Apr;30(4):820-6.
490. Toya Y, Schwencke C, Ishikawa Y. Forskolin derivatives with increased selectivity for cardiac adenylyl cyclase. *J Mol Cell Cardiol*. 1998 Jan;30(1):97-108.
491. Liu S, Veilleux A, Zhang L, Young A, Kwok E, Laliberte F, et al. Dynamic activation of cystic fibrosis transmembrane conductance regulator by type 3 and type 4D phosphodiesterase inhibitors. *J Pharmacol Exp Ther*. 2005 Aug;314(2):846-54.
492. Souness JE, Rao S. Proposal for pharmacologically distinct conformers of PDE4 cyclic AMP phosphodiesterases. *Cell Signal*. 1997 May-Jun;9(3-4):227-36.
493. Smith KJ, Baillie GS, Hyde EI, Li X, Houslay TM, McCahill A, et al. (1)H NMR structural and functional characterisation of a cAMP-specific phosphodiesterase-4D5 (PDE4D5) N-terminal region peptide that disrupts PDE4D5 interaction with the signalling scaffold proteins, betaarrestin and RACK1. *Cell Signal*. 2007 Sep 1.

Published material from this thesis

McEwan DG, Brunton VG, Baillie GS, Leslie NR, Houslay MD, Frame MC. Chemoresistant KM12C Colon Cancer Cells Are Addicted to Low Cyclic AMP Levels in a Phosphodiesterase 4-Regulated Compartment via Effects on Phosphoinositide 3-Kinase. *Cancer Res.* 2007 Jun 1;67(11):5248-57.

Chemoresistant KM12C Colon Cancer Cells Are Addicted to Low Cyclic AMP Levels in a Phosphodiesterase 4–Regulated Compartment via Effects on Phosphoinositide 3-Kinase

David G. McEwan,^{1,2} Valerie G. Brunton,¹ George S. Baillie,² Nicholas R. Leslie,³ Miles D. Houslay,² and Margaret C. Frame¹

¹The Beatson Institute for Cancer Research, Cancer Research UK Beatson Laboratories; ²Molecular Pharmacology Group, Division of Biochemistry and Molecular Biology, IBLS, University of Glasgow, Glasgow, United Kingdom; and ³Division of Molecular Physiology, College of Life Sciences, Wellcome Trust Biocentre, University of Dundee, Dundee, United Kingdom

Abstract

One of the major problems in treating colon cancer is chemoresistance to cytotoxic chemotherapeutic agents. There is therefore a need to devise new strategies to inhibit colon cancer cell growth and survival. Here, we show that a combination of low doses of the adenylyl cyclase activator forskolin together with the specific cyclic AMP (cAMP) phosphodiesterase-4 (PDE4) inhibitor rolipram, but not the cAMP phosphodiesterase-3 (PDE3) inhibitor cilostamide, causes profound growth arrest of chemoresistant KM12C colon cancer cells. Low-dose forskolin causes KM12C cells to exit the cell cycle in G₁ by inducing p27^{Kip1} and primes cells for apoptosis on addition of rolipram. The effect of the low-dose forskolin/rolipram combination is mediated by displacement of the phosphatidylinositol 3,4,5-trisphosphate/phosphoinositide 3-kinase signaling module from the plasma membrane and suppression of the Akt/protein kinase-B oncogene pathway, to which KM12C cells are addicted for growth. The cAMP and phosphoinositide 3-kinase pathways form a critical intersection in this response, and reexpression of the tumor suppressor lipid phosphatase, phosphatase and tensin homologue, which is commonly lost or mutated in colon cancer, sensitizes KM12C cells to growth inhibition by challenge with low-dose forskolin. Certain chemoresistant colon cancer cells are therefore exquisitely sensitive to subtle elevation of cAMP by a synergistic low-dose adenylyl cyclase activator/PDE4 inhibitor combination. Indeed, these cells are addicted to maintenance of low cAMP concentrations in a compartment that is regulated by PDE4. Well-tolerated doses of PDE4 inhibitors that are already in clinical development for other therapeutic indications may provide an exciting new strategy for the treatment of colon cancer. [Cancer Res 2007;67(11):5248–57]

Introduction

Colorectal cancer is the third commonest cancer in the United Kingdom, which can, at present, only be cured by complete resection of the primary tumor and isolated metastasis. In reality, the majority of metastatic tumors are not resectable, and

chemotherapy is the first-line treatment for a large number of patients. Currently, chemotherapy, which is usually 5-fluorouracil (5-FU), or capecitabine, which is processed to generate 5-FU in tumor cells, folinic acid, or newer agents such as irinotecan or oxaliplatin, improves survival in only a proportion of cases (reviewed in ref. 1). Although chemotherapy can also give a modest improvement in time to tumor progression and overall survival in more advanced disease, there remains an urgent need for new treatments to improve survival. Here, we have used cancer cells of various origins, including those from the Fidler model of colorectal metastasis (2), to examine whether modulators of cAMP may successfully intervene in chemoresistant cancers, and to identify both mechanism and circumstances in which this might be useful.

Cyclic AMP (cAMP) acts as a second messenger that controls a diverse range of cellular processes (3), usually through activation of either or both protein kinase A (PKA; ref. 4) and the cAMP-GTP exchange factor Epac (5). cAMP signaling is regulated in both spatial and temporal manner by cAMP phosphodiesterases (PDE; ref. 6), which provide the sole route for degradation of cAMP in cells (3, 7). Whereas a large and complex enzyme family provide for cAMP phosphodiesterase activity within cells, invariably the majority of cAMP-hydrolyzing activity is provided by members of the phosphodiesterase 3 (PDE3) and phosphodiesterase 4 (PDE4) families (7, 8). However, enzymes of the PDE4 family have attracted much recent interest because they play a key role in underpinning compartmentalized cAMP signaling in many cell types (9) and because PDE4-specific inhibitors seem to have therapeutic potential as anti-inflammatory agents for treating chronic obstructive pulmonary disease and as cognitive enhancers and antidepressants (7, 10).

In the cancer context, there are some reports suggesting that modulating intracellular cAMP levels may have effects on the behavior of cancer cells (11). For example, the archetypal PDE3-selective inhibitor cilostazol (12) and the archetypal PDE4-selective inhibitor rolipram (7) both suppress colon cancer cell motility (13), whereas inhibition PDE4 by rolipram can negatively affect chronic lymphocytic leukemia (14). Interestingly, rolipram can also induce expression of cyclin-dependent kinase (CDK) inhibitors, leading to growth inhibition and differentiation of glioma cells (15), although a high concentration of rolipram was required for these effects. The cAMP-elevating agent forskolin (16), when used at high doses, has been reported to inhibit DNA replication in lymphocytes via PKA-mediated effects on p21^{CIP1}, leading to dephosphorylation of the retinoblastoma protein (pRb) and disrupted tethering of proliferating cell nuclear antigen to DNA (17). Taken together, these reports tantalizingly suggest that modulating intracellular cAMP,

Note: Supplementary data for this article are available at Cancer Research Online (<http://cancerres.aacrjournals.org/>).

Requests for reprints: Margaret C. Frame, The Beatson Institute for Cancer Research, Cancer Research UK Beatson Laboratories, Garscube Estate, Switchback Road, Bearsden, Glasgow G61 1BD, United Kingdom. Phone: 44-141-330-3953; Fax: 44-141-942-6521; E-mail: m.frame@beatson.gla.ac.uk.

©2007 American Association for Cancer Research.
doi:10.1158/0008-5472.CAN-07-0097

perhaps in a localized manner by targeting particular PDE types, may affect the proliferation of cancer cells.

In the present study, we set out to test the hypothesis that some chemoresistant epithelial cancer cells are "addicted" to oncogenic growth-regulatory pathways that may be influenced by cAMP modulation. This would provide a novel, and much needed, way to inhibit such cancer cells, particularly if it could be achieved by well-tolerated synergistic low doses of cAMP modulators. We found that a combination of relatively low doses of forskolin and rolipram (but interestingly not cilostamide) can work together to cause growth arrest and apoptosis via sustained inhibition of the phosphoinositide 3-kinase (PI3K)/Akt pathway and effects on regulators of G₁ progression. Reexpression of the phosphatase and tensin homologue (PTEN) lipid phosphatase, which negatively regulates PI3K and is commonly lost or mutated in many human malignancies (18, 19), slows the growth of KM12C cells at low density and renders them more sensitive to growth inhibition by the low-dose forskolin/rolipram treatment. Therefore, KM12C colon cancer cells, which are resistant to cytotoxic agent-induced cell death, can be effectively growth inhibited and killed by particular modulators of cAMP degradation and synthesis; in this case, specifically by a mechanism that ablates signaling through the PI3K/Akt pathway, to which these cells are addicted for growth and survival. In a survey of 11 cancer cell lines (including 7 colon cancer cell lines), we found that up to 8 of these are sensitive to the forskolin/rolipram combination to a greater or lesser extent, implying that this may have more general applicability as a way of inhibiting cancer cells that are otherwise extremely difficult to kill.

Materials and Methods

Cell culture and cell lines. KM12C cells were provided by Prof. I. Fidler (Department of Cancer Biology, M.D. Anderson Cancer Center, Houston, TX) and KM12/2C4 cells were derived as previously reported (20). MCF7, HT29, A431, WiDr, RKO, A375, H630, Du145, SW480, and SW620 were obtained from the American Type Culture Collection. MCF7 and KM12C cells were cultured in Eagle's MEM with Earle's salts supplemented with MEM vitamins, nonessential amino acids, L-glutamine (2 mmol/L), and sodium pyruvate (1 mmol/L; all from Life Technologies) in the presence of 10% fetal bovine serum (Autogen Bioclear). HT29, A431, WiDr, RKO, A375, and Du145 cell lines were cultured in DMEM supplemented with L-glutamine (2 mmol/L; Life Technologies) and 10% fetal bovine serum (Autogen Bioclear). SW480, SW620, and H630 cells were cultured in RPMI (Invitrogen) supplemented with L-glutamine (2 mmol/L; Life Technologies) and 10% fetal bovine serum (Autogen Bioclear). All cells were routinely maintained in a humidified incubator at 37°C with 5% CO₂ and subcultured before reaching confluence. Cells expressing PTEN-green fluorescent protein (GFP; NH₂-terminal tag) were generated by retroviral infection of KM12C/2C4 cells with PTEN-GFP in pWZL vector, and single-cell clones were selected in growth media containing 400 µg/mL hygromycin B (Calbiochem).

Modified 3-(4,5-dimethylthiazol-2-yl)-2,5-diphenyltetrazolium bromide proliferation assay. Cell proliferation and viability was assayed indirectly by a modified 3-(4,5-dimethylthiazol-2-yl)-2,5-diphenyltetrazolium bromide (MTT) assay, based on the enzymatic reduction of MTT (Sigma) to formazan crystal by mitochondria and cellular dehydrogenase enzymes (21). Briefly, 50 µL of cell suspension containing 1,000 cells were dispensed into 96-well flat-bottomed microplates. Dilutions of pharmacologic agents in growth media were done in four replicate rows per cell type and per dilution. Plates were then incubated in a humidified incubator in 5% CO₂ at 37°C. At the time points indicated, 50 µL of MTT solution (5 mg/mL MTT in PBS) were added to a total volume of 100 µL and incubated in 5% CO₂ at 37°C for 4 h. Formazan crystals were dissolved with 100-µL DMSO and absorbance at 570 nm was determined with a plate reader.

Immunoblotting. Cells were treated with DMSO (vehicle), forskolin, rolipram (all obtained from Sigma-Aldrich), or LY294002 (obtained from Calbiochem) at the concentrations and times indicated before generation of cell extracts. Cell extracts were prepared in lysis buffer (20 mmol/L Tris, 150 mmol/L NaCl, 2 mmol/L EDTA, 1% Triton X-100, 10% glycerol pH 7.4) from subconfluent cell cultures and clarified by centrifugation at 4°C. Total protein was measured using microBCA reagent (Pierce). Proteins were resolved by 10% SDS-PAGE, transferred to nitrocellulose, and blocked before probing with indicated specific antibodies and detection by horseradish peroxidase (HRP)-conjugated secondary antibodies (antimouse and anti-rabbit HRP, Cell Signaling). Antibodies used in this study include anti-p27^{KIP1} (Becton Dickinson Transduction Laboratories); anti-vinculin (Sigma-Aldrich); anti-p21^{CIP1}, anti-cyclin A, anti-cyclin E, and anti-CDK1 (Cdc2 p34; Santa Cruz Biotechnology); and anti-phospho-Akt (Ser⁴⁷³ and Thr³⁰⁸) and total Akt (Cell Signaling Technologies). pRb was resolved by 7.5% SDS-PAGE (29.74% acrylamide/0.24% bis-acrylamide) gels before transfer and probed with anti-total pRb antibody (Becton Dickinson Transduction Laboratories). For immunoblotting, 50 to 100 µg of cellular proteins were resolved as above.

Cell cycle analysis and apoptosis detection. Cells were fixed in 70% ethanol in PBS overnight. For DNA content analysis, cells were pelleted and resuspended in PBS containing 1 µg/mL RNase (Qiagen Ltd.) and 10 µg/mL propidium iodide, incubated at room temperature for 30 min, then analyzed using a Becton Dickinson (Oxford, United Kingdom) FACScan flow cytometer. To monitor bromodeoxyuridine (BrdUrd) incorporation, cells were incubated with 20 µmol/L BrdUrd for the final hour of treatment, fixed, and incubated with an anti-BrdUrd antibody (Dako) followed by FITC-conjugated secondary antibody. Apoptosis was quantified using an Annexin V-FITC detection kit (Becton Dickinson) and staining was carried out per manufacturers' instructions. Briefly, KM12C cells were set up at low density and treated for 24, 48, or 72 h with the treatments indicated. At each time point, cells were washed with cold PBS, trypsinized, and resuspended in binding buffer (100 mmol/L HEPES, 1.4 mol/L NaCl, 25 mmol/L CaCl₂, pH 7.4) at a concentration of 1 × 10⁶/mL and 100 µL of resuspended cells were incubated with Annexin V-FITC and propidium iodide.

Microscopy and immunofluorescence. Cells were plated at a density of 1.5 × 10⁵ per glass coverslip for transfection and 7 × 10⁴ per glass coverslip for all other imagings. KM12C cells were transiently transfected with 1.5 µg of GFP fused to the plektstrin homology (PH) domain of Akt (GFP-PH; ref. 22) construct for 4 h using Polyfect (Qiagen) and left in fresh media overnight. Cells were treated with pharmacologic agents and then fixed using 4% paraformaldehyde for 15 min at room temperature. GFP was visualized with a confocal microscope (Leica).

Statistical analysis. Statistical analysis was done using the nonparametric Mann-Whitney test and *P* < 0.05 was considered significant.

Phosphodiesterase assay. PDE assays were done by a modification (23) of the two-step method by Thomson and Appleman (24). In brief, cells were lysed in KHEM buffer [50 mmol/L KCl, 50 mmol/L HEPES (pH 7.2), 10 mmol/L EGTA, 1.92 mmol/L MgCl₂] containing protease inhibitors (Roche Molecular Biochemicals). Cells were then subjected to 14,000 × *g* for 15 min at 4°C and the resulting supernatants were assayed for total PDE activity using 1 µmol/L cAMP and [³H]cAMP as a substrate. To determine the contribution of various PDE family members to the total PDE activity, family specific inhibitors were used at a final concentration that completely inhibited their activities. PDE3 and PDE4 activities were determined using 10 µmol/L cilostamide (PDE3; ref. 12) or 10 µmol/L rolipram (PDE4; refs. 7, 10).

Results

cAMP modulators cause growth suppression. Treatment of KM12C cells with the adenylyl cyclase activator forskolin (at 50 µmol/L) completely inhibits their growth (Fig. 1A), an effect that is mediated by cAMP as it is mimicked by challenging cells with the cell-permeant cAMP analogue 8-bromo-cyclic AMP (8-Br-cAMP; 300 µmol/L; Fig. 1A). However, treatment of KM12C cells

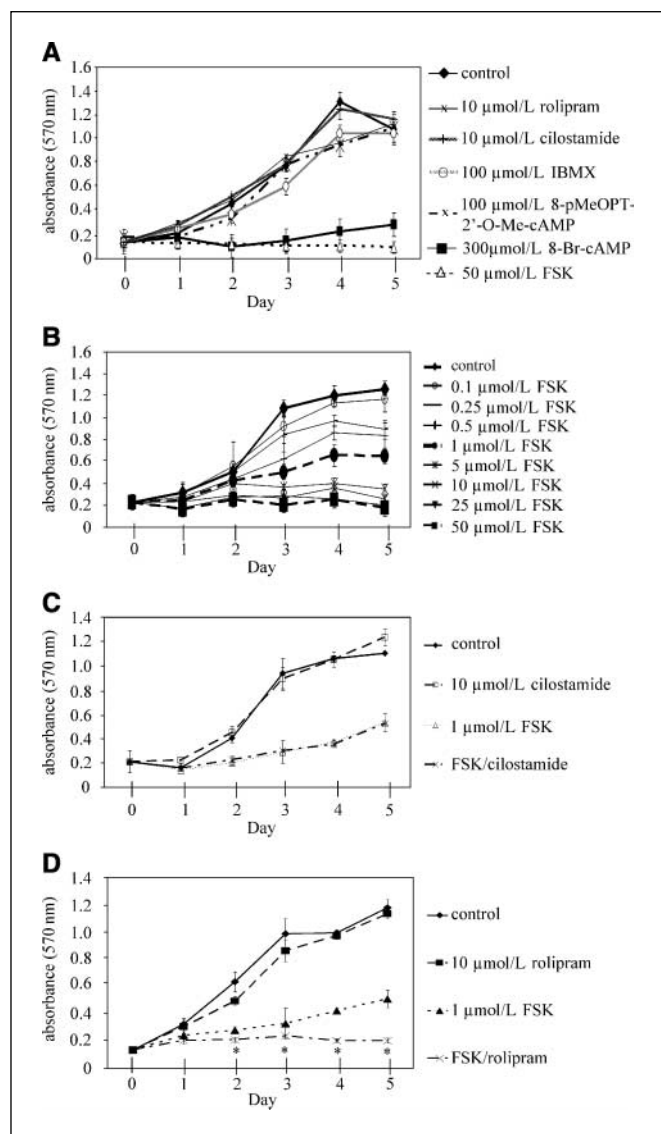


Figure 1. Specific cAMP elevation inhibits KM12C proliferation. Proliferation of KM12C cells was monitored over a 5-d period using a MTT dye-based assay, during which the cells were treated with modulators of cAMP. **A**, cells were treated with vehicle only (*control*; DMSO), 50 $\mu\text{mol/L}$ forskolin (FSK; a adenylyl cyclase activator), 300 $\mu\text{mol/L}$ 8-Br-cAMP (a nonhydrolyzable cAMP analogue), 100 $\mu\text{mol/L}$ 8-pMeOPT-2'-O-Me-cAMP (a Epac-specific activator), 100 $\mu\text{mol/L}$ IBMX (a nonspecific PDE inhibitor), 10 $\mu\text{mol/L}$ cilostamide (a PDE3-specific inhibitor), and 10 $\mu\text{mol/L}$ rolipram (a PDE4-specific inhibitor). **B**, a concentration range of forskolin (0.1–50 $\mu\text{mol/L}$) was carried out to establish which concentration (1 $\mu\text{mol/L}$) gave an $\sim 50\%$ inhibition of proliferation. **C**, stimulation of KM12C cells with low-dose forskolin (1 $\mu\text{mol/L}$) in combination with a PDE3 inhibitor (10 $\mu\text{mol/L}$ cilostamide) indicated that PDE3 enzymes do not control the cAMP pool that regulates proliferation on stimulation with forskolin. **D**, PDE4 inhibition (10 $\mu\text{mol/L}$ rolipram) in combination with a low forskolin concentration (1 $\mu\text{mol/L}$) completely inhibited the proliferation of KM12C cells, whereas neither agent alone (at these concentrations) was able to do this. *Points*, mean of three independent experiments; *bars*, SD. *, $P < 0.03$, compared with 1 $\mu\text{mol/L}$ forskolin alone.

with the cell-permeant cAMP analogue 8-pMeOPT-2'-O-Me-cAMP, which selectively activates Epac rather than PKA, did not result in growth suppression (Fig. 1A). Interestingly, treatment with the nonselective PDE inhibitor I-methyl-3-isobutylxanthine (IBMX; 100 $\mu\text{mol/L}$), the specific PDE3 inhibitor cilostamide (10 $\mu\text{mol/L}$), or the specific PDE4 inhibitor rolipram (10 $\mu\text{mol/L}$), at concen-

trations known to induce selective PDE inhibition (7, 9, 12), did not cause growth cessation (Fig. 1A).

We next titrated the action of forskolin and found that 1 $\mu\text{mol/L}$ forskolin gave rise to $\sim 50\%$ inhibition of KM12C cell growth (Fig. 1B). We therefore used this “low dose” of forskolin to look for potential synergistic action with inhibitors specific for the PDE3 and PDE4 families because these are collectively responsible for $\sim 35\%$ of cAMP-hydrolyzing activity in KM12C cells (Supplementary Table S1). We found that the PDE3-selective inhibitor cilostamide, when used at a dose known to maximally inhibit PDE3 (10 $\mu\text{mol/L}$; ref. 12), did not potentiate low-dose (1 $\mu\text{mol/L}$) forskolin-induced growth suppression (Fig. 1C). In marked contrast to this, addition of rolipram at a dose (10 $\mu\text{mol/L}$) known to maximally inhibit PDE4 (7, 10) enhanced the growth suppression induced by 1 $\mu\text{mol/L}$ forskolin (Fig. 1D); rolipram plus low-dose forskolin caused complete growth cessation of KM12C cells, despite rolipram having no effect on its own. Statistical analysis of the data indicated that there was no significant difference between control and rolipram ($P > 0.09$) for all time points; however, for control versus forskolin ($P < 0.03$), forskolin versus forskolin/rolipram ($P < 0.02$), and control versus forskolin/rolipram ($P < 0.02$), the data were deemed statistically significant from day 2 onward. Thus, under conditions of submaximal adenylyl cyclase activity, inhibition of specific cAMP-hydrolyzing PDE4 can suppress growth regulatory pathways in KM12C cells. The profound growth arrest is intriguing because these cancer cells are resistant to cytotoxic agents and to inhibitors of the major oncogenic Src and Ras pathways.⁴ We may therefore have uncovered an apparent “Achilles heel” for these chemoresistant cancer cells.

Effects of forskolin and rolipram on cell cycle regulators.

Next, we addressed known regulators of the G_1 -S transition in response to five conditions: (a) DMSO vehicle control; (b) high-dose (50 $\mu\text{mol/L}$) forskolin, which alone blocks KM12C cell proliferation; (c) low-dose (1 $\mu\text{mol/L}$) forskolin, which only suppresses proliferation by $\sim 50\%$; (d) low-dose (10 $\mu\text{mol/L}$) rolipram, which does not affect proliferation; and (e) the combined low doses of both forskolin (1 $\mu\text{mol/L}$) and rolipram (10 $\mu\text{mol/L}$; forskolin/rolipram), which causes complete growth cessation (Fig. 1). These treatments were used throughout of the remainder of this study to investigate mechanism of action.

We found no consistent difference in p21^{CIP1} expression induced by forskolin or rolipram (Fig. 2A, top). However, p27^{KIP1} expression was increased by treatments that blocked proliferation, particularly by high-dose forskolin and the synergistic low-dose combination of forskolin/rolipram (Fig. 2A, middle, lanes 2 and 5). In addition, Skp2, an oncogenic F-box protein component of the SCF ubiquitin ligase complex, which is known to target p27^{KIP1} for proteosomal degradation (25), is regulated in a reciprocal manner to p27^{KIP1} (Fig. 2B, top, lanes 2 and 5); Skp2 protein expression is reduced when p27^{KIP1} is enhanced after treatment with high-dose forskolin or the low-dose forskolin/rolipram combination (Fig. 2B, top, lanes 2 and 5). This suggests that the mechanism by which p27^{KIP1} accumulates during cell cycle withdrawal may be due, at least in part, to loss of Skp2-mediated degradation. As expected, the induction of p27^{KIP1} was paralleled by loss of phosphorylated pRb (and reduced pRb expression) as well as decreased expression of the pRb/E2F-regulated cyclins A, B1, and E, together with their

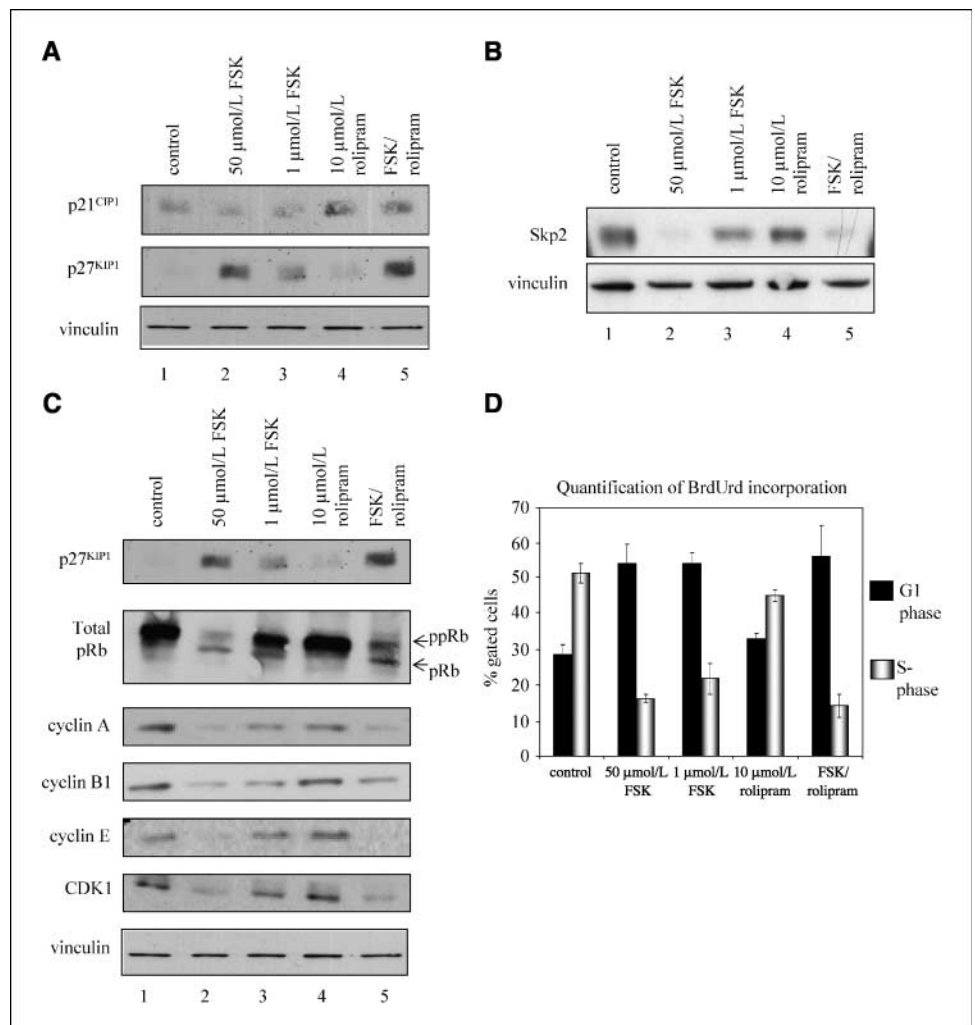
⁴ Our unpublished data.

kinase partner CDK1 (Fig. 2C, lanes 2 and 5). These results imply that high-dose forskolin and the low-dose forskolin/rolipram combination induce cell cycle arrest via inhibition of the pRb/cyclin/CDK pathway, which normally controls progression through G₁-S phase of the cell cycle, and that this is via stabilization of p27^{KIP1}.

Low-dose forskolin causes cell cycle arrest and primes KM12C cells for rolipram-induced apoptosis. To complement the results of the proliferation assays (Fig. 1) and analysis of cell cycle regulators (Fig. 2), we next cultured cells in the combination of cAMP-modulating agents for 24 h and then pulsed with BrdUrd during the final hour. Cells were stained with propidium iodide and analyzed by flow cytometry to determine BrdUrd incorporation into the DNA at various cell cycle stages. In keeping with the antiproliferative effects observed by MTT assays, quantification of BrdUrd incorporation showed that high-dose forskolin and the low-dose combination of forskolin/rolipram (forskolin/rolipram) caused a partial G₁ arrest, with ~20% of cells still in S phase (Fig. 2D). Surprisingly, low-dose (1 μmol/L) forskolin caused a similar G₁ arrest although these cultures were still able to grow to ~50% of control cells in proliferation assays (Fig. 1). To investigate the reason why high-dose forskolin and low-dose forskolin/rolipram cause complete growth cessation whereas low-dose forskolin-treated cultures can still proliferate, albeit more slowly,

we examined cell viability. Cells were treated with the cAMP-modulating agent combinations for 24, 48, or 72 h, and the cells were fixed and stained with propidium iodide (Fig. 3A) or an Annexin V-FITC conjugate (Fig. 3B) and analyzed by flow cytometry to detect apoptotic cells. Quantification and statistical analysis of sub-2n DNA by propidium iodide (Fig. 3C) and Annexin V staining (Fig. 3D) showed that whereas both high-dose (50 μmol/L) and low-dose (1 μmol/L) forskolin caused G₁ arrest (Fig. 2D), only high-dose forskolin-treated cells were apoptotic. In contrast to low-dose forskolin alone or rolipram alone, the low-dose forskolin/rolipram combination caused both G₁ arrest and apoptosis that was statistically significant from 48 h onward ($P < 0.05$) when compared with 1 μmol/L forskolin alone (Fig. 2D, quantified in Fig. 3C and D). This correlates with the data in Fig. 1D, in which a statistically significant difference in the proliferation between 1 μmol/L forskolin alone versus forskolin/rolipram combination is observed from day 2 onward and reflects the increase in apoptosis observed in forskolin/rolipram-treated cells (Fig. 3C and D). These data indicate that low-dose forskolin not only causes G₁ arrest but also primes KM12C cells to die, presumably from the G₁ arrested population, on addition of the PDE4 inhibitor rolipram (Fig. 3). Challenge with rolipram alone did not cause apoptosis (Fig. 3). This suggests that the combination of low-dose forskolin/rolipram can arrest and kill chemoresistant KM12C colon cancer cells. This

Figure 2. Combined low-dose forskolin/rolipram induces p27^{KIP1}, loss of Skp2, pRb phosphorylation, and cyclin/CDK components. Subconfluent KM12C cells were cultured for 24 h under normal conditions and in the presence of DMSO (control; lane 1), 50 μmol/L forskolin (lane 2), 1 μmol/L forskolin (lane 3), 10 μmol/L rolipram (lane 4), or 1 μmol/L forskolin + 10 μmol/L rolipram (FSK/rolipram; lane 5), and the protein levels of various cell cycle regulators were analyzed via immunoblotting with specific antibodies as probes. A, high forskolin and forskolin/rolipram combination treatment increases p27^{KIP1} (middle, lanes 2 and 5) but does not affect p21^{CIP1} levels (top). B, forskolin and forskolin/rolipram treatment causes a decrease in levels of the SCF ubiquitin ligase adapter protein Skp2 (top, lanes 2 and 5). C, high forskolin (lanes 2) and low-dose forskolin/rolipram treatment (lanes 5) causes loss of hyperphosphorylated (ppRb) and total pRb and deregulation of the pRb/E2F regulated cell cycle control proteins cyclin A, cyclin B1, cyclin E, and CDK1. Vinculin immunoblotting was used as a loading control in all of the above. D, quantification of BrdUrd pulse-labeled KM12C cells. Cell cycle distribution is presented as percentage of gated cells. Columns, mean of three independent experiments; bars, SD.



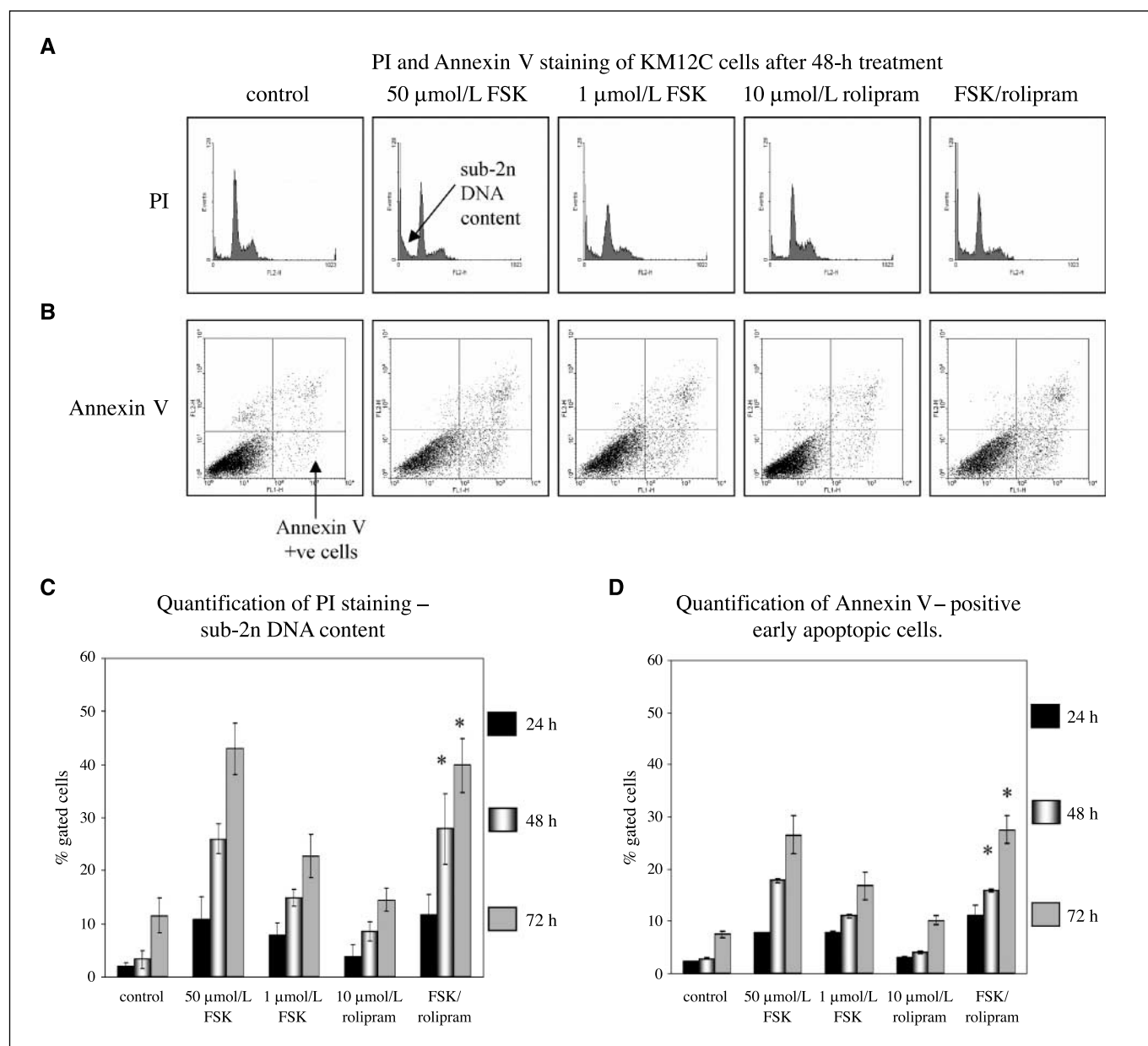


Figure 3. Forskolin/rolipram induces apoptosis of KM12C cells. Effects of treatments on cell viability. KM12C cells were cultured for 24, 48, or 72 h in the presence of DMSO, 50 $\mu\text{mol/L}$ forskolin, 1 $\mu\text{mol/L}$ forskolin, 10 $\mu\text{mol/L}$ rolipram, or 1 $\mu\text{mol/L}$ forskolin + 10 $\mu\text{mol/L}$ rolipram, and then washed, trypsinized, and incubated with either propidium iodide (PI; A) or anti-Annexin V-FITC conjugate and propidium iodide (B) and analyzed by fluorescence-activated cell sorting for the detection of apoptotic cells. Results shown are for 48 h. Quantification of sub-2n DNA regions of the histograms (C) and lower right quadrants of the dot plots for the detection of Annexin V-positive early apoptotic cells (D) were used to calculate percentages of gated cells (columns, mean of three independent experiments; bars, SD). *, $P < 0.05$, compared with 1 $\mu\text{mol/L}$ forskolin alone.

raises the exciting possibility that such combinations of relatively low doses of cAMP-elevating agents may provide a means of inhibiting the growth of some advanced cancer cells, which are otherwise extremely difficult to kill. This also indicates that KM12C cell viability and growth requires maintenance of cAMP at low levels, at least in the compartments that are regulated by PDE4.

Low-dose forskolin/rolipram works by suppressing PI3K signaling. Because the PI3K pathway plays a major role in regulating cell growth and survival (26), we examined whether it was important for continued proliferation of KM12C cells and whether it impinged on the novel, cAMP-induced, inhibitory effects on survival. Intriguingly, we found that GFP-PH [used as a reporter

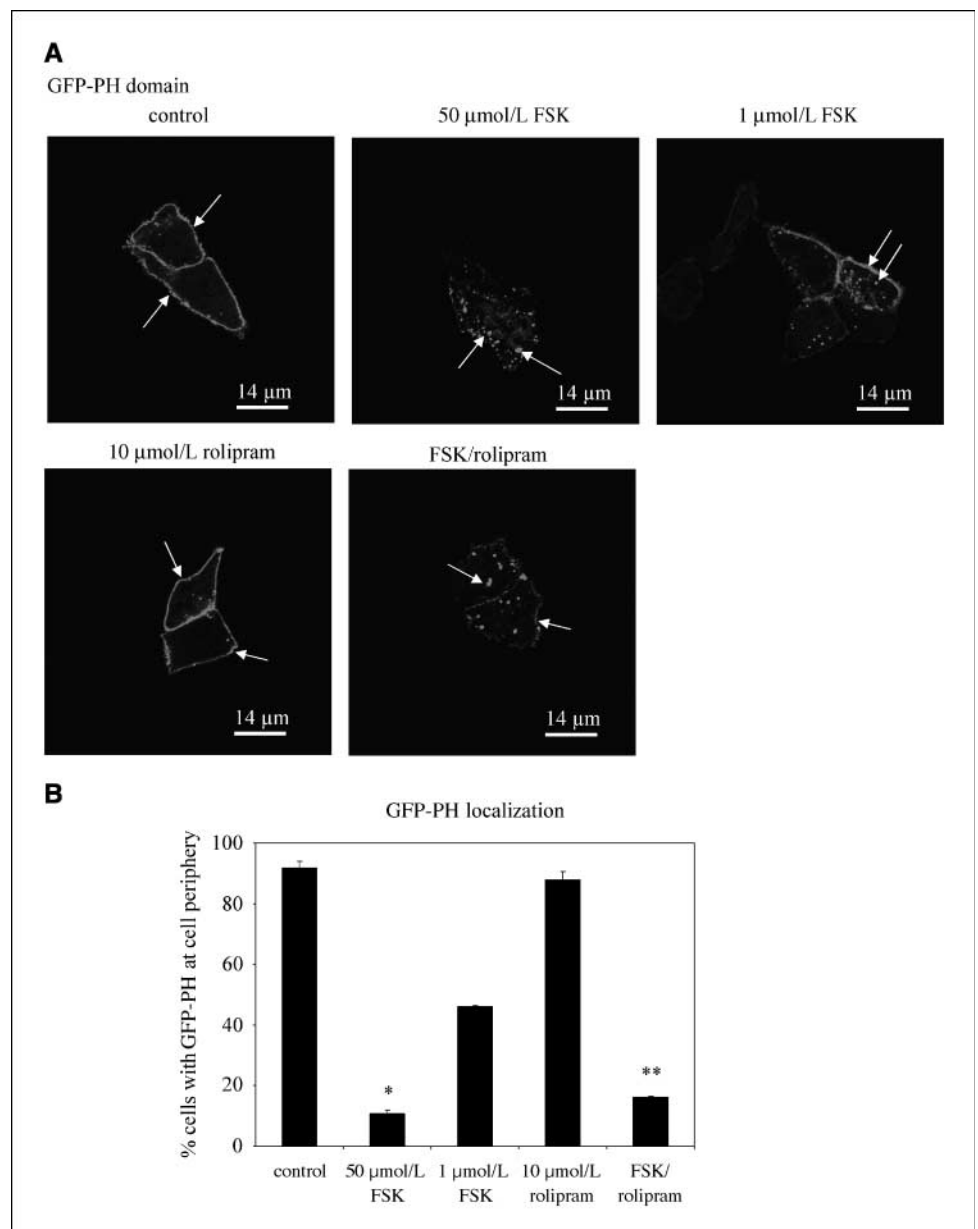
of phosphatidylinositol 3,4,5-trisphosphate (PIP₃) localization; ref. 22] was displaced from its normal membrane localization in cells treated with either high-dose forskolin ($P < 0.05$, compared with control) or the low-dose forskolin/rolipram combination ($P < 0.05$, compared with 1 $\mu\text{mol/L}$ forskolin alone), but not with rolipram alone ($P > 0.09$; Fig. 4A, quantified in Fig. 4B). We saw similar displacement of the membrane-proximal location of the PI3K regulatory subunit p85 α on treatment with forskolin or the lower-dose forskolin/rolipram combination (data not shown). These data indicate that under growth inhibitory cAMP-elevating conditions, there was loss of membrane-associated PI3K and PIP₃. In addition, low-dose forskolin/rolipram combination treatment

led to a rapid dephosphorylation of the PI3K/PIP₃-regulated protein kinase Akt/protein kinase B (PKB) at Ser⁴⁷³ (Fig. 5A). Moreover, although the biological effects of cAMP-elevating agents were long term and sustained, suppression of Akt/PKB phosphorylation was evident between 5 and 10 min after drug addition (Fig. 5A). Decreased phosphorylation of Akt/PKB, at both Ser⁴⁷³ and Thr³⁰⁸, which are known to regulate Akt/PKB activity (27), correlated with cell death induced by high-dose forskolin or the low-dose forskolin/rolipram combination (Fig. 5B). We confirmed the implied necessity for the PI3K/Akt pathway for continued proliferation and survival of KM12C cells by showing that the PI3K inhibitory drug LY294002 recapitulated the growth inhibitory effects induced by forskolin or the low-dose forskolin/rolipram combination (Fig. 5C). Indeed, more detailed analysis indicated that 20 $\mu\text{mol/L}$ LY294002 caused G₁ arrest, with <20% of cells still incorporating BrdUrd (Supplementary Fig. S1A, quantified in Fig. 5D), and also resulted in

accumulation of cells with sub-2n DNA content when compared with DMSO-treated controls (Supplementary Fig. S1B). In keeping with a similar mechanism of action, LY294002 also induced p27^{KIP1}, inhibited pRb phosphorylation, and reduced the expression of cyclins A, B1, and E and CDK1, effects that were similar to the forskolin/rolipram combination (Supplementary Fig. S2). These data show that PI3K membrane localization and phosphorylation of Akt/PKB were strongly inhibited by the low-dose forskolin/rolipram combination, and this is almost certainly how these agents induce growth arrest and cell death.

PTEN reexpression suppresses growth at low density and sensitizes KM12C cells to forskolin. To determine whether known oncogenic or tumor suppressor regulators of the PI3K pathway influenced KM12C cell growth, we examined cells in which either PTEN or Src had been modulated by exogenous expression. Src, which positively regulates PI3K (28), is commonly

Figure 4. Forskolin/rolipram perturbs PIP₃ localization. **A**, a GFP-PH-expressing plasmid was transiently transfected into KM12C cells to monitor PIP₃ distribution. Its localization after 3-h treatment with DMSO, 50 $\mu\text{mol/L}$ forskolin, 1 $\mu\text{mol/L}$ forskolin, 10 $\mu\text{mol/L}$ rolipram, or 1 $\mu\text{mol/L}$ forskolin + 10 $\mu\text{mol/L}$ rolipram was visualized by confocal microscopy. Arrows, distribution of the PIP₃ reporter. **B**, quantification of membrane-localized GFP-PH (Akt PH domain) reporter of PIP₃ after treatment with cAMP modulators or DMSO control was carried out by counting 100 transfected cells under each condition. Columns, mean number of cells (in percentage) from three independent experiments; bars, SD. *, $P < 0.05$, compared with control; **, $P < 0.05$, compared with 1 $\mu\text{mol/L}$ forskolin alone.



activated, or overexpressed, in late-stage colon cancer cells (29, 30), whereas PTEN, which acts as a PIP₃ lipid phosphatase to down-regulate the PI3K pathway (19), is frequently lost or mutated (26). We found that overexpressing a constitutively active Src-Y527F mutant did not alter the growth properties of KM12C colon cancer cells (specifically in KM12C/2C4 cells described in ref. 20; data not shown). However, reexpression of PTEN, the expression of which is lost in these cells, slows down growth rate of KM12C/2C4, particularly evident at lower cell densities (Fig. 6B), with accumulation of cells in G₁ (Fig. 6C). Reexpression of PTEN resulted in reduced Akt/PKB phosphorylation to levels found in colon cancer cells that have retained PTEN expression (shown for HT29 cells in Fig. 6A). However, although PTEN-mediated control of the PI3K/Akt pathway was restored, this did not result in complete growth cessation or cell death induced by complete loss of phospho-AKT caused by the PI3K inhibitor LY294002. Together, these data provide support for a critical role for the PI3K pathway in KM12C proliferation, presumably mediated, at least in part, by PTEN loss (Fig. 6A and B). Interestingly, we found that reexpression of PTEN resulted in a 4-fold greater inhibition of cell proliferation in the presence of 1 μmol/L forskolin (or 0.5 μmol/L forskolin; Fig. 6D).

Sensitivity to growth inhibition by cAMP modulation is not restricted to KM12C cells. In considering the potential therapeutic benefit of any new strategy (e.g., the potentiating low-dose combination of cAMP modulators), it is important to test whether the observed effects are not particular to one cell line, in this case KM12C colon cancer cells. We therefore examined a number for their ability to be growth inhibited by the low-dose forskolin/rolipram combination. Of the 11 cancer cell lines tested, 3 of these (KM12C, MCF7, and HT29) were extremely sensitive to forskolin/

rolipram, displaying ~80% inhibition of proliferation (Supplementary Fig. S3A). Another five cell lines (A431, WiDr, RKO, A375, and H630) were partially sensitive, displaying between 40% and 60% inhibition (Supplementary Fig. S3B), whereas three cell lines (Du145, SW480, and SW620) were all insensitive to forskolin/rolipram-induced growth inhibition (Supplementary Fig. S3C). Thus, there is a subset of cancer cells that respond to a greater or lesser extent to the forskolin/rolipram combination (8 of 11 in our study), implying that a significant proportion of cancer cells may be sensitive to this type of growth modulation.

Interestingly, we found that the sensitive cells were also highly sensitive to treatment with LY294002, whereas the forskolin/rolipram-resistant cancer cell lines were relatively insensitive to LY294002 (Supplementary Fig. S3A and C), showing a consistent link between sensitivity to cAMP modulation and PI3K dependence.

Discussion

Cancer cells, despite having many genetic, epigenetic, and chromosomal abnormalities, are often addicted to one or two oncogenic changes for continued proliferation and survival (31). Major therapeutic advances are likely to come from molecular profiling the oncogenic addictions of individual tumors. This would in turn allow tailored therapy to be more widely applied. There are now a number of spectacular examples of agents that attack critical molecular events having therapeutic benefit. For example, in non-small-cell lung cancer, a subset of patients with activating mutations in the kinase domain of the epidermal growth factor receptor (EGFR) exhibit impressive clinical responses to the EGFR inhibitor gefitinib (32). In this case, oncogene addiction is a result

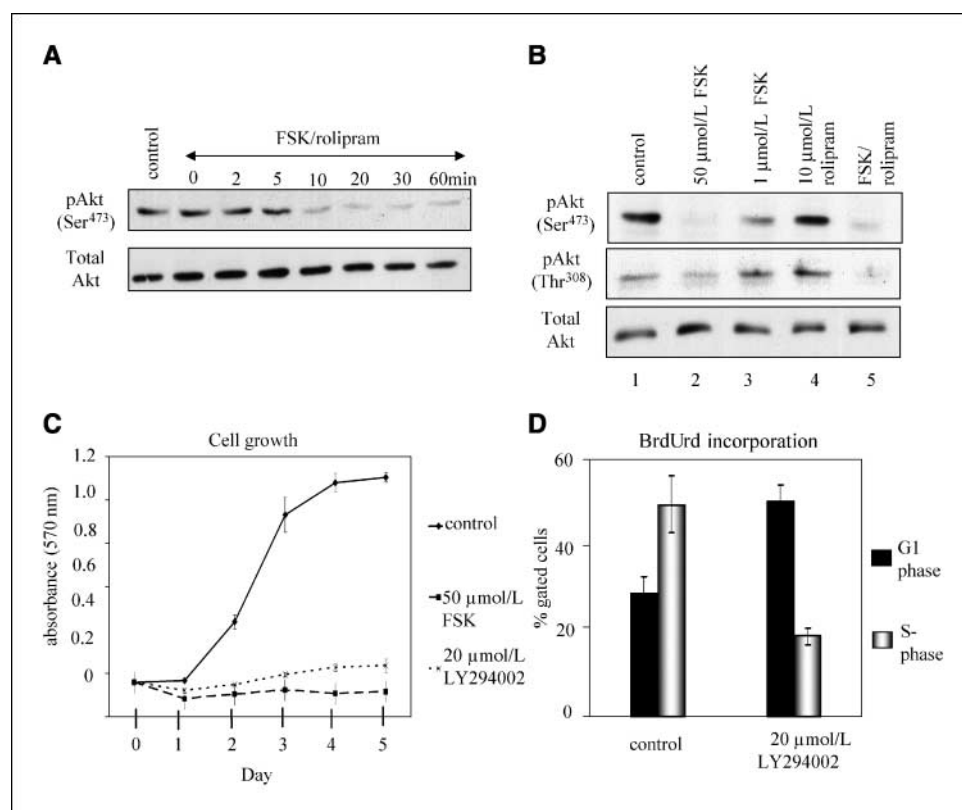


Figure 5. Forskolin/rolipram synergy causes loss of Akt/PKB phosphorylation. **A**, phosphorylated Akt (pAkt) was monitored by Western blot of lysates prepared from cells treated for various times up to 60 min and compared with total Akt. **B**, KM12C cells were treated continuously for 24 h with DMSO, 50 μmol/L forskolin, 1 μmol/L forskolin, 10 μmol/L rolipram, and 1 μmol/L forskolin + 10 μmol/L rolipram. Phospho-Akt (Ser⁴⁷³) (top) and phospho-Akt (Thr³⁰⁸) (middle) status was monitored by immunoblotting with phospho-specific antibodies and total Akt (bottom) was compared as a loading control. High forskolin and the low forskolin/rolipram combination (lanes 2 and 5, respectively) resulted in loss of phospho-Akt (at both Ser⁴⁷³ and Thr³⁰⁸). **C**, proliferation of KM12C cells was monitored by MTT assay over a 5-d period in the presence of DMSO, 50 μmol/L forskolin, or 20 μmol/L LY294002. Points, mean of three independent experiments; bars, SD. **D**, quantification of BrdUrd incorporation after 24 h of LY294002 treatment resulting in a partial G₁-S phase block.

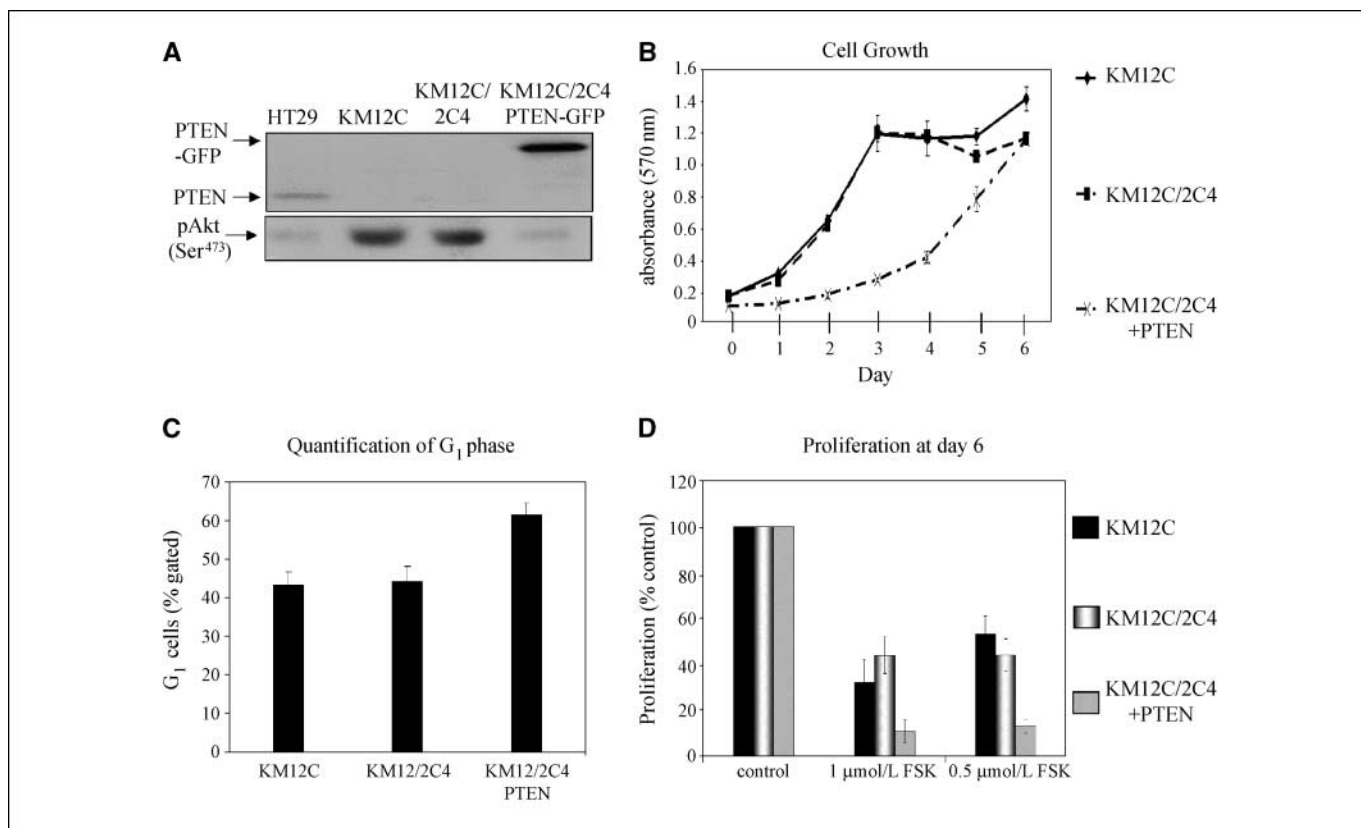


Figure 6. Exogenous expression of PTEN slows KM12C growth rate and sensitizes to forskolin/rolipram. Cells were plated at low density (5×10^5 in 60-mm² dish) for analysis. **A**, KM12C cells do not express PTEN and reintroduction restores lower phospho-Akt (Ser⁴⁷³) levels. Expression of endogenous PTEN in HT29 colon cancer cells and PTEN-GFP in KM12C/2C4 (top) correlates with reduced phospho-Akt (pAkt; Ser⁴⁷³), whereas lack of PTEN in KM12C and KM12C/2C4 cells correlates with increased phospho-Akt. Immunoblots were carried out with the specific PTEN and Akt antibodies as probes. **B**, reintroduction of PTEN affects low-density growth of KM12C cells. Proliferation of KM12C, KM12C/2C4, and KM12C/2C4 PTEN-GFP cells was monitored with an MTT assay over a 6-d period. **C**, PTEN increases percentage of cells in G₁ phase. Propidium iodide analysis of KM12C, KM12C/2C4, and KM12C/2C4-PTEN-GFP was carried out and the percentage of cells in G₁ calculated as described earlier. **D**, PTEN sensitizes cells to low concentrations of forskolin. Proliferation of KM12C, KM12C/2C4, and KM12C/2C4 PTEN-GFP cells in the presence of DMSO and 1 and 0.5 μmol/L forskolin was monitored over a 6-d period and the percentage proliferation of control (DMSO) at day 6 was calculated. Columns, mean of three independent experiments; bars, SD.

of mutation, not simply overexpression or inappropriate cellular activation, and it is thought that addiction may be mediated by constitutive activation of the prosurvival Akt/PKB pathway downstream of activated EGFR (33). Other clear examples of clinical benefit arising from the targeting of critical oncogenes come from treatment of breast cancers, in which the HER2 receptor tyrosine kinase is overexpressed, with the monoclonal antibody trastuzumab (Herceptin; ref. 34) and the use of imatinib (Gleevec) to treat chronic myeloid leukemia and gastrointestinal stromal tumors that are driven by the oncogenic BCR-Abl and c-Kit proteins, respectively (35). It is likely that identification of tumor oncogene addiction will thus provide a key part of delivering effective cancer treatments in the future.

Here, we establish for the first time that KM12C colon cancer cells, which are resistant to cell death induced by DNA-damaging or other cytotoxic agents commonly used to treat colorectal cancers,⁴ are critically dependent on the PI3K pathway for their continued proliferation and survival. The PI3K pathway is frequently deregulated in cancer through a variety of mechanisms, including PTEN loss (reviewed in ref. 36), as in KM12C cells, or activating mutations in PI3K α (37). One consequence of such mutations is activation of downstream effectors, including Akt/PKB and mammalian target of rapamycin (reviewed in ref. 38),

which promote proliferation and cell survival. In cancer cells, such as KM12C, which are addicted to the PI3K pathway, there is an urgent need to devise effective, yet relatively nontoxic, ways to inhibit tumor cell growth and survival. In this regard, inhibitors of PI3K have been developed with against various classes of PI3K (39), although these drugs are not particularly specific (40). Although there is optimism that ongoing efforts will lead to selective isoform-specific PI3K inhibitors as therapeutic agents, these are neither readily available nor at an advanced stage of clinical development (41).

Whereas reexpression of PTEN reduces phosphorylation of Akt/PKB and causes slowed proliferation at low density (Fig. 6), it does not recapitulate complete growth cessation and cell death induced by the PI3K inhibitor LY294002 (Fig. 5C and D and Supplementary Fig. S2). This implies that although loss of PTEN is a contributing factor to the apparent dependence of KM12C cells on PI3K, other mechanisms may also operate. Intriguingly, we show here that KM12C cells can also be efficiently growth arrested and killed by a low-dose combination of the adenylyl cyclase activator forskolin and the PDE4-selective inhibitor rolipram (Figs. 1, 2D, and 3), but not by forskolin and the PDE3-selective inhibitor cilostamide. Such selectivity is consistent with the now well-established notion that cAMP signaling is compartmentalized in cells, with PDE3 and

PDE4 activities contributing to distinct functional compartments (6, 7, 9).

In evaluating the mechanism of action of forskolin/rolipram on these cells, we found induced rapid and sustained inhibition of the PI3K pathway, as judged by displacement of a GFP-PH domain (Akt PH) protein (reporting PIP₃; Fig. 4), and inhibition of Akt/PKB phosphorylation on both Ser⁴⁷³ and Thr³⁰⁸ residues. Although we do not yet know the precise mechanism by which specific cAMP pools are mediating PIP₃ displacement, it is noteworthy that PKA has been shown to phosphorylate p85 α on Ser⁸³ and that this contributes to PKA-induced growth arrest (42). cAMP can also block the membrane localization of PDK1, an upstream activator of Akt/PKB (43). The forskolin/rolipram-induced inhibition of the PI3K pathway shown here is associated with clear changes in cell cycle regulators, including reduced Skp2, which is linked to induction of p27^{KIP1}, together with the dephosphorylation and reduced expression of pRb, cyclins A, B1, and E, and CDK1 (Fig. 2A–C). Such key changes, commonly associated with negative regulation of progression through the G₁ phase of the cell cycle (17, 44), are consistent with the observed accumulation of cells in G₁ (Fig. 2D). In addition, whereas low-dose forskolin (1 μ mol/L) can, by itself, induce a partial G₁ arrest (Fig. 2D), the coapplication of rolipram (10 μ mol/L), which has no effect on its own, potentiates the effects of low-dose forskolin to cause growth-arrested cells to undergo apoptosis (Fig. 3). Taken together, these data imply that whereas submaximal stimulation of adenylyl cyclase in KM12C colon cancer cells is sufficient to cause a partial growth arrest, it also primes cells for cell death on further elevation of cAMP in subcellular compartments that are specifically controlled by PDE4 rather than PDE3. This offers a unique opportunity for therapeutic exploitation. Whereas both PDE3 inhibitors and high-dose colforsin daropate, a water-soluble forskolin derivative, exert potent positive inotropic effects on heart, no such actions are evident using PDE4-selective inhibitors (45), which is consistent with PDE3 and PDE4 controlling distinct intracellular compartments also in cardiac myocytes (6, 9). Consistent with this, PDE4-selective inhibitors, which have undergone clinical trials for treating inflammatory lung disease, have shown no inotropic or chronotropic effects on cardiac function (10, 45). Thus, a combination therapy of low-dose forskolin coupled with a PDE4 inhibitor may provide a novel means of treating various colon cancers without associated cardiac toxicity.

We have here discovered a novel way of inhibiting the PI3K pathway by a synergistic combination of relatively low doses of cAMP modulators. Our data suggest that we have found another Achilles heel for these chemoresistant cancer cells: that these cells also critically require PDE4 activity, presumably during the normal adenylyl cyclase/PDE cycle that controls cAMP production and degradation in a localized manner. Thus, PDE4 inhibition, under conditions when adenylyl cyclase activity is stimulated endogenously, results in the death of these colon cancer cells, which display chemoresistance that is extremely hard to overcome. Such

a novel addiction to maintenance of low levels of cAMP in the appropriate subcellular locations, via PDE4 activity, is required to maintain signaling through the PI3K/Akt pathway. This, as we show here, is needed for the proliferation and survival of KM12C cells. It is interesting that by bringing it back under the normal regulatory control exerted by PTEN, the PI3K/Akt pathway acts to sensitize the cells to complete growth cessation and death induced by cAMP modulation, as shown by the enhanced responses to low doses of forskolin that do not normally kill these cells (Fig. 6).

To evaluate the generality of our discovery, we probed a number of cancer cells with forskolin/rolipram combinations. In doing this, we found that 8 of 11 of such cell lines were growth inhibited by the forskolin/rolipram combination to a greater or lesser extent (Supplementary Fig. S3). In particular, three of these cell lines were extremely sensitive to growth inhibition by forskolin/rolipram, suggesting that a significant number of cancer cells may be addicted to the need to maintain low levels of cAMP in the compartment regulated by PDE4. These data raise the exciting possibility that relatively low-dose combinations of (a) pharmacologic agonists that could prime adenylyl cyclase and (b) PDE4 inhibitors, which are undergoing clinical testing in other disease contexts, may have therapeutic benefit in treating advanced colon cancers that are refractory to existing cytotoxic therapies.

In summary, misregulation of signaling proteins occurs in many cancers, leading to distorted circuitry and the establishment of oncogene addiction to one or more signal transduction pathways. It is becoming clear that the identification of such addictions can provide therapeutic opportunities, and so understanding the molecular events driving oncogene addiction, and hence tumor cell proliferation and survival, is becoming increasingly important. Here, we identify for the first time two “addictions” of chemoresistant cancer cells. Both of these addictions are required for maintenance of cell proliferation and survival (i.e., activation of the PI3K pathway and the need to maintain low cAMP levels in compartments regulated by PDE4, which itself mediates effects on the PI3K/Akt pathway). We have therefore identified a key point of cross-regulation of two major second messenger-regulated pathways in these cells, those controlled by cAMP and PIP₃, which are critical for cancer cell viability. This raises the exciting possibility that the adenylyl cyclase/PDE4 axis may be exploited for therapeutic benefit.

Acknowledgments

Received 1/15/2007; revised 3/19/2007; accepted 4/5/2007.

Grant support: Cancer Research UK studentship (D.G. McEwan), Cancer Research UK Beatson Institute Core Grant (M.C. Frame and V.G. Brunton), and the Medical Research Council (M.D. Houslay and G.S. Baillie).

The costs of publication of this article were defrayed in part by the payment of page charges. This article must therefore be hereby marked *advertisement* in accordance with 18 U.S.C. Section 1734 solely to indicate this fact.

We wish to thank David Gillespie for advice on cell cycle analysis and Owen Sansom for advice on statistics.

References

- Folprecht G, Kohne CH. The role of new agents in the treatment of colorectal cancer. *Oncology* 2004;66:1–17.
- Morikawa K, Walker SM, Jessup JM, Fidler IJ. *In vivo* selection of highly metastatic cells from surgical specimens of different primary human colon carcinomas implanted into nude mice. *Cancer Res* 1988;48:1943–8.
- Beavo JA, Brunton LL. Cyclic nucleotide research—still expanding after half a century. *Nat Rev Mol Cell Biol* 2002;3:710–8.
- Taylor SS, Yang J, Wu J, Haste NM, Radzio-Andzelm E, Anand G. PKA: a portrait of protein kinase dynamics. *Biochim Biophys Acta* 2004;1697:259–69.
- Bos JL. Epac: a new cAMP target and new avenues in cAMP research. *Nat Rev Mol Cell Biol* 2003;4:733–8.

6. Baillie GS, Scott JD, Houslay MD. Compartmentalisation of phosphodiesterases and protein kinase A: opposites attract. *FEBS Lett* 2005;579:3264–70.
7. Houslay MD, Adams DR. PDE4 cAMP phosphodiesterases: modular enzymes that orchestrate signalling cross-talk, desensitization and compartmentalization. *Biochem J* 2003;370:1–18.
8. Conti M, Jin SL. The molecular biology of cyclic nucleotide phosphodiesterases. *Prog Nucleic Acid Res Mol Biol* 1999;63:1–38.
9. Mongillo M, McSorley T, Evellin S, et al. Fluorescence resonance energy transfer-based analysis of cAMP dynamics in live neonatal rat cardiac myocytes reveals distinct functions of compartmentalized phosphodiesterases. *Circ Res* 2004;95:67–75.
10. Houslay MD, Schafer P, Zhang KY. Keynote review: phosphodiesterase-4 as a therapeutic target. *Drug Discov Today* 2005;10:1503–19.
11. Lerner A, Epstein PM. Cyclic nucleotide phosphodiesterases as targets for treatment of hematological malignancies. *Biochem J* 2006;393:21–41.
12. Manganiello VC, Taira M, Degerman E, Belfrage P. Type III cGMP-inhibited cyclic nucleotide phosphodiesterases (PDE3 gene family). *Cell Signal* 1995;7:445–55.
13. Murata K, Sudo T, Kameyama M, et al. Cyclic AMP specific phosphodiesterase activity and colon cancer cell motility. *Clin Exp Metastasis* 2000;18:599–604.
14. Kim DH, Lerner A. Type 4 cyclic adenosine monophosphate phosphodiesterase as a therapeutic target in chronic lymphocytic leukemia. *Blood* 1998;92:2484–94.
15. Chen TC, Wadsten P, Su S, et al. The type IV phosphodiesterase inhibitor rolipram induces expression of the cell cycle inhibitors p21(Cip1) and p27(Kip1), resulting in growth inhibition, increased differentiation, and subsequent apoptosis of malignant A-172 glioma cells. *Cancer Biol Ther* 2002;1:268–76.
16. Cooper DM. Regulation and organization of adenylate cyclases and cAMP. *Biochem J* 2003;375:517–29.
17. Naderi S, Wang JY, Chen TT, Gutzkow KB, Blomhoff HK. cAMP-mediated inhibition of DNA replication and S phase progression: involvement of Rb, p21Cip1, and PCNA. *Mol Biol Cell* 2005;16:1527–42.
18. Sansal I, Sellers WR. The biology and clinical relevance of the PTEN tumor suppressor pathway. *J Clin Oncol* 2004;22:2954–63.
19. Stambolic V, Suzuki A, de la Pompa JL, et al. Negative regulation of PKB/Akt-dependent cell survival by the tumor suppressor PTEN. *Cell* 1998;95:29–39.
20. Jones RJ, Avizienyte E, Wyke AW, Owens DW, Brunton VG, Frame MC. Elevated c-Src is linked to altered cell-matrix adhesion rather than proliferation in KM12C human colorectal cancer cells. *Br J Cancer* 2002;87:1128–35.
21. Mosmann T. Rapid colorimetric assay for cellular growth and survival: application to proliferation and cytotoxicity assays. *J Immunol Methods* 1983;65:55–63.
22. Gray A, Van Der Kaay J, Downes CP. The pleckstrin homology domains of protein kinase B and GRP1 (general receptor for phosphoinositides-1) are sensitive and selective probes for the cellular detection of phosphatidylinositol 3,4-bisphosphate and/or phosphatidylinositol 3,4,5-trisphosphate *in vivo*. *Biochem J* 1999;344:929–36.
23. Marchmont RJ, Houslay MD. A peripheral and an intrinsic enzyme constitute the cyclic AMP phosphodiesterase activity of rat liver plasma membranes. *Biochem J* 1980;187:381–92.
24. Thompson WJ, Appleman MM. Multiple cyclic nucleotide phosphodiesterase activities from rat brain. *Biochemistry* 1971;10:311–6.
25. Pagano M. Control of DNA synthesis and mitosis by the Skp2-27-Cdk1/2 axis. *Mol Cell* 2004;14:414–6.
26. Vivanco I, Sawyers CL. The phosphatidylinositol 3-Kinase AKT pathway in human cancer. *Nat Rev Cancer* 2002;2:489–501.
27. Alessi DR, Andjelkovic M, Caudwell B, et al. Mechanism of activation of protein kinase B by insulin and IGF-1. *EMBO J* 1996;15:6541–51.
28. Jones RJ, Brunton VG, Frame MC. Adhesion-linked kinases in cancer; emphasis on src, focal adhesion kinase and PI 3-kinase. *Eur J Cancer* 2000;36:1595–606.
29. Bolen JB, Veillette A, Schwartz AM, Deseau V, Rosen N. Analysis of pp60c-src in human colon carcinoma and normal human colon mucosal cells. *Oncogene Res* 1987;1:149–68.
30. Cartwright CA, Coad CA, Egbert BM. Elevated c-Src tyrosine kinase activity in premalignant epithelia of ulcerative colitis. *J Clin Invest* 1994;93:509–15.
31. Weinstein IB. Cancer. Addiction to oncogenes—the Achilles heel of cancer. *Science* 2002;297:63–4.
32. Lynch TJ, Bell DW, Sordella R, et al. Activating mutations in the epidermal growth factor receptor underlying responsiveness of non-small-cell lung cancer to gefitinib. *N Engl J Med* 2004;350:2129–39.
33. Sordella R, Bell DW, Haber DA, Settleman J. Gefitinib-sensitizing EGFR mutations in lung cancer activate anti-apoptotic pathways. *Science* 2004;305:1163–7.
34. Slamon DJ, Leyland-Jones B, Shak S, et al. Use of chemotherapy plus a monoclonal antibody against HER2 for metastatic breast cancer that overexpresses HER2. *N Engl J Med* 2001;344:783–92.
35. Hughes TP, Kaeda J, Branford S, et al. Frequency of major molecular responses to imatinib or interferon- α plus cytarabine in newly diagnosed chronic myeloid leukemia. *N Engl J Med* 2003;349:1423–32.
36. Ali IU, Schriml LM, Dean M. Mutational spectra of PTEN/MMAC1 gene: a tumor suppressor with lipid phosphatase activity. *J Natl Cancer Inst* 1999;91:1922–32.
37. Bader AG, Kang S, Zhao L, Vogt PK. Oncogenic PI3K deregulates transcription and translation. *Nat Rev Cancer* 2005;5:921–9.
38. Choo AY, Blenis J. TORgeting oncogene addiction for cancer therapy. *Cancer Cell* 2006;9:77–9.
39. Knight ZA, Gonzalez B, Feldman ME, et al. A pharmacological map of the PI3-K family defines a role for p110 α in insulin signaling. *Cell* 2006;125:733–47.
40. Jacobs MD, Black J, Futer O, et al. Pim-1 ligand-bound structures reveal the mechanism of serine/threonine kinase inhibition by LY294002. *J Biol Chem* 2005;280:13728–34.
41. Ward SG and Finan P. Isoform-specific phosphoinositide 3-kinase inhibitors as therapeutic agents. *Curr Opin Pharmacol* 2003;3:426–34.
42. Cosentino C, Di Domenico M, Porcellini A, et al. p85 regulatory subunit of PI3K mediates cAMP-PKA and estrogens biological effects on growth and survival. *Oncogene* 2007;26:2095–103.
43. Kim S, Jee K, Kim D, Koh H, Chung J. Cyclic AMP inhibits Akt activity by blocking the membrane localization of PDK1. *J Biol Chem* 2001;276:12864–70.
44. Liang J, Slingerland JM. Multiple roles of the PI3K/PKB (Akt) pathway in cell cycle progression. *Cell Cycle* 2003;2:339–45.
45. Boswell-Smith V, Spina D, Page CP. Phosphodiesterase inhibitors. *Br J Pharmacol* 2006;147:S252–7.

Other publications

E. Sandilands, S. Akbazardeh, A. Vechionne, **D.G. McEwan**, M.C. Frame and J.K. Heath. Src kinase modulates the activation, trafficking and signalling dynamics of Fibroblast Growth Factor Receptors (EMBO Reports *in press*).

O. Tymchyshyn, S. Akbazardeh, **D.McEwan**, G.Norman, J.K Heath and M.Z. Kwiatkowska. Computational reasoning applied to FGF pathway: simulation, analysis and experimental validation. (Molecular Systems Biology, *under review*)

Src kinase modulates the activation, transport and signalling dynamics of fibroblast growth factor receptors

Emma Sandilands¹, Shiva Akbarzadeh², Anna Vecchione², David G. McEwan¹, Margaret C. Frame¹ & John K. Heath²⁺

¹Cancer Research UK Beatson Institute for Cancer Research, Glasgow, UK, and ²Cancer Research UK Growth Factor Group, School of Biosciences, University of Birmingham, Edgbaston, Birmingham, UK

The non-receptor tyrosine kinase Src is recruited to activated fibroblast growth factor receptor (FGFR) complexes through the adaptor protein factor receptor substrate 2 (FRS2). Here, we show that Src kinase activity has a crucial role in the regulation of FGFR1 signalling dynamics. Following receptor activation by ligand binding, activated Src is colocalized with activated FGFR1 at the plasma membrane. This localization requires both active Src and FGFR1 kinases, which are inter-dependent. Internalization of activated FGFR1 is associated with release from complexes containing activated Src. Src-mediated transport and subsequent activation of FGFR1 require both RhoB endosomes and an intact actin cytoskeleton. Chemical and genetic inhibition studies showed strikingly different requirements for Src family kinases in FGFR1-mediated signalling; activation of the phosphoinositide-3 kinase–Akt pathway is severely attenuated, whereas activation of the extracellular signal-regulated kinase pathway is delayed in its initial phase and fails to attenuate.

Keywords: Src; FGFR; phosphorylation; RhoB; actin

EMBO reports (2007) 8, 1162–1169. doi:10.1038/sj.embor.7401097

INTRODUCTION

The dynamics of signal propagation by receptor tyrosine kinases (RTKs) has a crucial role in cellular responses to ligands (Marshall, 1995). Mutations in fibroblast growth factor receptors (FGFRs), which slow ligand dissociation rates and extend signal duration, lead to phenotypic effects in skeletal development (Wilkie *et al*, 1995; Hajihosseini *et al*, 2004) and act as ‘driver’ mutations in various types of common tumour (Greenman *et al*, 2007). RTKs

are activated by ligand-mediated receptor homo- or heterodimerization (Schlessinger 2000; Pellegrini *et al*, 2000; Furdui *et al*, 2006); however, there is evidence that receptor activation might occur indirectly or be modified by recruitment and activation of other tyrosine kinases (Halford & Stacker, 2001). In the case of FGFR, Src kinase is recruited, by receptor-mediated phosphorylation, to the adaptor protein factor receptor substrate 2 (FRS2), influencing signalling dynamics by phosphorylation of the attenuator Sprouty (Li *et al*, 2004).

This finding prompted further analysis of the relationship between Src activity, FGFR1 activation and downstream signalling. As Src regulates endosomal transport of tyrosine kinases, including Src itself, through RhoB- and Rab11-containing endosomes (Sandilands *et al*, 2004), we reasoned that Src activation might have a role in FGFR activation through a directed transport mechanism. By using phospho-specific antibodies and Src inhibition, we show that Src activity, through a RhoB and actin-dependant pathway, controls FGFR activation and transport to and from the plasma membrane, and has both positive and negative roles in the activation and termination of FGFR signalling.

RESULTS AND DISCUSSION

Localization of activated FGFR and Src

Previous biochemical studies have shown that, following FGF2 stimulation, Src is recruited to FRS2 in a kinase-dependant manner, but the cellular location of this co-recruitment is unknown (Li *et al*, 2004). In the first set of experiments, phospho-specific antibodies directed against FGFR1/2-Tyr463 (characterized in supplementary Fig 1 online) and the activated form of Src were used to define the spatial relationship between Src localization, and Src and FGFR activation.

Mouse embryo fibroblasts (MEFs) were stimulated with FGF2, and endogenous FGFR1 and activated FGFR were detected at the plasma membrane and in endosomal vesicles throughout the cytoplasm (Fig 1A, upper left panels). In Src/Fyn/Yes^{-/-} (SYF) MEFs, endogenous FGFR1 was also detected at the plasma membrane and in endosomes; however, a lower basal level of

¹Cancer Research UK Beatson Institute for Cancer Research, Garscube Estate, Switchback Road, Glasgow G61 1BD, UK

²Cancer Research UK Growth Factor Group, School of Biosciences, University of Birmingham, Edgbaston, Birmingham B125 2TT, UK

+Corresponding author. Tel: +44 (0) 121 414 7533; Fax: +44 (0) 121 414 5925; E-mail: j.k.heath@bhm.ac.uk

Received 16 May 2007; revised 14 September 2007; accepted 19 September 2007; published online 2 November 2007

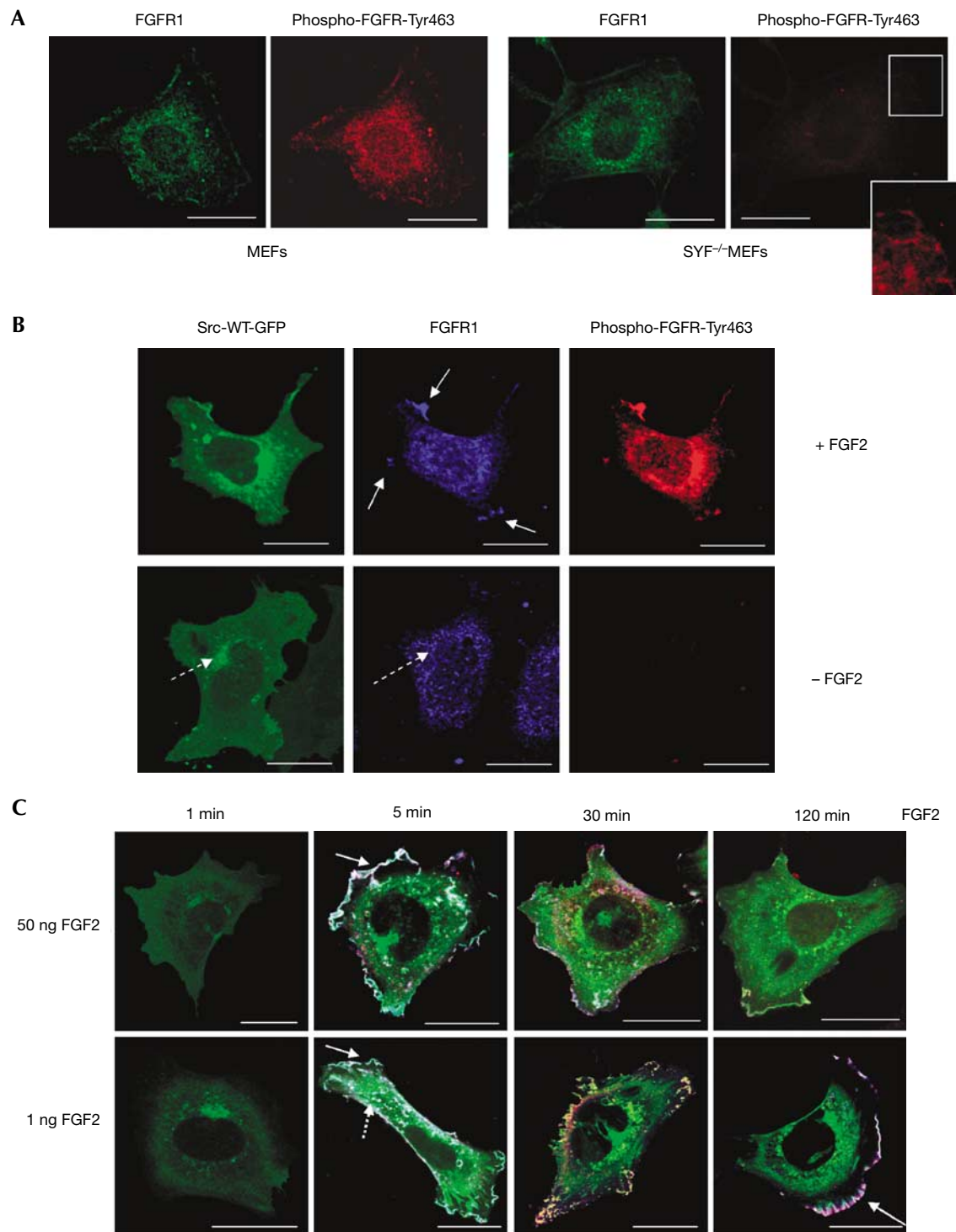


Fig 1 | FGF2 induces co-recruitment of active Src and active FGFR to the plasma membrane. (A) MEFs or SYF^{-/-}MEFs were maintained in serum-free media and then stimulated with FGF2 (50 ng/ml⁻¹) for 30 min. SYF^{-/-}MEFs expressing Src-WT-GFP were maintained in serum-free media overnight and then stimulated with FGF2 at (B) 50 ng/ml⁻¹ for 30 min or (C) 1 ng/ml⁻¹ and 50 ng/ml⁻¹ for 1, 5, 30 or 120 min. Total FGFR1 was detected with an FGFR1 antibody and active proteins were detected using anti-phospho-FGFR-Tyr463 or anti-phospho-Src-Tyr416. Solid arrows indicate protein localized to the plasma membrane, dashed arrows indicate protein maintained in the perinuclear region and dotted arrows show endosomes. Green, blue and red colours represent Src, phospho-Src-Tyr416 and phospho-FGFR-Tyr463, respectively. Scale bars, 25 µM. FGFR, fibroblast growth factor receptor; GFP, green fluorescent protein; MEF, mouse embryonic fibroblast; SYF^{-/-}MEF, Src/Yes/Fyn-deficient MEF; WT, wild type.

FGFR activation was detected in endosome-like structures in the perinuclear region of cells. On closer inspection, we also found that there was a trace of active FGFR at the plasma membrane (Fig 1A, upper right panels). When SYF^{-/-}MEFs were reconstituted with Src-WT-GFP (Sandilands *et al*, 2004), there was a substantial increase in the intensity of staining of activated FGFR, both at the plasma membrane and in endosomal structures (Fig 1B, upper panels). These findings show that Src protein is required for enhanced activation of FGFR at the plasma membrane in FGF2-stimulated cells, and that in the absence of Src, there is only a minor pool of Src-independent activated FGFR constitutively localized at the plasma membrane. This implies that FGF2 ligand stimulates an 'amplification' of active FGFR at the plasma membrane.

In the absence of FGF2 stimulation, Src-WT-GFP was localized in a cytoplasmic and tight perinuclear position, and no remarkable reactivity with anti-phospho-Src-Tyr416 or anti-phospho-FGFR-Tyr463 was observed, indicating that neither protein is activated under unstimulated conditions (Fig 1B; supplementary Fig 2 online). This experiment indicates that activity, and not simply overexpression of Src, is linked to the enhanced activation of FGFR at the plasma membrane. Furthermore, in unstimulated cells, total FGFR1 was retained in the cytoplasm in most of the cells (Fig 1B, lower panels), until stimulation with FGF2 when total FGFR1 was readily detected at the plasma membrane (Fig 1B, upper panels).

When SYF^{-/-}MEFs expressing Src-WT-GFP were stimulated for varying time durations with two different concentrations of FGF2, the location of Src-WT-GFP, activated Src and activated FGFR was visualized (Fig 1C). The results showed that, following FGF2 stimulation, there was a rapid (5 min) and prominent accumulation of both active Src and active FGFR at the plasma membrane. At higher concentrations of FGF2 (50 ng/ml), this localization and phospho-specific staining decayed over the following 120 min—implying receptor degradation. At low concentration (1 ng/ml), the colocalization of active Src and FGFR in the peripheral membrane location persisted for longer—for the duration of the time course (Fig 1C, solid arrows). At early time points, active Src and active FGFR were also observed in cytoplasmic vesicular structures (Fig 1C, dotted arrows). This colocalization occurred only in a sub-fraction of total cellular Src, as a significant proportion of Src-WT-GFP (Fig 1C, left panel) remained in a cytoplasmic and perinuclear location following stimulation, which is similar to the findings of Sandilands *et al* (2004). Thus, only a small proportion of Src is activated in a very tightly spatially regulated manner in response to FGF2 stimulation and what is activated is co-recruited with activated FGFR to the plasma membrane.

Together, these results show that FGF2 stimulation results in the co-activation of Src and FGFR and in the co-recruitment of the activated kinases to the peripheral plasma membrane, most likely through cytoplasmic endosomes. The peripheral signals derived from FGF2 decay in a manner that is inversely related to the concentration of FGF2 used. These findings raise the question of the mechanism of Src dependency of FGFR kinase activation at the plasma membrane.

The role of Src kinase activity in FGFR activation

SYF^{-/-}MEFs were reconstituted with either a dominant-negative kinase-deficient Src-251-GFP or a constitutively active Src-Tyr527Phe-GFP (Timpson *et al*, 2001; Sandilands *et al*, 2004). In the absence of functional Src kinase, FGF2 stimulation

failed to activate peripheral FGFR kinase activity, as determined by anti-phospho-FGFR staining (Fig 2A, upper panels). In the presence of constitutively active Src, FGFR was obviously phosphorylated (Fig 2A, lower panels) at peripheral membrane structures in a ligand-independent manner. One characteristic of these observations, as reported previously, is the localization of constitutively active Src in sub-membrane aggregates containing focal adhesion proteins (Avizienyte *et al*, 2002), whereas activated FGFR is correctly located in the peripheral membrane. These data imply that constitutively activated Src drives activated FGFR to its peripheral membrane sites of activity, even in the absence of ligand.

We also confirmed the requirement for Src kinase activation in FGFR activation by treating SYF^{-/-}MEFs expressing Src-WT-GFP with the selective Src inhibitor dasatinib (Lombardo *et al*, 2004; Serrels *et al*, 2006) before stimulation with FGF2. These results show that inhibition of Src kinase in the presence of FGF2 suppresses phosphorylation of both Src and FGFR, but does not prevent the translocation of Src-WT-GFP to the cell membrane (Fig 2B). Interestingly, the peripheral targeting of the low level of basal FGFR detected in cells at high laser intensities is also uninhibited (Fig 2B, right panel). By using a high-intensity CCD camera under fixed laser settings, images were captured that allowed quantification of the intensity of phospho-FGFR staining at the plasma membrane in the presence of Src-WT-GFP (Fig 2C). The results of this analysis showed that the active FGFR signal was reduced by approximately 80% in the presence of dasatinib. These findings show that Src is not necessary for the transport of the low basal level of active FGFR present in these cells, whereas it is both necessary and sufficient for 'amplification' of active FGFR at the plasma membrane.

The mechanism of Src and FGFR co-recruitment

We were interested to learn more about the mechanism by which Src is responsible for FGFR activation at the peripheral plasma membrane. When we overexpressed the late endosomal marker RhoB, we found that there was some colocalization with FGFR1 (Fig 3A). There was also a striking colocalization of Src, phospho-FGFR and RhoB in cytoplasmic endosomal structures (Fig 3A, right panel). This implies that activated FGFR might be a passenger in the Src/RhoB-dependent endosome delivery pathway previously described (Sandilands *et al*, 2004). We therefore interrogated the requirement for RhoB in FGFR activation and peripheral membrane localization. RhoB^{-/-}MEFs were stimulated with FGF2 and colocalization of Src, FGFR1 and phospho-FGFR examined (Fig 3B). We observed total FGFR1 at the plasma membrane and in intracellular vesicles in these cells. However, the translocation of Src-WT-GFP was inhibited by RhoB deficiency, as was the increase in phospho-FGFR normally detected in FGF2-stimulated MEFs expressing Src-WT-GFP (Fig 1A). Interestingly, a lack of RhoB also inhibited the transport of the low level of basal phospho-FGFR detected previously (Figs 1A,2C), as no signal was detected at the plasma membrane of RhoB^{-/-} cells (Fig 3B). Thus, peripheral membrane localization of activated FGFR is dependent on the presence of endosomal RhoB protein, and FGFR activation is suppressed in the absence of RhoB.

We have recently shown that RhoB is involved in the transport and activation of Src, using a farnesyl transferase inhibitor (FTI; Sandilands *et al*, 2007). FTIs are a class of biologically active anticancer drugs that inhibit farnesylation of many proteins such

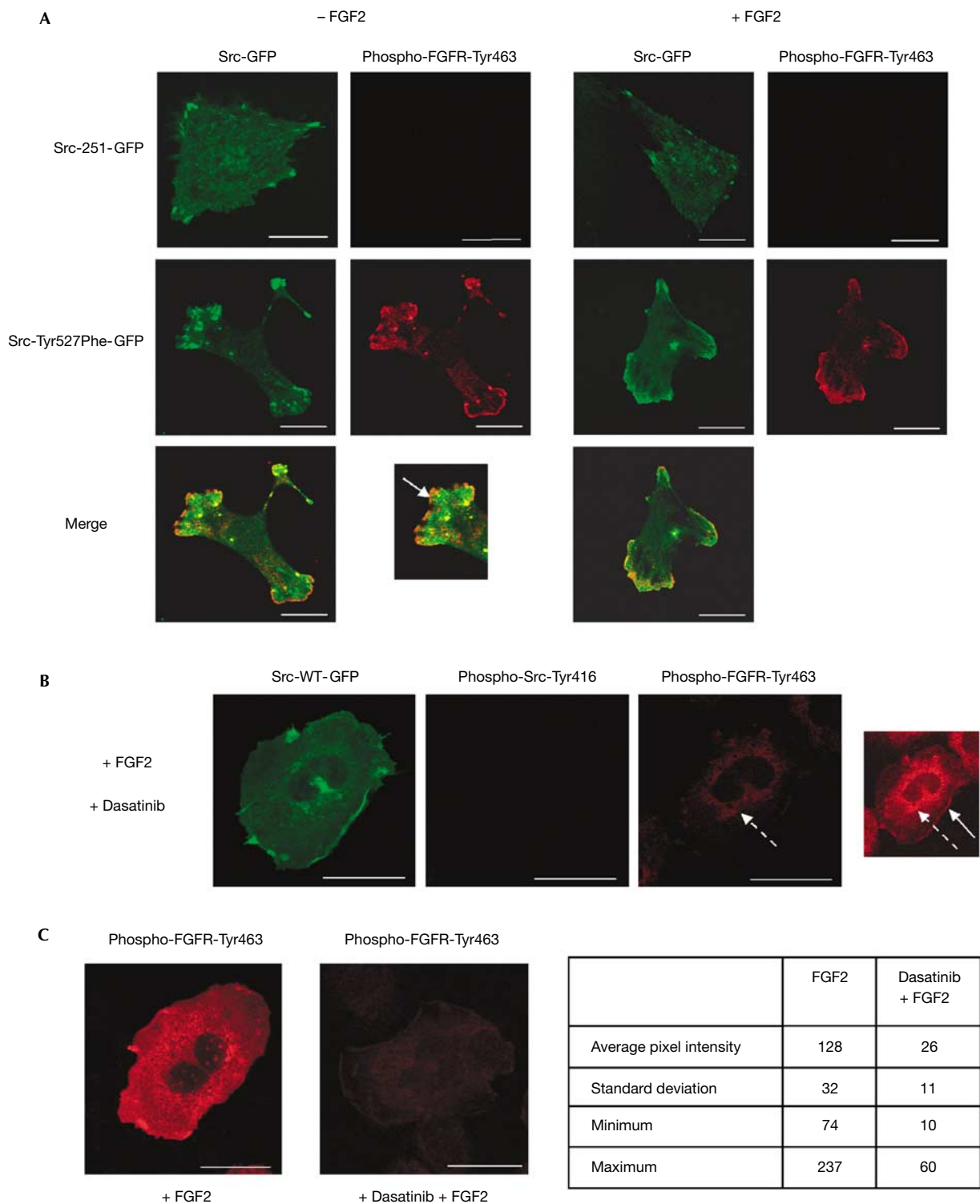


Fig 2 | Src activity is sufficient for increased peripheral membrane targeting of active FGFR. (A) *SYF*^{-/-} MEFs expressing Src-251-GFP or Src-Tyr527Phe-GFP were maintained in serum-free media or stimulated with FGF2. (B) *SYF*^{-/-} MEFs expressing Src-WT-GFP were treated with dasatinib (200 nM) for 2 h before stimulation with FGF2. (C) Images of 50 cells from (B) were taken under exactly the same conditions and the average pixel intensity at the membrane was calculated and compared. Active proteins were detected using anti-phospho-FGFR-Tyr463 or anti-phospho-Src-Tyr416. Solid arrows indicate protein localized to the plasma membrane and dashed arrows indicate protein maintained in the perinuclear region. Scale bars, 25 μ M. FGFR, fibroblast growth factor receptor; GFP, green fluorescent protein; MEF, mouse embryonic fibroblast; *SYF*^{-/-} MEF, Src/Yes/Fyn-deficient MEF.

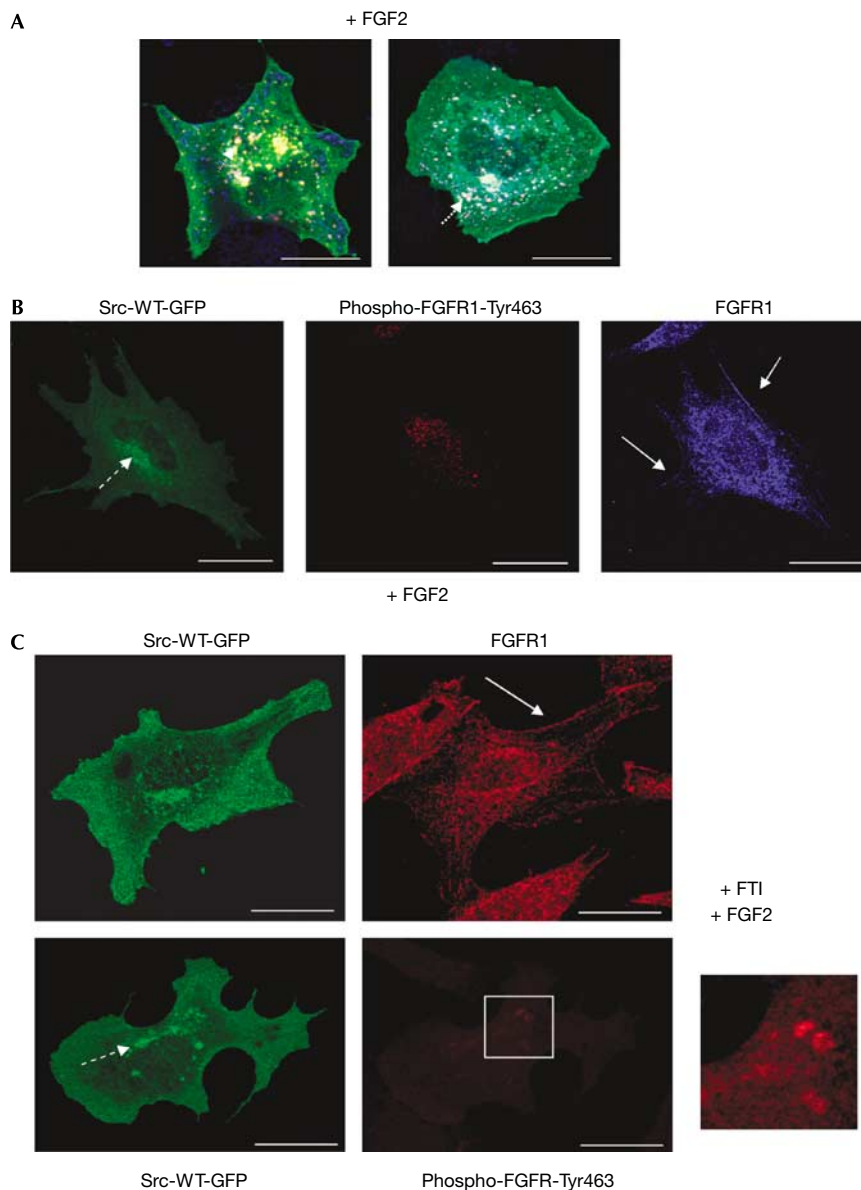


Fig 3 | Targeting of activated FGFR after FGF2 stimulation is RhoB dependent. (A) SYF^{-/-} MEFs expressing Src-WT-GFP and Myc-RhoB were stimulated with FGF2. Left panel: green, Src-WT-GFP; blue, FGFR; red, RhoB. Right panel: green, Src-WT-GFP; blue, phospho-FGFR-Tyr463; red, RhoB. (B) RhoB^{-/-} MEFs expressing Src-WT-GFP were stimulated with FGF2. (C) SYF^{-/-} MEFs expressing Src-WT-GFP were treated with L744832 (10 μM) for 2 h before stimulation with FGF2. RhoB, FGFR and active FGFR were detected with Myc, FGFR1 and phospho-FGFR1-Tyr463 antibodies, respectively. Solid arrows indicate protein localized to the plasma membrane, dashed arrows (B, left panel; C, bottom left panel) indicate protein maintained in the perinuclear region, whereas the dotted arrow (A, right panel) indicates endosomal proteins. Scale bars, 25 μm. FGFR, fibroblast growth factor receptor; GFP, green fluorescent protein; MEF, mouse embryonic fibroblast; SYF^{-/-} MEF, Src/Yes/Fyn-deficient MEF.

as Ras and RhoB through inhibition of the enzyme farnesyl transferase (Gibbs *et al*, 1994). Administration of an FTI, such as L744832, has been shown to affect the function of RhoB (Du & Prendergast, 1999), and therefore provides a test of the RhoB dependence of membrane targeting. To ascertain whether FTIs would influence the intracellular transport and activation of FGFR, we treated SYF^{-/-} MEFs expressing Src-WT-GFP with L744832 before stimulation with FGF2. The results indicate that although total FGFR1 could be detected at the plasma membrane, increased

activation of this protein was not detected (Fig 3C). We could, however, detect a low level of activation in endosomes throughout the cytoplasm (Fig 3C, right panel). Together, these data strongly indicate that FGFR activation and peripheral membrane targeting are tightly linked.

RhoB endosomes harbour actin-regulatory proteins, and Src and RhoB coordinate to control the actin assembly required for the transport of RhoB endosomes to the peripheral membrane; in essence, the RhoB/Src endosome shuttle is dependent on an intact

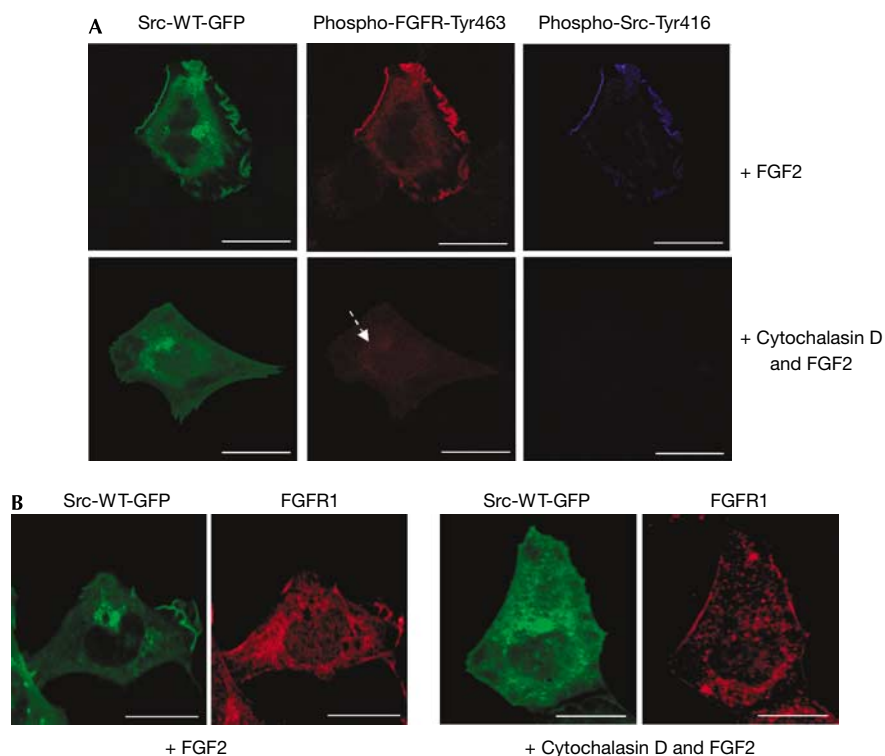


Fig 4 | Targeting of activated FGFR after FGF2 stimulation is actin dependent. SYF^{-/-}MEFs were treated with cytochalasin D (0.3 μg/ml) for 1 h before stimulation with FGF2. Cells were stained with (A) phospho-FGFR-Tyr463 antibody and anti-phospho-Src-Tyr416 or with (B) anti-FGFR1. Dashed arrows indicate protein maintained in the perinuclear region. Scale bars, 25 μm. FGFR, fibroblast growth factor receptor; MEF, mouse embryonic fibroblast; SYF^{-/-}MEF, Src/Yes/Fyn-deficient MEF.

actin cytoskeleton to drive vesicle movement (Sandilands *et al*, 2004). This predicts that FGFR activation might be dependent on actin and so abrogated by dissolution of the actin cytoskeleton. Indeed, we found that pretreatment of FGF2-stimulated MEFs by cytochalasin D inhibited activation of both FGFR and Src (Fig 4A), establishing that enhanced ligand-induced FGFR activation was dependent on both Src and an intact actin cytoskeleton. Low basal levels of activated FGFR were detected in the perinuclear regions of cytochalasin D-treated cells but were not visible at the plasma membrane (Fig 4A, lower middle panel). The localization of total FGFR1 did not seem to be affected by disruption of the actin cytoskeleton (Fig 4B). We have previously shown that the use of an interfering mutant of Scar1, a member of the WASP/Scar family of adaptor proteins, disrupts filamentous actin, and inhibits transport and activation of Src-WT-GFP (Sandilands *et al*, 2004). Here, we show that expression of this protein inhibits the increase in activation of FGFR1 and prevents translocation of basal activated FGFR to the plasma membrane (supplementary Fig 3 online).

Collectively, these data show that there is an essential requirement for the Src kinase/RhoB-dependent shuttle previously identified, which is driven by actin cytoskeleton assembly, in delivery of activated FGFR to the peripheral membrane. In the absence of this, the peripheral targeting steps of FGFR activation are blocked.

Role of Src in signalling pathways downstream of FGFR1

We were interested to learn how the engagement of Src in the process of FGFR activation and peripheral recruitment influenced

control of the dynamics of intracellular signalling pathways downstream of activated FGFR. MEFs were stimulated with FGF2 in the presence of dasatinib (Fig 5A) to block Src activation (data not shown), and we examined the kinetics of activation of the mitogen-activated protein kinase (MAPK) and phosphoinositide-3 kinase/Akt pathways. This showed a striking dependency of FGFR signalling on Src activity, and this was quite distinct for the two signalling pathways. In the case of Akt activation, FGF2 stimulation induced a rapid rise in Akt activation, which reached a maximum amplitude at about 4 min followed by a period of decay after 8 min (Fig 5A, upper panels). Pharmacological inhibition of Src activity resulted in attenuation of Akt activity. Although much weaker, the initial phase of residual activation reached peak amplitude at similar time points to control cells (Fig 5A, upper panels). An identical pattern was seen following inhibition of FGFR kinase activity (data not shown). This experiment was confirmed using SYF^{-/-}MEFs, which have significantly less active Akt than FGF2-stimulated MEFs (Fig 5B).

These data show that Akt activation is wholly dependent on the activation of Src, and is linked to Src-dependent peripheral membrane targeting of activated FGFR, presumably requiring FGFR to be at the plasma membrane.

A different pattern of kinetic behaviour was seen for the MAPK pathway following inhibition of Src activity. In this case, the rising phase of extracellular signal-regulated kinase-1 (ERK) activation was delayed compared with untreated cells (shown in Fig 5A for treatment with dasatinib and confirmed in Fig 4C with the Src inhibitor SU6656, right panels), consistent with a

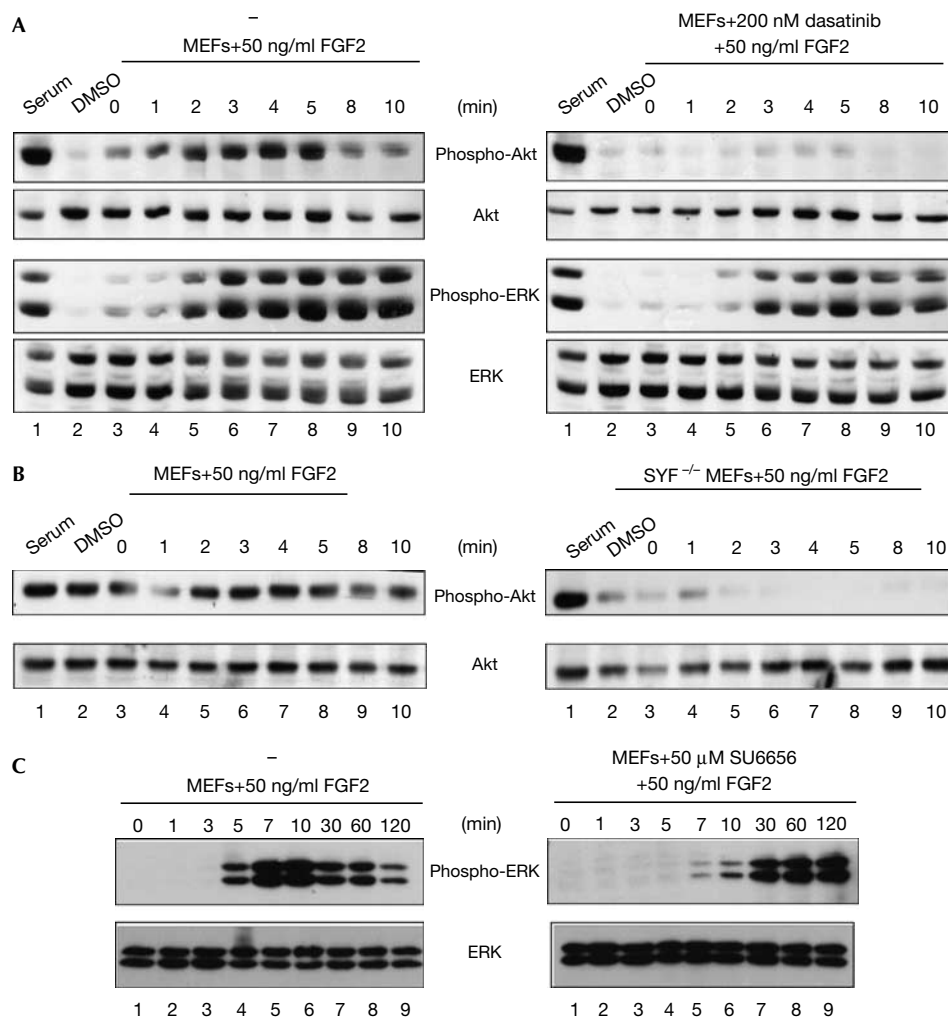


Fig 5 | Signalling from Src-dependent and Src-independent active FGFR pools. (A) MEFs were treated with dasatinib (200 nM) and stimulated with FGF2 for different durations. (B) SYF^{-/-}MEFs and MEFs alone were treated with FGF2. (C) MEFs were treated with 50 μM SU6656 before stimulation with FGF2 for different durations. Western blot analysis was carried out on cell lysates using Akt, phospho-Akt, ERK and phospho-ERK antibodies. ERK, extracellular signal-regulated kinase; FGFR, fibroblast growth factor receptor; MEF, mouse embryonic fibroblast; SYF^{-/-}MEF, Src/Yes/Fyn-deficient MEF.

requirement for Src activity for the correct FGFR-induced signalling response. However, in stark contrast to activation of Akt, robust activation of ERK persisted and it was the decay component of ERK activation that was markedly slowed down by inhibition of Src (Fig 5C, right panels). This inhibition of decay was also observed in SYF^{-/-}MEFs (data not shown). Thus, activation of ERK, which occurs through Grb2/SOS engagement of FRS2 (Ong *et al*, 2001), is delayed in its initial phase, which is consistent with the requirement for Src in FGFR activation, but prolonged in the decay phase, indicating an additional role for Src kinase in ERK attenuation after signal peak.

Several earlier studies have indicated that the Ras/Raf/ERK/MAPK cascade is activated at both the plasma membrane and cytosolic locations following growth factor stimulation (reviewed by Miaczynska *et al*, 2004), and that the two pools of signalling modules show markedly different dynamic properties (Harding *et al*, 2005). On a similar basis, we can explain the requirement for Src activation for attenuating ERK activity as a consequence

of Src releasing the activated ERK module to cytosolic locations where it requires higher signalling inputs to sustain activity; consequently, the amplitude of the signal degrades more quickly when Src is present. When Src is inhibited, the module is not released, continues to respond to inputs and fails to decay.

Given that Src activation is a common, if not indeed ubiquitous, characteristic of signalling from RTK receptors (Parsons & Parsons, 2004), it seems possible that a crucial role of Src in cellular signalling is to tune the dynamics of downstream processes by regulating the spatial localization and confinement of activated signalling complexes. This could also contribute to the functions of oncogenic forms of Src, as one consequence of constitutively activated Src is hypersensitization of RTK-mediated signalling pathways, thereby emulating the consequences of activating mutations in the RTKs themselves or downstream effectors. These considerations indicate that therapeutic intervention by the inhibition of Src might be accentuated in combination with agents that inhibit RTK kinase activity (Mohammadi *et al*, 1997). Indeed,

dasatinib is now licensed for clinical use in the treatment of chronic myeloid leukaemia, and this agent and other Src inhibitors are being clinically tested for activity against common solid tumours. Our work raises the exciting possibility that such agents might be useful in the treatment of cancers in which FGFR mutations are driving proliferation.

METHODS

Cell culture. Src/Yes/Fyn-deficient MEFs (SYF^{-/-}MEFs), control MEFs and RhoB^{-/-}MEFs were routinely grown in DMEM supplemented with 10% FCS and 1% glutamine. Cells were transiently transfected under serum-free conditions using FuGene6 (Roche Diagnostics Ltd, Sussex, UK) or Polyfect Transfection Reagent (Qiagen, Crawley, UK). Cells were treated with L744832 (10 μM) for 2 h (Biomol Int, Exeter, UK), cytochalasin D (0.3 μg/ml) for 1 h (Sigma, Poole, UK), dasatinib (200 nM) for 2 h (BMS, New York, NY, USA) or 50 μM SU6656 (Calbiochem, Nottingham, UK) before stimulation with FGF2 (50 ng/ml⁻¹ for 30 min) and 10 μg/ml heparin (Sigma, Poole, UK).

Immunofluorescence. Cells were fixed in 3% paraformaldehyde, washed in TBS/100 mM glycine and permeabilized with TBS/0.1% saponin/20 mM glycine. After blocking with TBS/0.1% saponin/10% FCS, cells were incubated with primary antibodies. Anti-phospho-Tyr463 FGFR1 was generated in sheep (Diagnostics Scotland, Edinburgh, UK) by immunization with a dendromeric form of the phosphopeptide LAGVSEY(P)ELPED (Alta Biosciences, Birmingham, UK) and purified by three cycles of affinity chromatography on an immobilized form of the phosphopeptide. Antibody specificity was confirmed by ELISA and in western blots, and immunohistochemistry was confirmed by inhibition with the phosphorylated form of the peptide. Anti-FGFR1 was used to detect total FGFR1 (Santa Cruz, Santa Cruz, CA, USA), 9E10 monoclonal antibody was used to detect Myc-tagged RhoB and anti-phospho-Tyr416-Src was used to detect active Src (Upstate Biotechnology, New York, NY, USA). Non-conjugated antibody detection was by reaction with species-specific fluorescein isothiocyanate-, Cy5- or Texas Red-conjugated secondary antibodies (Jackson ImmunoResearch, Luton, UK). Cells were visualized by using a Leica confocal microscope (Leica UK Ltd, Milton Keynes, UK). Each experiment was repeated a minimum of three times, 100 cells were counted for each condition for quantification purposes and an image that represented the phenotype of most of the cells was selected (supplementary Table 1 online).

Protein immunoblotting. Samples were lysed in radioimmuno-precipitation buffer (20 mM Tris, 150 mM NaCl, 2 mM EDTA, 1% Triton X-100, 10% glycerol, pH 7.4) containing protease and phosphatase inhibitors (2 mM phenylmethylsulphonyl fluoride, 10 μg/ml aprotinin, 1.5 mM sodium fluoride and 300 μM sodium vanadate) and then centrifuged at 40 °C for 15 min. Immunoblotting was carried out using 50–100 μg of lysate per sample. Proteins were separated by SDS–10% polyacrylamide gel electrophoresis, transferred to nitrocellulose, blocked with 5% BSA in TBS–0.2% Tween 20 (Sigma, Poole, UK) and probed with anti-ERK (Sigma, Poole, UK), anti-phospho-p44/42 MAP kinase (Thr202/Tyr204), anti-phospho-Akt (Ser473) and anti-Akt (Cell Signalling, Hertfordshire, UK). Detection was by incubation with horseradish peroxidase-conjugated secondary antibodies and visualization was by enhanced chemiluminescence (Amersham, Buckinghamshire, UK).

Supplementary information is available at *EMBO reports* online (<http://www.emboreports.org>).

ACKNOWLEDGEMENTS

We thank G. Superti Furga, H. Mellor and G. Prendergast for reagents, and M. O'Prey for help with imaging. This work was supported by the Cancer Research UK core grant to the Beatson Institute (M.C.F., E.S. and D.G.M.) and by a Cancer Research UK programme grant (J.K.H., S.A. and A.V.).

REFERENCES

- Avizienyte E, Wyke AW, Jones RJ, McLean GW, Westhoff MA, Brunton VG, Frame MC (2002) Src-induced de-regulation of E-cadherin in colon cancer cells requires integrin signalling. *Nat Cell Biol* **4**: 632–638
- Du W, Prendergast GC (1999) Geranylgeranylated RhoB mediates suppression of human tumor cell growth by farnesyltransferase inhibitors. *Cancer Res* **59**: 5492–5496
- Furdui CM, Lew ED, Schlessinger J, Anderson KS (2006) Autophosphorylation of FGFR1 kinase is mediated by a sequential and precisely ordered reaction. *Mol Cell* **21**: 711–717
- Gibbs JB, Oliff A, Kohl NE (1994) Farnesyltransferase inhibitors: Ras research yields a potential cancer therapeutic. *Cell* **77**: 175–178
- Greenman C *et al* (2007) Patterns of somatic mutation in human cancer genomes. *Nature* **446**: 153–158
- Hajihosseini MK, Lalioti MD, Arthaud S, Burgar HR, Brown JM, Twigg SR, Wilkie AO, Heath JK (2004) Skeletal development is regulated by fibroblast growth factor receptor 1 signalling dynamics. *Development* **131**: 325–335
- Halford MM, Stackler SA (2001) Revelations of the RYK receptor. *BioEssays* **23**: 34–45
- Harding A, Tian T, Westbury E, Frische E, Hancock JF (2005) Subcellular localization determines MAP kinase signal output. *Curr Biol* **15**: 869–873
- Li X, Brunton VG, Burgar HR, Wheldon LM, Heath JK (2004) FRS2-dependent SRC activation is required for fibroblast growth factor receptor-induced phosphorylation of Sprouty and suppression of ERK activity. *J Cell Sci* **117**: 6007–6017
- Lombardo LJ *et al* (2004) Discovery of *N*-(2-chloro-6-methyl-phenyl)-2-(6-(4-(2-hydroxyethyl)-piperazin-1-yl)-2-methylpyrimidin-4-ylamino)thiazole-5-carboxamide (BMS-354825), a dual Src/Abl kinase inhibitor with potent antitumor activity in preclinical assays. *J Med Chem* **47**: 6658–6661
- Marshall CJ (1995) Specificity of receptor tyrosine kinase signalling: transient versus sustained extracellular signal-regulated kinase activation. *Cell* **80**: 179–185
- Miaczynska M, Pelkmans L, Zerial M (2004) Not just a sink: endosomes in control of signal transduction. *Curr Opin Cell Biol* **16**: 400–406
- Mohammadi M, McMahon G, Sun L, Tang C, Hirth P, Yeh BK, Hubbard SR, Schlessinger J (1997) Structures of the tyrosine kinase domain of fibroblast growth factor receptor in complex with inhibitors. *Science* **276**: 955–960
- Ong SH, Hadari YR, Gotoh N, Guy GR, Schlessinger J, Lax I (2001) Stimulation of phosphatidylinositol 3-kinase by fibroblast growth factor receptors is mediated by coordinated recruitment of multiple docking proteins. *Proc Natl Acad Sci USA* **98**: 6074–6079
- Parsons SJ, Parsons JT (2004) Src family kinases, key regulators of signal transduction. *Oncogene* **23**: 7906–7909
- Pellegrini L, Burke DF, von Delft F, Mulloy B, Blundell TL (2000) Crystal structure of fibroblast growth factor receptor ectodomain bound to ligand and heparin. *Nature* **407**: 1029–1034
- Sandilands E, Cans C, Fincham VJ, Brunton VG, Mellor H, Prendergast GC, Norman JC, Superti-Furga G, Frame MC (2004) RhoB and actin polymerization coordinate Src activation with endosome-mediated delivery to the membrane. *Dev Cell* **7**: 855–869
- Sandilands E, Brunton VG, Frame MC (2007) The membrane targeting and spatial activation of Src, Yes and Fyn is influenced by palmitoylation and distinct RhoB/RhoD endosome requirements. *J Cell Sci* **120**: 2555–2564
- Schlessinger J (2000) Cell signaling by receptor tyrosine kinases. *Cell* **103**: 211–225
- Serrels A, Macpherson IR, Evans TR, Lee FY, Clark EA, Sansom OJ, Ashton GH, Frame MC, Brunton VG (2006) Identification of potential biomarkers for measuring inhibition of Src kinase activity in colon cancer cells following treatment with dasatinib. *Mol Cancer Ther* **5**: 3014–3022
- Timpson P, Jones GE, Frame MC, Brunton VG (2001) Coordination of cell polarization and migration by the Rho family GTPases requires Src tyrosine kinase activity. *Curr Biol* **11**: 1836–1846
- Wilkie AOM, Morriss-Kay GM, Jones EY, Heath JK (1995) Functions of fibroblast growth factors and their receptors. *Curr Biol* **5**: 500–507

Computational reasoning applied to FGF pathway: simulation, analysis and experimental validation

Oksana Tymchyshyn¹, Shiva Akbazardeh², David McEwan³, Gethin Norman^{1,4}, John K Heath² and Marta Z Kwiatkowska^{1,4,5}

School of Computer Science¹ and CRUK Growth Factor Group, School of Biosciences², University of Birmingham, Edgbaston, Birmingham B15 2TT, UK; CRUK Beatson Institute for Cancer Research, Switchback Road, Glasgow G61 1BD³

⁴ Current address: Oxford University Computing Laboratory, Parks Road, Oxford, OX1 3QD

⁵ Author for correspondence: Email mzk@comlab.ox.ac.uk, Tel +44 1865 283509, FAX +44 1865 273839

Subject Categories: Signal Transduction, Computational methods

Keywords: computational modelling / Fibroblast growth factor / pi-calculus / Sprouty / Src

Running title: Computational reasoning applied to FGF pathway

Character count: 29585 (excl. Methods, tables, supplementary material: 21984)

Abstract

Computational methods that assist in reasoning about biological processes provide an attractive framework for the formulation, evaluation and prioritisation of biological experiments. We use the stochastic pi-calculus proposed for analysing biological networks [Regev & Shapiro (2002) *Nature* **419**, 343] to devise a model of the Fibroblast growth factor (FGF) signalling pathway. This pathway has recently been identified as a cause of cancer and skeletal deformities, and yet its mechanisms are poorly understood. Parameter space exploration indicates that pathway dynamics are dominated by the inter-linked rates of receptor kinase activation and signalling complex endocytosis and degradation. In particular, simulation and analysis of the model predicts two unexpected features, which we validate by in vitro experiment. First, inhibition of Src kinase activity delays signal decay. Second, increasing receptor affinity for ligand (as occurs in pathogenic mutant forms of the FGFR) accelerates signal activation and inhibits signal decay at low receptor occupancy. Our results confirm that new biological hypotheses can be obtained with the pi-calculus approach and yield important insights into pathogenic receptor signalling dynamics.

Introduction

Ligand-initiated receptor mediated signalling controls fundamental biological responses in multi-cellular organisms. Abnormal signalling lies at the heart of common pathologies, e.g. cancer, inflammation and tissue repair. Receptor mediated signalling can be considered as a series of concurrently occurring transitions: molecules change properties as a consequence of covalent modification (phosphorylation, ubiquitinylation); associate or disassociate with partner proteins; change location within the cell; and change in concentration as a result of synthesis or degradation. These processes are intertwined: changes in interactions or concentration may be regulated concurrently or independently by covalent modification; changes in location may result in altered interaction opportunities and covalent modifications. Thus, although the component molecules exhibit simple properties, the system as a whole can exhibit emergent properties that are not easily analysed by biological intuition.

Computational modelling is therefore invaluable in analysing the dynamics of signalling pathways. Molecular species in a signalling system can be modelled using two basic approaches: (i) continuous concentrations, which is known to suffer from combinatorial explosion in the number of differential equations in presence of concurrent state changes such as phosphorylation (Tolle & Le Novere, 2006); and (ii) discrete molecular populations, which avoids the problem by employing Monte Carlo simulation and, furthermore, is more accurate for low numbers of molecules. Inspired by (Regev & Shapiro, 2002), we use the stochastic pi-calculus formalism to model a pathway as a network of molecular agents, interacting according to biochemical reaction rules (Priami et al, 2001). Stochastic pi-calculus affords a compact, textual description of a pathway and admits discrete stochastic simulation using Gillespie (Regev & Shapiro, 2004) or more powerful reasoning techniques (Heath et al, 2006; Kwiatkowska et al, 2007). One advantage of this approach is the ease with which molecular interactions can be modified to test alternative schemes. Therefore, pi-calculus models can be directly employed for robust hypothesis generation and selection to guide the design of experimental interventions. This is particularly desirable for signalling systems, since experimental technologies are currently labour-intensive, costly and extremely slow compared to computational models.

We apply the pi-calculus approach to model the FGF (Fibroblast growth factor) signalling pathway. We have chosen this pathway because mutations which affect quantitative features of pathway dynamics have been identified both as highly significant in common forms of human cancer (Greenman et al, 2007) and the underlying cause of congenital developmental skeletal dysmorphology syndromes (Kan et al, 2002). It is not, however, immediately obvious how these mutations might lead to pathogenic outcomes. Our goal is to use computational modelling supported by reasoning to characterize key parameters that shape pathway dynamics, which, in turn, can influence the prioritisation of biological experiments and development of effective therapeutic interventions. Noting that ODE models of the FGF pathway suffer from combinatorial explosion (Kwiatkowska et al, 2006), we develop and analyse a reusable family of stochastic pi-calculus models.

Simulation results for the derived stochastic pi-calculus model of the FGF pathway closely resemble the known dynamic behaviour. By interrogation of parameter space

and component dependencies ('in silico' genetics) we show that the behaviour of the pathway is dominated by two inter-linked variables: the rate of receptor kinase activation and the rate of signal attenuation by receptor complex internalisation. We confirm these findings in living cells by experimental intervention, which reveals that the interplay between receptor activation and attenuation exhibits counter-intuitive features, and that pathogenic mutations in FGF receptors lead to sustained signalling properties which are accentuated at low levels of receptor occupancy, thereby yielding novel insight into the function of oncogenic mutations.

Results and Discussion

Our approach consists of three steps: the derivation of the pi-calculus model; a series of simulation experiments to validate the model against existing experimental data and generate new predictions; and validation of the novel predictions by in vitro experiments.

Design of the FGF signalling model

The FGF model is based upon literature-derived information on the early steps of FGF signal propagation (described in Table I), and incorporates several features which have been reported to negatively regulate FGF signal propagation (reviewed (Dikic & Giordano, 2003; Tsang & Dawid, 2004)).

Identification of key variables that control pathway dynamics

The model accurately predicts the behaviour of the FGF pathway for known conditions described in the literature. The concentration of the signalling response component FRS2:Grb2 shows a rapid increase shortly after exposure to FGF, reaching its maximum level at about 15-20 min. Activation of the negative feedback loops (steps 8, 9, 12, and 14) results in signal downregulation after its successful transduction, thus preventing sustained pathway activation.

We interrogate the model in two ways: by exploration of parameter space to establish the key variables and by removing individual components to study their role in signal propagation. These steps are an advance on previous applications of pi-calculus to biological signalling (Phillips & Cardelli, 2005) in that they take computational modelling into the realm of experimental intervention rather than simulation, and are explicitly designed to formulate biological hypotheses.

The responses of the average signalling amplitude and duration upon changes in the rates of individual reactions are shown in Table III (Supplementary information). In most cases, the resulting deviations of the signalling responses do not exceed 0.1% of the changes of the respective parameters, proving that the system is robust against parameter perturbations. The only sensitive parameters are those controlling Src-mediated relocation of the receptor complex and FGFR kinase activation.

Reducing the rate constant of FGFR kinase activity leads to the reduction of maximal value of the signal, which now occurs after considerable delay. Fig. 1A shows the outcome of 10- and 100-fold reduction of the rate of FGFR. Maximal signal expression reaches 90 and 60% of its initial value and is delayed by 10 and 30 min,

respectively. A similar signal reduction and delay occurs in simulations in which the concentration of FGF was reduced to 10 and 5% (Fig. 1B).

The consequences of different signal attenuation mechanisms are evaluated by ‘in silico’ mutagenesis: removal of various model components before simulation. We observe that inhibition of Sprouty (Fig. 2A) does not affect the initial phase of signal upregulation, since it is synthesized after the signal passes its maximum value. Later, Sprouty attenuates signalling, primarily due to the competition for Grb2. Similar pattern of FRS2:Grb2 expression is generated when Shp2 is not present (Fig. 2A).

Another key determinant of FGFR signalling dynamics in the model is the rate of internalisation, which we have encoded (perhaps speculatively) by the action of Src. As Table III and Fig. 2A demonstrates, the suppression of Src activity is predicted to have a major impact on signalling dynamics: after fast increase, the signal fails to decrease substantially. This suggests that, in particular, other negative feedback mechanisms are not sufficient to reduce the signal if internalisation is abolished.

In sum, parameter variation and component removal studies of the model indicate that the overall dynamics of this system is dominated by two key variables: the rate of FGFR activation – as judged by varying the concentration of FGF or the rate constants of the FGFR kinase – and the rate of endocytosis modelled by the recruitment and activation of Src.

The role of Src in regulating FGF signalling: from model to experiments and back

Next, we turned to predictions which had not been experimentally validated previously. For this purpose we utilised an experimental model of activation of the Ras-MAPK (ERK) pathway in mouse embryonic fibroblasts (MEFs) stimulated with FGF2 using quantitation of phospho-ERK (pERK) by western blotting as the experimental readout. This approach assumes that the level of experimental pERK is a faithful surrogate for the computed value of the Grb2:FRS2 used in the modelling studies. We take this assumption to hold, as the quantitative behaviour of this output closely resembles the computed value in experimental reports and our own investigations (data not shown).

The prediction we addressed was that inhibition of Src kinase activity would lead to prolongation of signalling as a consequence of Src acting to remove the activated receptor complex. Quiescent MEFs were stimulated with 50ng/ml FGF2 for varying time points in the presence or absence of the highly specific Src family kinase inhibitor Dasatinib (Lombardo et al, 2004), harvested and examined for the presence of pERK. These results clearly show that untreated MEFs exhibit an FGF stimulus response that conforms to the predicted kinetics, and that pharmacological suppression of Src kinase activity (Fig. 2C) indeed produces the predicted extended duration of pERK activation (Fig. 2A).

In our initial model, Src encodes an abstraction of internalisation. Following conventional view of internalisation as termination of signalling, we assume that the internalised receptor complex disappears without specifying its subsequent fate. Fig. 2C and further experimental studies of our group (Sandilands et al, 2007) show that

Src exerts additional positive control on the initial phase of signalling by increasing the rate at which FGFR is recycled back to the membrane to re-engage with ligand. These results are consistent with previous reports of both negative and positive effect of receptor internalisation on signalling (reviewed (Clague & Urbe, 2001; Miaczynska et al, 2004)).

We revise the model by incorporating a positive feedback loop, in which initial activation of FGFR leads to recruitment of Src, which subsequently recycles more receptors thus amplifying the signal. Simulations of the refined model demonstrate delayed signal which reaches lower amplitude but fails to attenuate when Src is inhibited (Fig. 2B), consistent with the experimental data (Fig. 2C). Through reiteration of modelling and experiments we thus uncovered a positive feedback loop activated at the initial phase of signalling.

Cross-regulation between receptor activation and attenuation

Next, we simulate the effects of pathological mutations in FGFR by increasing the affinity of receptor-ligand interaction. The initial model, which does not account for a positive Src regulation, is not able to produce a phenotypic difference between normal and mutant signalling (Fig. 3A). Surprisingly, the revised model (Fig. 3B) predicts that the pathway amplitude is upregulated in a long run due to recycling of more receptors to the membrane in mutant. Increased ligand binding changes the equilibrium between activation and attenuation roles of Src, resulting in delayed signal attenuation.

We addressed the question if increasing the rate of receptor activation (i.e. pathogenic driver mutations) would lead to accelerated activation and delayed attenuation of signalling *in vitro*. For this purpose we employed a matched pair of MEFs: one derived from normal mouse embryos and the second derived from embryos harbouring the mutant Pro252Arg form of FGFR1 (Hajihosseini et al, 2004). The MEFs were rendered quiescent by serum starvation and then stimulated for varying time points with 0.1 ng/ml FGF2 and harvested for analysis as in the previous experiment. The result (Fig. 3C and D) reveals that the introduction of a single gene copy of the mutant driver form of FGFR1 has marked effect on signaling upon exposure to limiting concentrations of ligand. In the mutant cells peak amplitude is reached rapidly (~5 min) compared to wild type (~30 min) and signal duration is prolonged in the mutant cells, as the model predicts (Fig. 3B).

Decreasing the rate of FGFR activation by simulating the effects of FGFR kinase inhibitors accords well with many published studies and should come as no surprise. We showed, however, that increasing the rate of FGFR kinase activation – thereby simulating the effect of pathological mutations in FGFR associated with skeletal development syndromes (Anderson et al, 1998; Hajihosseini et al, 2004) and cancer (Greenman et al, 2007) – leads to extended duration of signalling which is not overcome by the action of inhibitory regulators such as Sprouty or degradation of the receptor complex.

Informed by these ‘*in silico*’ studies, we experimentally tested and confirmed two counter-intuitive predictions of the model: suppression of Src kinase prolongs the duration of FGF signalling and that driver mutations in FGFR exhibit fast activation

and slow attenuation in response to low level stimulation. These studies prove the utility of the pi-calculus modelling approach for selecting appropriate biological hypotheses from many possibilities and for deriving new insights into normal and pathological signalling dynamics.

Methods

Constructing a stochastic pi-calculus model

Stochastic pi-calculus and similar formalisms have been successfully applied to analyze small examples such as the Ras-MAPK signalling pathway (Phillips & Cardelli, 2005). This paper describes the first stochastic pi-calculus model of a realistic pathway that has been experimentally validated. The biochemical reactions 1-14 of the FGF pathway can be directly translated into pi-calculus processes following the translation scheme proposed in (Regev & Shapiro, 2002; Regev & Shapiro, 2004).

The stochastic pi-calculus model of FGF is described in more detail in Supplementary information. We have derived two further models directly from the FGF reactions 1-14, using ODEs (Gaffney et al, submitted) and PRISM (Kwiatkowska et al, 2007), and find that the three models are consistent with each other.

Rate parameters

The values of kinetic parameters of FGF reactions 1-14 were assembled based on the literature, see Table II in Supplementary information. The stochastic pi-calculus assumes exponentially distributed reaction rates; this is justified since, if collision times are small compared to the times between collisions, molecules are moving chaotically, and a constant ratio of overall collisions lead to reactions.

Simulation experiments

We use BioSPI (Regev & Shapiro, 2004) as the simulation platform. The BioSPI system inputs the pi-calculus process and performs simulations using the Gillespie algorithm, starting from a given initial state. Reactions are selected according to a certain probability distribution in order to account for the rates and times at which they occur. Each channel is associated with a rate constant, and the actual rate is determined by a combination of this rate and the quantities of the reactant. In all experiments, we plot values averaged over 100 simulations.

We run simulations starting with the initial number of FGF, unbound and unphosphorylated FGFR, unbound Src, Grb2, Cbl, PLC, and Sos set equal to 50 while unphosphorylated FRS2 is 100. Sprouty arrives into the system with the characteristic time of 20 min. Since the binding of Grb2 to FRS2 serves as the primary link between FGFR activation and ERK signalling, we examine the amount of Grb2 bound to FRS2 as the output. Concentrations of elements in mutagenesis study (Fig. 2) are reduced by 90%. Fig. 3 is generated using 10 molecules of FGF.

The role of the model

It is important to appreciate that the primary purpose of the model presented is as a tool to encode and evaluate biological hypotheses that are not easily obtained by intuition or manual methods, and not a detailed description of a real-life FGF pathway.

We explicitly draw attention to the following issues. The reactions selected are based upon their current biological interest rather than complete understanding of the components of FGF signalling. Indeed, at this stage we have ignored many reactions that could prove significant in regulation of FGFR signalling in real cells. The model is idealised in that it does not take into account variations in composition, affinities or rate constants that might occur in different cell types or physiological conditions. However, the design permits the incorporation of further modifications to the core model as biological understanding advances.

The model is based upon literature-defined events. It is probable that the reported biological significance of these processes reflects the experimental context, rather than the normal situation. For example, the significance of PLC in the relocation of FGFR signalling complexes has been the subject of some debate (Sorokin et al, 1994), as has the action of Sprouty (Hanafusa et al, 2002). The model can be easily modified and extended as new biological information becomes available.

In vitro investigations

Primary MEF cells isolated from WT or FGFR1 Pro252Arg +/- mice were cultured at 37°C, 5% CO₂, 3% O₂ in Dulbecco's modified Eagle medium supplemented with 2 mM glutamine (Invitrogen), 0.1 mg/mL streptomycin, 0.2 U/mL penicillin, 4.5 g/L glucose (Sigma) and 10% fetal calf serum (v/v) (Labtech International) for less than 10 passages. MEF cells were stimulated with FGF2 (0-60 ng/mL) for various times and lysed in 1× SDS sample buffer (5% glycerol (v/v), 1% SDS (w/v), 0.05% bromophenol Blue (w/v), 100 mM 1, 4-Dithiothreitol, 50 mM Tris-HCl, pH 6.8). Lysates were passed through 21G needle to shear DNA and heated at 95°C, 5 min. Cleared lysates were resolved on 10% SDS-PAGE and transferred to PVDF (Millipore) membrane with standard procedures. The membranes were dried according to manufacturer's instructions and probed with anti mouse pERK (Santa Cruz) for 2 hrs. Membranes were washed and incubated with anti mouse-HRP antibody (Amersham) for 1 hr. Following washes, the membranes were incubated with Super-Signal enzyme chemiluminescence (ECL, Pierce) according to manufacturer's instructions and exposed to X-ray films to detect signals. The membranes were stripped and re-probed with anti rabbit ERK-1 (Santa Cruz) or anti mouse Tubulin (Sigma) as loading controls.

Acknowledgements

We thank Muffy Calder, Jasmin Fisher, Margaret Frame, Eamonn Gaffney, Jeremy Gunawardena, Jane Hillston, and Dov Stekel for helpful discussions and advice. This work is part-sponsored by the EPSRC grants GR/S72023 and GR/S46727, Microsoft Research Cambridge contract MRL 2005-04 (MZK), and by a programme from Cancer Research UK (JKH).

References

- Anderson J, Burns HD, Enriquez-Harris P, Wilkie AO and Heath JK (1998) Apert syndrome mutations in fibroblast growth factor receptor 2 exhibit increased affinity for FGF ligand. *Hum Mol Genet* **7**: 1475-83
- Clague MJ and Urbe S (2001) The interface of receptor trafficking and signalling. *J Cell Sci* **114**: 3075-81
- Dikic I and Giordano S (2003) Negative receptor signalling. *Curr Opin Cell Biol* **15**: 128-35
- Foehr ED, Raffioni S, Murray-Rust J and Bradshaw RA (2001) The role of tyrosine residues in fibroblast growth factor receptor 1 signaling in PC12 cells. Systematic site-directed mutagenesis in the endodomain. *J Biol Chem* **276**: 37529-36
- Fong CW, Leong HF, Wong ES, Lim J, Yusoff P and Guy GR (2003) Tyrosine phosphorylation of Sprouty2 enhances its interaction with c-Cbl and is crucial for its function. *J Biol Chem* **278**: 33456-64
- Greenman C, Stephens P, Smith R, Dalgliesh GL, Hunter C, Bignell G, Davies H, Teague J, Butler A, Stevens C, Edkins S, O'Meara S, Vastrik I, Schmidt EE, Avis T, Barthorpe S, Bhamra G, Buck G, Choudhury B, Clements J, et al. (2007) Patterns of somatic mutation in human cancer genomes. *Nature* **446**: 153-158
- Hadari YR, Kouhara H, Lax I and Schlessinger J (1998) Binding of Shp2 tyrosine phosphatase to FRS2 is essential for fibroblast growth factor-induced PC12 cell differentiation. *Mol Cell Biol* **18**: 3966-73
- Hajihosseini MK, Lalioti MD, Arthaud S, Burgar HR, Brown JM, Twigg SR, Wilkie AO and Heath JK (2004) Skeletal development is regulated by fibroblast growth factor receptor 1 signalling dynamics. *Development* **131**: 325-35
- Hanafusa H, Torii S, Yasunaga T and Nishida E (2002) Sprouty1 and Sprouty2 provide a control mechanism for the Ras/MAPK signalling pathway. *Nat Cell Biol* **4**: 850-8
- Heath J, Kwiatkowska M, Norman G, Parker D and Tymchyshyn O (2006). Probabilistic model checking of complex biological pathways. In *Proc Comput Methods Syst Biol*, Lect Notes Bioinform, Springer **4210**: 32-47
- Kan SH, Elanko N, Johnson D, Cornejo-Roldan L, Cook J, Reich EW, Tomkins S, Verloes A, Twigg SR, Rannan-Eliya S, McDonald-McGinn DM, Zackai EH, Wall SA, Muenke M and Wilkie AO (2002) Genomic screening of fibroblast growth-factor receptor 2 reveals a wide spectrum of mutations in patients with syndromic craniosynostosis. *Am J Hum Genet* **70**: 472-86
- Kwiatkowska M, Norman G and Parker D (2007) Stochastic Model Checking. In *Lect Notes Comput Sc*, Bernardo M and Hillston J (ed) pp 220-270. Springer
- Kwiatkowska M, Norman G, Parker D, Tymchyshyn O, Heath J and Gaffney E (2006). Simulation and verification for computational modelling of signalling pathways. In *Proc Winter Simulation*: 1666-1674
- Li X, Brunton VG, Burgar HR, Wheldon LM and Heath JK (2004) FRS2-dependent SRC activation is required for fibroblast growth factor receptor-induced phosphorylation of Sprouty and suppression of ERK activity. *J Cell Sci* **117**: 6007-17
- Lombardo LJ, Lee FY, Chen P, Norris D, Barrish JC, Behnia K, Castaneda S, Cornelius LA, Das J, Doweyko AM, Fairchild C, Hunt JT, Inigo I, Johnston K, Kamath A, Kan D, Klei H, Marathe P, Pang S, Peterson R, et al. (2004)

- Discovery of N-(2-chloro-6-methyl-phenyl)-2-(6-(4-(2-hydroxyethyl)-piperazin-1-yl)-2-methylpyrimidin-4-ylamino)thiazole-5-carboxamide (BMS-354825), a dual Src/Abl kinase inhibitor with potent antitumor activity in preclinical assays. *J Med Chem* **47**: 6658-6661
- Miaczynska M, Pelkmans L and Zerial M (2004) Not just a sink: endosomes in control of signal transduction. *Curr Opin Cell Biol* **16**: 400-6
- Mohammadi M, McMahon G, Sun L, Tang C, Hirth P, Yeh BK, Hubbard SR and Schlessinger J (1997) Structures of the tyrosine kinase domain of fibroblast growth factor receptor in complex with inhibitors. *Science* **276**: 955-60
- Phillips A and Cardelli L (2005). A Graphical Representation for the Stochastic Pi-calculus. In *Proc Bioconcur'05*
- Priami C, Regev A, Shapiro EY and Silverman W (2001) Application of a stochastic name-passing calculus to representation and simulation of molecular processes. *Inf Process Lett* **80**: 25-31
- Regev A and Shapiro E (2002) Cells as computation. *Nature* **419**: 343
- Regev A and Shapiro E (2004) The pi-calculus as an Abstraction for Biomolecular Systems. In *Modelling in Molecular Biology*, Ciobanu G and Rozenberg G (ed) pp 219-266. Berlin-Heidelberg: Springer
- Sandilands E, Akbazardeh S, Vechionne A, McEwan DG, Frame MC and Heath JK (2007) Src kinase dictates activation, trafficking and signalling dynamics of Fibroblast Growth Factor Receptors. *Curr Biol*: to appear
- Schlessinger J (2004) Fibroblast Growth Factor Receptor Pathway. Sci. STKE (Connections Map) http://stke.sciencemag.org/cgi/cm/stkecm;CMP_15049.
- Sorokin A, Mohammadi M, Huang J and Schlessinger J (1994) Internalization of fibroblast growth factor receptor is inhibited by a point mutation at tyrosine 766. *J Biol Chem* **269**: 17056-61
- Tolle DP and Le Novere N (2006) Particle-based stochastic simulation in systems biology. *Curr Bioinform* **1**: 315-320
- Tsang M and Dawid IB (2004) Promotion and attenuation of FGF signaling through the Ras-MAPK pathway. *Sci STKE* **2004**: pe17
- Xu H and Goldfarb M (2001) Multiple effector domains within SNT1 coordinate ERK activation and neuronal differentiation of PC12 cells. *J Biol Chem* **276**: 13049-56

Fig 1. Varying FGFR kinase activity and FGF levels: (A) 10- (green) and 100-fold (red) decrease of FGFR kinase rate compared with the default rate (blue); (B) 100% (blue), 10% (green), and 5% (red) of FGF concentration.

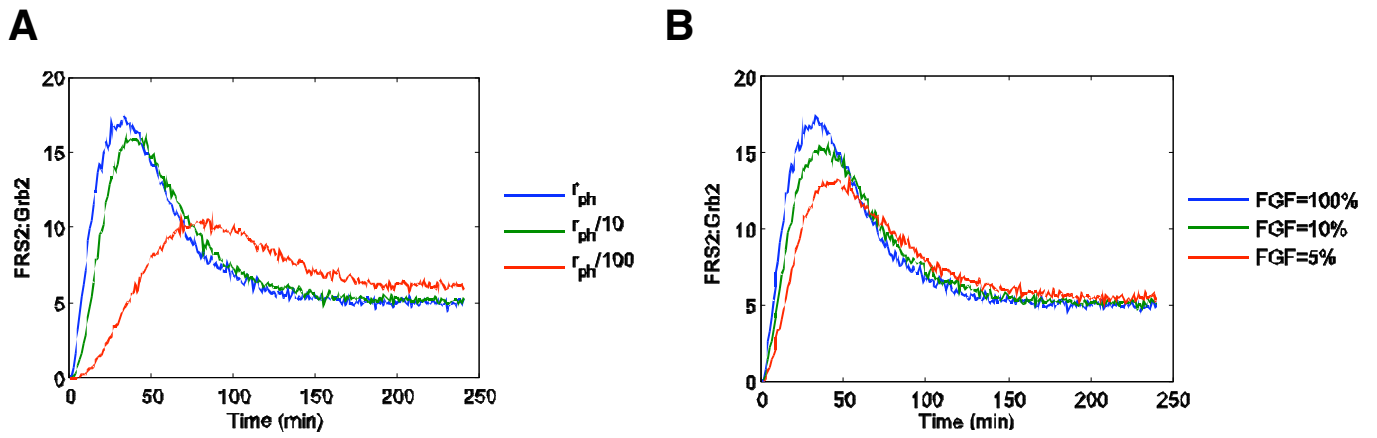


Fig 2. In silico mutagenesis: (A) simulations with inhibited Spry (green), Shp2 (red), and Src (cyan) and the full model (blue); (B) inhibition of Src (cyan) in the revised model (blue); (C and D) experimental validation of predictions with inhibited Src.

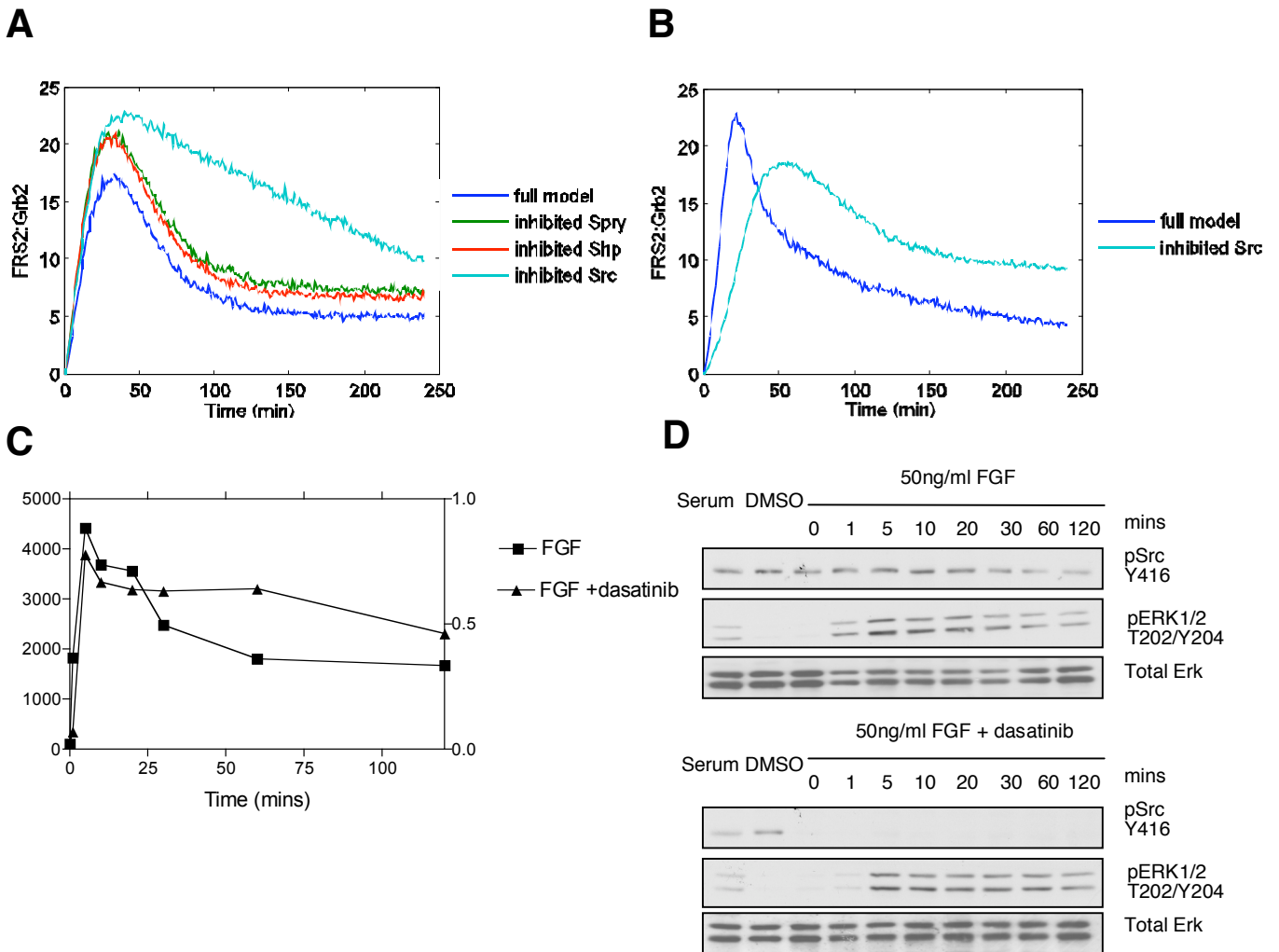


Fig 3. Effects of mutations: simulations with 10-fold inhibition of FGF:FGFR dissociation rate (green) compared to the normal rate (blue) in the initial (A) and revised (B) model; (C and D) experimental validation of phenotypic changes in mutant.

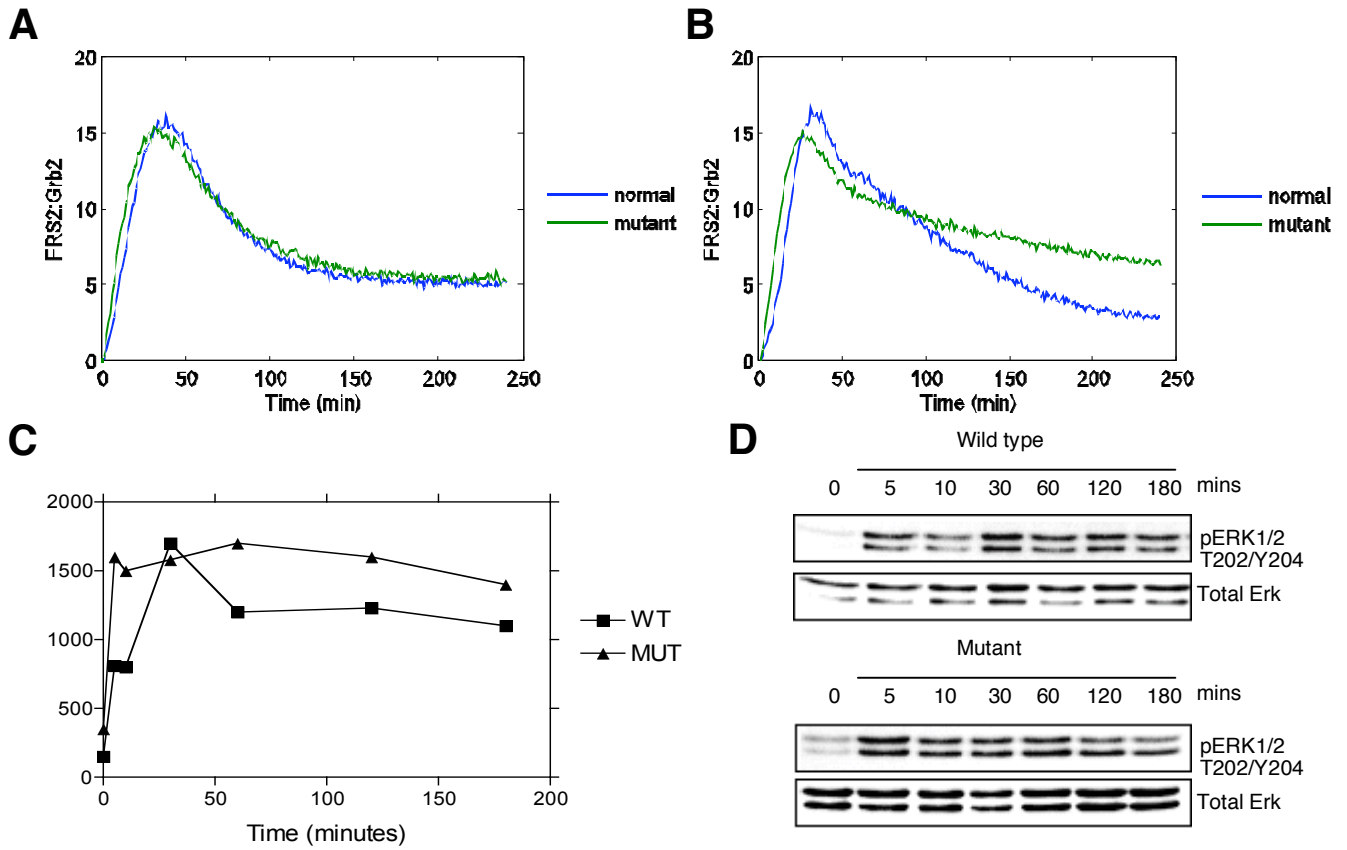


Table I. Reactions encoded in the model.

Reaction	Description	References
1	FGF ligand binds to the FGF receptor (FGFRs) creating a complex of two FGFRs and two FGF ligands	
2	The existence of an FGFR dimer leads to phosphorylation of FGFRs on two residues Y653 and Y654 in the activation loop of the receptor. Mutagenesis and structural studies have shown that phosphorylation of these residues is required for activation of FGFR kinase activity and phosphorylation of other substrates	(Mohammedi et al, 1997)
3	The dual Y653/654 form of the receptor leads to phosphorylation of other FGFR receptor residues (Y663, Y583, Y585, Y766) which have been shown in a number of studies to be required for execution of FGFR dependent signalling functions. In this paper we only consider Y766 further.	(Foehr et al, 2001)
4	FRS2 binds to both the phosphorylated and dephosphorylated forms of the FGFR. FRS2 has been shown in multiple studies to be an essential mediator of FGFR functions as a consequence of recruitment of effectors to specific phosphorylated sites on FRS2	(Xu & Goldfarb, 2001)
5	The dual Y653/654 form of the receptor leads to phosphorylation of the FGFR substrate FRS2	
6	We incorporate a step in which FRS2 is dephosphorylated by a phosphatase (denoted Shp2). Shp2 has been shown experimentally to be a negative regulator of FRS2 functions	(Hadari et al, 1998)
7	A number of effector proteins interact with the phosphorylated form of FRS2. In this model we include Src, Grb2:Sos and Shp2	(Schlessinger, 2004)
8	Src associated with the phosphorylated FRS2 Y219 leads to relocation (i.e. endocytosis and/or degradation) of FGFR:FRS2	
9	Another method of attenuating signal propagation is relocation/degradation of FGFR caused by PLCgamma being bound to Y766 of FGFR	(Sorokin et al, 1994)
10	The signal attenuator Sprouty is a known inhibitor of FGFR signalling and is synthesized in response to FGFR signalling. Here we include a variable to regulate the concentration of Sprouty protein in a time dependent manner	(Hanafusa et al, 2002)
11	We incorporate the association of Sprouty with Src and concomitant phosphorylation of Sprouty residue Y55	(Li et al, 2004)
12	The Y55 phosphorylated form of Sprouty binds Cbl, which leads to ubiquitin modification of FRS2 and a decrease in FRS2 concentration by ubiquitin mediated proteolysis	(Fong et al, 2003)
13	Y55P form of Sprouty is dephosphorylated by Shp2 bound to FRS2	(Hadari et al, 1998)
14	Sprouty Y55P competes with FRS2 for binding Grb2 as has been suggested from some studies in the literature	(Hanafusa et al, 2002)

Supporting Information

Supporting Methods

Representing signalling pathway models in stochastic pi-calculus. Stochastic pi-calculus (Priami et al, 2001) is an extension of the pi-calculus (Milner, 1999) with exponential distributions. A pi-calculus model is a network of concurrent processes operating according to explicitly given reaction rules. The pi-calculus was proposed as a representation for biological systems in (Regev & Shapiro, 2002) and in (Regev & Shapiro, 2004) a translation scheme for molecular reactions was formulated. We use this scheme, described in more detail below, to represent biochemical reactions 1-14 of the FGF pathway, and subsequent variants corresponding to new hypotheses. Under such translation scheme, the model describes a molecular network whose states contain sets of interacting proteins and complexes. The behaviour of each protein is governed by the reaction rules it participates in. Protein interactions do not depend on the precise sequence, but on conformation and binding of domains. Therefore, we encode proteins as sequences of subcomponents, each of which enables binding to other proteins or phosphorylation, which can further modify protein interaction capabilities. Subcomponents serve as both protein internal states and its interfaces through which the interactions with other proteins occur. Any subcomponent can undergo state transition between free and bound, or phosphorylated and unphosphorylated, independently of the other protein sites. The pi-calculus processes can be represented in a machine-readable textual format (here BioSPI (Regev & Shapiro, 2004)) or that of a graphical pi-calculus (Phillips & Cardelli, 2005).

The BioSPI system. The BioSPI (Regev & Shapiro, 2004) system is a simulation platform for stochastic pi-calculus implemented at the Weizmann Institute using Concurrent Prolog. BioSPI 2.0, which implements the Gillespie algorithm, allows one to obtain a full record of the time evolution of the system. Extensive examples of biological networks modelled using BioSPI are available from (Regev & Shapiro, 2004) and the website <http://www.wisdom.weizmann.ac.il/~biospi/> as well as Supplementary Material for (Regev & Shapiro, 2002).

The graphical pi-calculus and the SPiM system. SPiM (Phillips & Cardelli, 2005) is a simulation platform for the stochastic pi-calculus based on an abstract machine implemented by Phillips (Phillips & Cardelli, 2005). The graphical stochastic pi-calculus is a front-end to SPiM. The formalism was introduced in (Phillips & Cardelli, 2005) and applied to a number of case studies, for example the MAPK cascade. More detail about the biological case studies and the tool is available from the websites <http://www.doc.ic.ac.uk/~anp/spim/> and <http://www.luca.demon.co.uk/BioComputing.htm>.

Representing biochemical reactions in graphical pi-calculus. A model in the graphical stochastic pi-calculus is a graph whose nodes correspond to pi-calculus processes (here proteins) and edges between the nodes correspond to biochemical reactions and subsequent modifications of proteins. Fig. 4 illustrates how basic reactions can be modelled. A formation of the complex is modelled by communication of the processes A and B over a channel `bind`. Reactant A

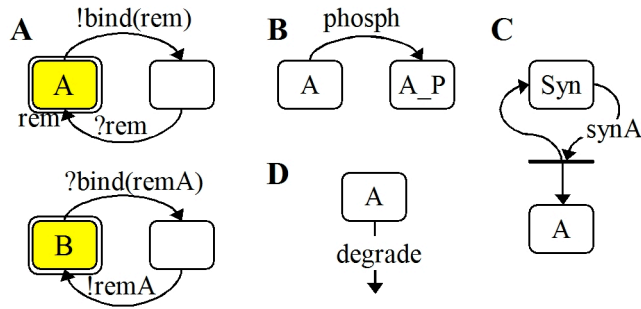


Fig 4. . Pi-calculus representation of complexation (A), phosphorylation (B), synthesis (C), and degradation (D) reactions.

performs a send on `bind`, sending its private channel `rem` (denoted by a bubble around `A` labelled with `rem`). After becoming bound, `A` can unbind by performing receive on `rem`. Respectively, `B` can bind to `A` by receiving on channel `bind` or unbind by sending on `remA` (which will be substituted by `rem` in the course of program execution). Highlighted nodes denote processes that perform substitution.

In the course of some interactions, members of the complex can undergo phosphorylation changing the visibility of binding sites. This is modelled as a state transition of `A` on channel `phosph`, Fig. 4B. Proteins can also be synthesized and degraded as shown in Fig. 4C and D. Note that the synthesis operation corresponds to the creation of a new instance of `A` while the process actually performing the creation (`Syn`) returns to its original state.

More complex reactions can be built up from basic building blocks. We illustrate parallel, competitive and context-dependent reactions. In a parallel reaction, an element can be simultaneously involved in different reactions, for example, binding of `A` to `B` and `C` can be done in parallel (FGF reactions 12 and 14). This corresponds to the existence of two independent binding sites in `A` through which bindings can be established. This can be represented by two parallel, unlabelled edges from node `A`, each of which denotes a concurrent execution path in the system. The node `A` in this case is represented as a solid rectangle (Fig. 5A).

In a competitive reaction, the reactant `A` participates in two mutually exclusive reactions when its different partners, `B` and `C`, compete for the same binding site in `A` (FGF reaction 7 and 14). Such a reaction is presented in Fig. 5B. Each edge from `A` now denotes an alternative execution path by being labelled with separate action, `bindB` and `bindC`.

Contextual reactions define an application of a basic reaction rule only when the reactants themselves are within the desired contexts. An example would be a rule stating that, if `B` is bound to `A`, `B` can undergo further state changes, for example, become phosphorylated on some residue (FGF reactions 2, 3, and 4). First, note that, since dephosphorylation of `B` is generally not connected to its binding to `A`, `B` can appear in either phosphorylated or unphosphorylated state while being bound to `A`. Therefore, we need to represent the binding site and phosphorylation site of `B` independently, as `B1` and `B2`. We use the following protocol illustrated in Fig. 5C: `B2` can be phosphorylated following the receive operation from `B1` binding site on channel `pre`. When `B1` is bound, it notifies `B2` about the possibility to phosphorylate.

Channel pre is restricted to processes B1 and B2, as represented by a bubble around the processes labelled with the corresponding channel name.

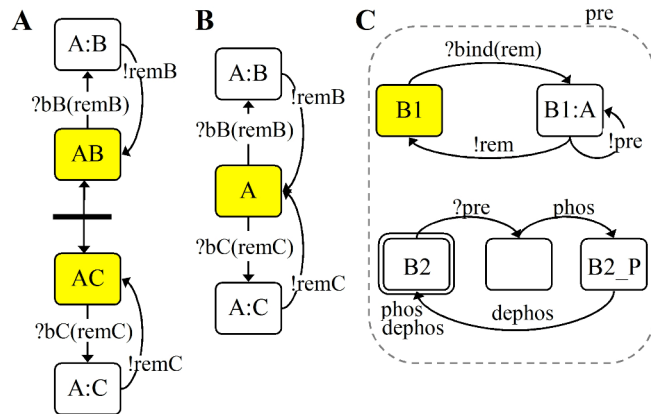


Fig 5. Representation of parallel (A), competitive (B), and contextual (C) reactions.

A clickable map of the FGF pathway (as in Fig. 6) giving access to the pi-calculus code for each component of the pathway is available from the website:

<http://www.cs.bham.ac.uk/~oxt/fgfmap.html>

The full machine-readable code (BioSPI 2.0, (Regev & Shapiro, 2004)) is also available below, as is the corresponding graphical pi-calculus variant based on (Phillips & Cardelli, 2005).

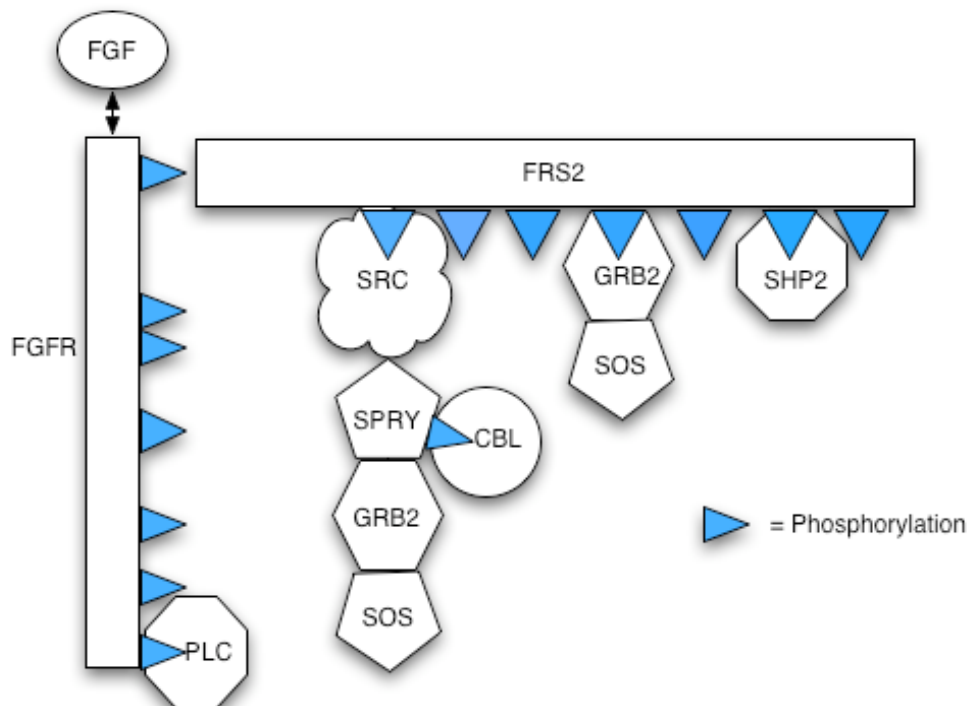


Fig 6. A diagrammatic representation of FGF pathway map.

The model code in stochastic pi-calculus

```
-language(spifcp).
-include(fgfrates).

public(fb(FGFBind), frb(FRSBind), sb(SRCBind), grb(GRBBind),
srb(SPRYBind), shb(SHPBind), pb(PLCBind), cb(CBLBind), sosb(SOSBind),
gsb(GSBind), ph653(FGFRPh1), ph766(FGFRPh2), phFRS(FRSPh),
phSpry(SPRYPh), dph4(FRSDph), create_spry(SPRYIn), dph196(FRSDph),
dph306(FRSDph), dph471(FRSDph)).

System(N1,N2,N3) ::= <<
    CREATE_FGFR(N1) | CREATE_FGF(N2) | CREATE_FRS(N3) |
    CREATE_SRC(N1) | CREATE_SHP(N1) |
    CREATE_GRB(N1) | CREATE_PLC(N1) | CREATE_CBL(N1) |
    CREATE_SOS(N1) | CREATE_DSPRY(N1) | Clock .

CREATE_FGF(N) ::= {N =< 0}, true ; {N > 0}, {N--} | FGF | self .
CREATE_FGFR(N) ::= {N =< 0}, true ; {N > 0}, {N--} | FGFR | self .
CREATE_FRS(N) ::= {N =< 0}, true ; {N > 0}, {N--} | FRS2 | self .
CREATE_SRC(N) ::= {N =< 0}, true ; {N > 0}, {N--} | Src | self .
CREATE_GRB(N) ::= {N =< 0}, true ; {N > 0}, {N--} | Grb2 | self .
CREATE_SHP(N) ::= {N =< 0}, true ; {N > 0}, {N--} | Shp | self .
CREATE_DSPRY(N) ::= {N =< 0}, true ; {N > 0}, {N--} | Spry | Dself(N)
.
Dself(N) ::= create_spry ! [], CREATE_DSPRY(N) .
CREATE_CBL(N) ::= {N =< 0}, true ; {N > 0}, {N--} | Cbl | self .
CREATE_PLC(N) ::= {N =< 0}, true ; {N > 0}, {N--} | Plc | self .
CREATE_SOS(N) ::= {N =< 0}, true ; {N > 0}, {N--} | Sos | self >> .

FGF ::= << f(FGFUn), remFgf(infinite), degFgf(infinite) .
    %private channels
    fb ? {f, remFgf, degFgf}, FGF_Bound .
    %binding to the receptor

FGF_Bound ::= f ! [], FGF ;
    %dissociation from FGFR
    remFgf ? [], FGF ;
    %immediate dissociation
    degFgf ? [], true >> .
    %degradation

FGFR ::= << f(FGFUn), fr(FRSUn), p(PLCUn), degPlc(PLCDeg),
degPlcInf(infinite), pre653(infinite), preFRS1(10000),
preFRS2(10000), pre766(infinite), remFgfr(infinite),
remFrs(infinite), degFrs(infinite), remFgf(infinite),
degFgf(infinite), degFGFR10(infinite), degFGFR11(infinite),
degFGFR12(infinite), degFGFR20(infinite), degFGFR22(infinite),
degFGFR23(infinite), degFGFR14(infinite), degFGFR24(infinite) .
%the rates of phosphorylation notification messages are not infinite
because of the memory error in the BioSPI implementation

    FGFR_Ligand_Binding | FGFR_FRS2_Binding | FGFR_653 | FGFR_766 .
%four independent domains (activities)

FGFR_Ligand_Binding ::= fb ! {f, remFgf, degFgf}, FGFR_Ligand_Bound ;
    %binding to FGF, allow phosphorylation of res 653
    degFGFR10 ? [], true;
    %requested degradation
```

```

        degFGFR20 ? [], true .
    %requested degradation
FGFR_Ligand_Bound ::= f ? [], FGFR_Ligand_Binding ;
    %dissociation from FGF
        pre653 ! [], FGFR_Ligand_Bound ;                               %while
bound, allow phosphorylation of res 653
        degFGFR10 ? [], remFgf ! [], true ;
    %requested degradation, remove FGF
        degFGFR20 ? [], degFgf ! [], true .
    %requested degradation, pass to FGF

FGFR_FRS2_Binding ::=
    frb ! {fr, preFRS2, remFrs, degFrs, remFgfr},
FGFR_FRS2_Bound ; %binding to FRS2
    degFGFR11 ? [], true .
    %requested degradation
FGFR_FRS2_Bound ::=
    fr ? [], FGFR_FRS2_Binding ;
    %FRS2 dissociation
        preFRS1 ? [], FGFR_FRS2_BoundP ;
        remFrs ? [], FGFR_FRS2_Binding ;
        degFrs ? [], degFGFR20 ! [], degFGFR22 ! [], degFGFR23 !
[], true ; %remove FGFR together with all bound partners
        degFGFR11 ? [], remFgfr ! [], true .
FGFR_FRS2_BoundP ::=
    preFRS2 ! [], FGFR_FRS2_BoundP ;
    fr ? [], FGFR_FRS2_Binding ;
    remFrs ? [], FGFR_FRS2_Binding ;
    degFrs ? [], degFGFR20 ! [], degFGFR22 ! [], degFGFR23 !
[], true;
        degFGFR11 ? [], remFgfr ! [], true .

FGFR_653 ::= pre653 ? [], (ph653 ! [], FGFR_653P ;
    %phosphorylate, once condition pre653 is satisfied
        degFGFR12 ? [], true ;
        degFGFR22 ? [], true ) ;
        degFGFR12 ? [], true ;
        degFGFR22 ? [], true .
FGFR_653P ::=
    preFRS1 ! [], FGFR_653P ;                               %allow
phosphorylation of FRS2 if bound
    pre766 ! [], FGFR_653P ;                               %allow
phosphorylation of res 766
        degFGFR12 ? [], true ;
        degFGFR22 ? [], true .

FGFR_766 ::= pre766 ? [], (ph766 ! [], FGFR_766P ; degFGFR23 ? [],
true ) ;
        degFGFR23 ? [], true .
FGFR_766P ::= pb ! {p, degPlc, degPlcInf}, FGFR_Plc_Bound ;
    %bind Plc if phosphorylated
        degFGFR23 ? [], true .
FGFR_Plc_Bound ::= p ? [], FGFR_766P ;
        degPlc ? [], ( degFGFR10 ! [], degFGFR11 ! [], degFGFR12
! [], true ; degFGFR23 ? [], true ) ; %remove FGFR but leave all
bound partners
        degFGFR23 ? [], degPlcInf ! [], true >> .

FRS2 ::= << s(SRCUn), fr(FRSUn), degSrc(SRCDeg), remFrs(infinite),
degFrs(infinite), remFgfr(infinite), remSrc(infinite),

```

```

degCbl3(infinite), remShp(infinite), degShp(infinite),
remGrb(infinite), degGrb(infinite), gr(GRBUn), sh(SHPUn),
pre196(infinite), pre306(infinite), pre471(infinite), preFRS2(10000),
preFRS3(10000), post196(infinite), post306(infinite),
degFRS11(infinite), degFRS12(infinite), degFRS13(infinite),
degFRS20(infinite), degFRS22(infinite), degFRS23(infinite) .

FRS2_FBinding | FRS2_196 | FRS2_306 | FRS2_471 .
%four independent domains

FRS2_FBinding ::=
  frb ? {fr, preFRS2, remFrs, degFrs, remFgfr}, FRS2_FBound ;
  %FGF binding site
  degFRS20 ? [], true ;
  degCbl3 ? [], degFRS12 ! [], degFRS11 ! [], degFRS13 ! [], true
.
FRS2_FBound ::= preFRS2 ? [], FRS2_FBoundP ;
  fr ! [], FRS2_FBinding ;
  remFgfr ? [], FRS2_FBinding ;
  degCbl3 ? [], degFRS12 ! [], degFRS11 ! [], degFRS13 ! [],
remFrs ! [], true ;
  degFRS20 ? [], (degFrs ! [], true ; remFgfr ? [], true) .
FRS2_FBoundP ::= fr ! [], FRS2_FBinding ;                               %no
subsequent dephosphorylation of 196, 306, 471
  remFgfr ? [], FRS2_FBinding ;
  degCbl3 ? [], degFRS12 ! [], degFRS11 ! [], degFRS13 ! [],
remFrs ! [], true ;
  degFRS20 ? [], (degFrs ! [], true ; remFgfr ? [], true) ;
  preFRS3 ! [], FRS2_FBoundP .                                         %allow
phosphorylation of res 196, 306, 471 whenever bound

FRS2_196 ::= preFRS3 ? [], (phFRS ! [], FRS2_196P ;
  %Src binding site, precondition for phosphorylation
  post196 ? [], FRS2_196 ;
  degFRS11 ? [], true ) ;
  post196 ? [], FRS2_196 ;
  degFRS11 ? [], true .
FRS2_196P ::= sb ! {s, degCbl3, remSrc, degSrc}, FRS2_Src_Bound ;
  post196 ? [], FRS2_196 ;
  degFRS11 ? [], true .
FRS2_Src_Bound ::= s ? [], FRS2_196P ;
  degSrc ! [], ( degFRS20 ! [], degFRS22 ! [], degFRS23 ! [],
true ; %degrade together with all bound partners
  degFRS11 ? [], true ) ;
  post196 ? [], remSrc ! [], FRS2_196 ;
  degFRS11 ? [], true .

FRS2_306 ::= preFRS3 ? [], (phFRS ! [], FRS2_306P ;
  %Grb binding site
  post306 ? [], FRS2_306 ; degFRS12 ? [], true ;
  degFRS22 ? [], true) ;
  post306 ? [], FRS2_306 ;
  degFRS12 ? [], true ;
  degFRS22 ? [], true .
FRS2_306P ::= grb ! {gr, remGrb, degGrb}, FRS2_Grb_Bound ;
  post306 ? [], FRS2_306 ;
  degFRS12 ? [], true ;
  degFRS22 ? [], true .
FRS2_Grb_Bound ::= gr ? [], FRS2_306P ;
  post306 ? [], remGrb ! [], FRS2_306 ;
  degFRS12 ? [], remGrb ! [], true ;

```

```

degFRS22 ? [], degGrb ! [], true .

FRS2_471 ::= preFRS3 ? [], (phFRS ! [], FRS2_471P ;
    %Shp binding site
        degFRS13 ? [], true ;
        degFRS23 ? [], true) ;
degFRS13 ? [], true ;
degFRS23 ? [], true .
FRS2_471P ::= shb ! {sh, remShp, degShp}, FRS2_Shp_Bound ;
degFRS13 ? [], true ;
degFRS23 ? [], true .
FRS2_Shp_Bound ::= sh ? [], FRS2_471P ;                               %Shp
dissociation
    dph196 ! [], post196 ! [], FRS2_Shp_Bound ;
    %dephosphorylation of res 196
    dph306 ! [], post306 ! [], FRS2_Shp_Bound ;
    %dephosphorylation of res 306
    dph471 ! [], remShp ! [], FRS2_471 ;
    %dephosphorylation of res 471
    degFRS13 ? [], remShp ! [], true ;                               %request
for degradation
    degFRS23 ? [], degShp ! [], true >> .
    %request for degradation

Src ::= << degCbl3(infinite), degCbl2(infinite), cbl3(infinite),
degSpry(infinite), sr(SPRYUn), srp(SPRYPUn), remSpry(infinite),
s(SRCUn), remSrc(infinite), degSrc(SRCDeg).

Src_FBinding | Src_SBinding .
%independent FRS2 and Spry binding sites

Src_FBinding ::=
    sb ? {s, degCbl3, remSrc, degSrc}, Src_FBound ;
    %Src binding
    cbl3 ? [], Src_FBinding .
Src_FBound ::= s ! [], Src_FBinding ;
remSrc ? [], Src_FBinding ;
degSrc ? [], degSpry ! [], true ;
cbl3 ? [], ( degCbl3 ! [], Src_FBinding ;
    remSrc ? [], Src_FBinding ;
    degSrc ? [], degSpry ! [], true ) .

Src_SBinding ::= srb ! {sr, srp, remSpry, degCbl2}, Src_SBound ;
degSpry ? [], true .
Src_SBound ::= sr ? [], Src_SBinding ;
srp ? [], Src_SBinding ;
degSpry ? [], remSpry ! [], true ;
degCbl2 ? [], cbl3 ! [], Src_SBound >> .

Spry ::= << c(CBLUn), sr(SPRYUn), srp(SPRYPUn), remSpry(infinite),
gs(GSUn), degSpry(infinite), degGrb(infinite), degCbl(infinite),
degCbl2(infinite), degCbl1(CBLDeg), remGrb(infinite),
remCbl(infinite), spryp(infinite), dspryp(infinite) .

Spry_SBinding | Spry_CBinding | Spry_GBinding .
%independent binding to Src, Cbl and Grb

Spry_GBinding ::= spryp ? [], SpryP_GBinding ;
%can bind Grb after being phosphorylated

```

```

    degSpry ? [], true .
SpryP_GBinding ::= gsb ! {gs, remGrb, degGrb}, SpryP_GBound ;
    dspryp ? [], Spry_GBinding ;
    degSpry ? [], true .
SpryP_GBound ::= gs ? [], SpryP_GBinding ;
    dspryp ? [], ( remGrb ! [], Spry_GBinding ;
        degSpry ? [], degGrb ! [], true) ;
    degSpry ? [], degGrb ! [], true .

Spry_CBinding ::= spryp ? [], SpryP_CBinding ;
    %can bind Cbl after being phosphorylated
    degSpry ? [], true .
SpryP_CBinding ::= cb ! {c, remCbl, degCbl1, degCbl}, SpryP_CBound ;
    dspryp ? [], Spry_CBinding ;
    degSpry ? [], true .
SpryP_CBound ::= c ? [], SpryP_CBinding ;
    dspryp ? [], ( remCbl ! [], Spry_CBinding ;
        degSpry ? [], degCbl ! [], true) ;
    degSpry ? [], degCbl ! [], true .

Spry_SBinding ::= srb ? {sr, srp, remSpry, degCbl2}, Spry_SBound ;
    dspryp ! [], Spry_SBinding .
Spry_SBound ::= phSpry ! [], SpryP_SBound ;
    sr ! [], Spry_SBinding ;
    remSpry ? [], degSpry ! [], degSpry ! [], true ;
    dspryp ! [], Spry_SBound .
SpryP_SBound ::=
    srp ! [], SpryP_SBinding ;
    remSpry ? [], degSpry ! [], degSpry ! [], true ;
    degCbl1 ? [], ( degCbl2 ! [], SpryP_SBound ;
        remSpry ? [], degSpry ! [], degSpry ! [], true) ;
    spryp ! [], SpryP_SBound .
SpryP_SBinding ::= srb ? {sr, srp, remSpry, degCbl2}, SpryP_SBound ;
    degCbl1 ? [], SpryP_SBinding ;
    spryp ! [], SpryP_SBinding >> .

Cbl ::= << degCbl1(CBLDeg), c(CBLUn), remCbl(infinite),
degCbl(infinite) .
    cb ? {c, remCbl, degCbl1, degCbl}, Cbl_Bound .
Cbl_Bound ::= c ! [], Cbl ;
    remCbl ? [], Cbl ;
    degCbl ? [], true ;
    degCbl1 ! [], Cbl_Bound >> .

Grb2 ::= << gr(GRBUn), gs(GSun), remGrb(infinite), degGrb(infinite),
sos(SOSUn), remSos(infinite), degSos(infinite) .
    grb ? {gr, remGrb, degGrb}, Grb2_FBound ;
    gsb ? {gs, remGrb, degGrb}, Grb2_Spry_Bound .

Grb2_FBound ::= sosb ! {sos, remSos, degSos}, Grb2_FSBound ;
    gr ! [], Grb2 ;
    remGrb ? [], Grb2 ;
    degGrb ? [], true .
Grb2_FSBound ::= sos ? [], Grb2_FBound ;
    gr ! [], remSos ! [], Grb2 ;
    remGrb ? [], remSos ! [], Grb2 ;
    degGrb ? [], degSos ! [], true .

Grb2_Spry_Bound ::= gs ! [], Grb2 ;

```

```

    degGrb ? [], true ;                                %request
for degradation
    remGrb ? [], Grb2 >> .

Sos ::= << sos(SOSUn), remSos(infinite), degSos(infinite) .
    sosb ? {sos, remSos, degSos}, Sos_Bound .
Sos_Bound ::= sos ! [], Sos ;
    degSos ? [], true ;
    remSos ? [], Sos >> .

Shp ::= << sh(SHPUn), remShp(infinite), degShp(infinite) .
    shb ? {sh, remShp, degShp}, Shp_FBound .

Shp_FBound ::= sh ! [], Shp ;
    remShp ? [], Shp;
    degShp ? [], true >> .

Plc ::= << p(PLCUn), degPlc(PLCDeg), degPlcInf(infinite).
    pb ? {p, degPlc, degPlcInf}, Plc_Bound.
Plc_Bound ::= p ! [], Plc; degPlc ! [], true ; degPlcInf ? [], true
>>.

Clock ::=
    ph653 ? [], Clock ;
    ph766 ? [], Clock ;
    phFRS ? [], Clock ;
    phSpry ? [], Clock ;
    dph196 ? [], Clock ;
    dph306 ? [], Clock ;
    dph471 ? [], Clock ;
    create_spry ? [], Clock .

```

Table II. Rate constants used in simulation studies.

Reaction	Parameter	Value	Ref
1	FGF binding	$b_{\text{FGF}} = 5 \times 10^6 \text{ M}^{-1} \text{ s}^{-1}$, $r_{\text{FGF}} = 5 \times 10^{-3} \text{ s}^{-1}$	(Felder et al, 1993; Mohammadi et al, 2005)
2	FGFR Y653/654 phosphorylation	$ph_{\text{FGFR1}} = 0.013 \text{ s}^{-1}$	(Furdui et al, 2006)
3	FGFR Y766 phosphorylation	$ph_{\text{FGFR2}} = 0.004 \text{ s}^{-1}$	(Furdui et al, 2006)
4, 7, 9	FRS2, Src, Grb2, Shp2, PLC binding	$b_{\text{FRS, SRC, Grb, Shp, PLC}} = 2.5 \times 10^6 \text{ M}^{-1} \text{ s}^{-1}$, $r_{\text{FRS, SRC, Grb, Shp, PLC}} = 5 \times 10^{-2} \text{ s}^{-1}$	(Panayotou et al, 1993; Skolnik et al, 1993)
5	FRS2 phosphorylation	$ph_{\text{FRS}} = 0.005 \text{ s}^{-1}$	(Furdui et al, 2006)
6, 13	FRS2, Spry dephosphorylation	$dph_{\text{FRS, Spry}} = 12 \text{ s}^{-1}$	(Montalibet et al, 2005)
7,11,14,12	Sos, Spry, Cbl binding	$b_{\text{Sos, Spry, Cbl}} = 10^5 \text{ M}^{-1} \text{ s}^{-1}$, $r_{\text{Sos, Spry, Cbl}} = 10^{-4} \text{ s}^{-1}$	(Sastry et al, 1995)
8	FRS2:Src relocation	$t_{\text{SRC}} = 1/\text{deg}_{\text{SRC}} = 15 \text{ min}$	(Ware et al, 1997)
9	FGFR:PLC relocation	$t_{\text{PLC}} = 1/\text{deg}_{\text{PLC}} = 60 \text{ min}$	(Sorokin et al, 1994)
10	Spry induction	$\text{syn}_{\text{Spry}} = 0.083 \text{ nM s}^{-1}$	(Hanafusa et al, 2002)
11	Spry phosphorylation	$ph_{\text{Spry}} = 10 \text{ s}^{-1}$	estimated
12	FRS2 ubiquitinylation and proteolysis	$t_{\text{Spry}} = 1/\text{deg}_{\text{Spry}} = 25 \text{ min}$	(Wong et al, 2001)

Table III. Sensitivity coefficients calculated for the reference state: $FGF_0=50$ nM , $FGFR_0=50$ nM , $PLC_0=50$ nM , $FRS_0=100$ nM , $SRC_0=50$ nM , $Grb2_0=50$ nM , $Shp2_0=50$ nM , $Spry_0=0$ nM , $Cbl_0=50$ nM . Values smaller than 1×10^{-5} are annotated as ~ 0 .

Parameter j		C_j^A	C_j^D
FGF bind/release	b_{FGF}/r_{FGF}	0.003/-0.002	0/0
FGFR Y653/654 phosphorylation	ph_{FGF1}	0.12	-0.02
FGFR Y766 phosphorylation	ph_{FGF2}	~ 0	0
PLC bind/release	b_{PLC}/r_{PLC}	$\sim 0 / -2 \times 10^{-5}$	0/0
FRS2 bind/release	b_{FRS}/r_{FRS}	$-2 \times 10^{-5} / 0.008$	0/-0.001
FRS2 phosphorylation	ph_{FRS}	0.01	-0.01
FRS2 dephosphorylation	dph_{FRS}	2×10^{-4}	0
SRC bind/release	b_{SRC}/r_{SRC}	$-0.001 / 4 \times 10^{-4}$	-0.03/0.02
Grb2 bind/release	b_{Grb}/r_{Grb}	0.008/-0.005	0.004/-0.003
Shp2 bind/release	b_{Shp}/r_{Shp}	$-3 \times 10^{-4} / \sim 0$	0/0
SRC-mediated relocation	deg_{SRC}	-0.14	-0.97
PLC-mediated degradation	deg_{PLC}	0.0005	0
Spry synthesis	syn_{Spry}	-0.002	-0.004
Spry degradation	deg_{Spry}	-0.02	-0.04
Spry bind/release	b_{Spry}/r_{Spry}	-0.006/ ~ 0	-0.006/0
Spry phosphorylation	ph_{Spry}	-0.0007	0
Spry dephosphorylation	dph_{Spry}	0.013	0.011
Cbl bind/release	b_{Cbl}/r_{Cbl}	0.0003/ ~ 0	-0.002/0
Cbl-mediated degradation	deg_{Cbl}	-0.0002	-0.004
Grb/Spry bind/release	b_{GS}/r_{GS}	-0.006/ ~ 0	-0.002/0

References

- Felder S, Zhou M, Hu P, Urena J, Ullrich A, Chaudhuri M, White M, Shoelson SE and Schlessinger J (1993) SH2 domains exhibit high-affinity binding to tyrosine-phosphorylated peptides yet also exhibit rapid dissociation and exchange. *Mol Cell Biol* **13**: 1449-55
- Furdui CM, Lew ED, Schlessinger J and Anderson KS (2006) Autophosphorylation of FGFR1 Kinase Is Mediated by a Sequential and Precisely Ordered Reaction. *Mol Cell* **21**: 711-7
- Hanafusa H, Torii S, Yasunaga T and Nishida E (2002) Sprouty1 and Sprouty2 provide a control mechanism for the Ras/MAPK signalling pathway. *Nat Cell Biol* **4**: 850-8
- Milner R (1999). *Communicating and Mobile Systems: The pi-Calculus*. Cambridge, Cambridge University Press
- Mohammadi M, Olsen SK and Ibrahimi OA (2005) Structural basis for fibroblast growth factor receptor activation. *Cytokine Growth Factor Rev* **16**: 107-37
- Montalibet J, Skorey KI and Kennedy BP (2005) Protein tyrosine phosphatase: enzymatic assays. *Methods* **35**: 2-8
- Panayotou G, Gish G, End P, Truong O, Gout I, Dhand R, Fry MJ, Hiles I, Pawson T and Waterfield MD (1993) Interactions between SH2 domains and tyrosine-phosphorylated platelet-derived growth factor beta-receptor sequences: analysis of kinetic parameters by a novel biosensor-based approach. *Mol Cell Biol* **13**: 3567-76
- Phillips A and Cardelli L (2005). A Graphical Representation for the Stochastic Pi-calculus. In *Proc Bioconcur'05*
- Priami C, Regev A, Shapiro EY and Silverman W (2001) Application of a stochastic name-passing calculus to representation and simulation of molecular processes. *Inf Process Lett* **80**: 25-31
- Regev A and Shapiro E (2002) Cells as computation. *Nature* **419**: 343
- Regev A and Shapiro E (2004) The pi-calculus as an Abstraction for Biomolecular Systems. In *Modelling in Molecular Biology*, Ciobanu G and Rozenberg G (ed) pp 219-266. Berlin-Heidelberg: Springer
- Sastry L, Lin W, Wong WT, Di Fiore PP, Scoppa CA and King CR (1995) Quantitative analysis of Grb2-Sos1 interaction: the N-terminal SH3 domain of Grb2 mediates affinity. *Oncogene* **11**: 1107-12
- Skolnik EY, Lee CH, Batzer A, Vicentini LM, Zhou M, Daly R, Myers MJ, Backer JM, Ullrich A, White MF and Schlessinger J (1993) The SH2/SH3 domain-containing protein GRB2 interacts with tyrosine-phosphorylated IRS1 and Shc: implications for insulin control of ras signalling. *EMBO J* **12**: 1929-36
- Sorokin A, Mohammadi M, Huang J and Schlessinger J (1994) Internalization of fibroblast growth factor receptor is inhibited by a point mutation at tyrosine 766. *J Biol Chem* **269**: 17056-61
- Ware MF, Tice DA, Parsons SJ and Lauffenburger DA (1997) Overexpression of cellular Src in fibroblasts enhances endocytic internalization of Epidermal Growth Factor receptor. *J Biol Chem* **272**: 30185-90
- Wong ES, Lim J, Low BC, Chen Q and Guy GR (2001) Evidence for Direct Interaction between Sprouty and Cbl. *J Biol Chem* **276**: 5866-75